STUDIES ON HIGHER VALENT MANGANESE COMPLEXES AND POLYIODIDE SALTS OF METAL COMPLEX CATIONS

A Thesis

Submitted for the Degree of

DOCTOR OF PHILOSOPHY

By

D. RAMALAKSHMI

SCHOOL OF CHEMISTRY

UNIVERSITY OF HYDERABAD

HYDERABAD 500 046

INDIA

MAY 1999

with respect,

to my Parents and Guide

CONTENTS

STATEMENT

I hereby declare that the matter embodied in this thesis is the result of investigations carried out by me in the School of Chemistry, University of Hyderabad, Hyderabad, under the supervision of Dr. M. V. Rajasekharan.

In keeping with the general practice of reporting scientific observations, due acknowledgement has been made wherever the work described is based on the findings of other investigators.

D. Ramalakshmi

CERTIFICATE

Certified that the work contained in this thesis entitled **"STUDIES ON HIGHER VALENT MANGANESE COMPLEXES AND POLYIODIDE SALTS OF METAL COMPLEX CATIONS"** has been carried out by Ms. D. Ramalakshmi under my supervision and the same has not been submitted elsewhere for a degree.

Hyderabad
May 1999

M. V. RAJASEKHARAN
(Thesis supervisor)

DEAN
SCHOOL OF CHEMISTRY

ACKNOWLEDGEMENTS

I would like to give my sincere thanks to my teacher and guide, Dr. M. V. Rajasekharan for his guidance and direction of this work.

I thank the present and past dean(s) of the School of Chemistry for extending all the facilities of the Department. I also thank all the faculty members of the School.

The bulk of the x-ray data were collected at the Regional Sophisticated Instrumentation Centre, Indian Institute of Technology, Madras and at the National single crystal x-ray diffraction facility recently established in our school.
Prof. W. T. Robinson, University of Canterbury, New Zealand, Dr. N. Arulsamy, Prof. D. J. Hodgson, University of Wyoming, Laramie and Dr. A. Vij, University of Idaho, Idaho, provided data for two samples (compound 1 and 2). I would like to thank Dr. T. P. Radhakrishnan for allowing me to do resistivity measurements in his lab and Dr. Sathya Prasanna for his help. The Raman measurements were made in the laboratory of Prof. H. U. Guedel, University of Bern, Switzerland. Dr. F. von Helmont and Dr. P. Tregannane, helped with the measurements. I thank Prof. K. -F. Tebbe for sending me several useful re-prints of his work.

I thank all the technical and non-teaching staff of the School of Chemistry and Central Instrumentation Lab for their help and cooperation.

I thank my labmates Dr. G. Swarnabala, Dr. K. Rajender Reddy and Dr. Sindhu Menon and Ms. S. Sailaja for their help and cooperation.

I thank all the staff and research scholars of R.S.I.C., LIT., Madras, especially Dr. Babu Varghese, Dr Manisekharan, Dr. R. Muthukumaran, Dr. G. V. R. Chandramouli, Dr. Asokan, Dr. Baby and Ms. Vani.

I thank all my teachers of M.Sc, whose lectures, made *Chemistry* more convincing and interesting to me. I would like to thank Prof. R. Jagannathan for

his advice and support on many occasions. I would like to thank Prof. M. Perisamy for kindly allowing me to take laser print-out. I would also like to thank Dr. P. Appa Rao for allowing me to do anti-microbial testing in his lab and Ms. Sangeetha for her help.

I extend special thanks to my family members whose support and encouragement was always with me and also to my friends Hema and Leena. The cheerful company of all my M.Sc. classmates, especially Anthony, is always remembered. The pleasant memories with my friends on campus, Sindhu, Chandrakala, Aneetha, Vijjulatha, Madhavi, Mangai, Sailaja, Manjula, Sudha, Saroja, Anita, Soujanya, Gayatri, Nisha, Padmaja, Sangeetha, Sonika, Padma, Subbalakshmi,. . . . .the list goes on. Special thanks to my junior labmates (M.Sc.&M.Phil.), who remember the lab even after the completion of their project. My thanks to the Upper lab association members, Satyen, Sankaran, Srinivasan, Senthil ... for their cheerful company. In fact, all the students in the school were friendly and helpful, the record of which is left for memory.

Financial Assistance from UGC is gratefully acknowledged.

ABBREVIATIONS

aneN4	1,5,9,13-tetraazacyclohexadecane	
aneN2S4	1,4,10,13-tetrathia-7,16-diazacyclohexadecane	
aneO5	1,4,7,10,13-pentaoxacyclopentadecane	
aneS3	1,4,7-trithiacyclononane	
aneS4	1,5,9,13-tetrathiacyclohexadecane	
aneS5	1,4,7,10,13-pentathiacyclopentadecane	
aneS6	1,4,7,10,13,16-hexathiacyclooctadecane	
1-azo-prop	1-azapropellane	
benz	benzamide	
benzo	benzophenone	
bntMe	N-methylbenzothiazole-2(3*H*)-thione	
bpy	2,2'-bipyridine	
nBu	N-butyl	
tBu	tert-butyl	
18-C-6	18-Crown-6	

caf	caffeine	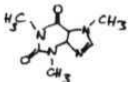
α-CD	α-cyclodextrin	
Cp	cyclopentadiene	
Cryp(2.2)	diaza-18-Crown-6	
Cryp(2.2.2)	cryptand	
D	N-methylbenzothiazole-2(3*H*)-selone	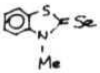
Dabco	1,4-diazabicyclo[2.2.2]octane	
dafone	4,5-diazaflour -9-one	
dibenz(18-C-6)	dibenzo-18-Crown-6	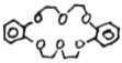
en	ethylenediamine	
EOST	4,5-ethylenedithio-4',5'-(2-oxatrimethylenedithio)diselenadithiafulvalene	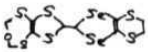
EPR	electron paramagnetic resonance	
ET	bis(ethylenedithiotetrathiafulvalene) or BEDT-TTF	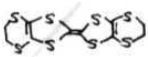
Et	ethyt	
(EtNH2)dt	3,5-bis(ethylamino)-1,2-dithioline	
imd	imidazole	
Me	methyl	
MeCp	1-methylcyclopentadiene	

Me-Piper	N-Me-piperazine	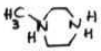
Me-N_4-Adam	1-methyl-1,3,5,7-tetraazaadamantan-1-ane	
Me_2-Piper	N,N'-Me_2-piperazine	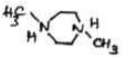
Me_4-1,2Etham	N,N,N',N'-Me_4-1,2-ethanediammonium	
Me_4-1,3Propam	N,N,N',N'-Me_4-1,3-propanediammonium	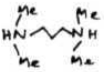
Me_5Cp	pentamethylcyclopentadiene	
n-Me-γ-pico	N-methyl-γ-picolinium	
mo	morpholine	
mod	morpholine-carbodithioato	
morH	3,5-bis(N-morphotino)-l,2,4-trithioIane	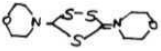
naphMeCp	1 -naphthylmethylcyclopentadiene	
β-Naphtham	β-naphthylammonium	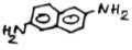
OETPP	2,3,7,8,12,13,17-octaethyl-5,10,15,20-tetraphenyporphyrine	
pc	phthalocyanine	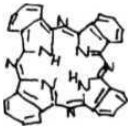 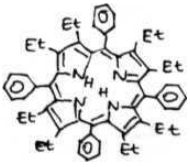
Ph	phenyl	

phen	1,10-phenanthroline
phena	phenacitin (N-(4-ethoxyphenyl)-acetamide) 
PPBQ	poly(cyclophosphazenebenzoquinone) 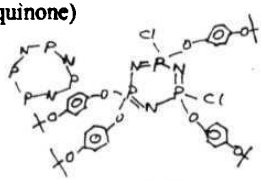
iPr	iso-propyl
nPr	N-propyl
PVA	poly(vinylalcohol) 
py	pyridine
TAAB	tetrabenzo[b,f,j,n][1,5,9,13]tetraazacyclohexadecine
tatbp	triazatetrabenzoporphyrine 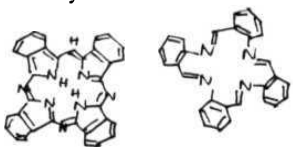
Taz	1,3,5-triazine 
tbp	5,10,15,20-tetrabenzoporphyrine 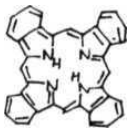
tetrazole	2,3-diphenyl-5-methyltetrazolium 
TMA	trimesic acid 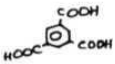
tmp	5,10,15,20-tetramethytporphynne 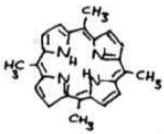
tphpn	N,N,N',N'-tetra(2-methyl pyridyl)-2-hydroxypropanediamine 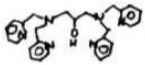
Ur	Urotropine 

PREFACE

The study on the role of the Mn complex involved in the water oxidation centre (WOC) of the photo system II has resulted in syntheses of a large number of higher valent Mn complexes. In our effort towards the same, several higher valent Mn complexes have been synthesised, earlier in our laboratory, by oxidising Mn(II) using Ce(IV) as oxidising agent or disproportionation of Mn(III). Besides the synthesis, the complexes were tested for their catalytic oxygen gas evolution in heterogeneous phase, using external oxidising medium.

The present thesis deals with the synthesis of higher valent Mn complexes, following a Ce(IV) oxidation of Mn(II) in non-aqueous media, which resulted in the formation of the $Ce(NO_3)_6^{3-}$ salt of $[Mn_2O_2(bpy)_2]^{3+}$. Water oxidation studies involving $[Mn_2O_2(bpy)_4]^{3+}$ systems in pure as well as dilute forms (as dopants in polymeric matrices) in heterogeneous phase, showed catalytic evolution of oxygen gas. Attempts towards synthesis of Mn complexes using Mn(III) in dilute nitric acid media, resulted in the isolation of some Mn cores, depending on the conditions.

The equivalent weight determination (by iodometry) of the above complexes (with bpy or phen as ligands), in water-acetonitrile medium, led to the accidental detection of the complexes, $[Mn(phen)_3](I_3)_2$ and $[Mn(bpy)_3](I_3)_{1.5}(I_8)_{0.25}$. Goodwin and Sylva, earlier in 1966, had noticed the formation of "highly insoluble $Mn(base)_3(I_3)_2$" when iodide was added to acidified $KMnO_4$ containing ligand base, but did not study it further. The structural studies of the above complexes revealed the presence of novel triiodide and polyiodide anions in the crystals. Subsequently, a new method was developed, using Mn(II) as starting material, in a two phase (water/dichloromethane) procedure for their synthesis.

Although a lot of polyiodides have been studied and structurally characterised in the past (especially tetraalkylammonium salts), most of them happen to involve an organic moiety as the cation. We, therefore, started preparing polyiodide salts of transition metal tris chelate complex cations, which have not been studied earlier. The polyiodides are prepared using simple bidentate neutral ligands such as 2,2'-bipyridine (bpy) and 1,10-phenanthroline (phen) with various transition metals in their 2+ oxidation states. It has been further extended later, by use of other similar substituted ligands like 4,5-diazafluoren-9-one (dafone), and various metals other than transition metals.

The studies on polyiodide anions include a literature survey on the work done in this field, in the past two decades. The complexes synthesised by us, have been classified into two categories: one with normal iodine content, where mainly triiodides are the anions and the other with higher iodine content, where higher polyiodide anions such as I_8^{2-}, I_{12}^{2-} are involved. The complexes characterised in the first category include $[Mn(phen)_3](I_3)_2$, $[Mn(bpy)_3](I_3)_{1.5}(I_8)_{0.25}$ and the solvent included $[Ni(phen)_3](I_3)_2 \cdot CH_3CN$. The higher iodine content complexes include $[Cu(bpy)_3]I_8 \cdot CH_2Cl_2$, where I_8^{2-} anion packs in layers to form channels along an axis direction that are filled with disordered solvent molecules. In $[Fe(bpy)_3]I_9$, 3-dimensional polyiodide networks are formed with the $[Fe(bpy)_3]^{2+}$ cations sitting inside the anionic channels. The structure of $[Zn(bpy)_3]I_{12}$ and $[Zn(phen)_3]I_{12}$ show two different types of I_{12}^{2-} units. Two $[Zn(phen)_3]^{2+}$ cations sit inside a dimeric 24-member, nearly planar ring, formed by a new unbranched I_{12}^{2-} anion. An attempted synthesis of polyiodide salts of $[Al(bpy)_3]^{3+}$ and $[Co(bpy)_3]^{2+}$ resulted in the formation of $[bpyH]I_5$ and $[bpyH]I_7$ respectively.

The spectroscopic studies of all the polyiodide salts reported in this thesis have been discussed. Most of them have been studied using Far-IR, Raman

techniques and electronic spectroscopy of solutions in CH_2Cl_2 and correlated with structural information.

Finally, a general comparison of all the structures of polyiodide salts of metal complex cations is done which includes a comparison of the structure of tris chelate cations, polyiodide anions and the crystal packing. Preliminary work on the anti-microbial properties of the polyiodide salts is presented in the Appendix N.

Part of the work has been published or communicated in a preliminary form: "1,10-phenanthroline and 2,2'-bipyridine tris-chelates of manganese(II) with polyiodides as anions", D. Ramalakshmi and M. V. Rajasekharan, *Proc. National Symposium on Current Trends in Coordination Chemistry, Cochin* (1995), p. 10; "Synthesis, Crystal Structure and EPR Simulation of a Water Stable Binuclear di-u-oxo Mn(III,IV) Complex", D. Ramalakshmi, G. Swarnabala and M. V. Rajasekharan, *Proc. Symposium on Modern Trends in Inorganic Chemistry, Hyderabad* (1995), P29; *Proc. Indian Acad. Sci. (Chem. Sci.),* 1996,*108,* 291; "EPR and Oxygen Evolution Studies of a Polymer Bound Mixed Valent Manganese Complex", D. Ramalakshmi and M. V. Rajasekharan, *Proc. First Asia-Pacific EPR/ESR Symposium, Hongkong* (1997), p. 108; "Synthesis and Structural Investigations of Polyiodides of Transition Metal Tris-Chelate Cations: Formation of a new polyiodide in $[Fe(bpy)_3]I_9$", D. Ramalakshmi and M. V. Rajasekharan, *Proc. Symposium on Modern Trends in Inorganic Chemistry, Kanpur* (1997), P12. "Polyiodides of Transition Metal Tris-Chelate Cations: Syntheses, Structures, Spectral and Electrical Conductivity Studies of $[Mn(phen)_3](I_3)_2$ and $[Mn(bpy)_3](I_3)_{1.5}(I_8)_{0.25}$", D. Ramalakshmi, K. Rajender Reddy, D. Padmavathy, M. V. Rajasekharan, N. Arulsamy and D. J. Hodgson *Inorg. Chim. Acta* 1999 *284,* 158-166; "Crystallographic Disorder in mixed valent Mn complex $[Mn_2O_2(bpy)_4][Ce(NO_3)_6]\cdot 5H_2O$ ", D. Ramalakshmi and M. V. Rajasekharan. *Acta Crystallographica Sec. B* 1999, *55, (in press).*

STUDIES ON HIGHER VALENT MANGANESE COMPLEXES

CHAPTER 1

Synthesis and Characterisation of High Valent Mn Complexes in Non-Aqueous and Low p// Media and Catalytic Water Oxidation Studies

Higher valent manganese chemistry has generated a lot of interest during the past two decades.' On the one hand, dinuclear, trinuclear and tetra nuclear complexes having Mn in oxidation states higher than 2+ are sought as models for the, not yet fully understood, water oxidation centre (WOC) of photosystem II (PS II) (Figure 1.1). On the other hand, compounds with even higher nuclearity often possess high spin ground states and are studied as models for molecular magnetism.

Previous studies in our lab have used aqueous $(NH_4)_2Ce(NO_3)_6$ to prepare high valent Mn complexes by oxidation of Mn^{2+} in presence of bpy and phen.[3] A non-aqueous modification of this procedure resulted in the formation of $[Mn_2O_2(bpy)_4][Ce(NO_3)_6]\cdot 5H_2O$, which is described in the first section of this chapter. Catalytic water oxidation studies involving $[Mn_2O_2(bpy)_4]^{3+}$ systems in pure as well as dilute forms (as dopants in polymeric matrices) in heterogeneous phase comprise the next section. Attempts towards the synthesis of Mn complexes using Mn(III) in dilute nitric acid media, resulted in the isolation of various Mn complexes, which have been studied in the last section.

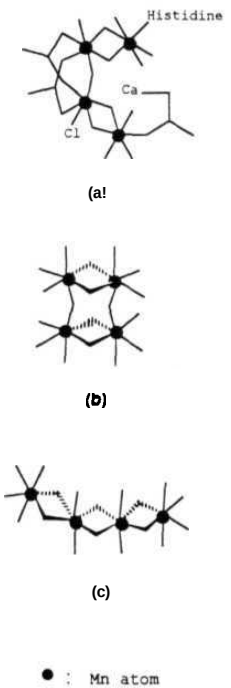

Figure 1.1 Tetranuclear Mn complexes proposed as PS II models (Ref. 2). (a) proposed $[Mn_4O_5]^{n+}$ model (3<n<5), (b) Dimer of dimers **and** (c) open chain **model.** [(b) and (c) **are** complexes synthesised and characterised as $[(Mn_2O_2)_2(tphpn)_2](ClO_4)_4$ (Ref. 2b) **and** $[Mn_4O_6(bpy)_6](ClO_4)_4 \cdot H_2O$ (Ref. 2c) respectively.]

1.1 Synthesis, Crystal Structure, EPR, and Solution Studies of $[Mn_2O_2(bpy)_4]Ce(NO_3)_6 \cdot 5H_2O$

A large number of higher valent Mn complexes synthesised have predominantly, the $Mn_2O_2^{3+/4+}$ core.[4-6] The synthesis generally involves oxidation of Mn(II) using O_2 (air), MnO_4^-, H_2O_2, Ce(IV), etc. or disproportionation of Mn(III) complexes. Diverse manganese complexes could be crystallised from aqueous solutions containing Mn(II), bpy, phen and Ce(IV) (bpy = 2,2'-bipyridine; phen = 1,10-phenanthroline) depending on the experimental conditions.[3] The synthesis and characterisation of $[Mn_2O_2(bpy)_4][Ce(NO_3)_6] \cdot 5H_2O$ (1), which is obtained by Ce(IV) oxidation in methanol are discussed. The cation $[Mn_2O_2(bpy)_4]^{3+}$, has been structurally characterised twice before.[4a,b] In both cases geometrically distinct Mn centres were observed. However, in this case, the Mn atoms are not crystallographically distinguishable. This is, in fact, the situation for 7 of the 23 dinuclear $Mn_2O_2^{3+}$ complexes reported to-date. An analysis of the thermal vibration ellipsoids obtained from the structure of the cation determined at 132 K is presented. An unusual feature of the $Ce(NO_3)_6^{3-}$ salt of the now well-known cation, $[Mn_2O_2(bpy)_4]^{3+}$ is its stability in water even in the absence of added buffer. This has enabled a study of the electronic spectra in water in the absence of excess ligand. The phen analogue of 1 was also prepared in a similar way, but it turned out to be the nitrate salt rather than the $Ce(NO_3)_6^{3-}$ salt.

1.1.1 Experimental

1.1.1(a) Synthesis. Preparation of $[Mn_2O_2(bpy)_4][Ce(NO_3)_6] \cdot 5H_2O$ (1). To a solution of $Mn(CH_3CO_2)_2 \cdot 4H_2O$ (0.508g, 2.07mmol) and 2,2'-bipyridine (0.648g,

4.2mmol) in methanol (5mL), a solution of $(NH_4)_2Ce(NO_3)_6$ (2.16g, 3.94mmol) in methanol (10mL) was added, drop-wise, with stirring. The solution turned yellow initially, and on further addition, a green coloured solution was obtained which was allowed to stand for 10 minutes. The green precipitate that formed was filtered and dried under vacuum and recrystallized from water to give dark rectangular rods; Yield : 0.770g (0.562mmol, 54%). Anal. Calcd. for $C_{40}CeH_{42}Mn_2N_{14}O_{25}$ (MW 1368.88) : C, 35.10 ; H, 3.09 ; N, 14.32 ; Mn, 8.03. Found : C, 33.84; H, 2.74; N, 14.16; Mn, 8.5. Equivalent weight : calcd, 456.3; determined by iodometry, 454. IR (KBr/cm^{-1}) : 3383(b), 3088(w), 1605(s), 1566(w), 1445(vs), 1314(vs), 1161(s), 1111(w), 1020(s), 820(s), 770(s), 731(s), 693(s), 656(s).

Preparation of $[Mn_2O_2(phen)_4](NO_3)_3{\cdot}8H_2O$ (2). To a solution of $Mn(CH_3CO_2)_2{\cdot}4H_2O$ (0.750g, 3.06mmol) and 1,10-phenanthroline (1.190g, 6.0mmol) in methanol (5mL), a solution of $(NH_4)_2Ce(NO_3)_6$ (3.39g, 6.18mmol) in methanol (10mL) was added, drop-wise, with stirring. The solution turned yellow initially, and on further addition, a green coloured solution was obtained which was allowed to stand for 10 minutes. The dark green sticky precipitate that formed was washed with methanol, filtered and dried under vacuum and recrystallized from water to give dark needles. The crystals obtained were of low quality and not suitable for collecting the X-ray diffraction data. Yield : 1.088g (0.912mmol, 60%). Anal. Calcd. for $C_{48}H_{42}Mn_2N_{11}O_{19}$ (MW 1192.84) : C, 48.33 ; H, 4.06 ; N, 12.92 ; Found : C, 48.34; H, 2.79; N, 13.24. Equivalent weight : calcd, 397.6; determined by iodometry, 400. IR (KBr/cm^{-1}) : 3426(b), 3056(s), 1628(w), 1605(w), 1582(w), 1518(s), 1428(s), 1352(vs), 1225(w), 1146(w), 1105(w), 851(s), 777(w), 720(s), 691(s), 640(w), 588(w), 422(w).

1.1.1(b) Physical Measurements. I.R. spectra were obtained using KBr pellets on a Perkin-Elmer 297 infrared spectrophotometer. C, H, N elemental analysis were performed on a Perkin-Elmer 240C elemental analyser. Electronic spectra were recorded in water as solvent, in the range of 300-1100 nm on a JASCO 7800 spectrophotometer using quartz cells of 1cm length. Room temperature magnetic data were obtained on a Cahn-3000 microbalance using Faraday's method. $Hg[Co(CNS)_4]$ was used as a primary standard. Diamagnetic corrections were done using Pascal's constants.[7] EPR spectra were recorded for frozen solutions (in acetonitrile or dimethylformamide or water), powder and aqueous solution samples on a JEOL FE-3X spectrophotometer using DPPH as the internal standard. JEOL NM-7700 temperature controller was used for low temperature measurements in the 123 to 300 K range.

1.1.1(c) X-ray Crystallography. (1) Data for a dark rectangular rod type crystal were collected at 132 K on a Siemens P4 diffractometer (at University of Canterbury, New Zealand) using MoKa radiation with graphite monochromator. The data were corrected for absorption.[8] The structure was solved by patterson followed by direct methods (SHELXS 86)[9] and refined (over F^2) by least squares techniques (SHELXL 93).[10]

The complex crystallises in the monoclinic system, space group C2/c, with 4 molecules in the unit cell. A total of 6034 reflections (6021 unique, 5645 with $F > 4\sigma F$) were collected in the 2θ range 4 to 55°, with indices $-16 < h < 0$, $0 < k < 23$, $-28 < 1 < 29$. Non-hydrogen atoms were refined anisotropically and all ring hydrogen atoms were included in calculated positions using a riding model. The hydrogen atoms on water molecules were located from the fourier map and refined. The final cycle of full matrix least squares refinement on F^2 converged with unweighted and weighted agreement factors of R1 = 0.0357 and wR2 =

0.0819. The goodness of fit was S = 1.105 with 5645 observations and 409 parameters. The maximum and minimum peaks on the final fourier map corresponded to 0.925 and -0.589 e/A^3 respectively. Crystallographic data and selected bond angles and bond distances are in Table 1.1 and Table 1.2 respectively. Full crystallographic data and other positional parameters are listed in Appendix A. There are four different types of water molecules in the lattice; One of them, OW1, is at a distance of 2.724 A from the bridging oxygen (O1) lying on the 2-fold axis of cation. The hydrogens for this water molecule were located from the fourier map at ~ 1 A distance from OW1, but were fixed at 0.97 A (O-H distance) due to extreme shortening of the bonds on free refinement. One of the hydrogens HW1A, lies on the same 2-fold axis, while the other (HW1B) has a site occupancy of 0.5 (implying disorder about the 2-fold axis).

Table 1.1 Crystallographic Data for $[Mn_2O_2(bpy)_4][Ce(NO_3)_6]\cdot 5H_2O$ (1)

formula	$C_{40}H_{42}CeMn_2N_{14}O_{25}$	Z	4
formula weight	1368.88	space group	C2/c (No. 15)
a	12.940(3)	T	132(2) K
b	18.060(2)	*X*	0.71073 A
c	22.54(1)	ρ(obsd)	1.74 Mg/m^3
a	90°	p(calcd)	1.736 Mg/m^3
β	96.29(2)0	u	1.429 mm-^{1}
γ	90°	R1	0.0358
V	5237(3) A^3	wR2	0.0783

$R1 = \Sigma||F_o| - |F_c||/\Sigma|F_o|$

$wR2 = [\Sigma\{w(F_o^2 - F_c^2)^2\}/\Sigma(wF_o^4)]^{1/2}$

$w^{-1} = [\sigma^2(F_o^2) + (0.0342\ P)^2 + 13.2986P]$, $P = (F_o^2 + 2F_c^2)/3$

Table 1.2 Selected bond lengths [A] and angles [deg] for 1.

Bond distances :

Mn-0(2)	1.811(2)	Mn-O(l)	1.817(2)	Mn-N(2)	2.089(2)
Mn-N(3)	2.091(2)	Mn-N(l)	2.121(2)	Mn-N(4)	2.133(3)
Mn-Mn#1	2.7188(9)	Ce-O(3)	2.601(2)	Ce-O(5)	2.602(2)
Ce-O(8)	2.636(2)	Ce-O(9)	2.637(2)	Ce-O(ll)	2.648(2)
Ce-O(6)	2.720(2)				

Bond angles :

O(2)-Mn-O(1)	82.92(8)	O(1)-Mn-N(2)	90.97(8)
O(2)-Mn-N(3)	94.53(8)	N(2)-Mn-N(3)	94.46(8)
O(2)-Mn-N(1)	90.36(6)	O(1)-Mn-N(1)	100.59(6)
N(2)-Mn-N(l)	77.34(8)	N(3)-Mn-N(l)	92.66(9)
O(2)-Mn-N(4)	100.41(6)	O(1)-Mn-N(4)	90.59(6)
N(2)-Mn-N(4)	93.23(8)	N(3)-Mn-N(4)	76.80(9)
Mn-O(1)-Mn#1	96.87(11)	Mn#1-O(2)-Mn	97.29(11)
O(3)-Ce-O(5)	49.15(6)	O(9)-Ce-O(1 1)	48.10(6)
O(8)-Ce-O(6)	47.58(6)		

Intermolecular contacts :

(a) Hydrogen bonds :

O(1)--HW1A	1.754(3)	O(7)--HW4B	2.257(6)	O(10)--HW2B	2.071(7)
OW1#3--HW3B	2.136(7)	OW2--HW2A#1	1.933(4)	OW2#5-HW4A	1.872(6)
OW3#4--HW1B	1.813(4)	OW4#4--HW1B	1.947(5)		

O(1)-HW1A-OW2	180.0	O(10)-HW2B-OW2	160(1)
OW1-HW1B-OW3#4	164(1)	OW1-HW1B-OW4#4	153.5(6)

OW3#4-HW1B-OW4#4	23.98(8)	OW4-HW4A-OW2#5	120.1(4)
OW3-HW3B-OW1#3	120.6(4)	OW4-HW4B-O(7)	162(1)
OW2-HW2A-OW2#1	146.7(5)		

Symmetry transformations used to generate equivalent atoms:

1 -x, y, -z+1 /2 #2 -x, -y, -z #3 -x-1/2, -y-1/2, -z #4 x+1/2, -y-1/2, z+1/2

#5-x-l/2, -y+1/2, -z

1.1.2 Results and Discussion

1.1.2(a) Synthesis. Oxidation by Ce(IV) in aqueous medium has been previously used in the preparation of $[Mn(phen)_2Cl_2]^+$, $[Mn_2O_2(OAc)(bpy)_2(H_2O)_2]^{3+}$, $[Mn_2O(OAc)_2(H_2O)(NO_3)(bpy)_2]^{3+}$, and $[Mn_3O_4(phen)_4(H_2O)_2]^{4+}$ as their chloride or perchlorate salts.[3] These preparations involve the initial one electron oxidation of Mn(II) to Mn(III) followed by disproportionation and aggregation via the formation of $[Mn_2O_2]^{3+/4+}$ or $[Mn_2O(OAc)_2]^{2+}$ core. The precipitation is governed by the solubility of the salts of different complex cations present in equilibrium in the solution.[3d] The Mn(HI,IV) cation of 1 was not precipitated from the aqueous solution even by ClO_4^- or PF_6^- . The use of methanol as solvent readily leads to the precipitation of $[Mn_2O_2(bpy)_4][Ce(NO_3)_6]$. The incorporation of $Ce(NO_3)_6^{3-}$ (formed by reduction of $Ce(NO_3)_6^{2-}$) in the crystal lattice is probably due to its low solvation energy in methanol compared to water.

All the other salts ($S_2O_8^{2-}$, PF_6^-, ClO_4^-) of $[Mn_2O_2(bpy)_4]^{3+}$ are stable in water only when the *pH* is maintained at 4.5 by addition of bpy/bpyH$^+$ or CH_3COO^-/CH_3COOH buffers. However, $[Mn_2O_2(bpy)_4][Ce(NO_3)_6]$ is stable in water and can be crystallised as its pentahydrate. The buffering action is provided by the hydrolysis of the anion which maintains the *pH* at 4.5.

$$[Ce(NO_3)_6]^{3-} + H_2O \rightleftarrows [Ce(NO_3)_5(OH)]^{3-} + H^+ + NO_3^-$$

The phen analogue of 1, $[Mn_2O_2(phen)_4](NO_3)_3$, however, prefers NO_3^- as the counter-anion instead of $Ce(NO_3)_6^{3-}$. This complex is also stable in water (with a *pH* of 5.0), and can be recrystallised from it, accomodating as many as eight water molecules in the lattice.

1.1.2(b) Structure. (1) Cation: The $[Mn_2O_2(bpy)_4]^{3+}$ cation is shown in Figure 1.2 along with a water molecule H-bonded to one of the bridging O atoms. Unlike in the previously reported ClO_4^- or BF_4^- salts, in the present compound, the two Mn atoms are not distinguishable due to the presence of crystallographic 2-fold axis passing through the two O atoms.

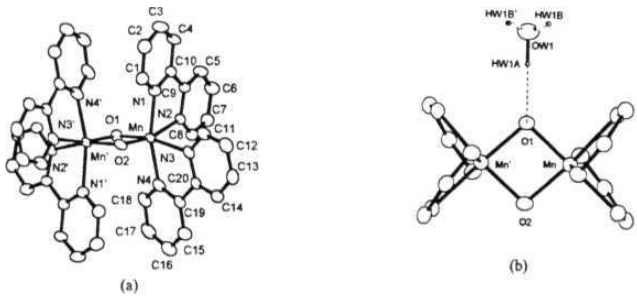

Figure 1.2 (a) $[Mn_2O_2(bpy)_4]^{3+}$ (cation of 1); (b) Cation of 1 showing the H-bonded water molecule.

Keeping this in view, it is possible to compare the parameters with those of the previous reports on this ion as well as its phen analog. There are two main

factors that influence the geometry of a dioxo bridged $Mn_2(III,IV)$ complex : (i) the Mn(III) centre is susceptible to the Jahn-Teller effect which usually manifests as a tetragonal elongation;[3d,e] (ii) the bonds opposite the oxo ligand for both Mn centres experience a strong *trans* influence leading to their elongation (this effect is more for Mn(IV) which has the shorter Mn-0 distance). The net result is that N^{III}_{ax} bonds are longer than N^{III}_{eq} bonds, while N^{IV}_{ax} bonds are shorter than N^{IV}_{eq} bonds. This is borne out by the average bond distances shown in Table 1.3.

As expected, for the crystallographically averaged structures, the axial - equatorial difference is less, but still significant. By a detailed analysis of the thermal motion parameters for $[Mn_2O_2(phen)_4](PF_6)_3 \cdot CH_3CN$, it has been shown that the averaged structure results from a dynamic or static disorder about a crystallographic symmetry element, and not from any electronic delocalisation.[5a] A similar analysis leads to the same conclusion for the present structure. The $\Delta U^{1/2}(z)$ values are included in Table 1.3. It is worth emphasising that the greater trans influence of the oxo ligands attached to Mn(IV) smears out, to a great extent, the expected differences for N_{eq} bond distances for the 3+ and 4+ oxidation states. On the other hand, the Jahn-Teller effect magnifies this difference for the N_{ax} bonds. Thus, N^{III}_{ax} - N^{IV}_{ax} are in the range 0.19 - 0.21 A for the three complexes with distinguishable sites, while N^{III}_{eq} - N^{IV}_{eq} is only 0.03-0.06 A.

The same trend is observed when the $\Delta U^{1/2}(z)$ values are compared for the disordered structure. The values along the axial bonds are in the range of 0.09-0.14 A, while along the equatorial bonds they are only 0.05-0.06 A which is in the range normally seen in the absence of any disorder. Therefore, to build a simplified picture of disorder in these type of complexes, one need consider only the axial bonds.

Table 1.3 Distortion Parameters[a] (A) and Difference Displacement Parameters[b] (A) for Dioxo Bridged $[Mn_2O_2L_4]^{3+}$ Systems.[c]

Compounds with distinct Mn sites:

	N_{ax}(III)-N_{eq}(III)	N_{ax}(IV)-N_{eq}(IV)	N_{ax}(III)-N_{ax}(IV)	N_{eq}(III)-N_{eq}(IV)
$[Mn_2O_2(bpy)_4](ClO_4)_3 \cdot 3H_2O$[d]	0.085(7,14)	-0.053(7,9)	0.195(7,16)	0.057(7,4)
$[Mn_2O_2(bpy)_4](BF_4)_3 \cdot 2.8H_2O$[e]	0.089(4,6)	-0.070(4,20)	0.207(4,11)	0.048(4,18)
$[Mn_2O_2(phen)_4](ClO_4)_3 \cdot 2CH_3COOH \cdot 2H_2O$[f]	0.107(6,14)	-0.061(6,12)	0.195(6,14)	0.028(6,12)

Compounds with equivalent Mn sites:

	N_{ax}-N_{eq}	$\Delta U^{1/2}(z)N_{ax}$	$\Delta U^{1/2}(z)N_{eq}$
$[Mn_2O_2(bpy)_4]Ce(NO_3)_6 \cdot 5H_2O$	0.037(2,9)	0.093(5);0.136(5)	0.050(5);0.060(5)
$[Mn_2O_2(phen)_4](PF_6)_3 \cdot CH_3CN$[g]	0.023(2,21)	0.116(10)	0.037(33)

[a] Bond length differences for Mn-N bonds. N_{ax}(III) stands for Mn^{III}-N_{axial} bond distance. [b] along Mn-N bonds for averaged structures calculated as given in Ref. 5a. [c] The values are averages for chemically equivalent bonds in a structure. The two standard deviations in paranthesis are calculated as: $\sigma^2[f(p_1..)] = *L(dfldp\backslash y\text{-}s\$$- and σ_{mean}= £ $(x_i-\bar{x})^2/(n-1)$, respectively. [d] Ref. 4a. [e] Ref. 4b./Ref. 4c. [f] Ref. 5a.

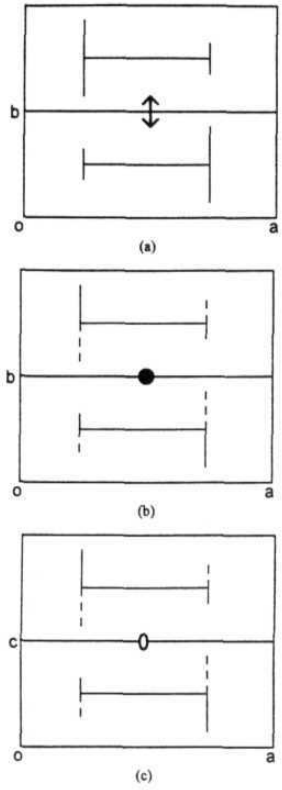

Figure 1.3 Simplified model of disorder of $[Mn_2O_2L_4]^{3+}$ ion in monoclinic crystals. The horizontal line represents the Mn_2O_2 core, while the vertical lines denote the axial direction of the coordination 'octahedra'.

The three resulting possibilities for a monoclinic crystal are shown schematically in Figure 1.3. In (a) the symmetry element involved is the monoclinic symmetry axis, normal to the Mn_2O_2 mean plane, while in (b) it is the inversion centre, and in (c) the b axis is passing through the two O atoms. Of the 7 previously reported disordered structures two belong to (a) and five to (b). In (c)

the symmetry axis is perpendicular to the axial (disorder) direction of the molecule. The present structure belongs to this category. This mode is obtained here due to the presence of a water molecule H-bonded to only one of the O-atoms. The other modes (a or b) in this situation would have meant a 2-dimensional disorder in the lattice which is probably energetically costlier. The Mn_2O_2 plane is strictly planar while in the undistorted structures small deviations (~ 0.03 A) from planarity are seen. The equatorial N atoms show large deviation (±0.48, ±0.49 A) from this plane, which has also been observed for the undistorted structures.

Anion: $Ce(NO_3)_6^{3-}$ has a distorted icosahedral structure with Ce located on a crystallographic inversion centre (Figure 1.4). Two of the three independent NO3" ions conform closely to the symmetric chelating mode (average Ce-O, 2.622(2) A) while the third NO_3^- shows considerable asymmetry in the chelation (Ce-O, 2.720(2), 2.636(2) A). This ion has been previously characterised in $Ce_2Mg_3(NO_3)_{12}\cdot 24H_2O$[11] and more recently in $K_3Ce_2(NO_3)_9$.[12] The later compound has a three-dimensional network of irregular icosahedra linked by NO_3^- ions.

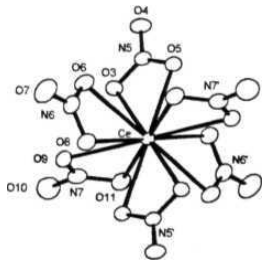

Figure 1.4 Anion of 1, $Ce(NO_3)_6^{3-}$

The $Ce(NO_3)_6^{3-}$ ion in all these compounds is more distorted than the $Ce(NO_3)_6^{2-}$ ion in $(NH_4)_2Ce(NO_3)_6$[13] and $K_2Ce(NO_3)_6$.[14] It is tempting to ascribe this difference to the Jahn-Teller effect in the Ce(III) complex ion. However the weak distortions expected for the f^1 configuration might be comparable in magnitude to distortions arising from H-bonding and other lattice perturbation.

One lattice water forms a strong H-bond with an O-atom of the dioxo bridge (O(1)---HW1A = 1.754(3) A, O(1)---OW1 = 2.724(3) A), while another water molecule forms a H-bonded network (OW2---HW2A' = 1.933(4) A, 0W2—0W2' = 2.795(3) A, ' = -x, y, 0.5-z) and also interacts with the anion (0(10)—HW2B = 2.071(7) A, O(10)---OW2 = 3.002(3) A). The third water molecule is disordered and interacts with OW1 as well as the 0(7) atom of the anion.

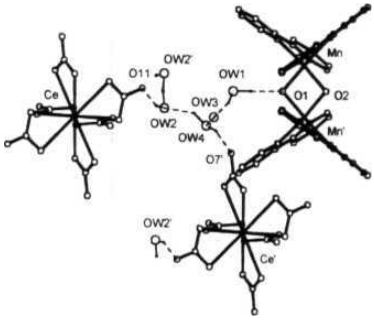

Figure 1.5 H-bonding network between cation and anion in 1, *via* water molecules.

There appear to be no significant contacts between the anion and the Mn_2(III,IV) complex ion except via the H-bond network involving two interacting water molecules (OW1, OW4), as seen in Figure 1.5.

1.1.2(c) EPR and Magnetic Moment. The room temperature magnetic moment of 1 was found to be 3.60 μ_B based on the paramagnetic susceptibility of a powdered sample. The corresponding perchlorate salt has a room temperature moment of 2.53 μ_B, arising from strong anti-ferromagnetic coupling in the $[Mn_2O_2(bpy)_4]^{3+}$ ion (J = -150 (7) cm^{-1}, $H_{ij} = -2J_{ij}S_i.S_j$)[15]. If the susceptibility of the $Ce(NO_3)_6^{3-}$ ion (μ = 2.40 μ_B)[16] is subtracted, a value of 2.68 μ_B is obtained for $[Mn_2O_2(bpy)_4]^{3+}$ ion in the present compound. The room temperature magnetic moment of the powdered sample of 2 was found, to be 2.66 μ_B, as expected. The $Ce(NO_3)_6^{3-}$ ion is not expected to give an EPR signal above ~ 10 K due to fast spin lattice relaxation time.[17] Accordingly, a well resolved '16-line spectrum' is obtained for a frozen aqueous solution of 1 at 123 K (Figure 1.6). Frozen aqueous solution of complex 2 also gave a 16-line spectrum with a base-line shift. The frozen dmf solution of 1 shows a slow decomposition to Mn(II), while a stable 16-line pattern with hyperfine features are obtained for frozen dmf solution samples of 2. The polycrystalline samples for both complexes give only a dipolar broadened signal at g ~ 2.

1.1.2(d) Electronic Spectra. The complexes 1 and 2 are highly soluble in water and DMF and insoluble in CH_3CN. As discussed before aqueous solutions have a p*H* in the range 4.5 - 5.0. The electronic spectra (Figure 1.7) of a 2 x 10^{-3} M aqueous solution of 1, shows only one band at 679 nm.

Only at higher concentration (6 x 10^{-3} M), does one observe the 557 nm shoulder and the broad 830 nm band arising mainly due to charge transfer (CT) transitions of oxo to Mn(IV),[18] which was earlier referred to as the inter valence transfer band between the Mn(III) and Mn(IV).[15b] The spectrum in ligand buffer (bpy/bpyHNO_3, p*H* - 4.5) is similar to that reported for the perchlorate salt.

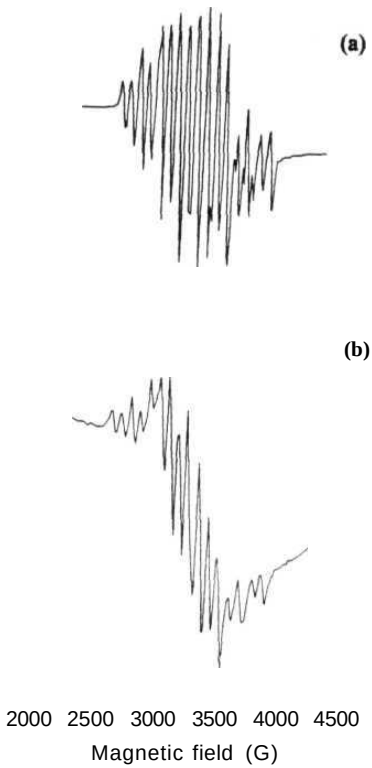

Figure 1.6 X-band EPR spectra of frozen solution of (a) 1 in water at 123 K (v = 9.217 GHz), (b) 2 in water at 123 K (v = 9.215 GHz).

However, the molar extinction coefficients (E) for all the peaks of this $Ce(NO_3)_6^{3-}$ salt are 80% that of the perchlorate salt. Similar spectra with nearly same ε values could be obtained when pure bpy was added to 2 x 10^{-3} M aqueous solution. The *pH,* in this case, went up slightly (to 5.0) and the ε value of 557 nm and 525 nm were about 20% higher. In the case of the perchlorate salt, it was observed that an increase in *pH* from 4.5 to 4.7 of the ligand buffered solutions resulted in a decrease in intensity of about 20% for all the peaks.

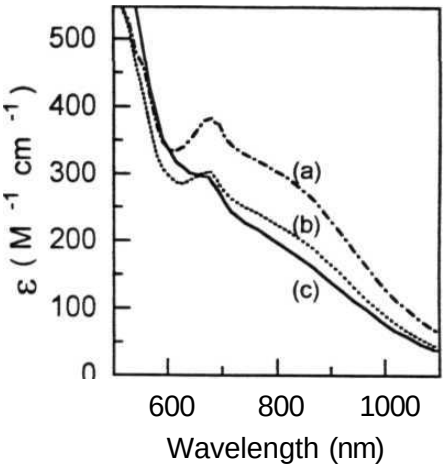

Figure 1.7 Electronic spectra of 1 in water at different concentrations, (a) 6 x 10^{-3} M, (b) 4 x 10^{-3} M and (c) 2 x 10^{-3} M

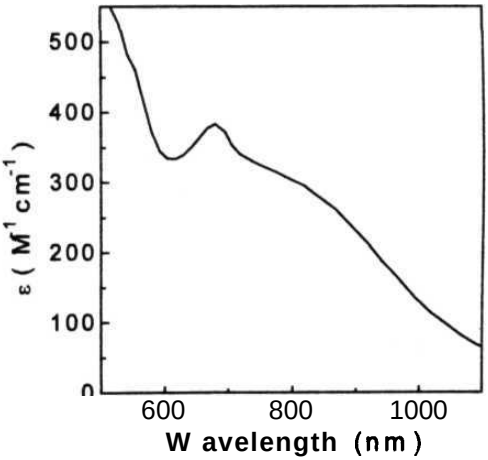

Figure 1.8 Electronic spectrum of 2 in water at 2 x 10^{-3} M concentration.

The presence of excess ligand is essential for the proper development of the band centred around 830 nm. Similar observations have been made before.[15b] It has been observed that solvent substitution on the labile Mn(III) centre drastically reduces the above band intensity.[19] Presence of excess ligand is therefore necessary to maintain equilibrium concentration of the unsubstituted, symmetrical mixed valence complex. It has been previously reported that solvent substituted complexes are precipitated from solutions of $[Mn_2O_2(phen)_4](PF_6)_3$ in DMF, However, they were not structurally characterised.[19]

In contrast the EPR spectra are totally insensitive to solvent substitution, identical spectra being obtained in various solvents. The electronic spectra of 2 at 2 x 10^{-3} M showed peaks at 680nm with strong overlapping band at around 830 nm, and clear overlapping shoulders at 552 nm and 526 nm (Figure 1.8). The spectrum is similar to the earlier reported spectrum for the cation in ligand buffer.

1.1.3 Conclusions

The preparation of 1 and 2 in methanol medium illustrates the role of solvation energies in the precipitation of oxo-manganese cluster compounds. Similar reactions in water do not lead to precipitation in the absence of added anions (like ClO_4^-, PF_6^-), in which case, Mn_2(III,III) complexes having the $Mn_2O(OAc)_2$ core were obtained.[3d]

The widespread occurence of the dioxo-bridged Mn_2(III,IV) complexes with averaged geometries is a consequence of crystallographic disorder jointly influenced by Jahn-Teller elongation (at Mn^{III}) and *trans* effect of the oxo-ligands. The H-bonding with a lattice water leads to a novel type of disorder in 1, wherin the crystallographic 2-fold axis passes through the dioxo O atoms.

The complexes 1 and 2 are stable in aqueous solution even in the absence of added buffer. The electronic spectral intensities are sensitive to *pH* as well as the presence of excess ligand. The EPR spectra are insensitive to solvent substitution.

1.2 Catalytic Water Oxidation Studies involving $[Mn_2O_2(bpy)_4]^{3+}$ Systems Doped in Polymeric Matrices

Various salts of this Mn_2(III,IV) cation and its phen analog were previously reported to evolve O_2 when in contact with a concentrated aqueous solution of $(NH_4)_2Ce(NO_3)_6$.[20] A monomeric Schiff base complex of Mn(III) was found to evolve a mixture of O_2 and N_2 under similar conditions.[21] O_2 evolution was also reported under electrochemical conditions when Schiff base complex was contained in a polymer membrane.[22] In this section it is shown that the $[Mn_2O_2(bpy)_4]^{3+}$ complex incorporated in polymer and silica gel matrices have been found to have higher turnover numbers for O_2 evolution from $(NH_4)_2Ce(NO_3)_6$ solutions.

1.2.1 Experimental

1.2.1(a) Preparation of Silica Gel Doped with 1. The acid catalysed hydrolysis of tetraethyl orthosilcate (TEOS) in 2 : 5 alcohol - water mixture produces a silica gel.[23] In a typical experiment 1mL of TEOS was stirred into a mixture of 2mL ethanol and 5mL water. 1mL of dil. sulphuric acid was added and the beaker containing the solution was kept undisturbed for a week. The transparent dry gel which formed could be cut into pieces with a knife. The doped gel was prepared by using an aqueous solution (0.004M) of 1, in place of water. No acid was required in this case since the solution itself was acidic (see later). The doping

level was 10% by weight. A more dilute gel (5% doping) was found suitable for electronic spectra. The dark coloured gel was found to be stable in water and in $(NH_4)_2Ce(NO_3)_6$ solution. Both EPR and electronic spectra confirmed the presence of Mn_2(III,IV) in the gel.

1.2.1(b) Preparation of Polymer Film Doped with [M

Polymethylmethacrylate (PMMA) films could be made by slow evaporation of an acetonitrile solution of the polymer. Both commercial grade PERSPEX and Aldrich (low molecular weight grade) polymer were found to give clear transparent films. In a typical experiment to make doped films, 15 mg of the powdered perchlorate salt, prepared by a reported procedure,[15a] complex was added to 25 ml of acetonitrile solution containing 0.70 g of the dissolved polymer. The solution was poured into a petri dish and kept undisturbed for a week. The resulting olive green transparent film (doping level 2% by weight) was examined by electronic spectral and EPR measurements to confirm the presence of the Mn_2(III,IV) complex. The film was found to be stable in water and 50% $(NH_4)_2Ce(NO_3)_6$ solution.

1.2.1(c) Physical Measurements. Electronic spectra were recorded in the range of 300-1100 nm on a JASCO 7800 spectrophotometer for polymer films and gel doped with the complexes. Low temperature spectra were measured by mounting the gel or film sample on the cold finger of a liquid nitrogen cryostat equipped with quartz windows. EPR spectra were recorded for polymer films and gel doped with the complexes on a JEOL FE-3X spectrophotometer using DPPH as the internal standard. JEOL NM-7700 temperature controller was used for low temperature measurements (130 to 300 K).

1.2.1(d) Oxygen Evolution Studies. The Mn_2(III,IV) complex in different forms, viz., gel doped ($Ce(NO_3)_6^{3-}$ salt) or film doped (ClO_4^- salt) produced gas bubbles when dropped into a 50% $(NH_4)_2Ce(NO_3)_6$ solution. The gas evolved was measured using a gas burette and confirmed to be O_2 by its quantitative absorption in alkaline pyrogallol. In a typical experiment 0.40g of the pure complex or 0.1 Og of the 2% doped film or 0.1 Og of the 10% doped gel was added **to** 50% aqueous solution of $(NH_4)_2Ce(NO_3)_6$ solution in a round bottom flask and it was connected to the gas burette (pressure equalising manometer type). Two controls were also set up, one containing pure water or blank film or gel as appropriate and another containing the same amount of the active substance taken in a flask with a side arm which was connected to a flask containing alkaline pyrogallol (The flasks were initially purged with nitrogen). The blank film or gel did not evolve any gas in most experiments or showed an insignificant amount of bubbles during the first few hours. The oxygen evolution was followed for several days.

1.2.2 Results and Discussion

1.2.2(a) EPR. The PMMA film and silca gel doped with $[Mn_2O_2(bpy)_4]^{3+}$ gave well resolved '16-line spectrum' (Figure 1.9 (a), (b)). Additional broad low field and high field signals arising from population of excited quartet state are seen at room temperature (Figure 1.9 (c)). However hyperfine splitting could not be resolved in the quartet state signals.

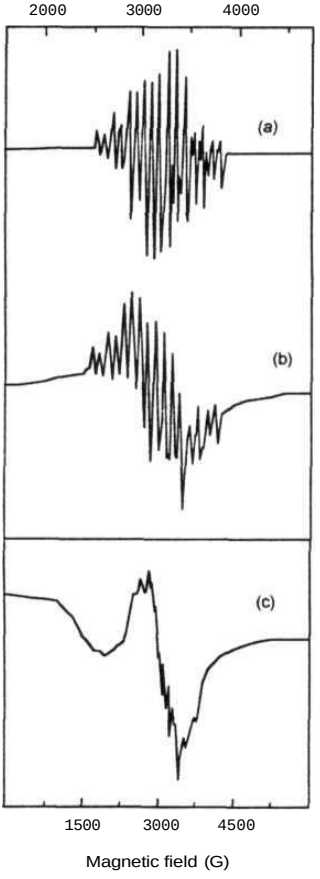

Figure 1.9 X-band EPR spectra (v = 9.165 GHz) of (a) PMMA film doped with $[Mn_2O_2(bpy)_4](ClO_4)_3$ at 133 K, (b) silica gel doped with 1 at 153 K and (c) sample as in (a) at 300 K. [The upper scale refers to (a) and (b) while the lower refers to (c)].

1.2.2(b) Electronic Spectra. The low temperature (77 K) electronic spectra in PMMA film and silica gel are shown in Figure 1.10 (a), (b). There is no significant improvement in resolution compared to the room temperature spectra. However, there is a 10 to 25 % reduction in intensity at 77 K indicating appreciable vibrionic contribution to the intensities. The film spectrum which is more similar to solution spectra in CH_3CN[19] rather than water, has much less intensity in 800 - 1000 ran region. The gel spectrum, on the other hand, is different from both aqueous solution and film spectra. The 680 run maximum is absent and a new broad maximum is seen at 1000 nm. The 680 nm maximum is generally assumed to arise from the overlap of single ion (Mn^{3+}) transition with other bands centred around 830 nm.[15a,25] Therefore, in the gel the 830 nm band experiences a remarkable red shift of about 2000 cnr[1].

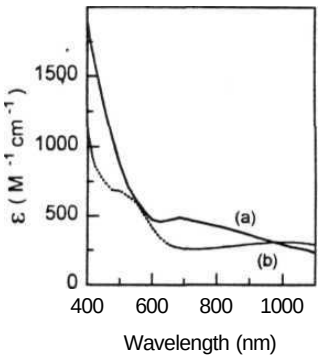

Figure 1.10 Electronic spectra (at 77 K) of (a) PMMA film doped with $[Mn_2O_2(bpy)_4](ClO_4)_3$ and (b) silica gel doped with 1

1.2.2(c) Oxygen Evolution Studies. It has been previously reported that the perchlorate and the PF_6^- salts of $[Mn_2O_2(bpy)_4]^{3+}$ and its phen analog as well as solvent substituted products crystallised from DMF, evolve O_2 when suspended in

a concentrated solution of $(NH_4)_2Ce(NO_3)_6$.[19] In the present study we find that the $Ce(NO_3)_6^{3-}$ salt, behaves similar to the perchlorate salt, giving a turnover number of 7 over a period of one week (turnover number, here, is defined as the number of moles of O_2 evolved per mole of the complex). The solution after O_2 evolution contains MnO_4^-, as observed before,[19] but significantly the solid residue from both ClO_4^- and $Ce(NO_3)_6^{3-}$ salts had very similar IR spectra. The absence of ClO_4^- band in the former case and the presence of NO_3^- band in both cases implies that the solid goes into solution during O_2 evolution and crystallises back as the $Ce(NO_3)_6^{3-}$ salt. EPR of the solid residue gives evidence for the presence of Mn(II). Upon slow evaporation of the solution of the residue in water, dark rod shaped crystals were obtained. These appear to be the crystals of the nitrate salt of the previously characterised Mn_3(IV,IV,IV) complex, $[Mn_3O_4(bpy)_4(H_2O)_2]^{4+}$,[26a] based on the IR spectrum (600-800 cm^{-1}) of the perchlorate salt of this ion. Since this complex does not oxidise water, it must be one of the side products formed during oxygen evolution and responsible for the degeneration of O_2 evolution activity of Mn_2(III, IV) complex.

The above experiments were repeated for the gel and films doped with the cation of complex 1. Both the gel and the film contained $[Mn_2O_2(bpy)_4]^{3+}$ ion and very little, if any, Mn(II) impurity as can be seen from their EPR (Figure 1.9) and electronic spectra (Figure 1.10). In both cases the suspensions in $(NH_4)_2Ce(NO_3)_6$ solution evolved O_2 for several days with turnover numbers of 30-40 for the gel samples and 5-10 for the films. In both cases the initial rates were nearly equal and they were much greater than the rates observed for the pure crystalline compounds. The oxygen evolution reached a plateau after 20-30 days (Figure 1.11). The film and gel could be reactivated by washing with water. The reactivated samples continued to evolve O_2 with somewhat less efficiency. Reduced efficiency is correlated with the gradual increase in the Mn(II) content in

the samples as seen by EPR. In the residual solution from experiments involving polymer films, Mn(III) bands could be seen at 568 and 544 run.

O_2 evolution from doped films and gels which contain well separated Mn_2(III,IV) complex ions rules out the possibility of a cluster of four Mn_2(III,IV) centres being responsible for the oxidation of water in these systems. Absence of O_2 evolution from homogeneous solutions and the enhanced efficiency of the gel and film compared to the bulk sample indicates that the reaction is a surface phenomenon.

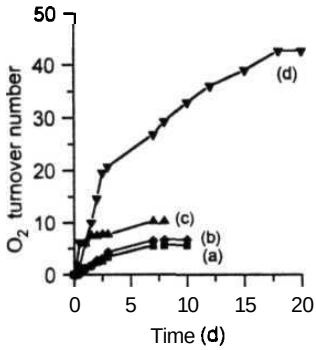

Figure 1.11 Oxygen evolution from 50% $(NH_4)_2Ce(NO_3)_6$ solution: (a) $[Mn_2O_2(bpy)_4](ClO_4)_3$, (b) 1, (c) PMMA film doped with $[Mn_2O_2(bpy)_4](ClO_4)_3$ and (d) silica gel doped with 1.

The species involved cannot be definitely known from these experiments. One possibility is a Mn_2(IV,IV) centre which gets reduced to Mn_2(II,II) or two Mn(II) upon O_2 evolution. The role of Ce(IV) will be to maintain sufficient concentration of Mn_2(IV,IV) centres by one electron oxidation: Mn_2(III,IV) $\rightarrow$ Mn_2(IV,IV); Mn_2(II,II) $\rightarrow$ $\rightarrow$ Mn_2(IV,IV). The accumulation of isolated Mn(II) during this process might be ultimately leading to the loss of activity of the samples. The

lower valent dinuclear ions in this chain may be based on $Mn(\mu\text{-}OH)(\mu\text{-}O)Mn$ or $Mn(\mu\text{-}OH)_2Mn$ core. No solid complexes of this type have been isolated so far, even though protonation of $Mn_2O_2^{3+/4+}$ core may be a definite possibility in redox reactions in solution.[26] The main drawback of the above model is that the $Mn_2(IV,IV)$ complex, $[Mn_2O_2(phen)_2](ClO_4)_4$ does not oxidise water at any significant rate. An alternate possibility is the formation of a reactive form of "MnO_2" on the surface which in turn oxidises water. This could explain the heterogenous nature of reaction in bulk as well as in dilute composites (polymer or gel). Most high valent manganese complexes decompose in water giving insoluble brown precipitates whose nature is not known with any certainty. The active species in O_2 evolution could be an intermediate in the normal decomposition reaction which is not allowed to go to completion due to the highely oxidising medium provided by the Ce(IV) ions.

1.2.3 Conclusions

The electronic spectrum of the PMMA film is similar to the spectrum observed in acetonitrile solution. There is a 10 to 25 % reduction in intensity at 77 K for the PMMA film and gel, indicating appreciable vibronic contribution to the intensities. The 830 nm band observed in the solution and film spectra, experiences a remarkable red shift of about 2000 cm"' in the gel. The EPR spectra are however, insensitive to matrix effects. MCD studies[18] in solution have been interpreted based on a band system consisting of 13 different electronic transitions in $[Mn_2O_2(bpy)_4]^{3+}$. In view of this, it is not possible to draw any definite inferences about the origin of solvent effects on the broad features observed in absorption spectra (both in solution and solid phases). Suffice it to say that electronic absorption intensities and EPR parameters (g, A) are controlled by

different components of the electronic wave functions, and therefore, need not show similar dependence on the changes in ligand field brought about by solvent interactions.

The oxygen evolution studies using $[Mn_2O_2(bpy)_4]^{3+}$ salts in pure as well as polymer and gel doped forms indicate enhanced activity for doped composites for water oxidation in $(NH_4)_2Ce(NO_3)_6$ solution. The active species is likely to be reactive form of 'MnO_2' rather than a Mn_2(IV,IV) center.

1.3 Synthesis, Crystal Structure, EPR, and Solution Studies of $[Mn_2O(OAc)_2(bpy)_2(H_2O)_2](NO_3)_2{\cdot}5H_2O$ and $[Mn_3O_4(phen)_4(H_2O)_2](ClO_4)(NO_3)_3{\cdot}2CH_3OH{\cdot}2H_2O$

The disproportionation of Mn(III) under various conditions of p*H*, concentration, etc. have resulted in the formation of a number of high valent multinuclear Mn complexes. The disproportionation of 'manganic acetate' $Mn(OAc)_3{\cdot}2H_2O$, with equimolar amount of ligand, in dilute nitric acid, resulted in the isolation of a dinuclear Mn_2(III,IV) complex, $[Mn_2O_2(OAc)(bpy)_2(H_2O)_2](ClO_4)_2{\cdot}HNO_3$[3f] and a tetranuclear Mn(IV) complex, $[Mn_4O_6(bpy)_6](ClO_4)_4{\cdot}H_2O$[2c]. In a continuing effort, a careful study of the Mn(III) in dilute nitric acid medium using equimolar amount of bpy or phen as the ligands, resulted in the isolation of various high valent Mn species, such as $[Mn_2O(OAc)_2]^{2+}$, $[Mn_2O_2(OAc)]^{2+}$ and $[Mn_3O_4]^{4+}$. Two of these have been structurally characterised as $[Mn_2O(OAc)_2(bpy)_2(H_2O)_2](NO_3)_2{\cdot}5H_2O$ (3) and $[Mn_3O_4(phen)_4(H_2O)_2](ClO_4)(NO_3)_3{\cdot}2CH_3OH{\cdot}2H_2O$ (4)

1.3.1 Experimental

1.3.1(a) Synthesis. Preparation of $[Mn_2O(OAc)_2(bpy)_2(H_2O)_2](NO_3)_2 \cdot 5H_2O$ (3). 0.750 g (5.6 mmol) of 'manganic acetate' $Mn(OAc)_3 \cdot 2H_2O$, was dissolved in 5mL of 1.6 N HNO_3 containing 0.500 g (3.2 mmol) of 2,2'-bipyridine. The resulting dark brown solution was filtered and kept in desiccator when brown crystals of 3 deposited within a few hours. The rectangular crystals were filtered and dried in vacuo. Yield : 0.650g (0.806mmol, 50%). Anal. Calcd. for $C_{24}H_{36}Mn_2N_6O_{18}$ (MW 806.47): C, 35.92 ; H, 3.09 ; N, 10.78. Found : C, 35.74; H, 4.50; N, 10.42; Equivalent weight : calcd, 403.2; determined by iodometry, 387. IR (KBr/cm^{-1}) : 3368(b), 1578(s), 1497(w), 1472(w), 1352(s), 1157(w), 1103(w), 1057(w), 1032(s), 829(w), 776(s), 731(s), 664(s), 417(w).

Preparation of $[Mn_3O_4(phen)_4(H_2O)_2](ClO_4)(NO_3)_3 \cdot 2CH_3OH \cdot 2H_2O$ (4). 0.750 g (5.6 mmol) of 'manganic acetate' $Mn(OAc)_3 \cdot 2H_2O$ was dissolved in 5mL of 1.6 N HNO_3 containing 0.610 g (3.1 mmol) of 1,10-phenanthroline and 50mL of methanol is added to it. The resulting dark solution was filtered and 0.20 g(1.6 mmol) of $NaClO_4$ dissolved in minimum amount of water was added to it. The solution was stirred and kept in a refrigerator. Dark coloured crystals of 4 deposited after 2-3 days, were filtered, washed with cold methanol and dried in vacuo. Yield : 0.745g (0.54mmol, 70%). Anal. Calcd. for $C_{50}H_{48}Mn_3N_{11}O_{23}$ (MW 1370.5) :C, 43.78 ;H, 3.50 ;N, 11.24. Found : C, 41.19; H, 3.09; N, 10.85; Equivalent weight : calcd, 228.4; determined by iodometry, 210. IR (KBr/cm^{-1}) : 3393(b), 1607(w), 1582(w), 1518(s), 1456(w), 1354(s,br), 1225(w), 1152(w), 1084(s), 874(w), 845(s), 774(w), 716(s), 621(s).

Preparation of $[Mn_3O_4(bpy)_4(H_2O)_2](ClO_4)_4 \cdot 0.5[bpyH_2(NO_3)_2] \cdot 2H_2O$ (5). 0.750 g (5.6 mmol) of 'manganic acetate' $Mn(OAc)_3 \cdot 2H_2O$ was dissolved in 5mL of 1.6 N HNO_3 containing 0.500 g (3.2 mmol) of 2,2'-bipyridine. The resulting

dark green solution was filtered and 0.43 g (3.5 mmol) of $NaClO_4$ dissolved in minimum amount of water was added to it. The solution was stirred and kept in desiccator. After one day, large dark coloured crystals of 5 deposited, were filtered and dried in **vacuo.** Yield : 0.985g (0.673mmol, 84%). Anal. Calcd. for $C_{45}Cl_4H_{45}Mn_3N_{10}O_{27}$ (MW 1464.36) : C, 36.91 ; H, 3.10 ; N, 9.56. Found : C, 36.99; H, 3.10; N, 9.48; Equivalent weight : calcd, 244.1; determined by iodometry, 259. IR (KBr/cm^{-1}) : 3424(b), 3084(s), 1603(s), 1566(w), 1497(s), 1470(w), 1447(s), 1312(s), 1250(w), 1102(s,br), 1032(s), 926(w), 768(s), 696(s), 621(s), 450(w).

Preparation of $[Mn_2O(OAc)_2(phen)_2(H_2O)_2](NO_3)_2 \cdot H_2O$ (6). 0.750 g (5.6 mmol) of 'manganic acetate' $Mn(OAc)_3 \cdot 2H_2O$ was dissolved in 5ml of 1.6 N HNO_3 containing 0.605g (3.1 mmol) of 1,10-phenanthroline. The resulting dark solution was filtered and kept in desiccator when brown crystals of 6 deposited within a few hours. The flat diamond shaped crystals were filtered and dried in vacuo. Yield : 0.510g (0.65mmol, 42%). Anal. Calcd. for $C_{28}H_{30}Mn_2N_6O_{14}$ (MW 782.42) : C, 42.98 ; H, 3.35 ; N, 10.74. Found : C, 42.79; H, 3.38; N, 11.22; Equivalent weight : calcd, 391.2; determined by iodometry, 398. IR (KBr/cm^{-1}) : 3376(b), 1570(s), 1516(s), 1339(s,br), 1146(w), 1105(w), 1024(w), 874(w), 853(w), 828(w), 721(s), 662(s).

1.3.1(b) Physical Measurements. All physical measurements were performed as described in Experimental Section 1.1.1 of this chapter.

1.3.1(c) X-ray Crystallography. (3) : Data for a dark rectangular plate-like crystal were collected at 298 K on a CAD4 diffractometer using graphite monochromated Mo-K_α radiation. The structure was solved by direct methods (SHELXS) and refined (over F^2) by least squares techniques (SHELXL).[27]

The complex crystallises in the monoclinic system, space group $P2_1/n$, with 4 molecules in the unit cell. A total of 6306 reflections (6039 unique, 3014 with F > 4σF) were collected in the 2θ range 3.5 to 55°, with indices 0 < h < 2 1 , 0 < k < 11, -22 < 1 < 22. Non-hydrogen atoms were refined anisotropically and all ring hydrogen atoms were included in calculated positions using a riding model. The hydrogen atoms on water molecules were located from the fourier map and bond length constraints were applied. The final cycle of full matrix least squares refinement on F^2 converged with unweighted and weighted agreement factors of R1 = 0.0569 and wR2 = 0.1358. The goodness of fit was S = 0.951 with 3014 observations and 503 parameters. The maximum and minimum peaks on the final fourier map corresponded to 0.476 and -0.351 e/A^3 respectively. Crystallographic data and selected bond angles and bond distances are listed in Table 1.4 and Table 1.5 respectively. Full crystallographic data and other positional parameters are listed in Appendix B. There are seven water molecules out of which two are coordinated to the metal and other five are lattice water.

Table 1.4 Crystallographic Data for $[Mn_2O(OAc)_2(bpy)_2(H_2O)_2](NO_3)_2 \cdot 5H_2O$ (3)

formula	$C_{24}H_{36}Mn_2N_6O_{18}$	2	4
formula weight	806.47	space group	$P\ 2_1/n$ (No. 14)
a	18.251(4) A	T	293(2) K
b	9.968(3) A	^	0.71073 A
c	19.157(3) A	p(obsd)	1.50 Mg/m^3
a	90°	p(calcd)	1.557 Mg/m^3
P	99.33(1)0	μ	0.819 mm^{-1}
y	90°	R1	0.0569

V	3439(1) A^3	wR2	0.1358

$R1 = \Sigma||F_o| - |F_c||/\Sigma|F_o$

$wR2 = [\Sigma\{w(F_o^2 . F_c^2)^2\}/\Sigma(wF_o^4)]^{1/2}$

$w^{-1} = [\sigma^2(F_o^2) + (0.0847P)^2 + 0.0000P]$, $P = (F_o^2 + 2F_c^2)/3$

Table 1.5 Selected bond lengths [A] and angles [deg] for 3.

Bond distances

Mn(1)-O(1)	1.779(3)	Mn(1)-O(5)	1.943(3)
Mn(1)-N(2)	2.070(4)	Mn(1)-N(1)	2.071(3)
Mn(1)-OW2	2.196(2)	Mn(1)-O(2)	2.206(3)
Mn(1)-Mn(2)	3.1350(9)	Mn(2)-O(1)	1.784(2)
Mn(2)-O(3)	1.938(3)	Mn(2)-N(3)	2.061(4)
Mn(2)-N(4)	2.074(3)	Mn(2)-O(4)	2.158(3)
Mn(2)-OW1	2.239(2)		

Bond angles :

O(1)-Mn(1)-O(5)	98.66(12)	O(1)-Mn(1)-N(2)	93.30(13)
O(5)-Mn(1)-N(1)	90.66(13)	N(2)-Mn(l)-N(l)	77.59(14)
O(1)-Mn(1)-OW2	92.58(10)	O(5)-Mn(1)-OW2	91.05(11)
N(2)-Mn(1)-OW2	91.82(12)	N(1)-Mn(1)-OW2	84.27(11)
O(1)-Mn(1)-O(2)	95.28(12)	O(5)-Mn(1)-O(2)	88.88(12)
N(2)-Mn(1)-O(2)	86.62(13)	N(1)-Mn(1)-O(2)	87.80(12)
Mn(1)-O(1)-Mn(2)	123.29(16)		

Intermolecular contacts:

(a) Hydrogen bonds:

O(6)--HW1B	1.812(6)	OW7--HW1A	1.777(5)	O(9)--HW2B	1.971(8)
OW4--HW2A	1.791(5)	O(7B)#1--HW3B	2.09(1)	O(10)--HW5A	1.760(7)

OW3#2--	1.880(7)		
HW5B			
O(6)-HW1B-OW1	168.0(6)	OW7-HW1A-OW1	150.8(4)
O(9)-HW2B-OW2	168.9(8)	OW4-HW2A-OW2	172.8(5)
OW3-HW3B-O(7B)#1	130.0(6)	OW5-HW5A-O(10)	146.6(7)
OW5-HW5B-OW3#2	174.9(7)		

Symmetry transformations used to generate equivalent atoms:

#1 -x+1/2, y+1/2, -z+1/2 #2 x+1/2, -y+3/2, z+1/2

(4) : Data for a thin plate-like crystal were collected at 298 K on a CAD4 diffractometer using graphite monochromated Mo-K_α radiation. The data were corrected for absorption.[8] The structure was solved by direct methods (SHELXS86)[9] and refined (over F^2) by least squares techniques (SHELXL93).[10]

The complex crystallises in the triclinic system, space group P1, with 2 molecules in the unit cell. A total of 8485 reflections (7996 unique, 4204 with F > 4σF) were collected in the 2θ range 4 to 55°, with indices 0 < h < 13, -16 < k < 16, -20 < 1 < 20. All the non-hydrogen atoms except the nitrate anions and lattice solvent molecules, were refined anisotropically and all ring hydrogen atoms were included in calculated positions using a riding model, while the solvent hydrogens were not located. The full matrix least squares refinement on F^2 converged at a high unweighted and weighted agreement factors of R1 = 0.1067 and wR2 = 0.2775. Crystallographic data and selected bond distances and angles are listed in Appendix C.

1.3.2 Results and Discussion

1.3.2(a) Synthesis. The disproportionation of Mn(III) and aggregation to various binuclear and trinuclear $[Mn_2O_2(OAc)_2]^{2+}$, $[Mn_2O(OAc)_2]^{2+}$ or $[Mn_3O_4]^{4+}$ cores has been observed in dilute nitric acid. (Scheme 1)

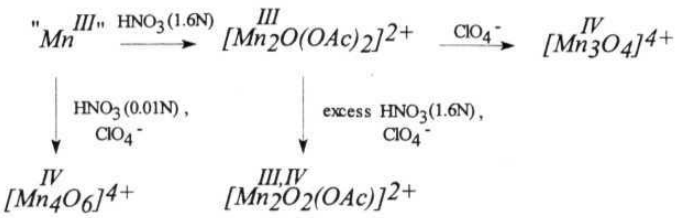

Scheme 1

It has been observed that the disproportionation of Mn(III) in dilute nitric acid media, at *pH = 2,* results in the aggregation to tetranuclear Mn(IV) complex.[2c] The precipitation of various products is controlled by the concentration of nitric acid and the anions present in the solution. The Mn(III), first forms the dinuclear $[Mn_2O(OAc)_2]^{2+}$ core which has been isolated with bpy and phen as ligands (complex 3 and 6). With time the Mn(III) gets oxidised to Mn(IV) and then $[Mn_3O_4(H_2O)_2(L)_4]^{4+}$ species is formed. Using perchlorate as the anion the Mn_3(IV,IV,IV) species (complex 4 and 5) has been isolated and characterised with bpy and phen as the ligands. An increase in the amount of nitric acid results in isolation of mixed valent species of $[Mn_2O_2(OAc)]^{2+}$. The species has been isolated and structurally characterised with bpy as ligand.[3f] However with phen, a sticky precipitate formed, which was difficult to analyse.

1.3.2(b) Structure. (3) The $[Mn_2O(OAc)_2(bpy)_2(H_2O)_2]^{2+}$ cation is shown in Figure 1.12. The cation has been characterised three times previously as PF_6^- and

ClO_4^- salts.[28], 3d,f. The binuclear unit of Mn(III) shows an average $Mn\text{-}O_{oxo}$ distance of 1.782 A and Mn-O-Mn angle of 123.2°. The $Mn\text{-}O_{OAc}$ distance ranges from 1.938 to 2.206 A (average 2.182 A (long) and 1.941 A (short)) and the Mn-Mn distance is 3.1350 A. The Mn-OW(water) distances are 2.196 and 2.239 A and the average Mn-N distance is 2.069 A. All the structural parameters are similar to the ones reported[28], 3d,f except for slight difference in Mn-OW(water) bond distances which are influenced by the molecules H-bonded to it. One of the nitrate oxygen (07) is disordered in two postions. The N-0 bond distance in one of the nitrate is symmetrical (av. 1.25 A), while the other has unsymmetrical distances of 1.094, 1.265 and 1.227 A.

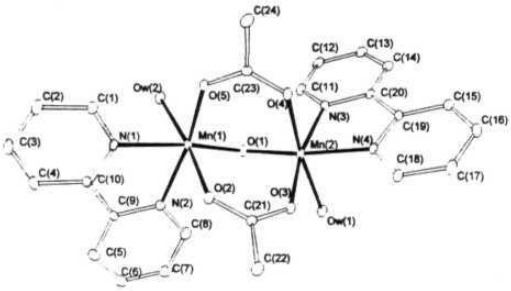

Figure 1.12 Cation of 3, $[Mn_2O(OAc)_2(bpy)_2(H_2O)_2]^{2+}$

The coordinated waters are hydrogen bonded to a nitrate and lattice water each (OW1 to OW3, 06 and 0W2 to OW4, O9), as shown in Figure 1.13. In 3 the nitrato ions are outside the coordination sphere, while there is a related compound, viz., $[Mn_2O(OAc)_2(bpy)_2(H_2O)(NO_3)]ClO_4{\cdot}CH_3COOH$, in which the nitrate is found coordinated to one of the Mn atom.3d

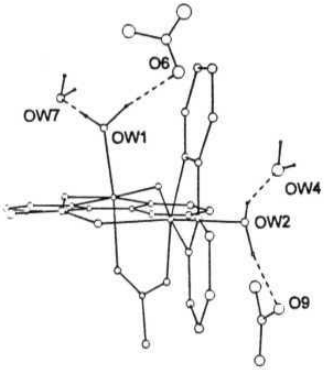

Figure 1.13 H-bonding of water molecules on the cation of 3 with a water and a nitrate each.

(4): The cation of 4 has been synthesised and structurally characterised, earlier in our lab, by Ce(IV) oxidation of Mn(II).[3c] However, the present structure could not be refined to a good agreement factor. The cation has been refined anisotropically, and shows 3 manganese atoms bridged in a triangular way (Figure 1.14).

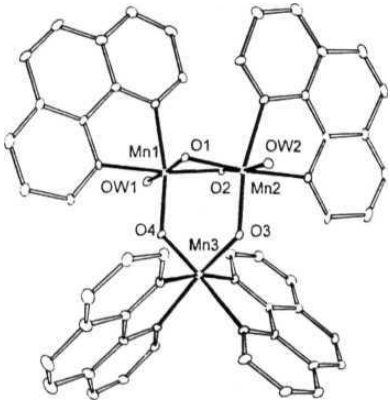

Figure 1.14 Cation of 4,

There is one di-μ-oxo and two mono-μ-oxo bridges at Mn-Mn distances of 2.670, 3.234 and 3.250 A respectively. The Mn-water distances are similar 2.013 A. The nitrate anions and the lattice waters were found to be disordered and could not be modelled well due to insufficient number of observed reflections and they were left isotropic. All other structural parameters are similar to those in the previously reported structure.[3c]

1.3.2(c) EPR and Magnetic Moment. The room temperature magnetic moment of 3 was found to be 6.76 μ_B based on the paramagnetic susceptibility of a powdered sample which corresponds to a magnetic moment of 4.78 μ_B per Mn (d^4 system). The $[Mn_3O_4]^{4+}$ complexes 4 and 5 have molar magnetic moments of 4.46 μ_B and 4.25 μ_B respectively. The polycrystalline samples of 3, 4 and 6 show a broad signal at g ~ 2, while the complex 5 does not show any signal at room temperature. The low temperature spectrum of 5, however shows broad signal at g ~ 2. The spectra in frozen dimethylformamide and acetonitrile solution of 3 and 6 show a '6-line feature' at g ~ 2 and of complexes 4 and 5 show a '16-line spectrum' with '6-line feature'. This indicates the decomposition of 3 and 6 to Mn(II) species and the trinuclear units of 4 and 5 to Mn_2(III,IV) and Mn(II) species.

1.3.2(d) Electronic Spectra. The complexes 3-6 are soluble in water, DMF and CH_3CN. The electronic spectra in water for all the complexes show weak shoulders at around 720 and 660 nm.

1.3.3 Conclusions

Disproportionation of '$Mn(OAc)_3$' in dilute nitric acid leads to the formation of several higher valent Mn complexes having nuclearity two to four.

References

(1) Recent reviews: (a) K. Wieghardt *Angew. Chem. Int. Ed. Engl.* **1989,** *28,* 1153. (b) G. C. Dismukes *Chem. Rev.* **1996,** *96,* 2909. (c) K. Wieghardt *Angew. Chem. Int. Ed. Engl.* **1994,** *33,* 725. (d) V. L. Pecoraro, M. J. Baldwin and A. Gelasco *Chem. Rev.* **1994,** *94,* 807. (e) R. Manchanda, G. W. Brudvig and R. H. Crabtree *Coord Chem. Rev.* **1995,** *144,* 1. (f) V. K. Yachandra, K. Sauer and M. P. Klein *Chem. Rev.* **1996,** *96,* 2927. (g) A. Caneschi, D. Gatteschi and R. Sessoli *J. Chem. Soc, Dalton Trans.* **1997,** 3963. (h) W. Ruttinger and G. C. Dismukes *Chem. Rev.* **1997,** *97,* 1.

(2) (a) V. K. Yachandra, V. J. DeRose, M. J. Latimer, I. Mukerji, K. Sauer and M. P. Klein *Science* **1993,** *260,* 675. (b) M. L. Kirk, M. K. Chan, W. H. Armstrong and E. I. Solomon *J. Am. Chem. Soc.* **1992,** ***114,*** 10432. (c) C. Philouze, G. Blondin, J. -J. Girerd, J. Guilhem, C. Pascard and D. Lexa *J. Am. Chem. Soc.* **1994,** *116,* 8557.

(3) (a) K. R. Reddy, M. V. Rajasekharan, S. Padhye, F. Dahan and J. -P. Tuchagues *Inorg. Chem.* **1994,** *33,* 428. (b) K. R. Reddy and M. V. Rajasekharan *Polyhedron* **1994,** *13,* 765. (c) K. R. Reddy, M. V. Rajasekharan, N. Arulsamy and D. J. Hodgson *Inorg. Chem.* **1996,** *35,* 2283; (d) K. R. Reddy, M. V. Rajasekharan and S. Sukumar *Polyhedron* **1996,** *15,* 4161. (e) G. Swarnabala, K. R. Reddy, J. Tirunagar and M. V. Rajasekharan *Transition Met. Chem.* **1994,** *19,* 506. (f) K. R. Reddy, Ph. D. Thesis, University of Hyderabad, Hyderabad, India, 1993.

(4) Mn_2(III,IV) complexes with crystallographically distinct Mn atoms: (a) P. M. Plaksin, R. C. Stoufer, M. Mathew and G. J. Palenik *J. Am. Chem. Soc.* 1972, *94,* 2121. (b) A. F. Jensen, Z. Su, N. K. Hansen and F. K. Larsen

(15) (a) S. R. Cooper and M. Calvin *J. Am. Chem. Soc.* **1977,** *99,* 6623. (b) S. R. Cooper, G. C. Dismukes, M. P. Klein and M. Calvin *J. Am. Chem. Soc.* **1978,***100,* 7248.

(16) A. T. Casey and S. Mitra in *Theory and Applications of Molecular Paramagnetism*; E. A. Boudreaux and L. N. Mulay, Eds.; Wiley - Interscience: New York (USA), 1976, p.276.

(17) (a) A. H. Cooke, H. J. Duffus and W. P. Wolf *Phil. Mag.* **1953,** *44,* 623. (b) C. Y. Wu, R. Alben and W. P. Wolf *Solid State Commun.* **1972,***11,* 1599.

(18) D. R. Gamelin, M. L. Kirk, T. L. Stemmler, S. Pal, W. H. Armstrong, J. E. Penner-Hahn and E. I. Solomon *J. Am. Chem. Soc.* **1994**, *116*, 2392.

(19) (a) G. Swarnabala, Ph.D. Thesis. University of Hyderabad, Hyderabad, India, 1989. (b) G. Swarnabala and M. V. Rajasekharan *Proc. Indian Acad. Sci.(Chem. Sci.)* **1990**, *102*, 87.

(20) R. Ramaraj, A. Kira and M. Kaneko *Angew. Chem. Int. Ed. Engl.* **1986,** *25,* 825.

(21) K. V. Gobi, R. Ramaraj and M. Kaneko *J. Mol. Catal.* **1993,** *81,* L7.

(22) R. Ramaraj and M. Kaneko *Adv. Polym. Sci.* **1995,** *123*, 215.

(23) N. Garcia, P. Crespo, A. Hernando, C. Bovier, J. Semghetti and E. Duval *Phys. Rev. B* **1993,** *47,* 570.

(24) K. Chandramauli, M. Sc. Dissertation. Jawaharlal Nehru Technological University, Hyderabad, India, 1993.

(25) R. Dingle *Acta Chem. Scand.* **1966,** *20,* 33.

(26) (a) J. E. Sarneski, H. H. Thorp, G. W. Brudvig, R. H. Crabtree and G. K. Schulte *J. Am. Chem. Soc.* **1990**, *112*, 7255. (b) H. H. Thorp, J. E. Sarneski, G. W. Brudvig and R. H. Crabtree *J. Am. Chem. Soc.* **1989,** *111*, 9249.

(27) G. M. Sheldrick, SHELX-97; University of Gottingen, Gottingen, 1997.

(28) (a) S. Menage, J. -J. Girerd and A. Gleizes *J. Chem. Soc, Chem. Commun.* 1988, 431. (b) J. B. Vincent, H. L. Tsai, A. G. Blackman, S. Wang, P. D. W. Boyd, K. Folting, J. C. Huffman, E. B. Lobkovsky, D. N. Hendrickson and G. Christou *J. Am. Chem. Soc.* **1993,** *115*, 12353.

POLYIODIDE SALTS OF METAL COMPLEX CATIONS

CHAPTER 2

Polyiodide Anions : A Review

2.1. Introduction

The study of anionic aggregates of iodine and iodide is the main focus of this thesis. A brief review of such systems is therefore presented in this chapter.

It is natural to begin with a quick glance at some of the basic facts known about iodine.[1] Molecular iodine is synthesised by oxidizing iodide under acidic conditions. It is a black solid with slight metallic luster which directly sublimes to violet vapours on heating. The violet colour is usually assigned to the *n-n** transtions. It is slightly soluble in water, but readily dissolves in non-polar solvents to form violet solutions. It forms brown solution in unsaturated hydrocarbons, alcohols, ketones and pinkish brown solution in benzene. Charge transfer complexes formed with solvent molecules as well as $2I_2 \rightleftarrows I_4$ equilibrium may contribute to the solution colour. Molten iodine is electrically conducting due to self ionisation, $3I_2 \rightleftarrows I_3^- + I_3^+$

In the solid state, iodine has a layer structure with an I-I bond distance of 2.715 A (The bond distance in the vapour phase is only 2.666 A). There are two types of intermolecular contacts within each layer, at distances of 3.50 A and 3.97 A. The interlayer contacts are at 4.27 A which is close to the van der Waals diameter of I atom (4.30 A). At ambient conditions iodine is a two dimensional

semiconductor with a band gap of 1.3 eV. Under a pressure of 350 kbar iodine crystals become metallic.

The ability of iodine to catenate has led to the isolation of several compounds containing polyiodine species : anionic (I_3^-, I_4^{2-}, I_5^-, I_7^-, I_8^{2-}, I_9^-, I_{10}^{2-}, I_{10}^{4-}, I_{12}^{2-}, I_{16}^{2-}, I_{16}^{4-}, I_{18}^{4-}, I_{22}^{4-}) ; cationic : (I_2^+, I_3^+, I_4^{2+}, I_5^+, I_{15}^{3+})[2] ; neutral : $((I_2)_7)$.[3] Anionic species are the most numerous and several reviews dealing with them have been published.[4] In solution, I_3^- is the most stable polyiodide anionic species and it has been found to be linear and symmetrical, whereas in the solid state the I_3^- ion is found to be linear or nearly linear with both symmetrical and unsymmetrical forms. A complete review on the polyiodide anions was last done by K. -F. Tebbe, as part of the review on polyhalogen cations and polyhalide ions.[4d] A few years later, some specific studies on structure and conductivity on iodine containing low dimensional materials was also done[4e-g] and more recently structural studies on triiodides[4h,i] and template assembly of polyiodide networks for a special class of cations have been reviewed.[4j]

2.2 Synthesis.

The general methods of preparation of polyiodide anions include reaction between solid iodide or polyiodide and gaseous iodine or reaction between iodine and iodide in an appropriate solvent. The former procedure is not preferred due to low yield and cumbersome reaction conditions. The solid-solution reactions are affected by solvents that are easily susceptible to halogenation or which cause solvolysis reactions. Some inert solvents cannot dissolve halide salts, hence methanol or glacial acetic acid have been found to be better solvents for the reaction.[5] Other synthetic techniques employed include electrocrystallisation using cationic host and polyiodide salt in a solvent like tetrahydrofuran (THF) or chlorobenzene to obtain crystals suitable for conductivity studies.[6]

The stability of the polyiodide anion is largely dependent on the cation chosen. It has been found that most stable salts are formed when the cation and anion are of nearly same size. However, it has also been observed that the same cation forms a number of stable polyiodide species either on varying the ratio of number of moles of iodine to iodide[7] or on adding one mole of iodine successively to the triiodide.[8] It has also been observed that recrystallisation of the same compound from different solvents sometimes, resulted in different polyiodides.[9] The polyiodides reported in this thesis were prepared using a two phase procedure, according to which the iodide and cation in aqueous phase are extracted into organic phase containing dissolved I_2 after the formation of polyiodide at the inter phase.[10]

Iodine doped systems are becoming important these days due to their electrical properties. Partial oxidation of Co(II) and Ni(II) complexes with iodine in organic solvents sometimes results in columnar stacks of metal complex moieties along with polyiodide chains.[11] Poly(vinyl alcohol) (PVA) films when treated with aqueous I_2 in presence of KI form dark blue I-doped PVA.[12] Doping is sometimes done by electrochemical generation of I_2 in a solution of KI in dilute sulphuric acid or by exposure of the films to I_2 vapour.[13]

2.3 Structure and Bonding.

The interatomic spacing in I_3^-, which is generally linear, formed as a result of a neutral I_2 molecule bound to a negative I" ion has been studied earlier.[14] By analogy to theoritical results on H_3, it was argued that when the distance between the extreme atoms is below a certain critical value, there is a single minimum for the energy of the molecule when the central atom is midway between the two other atoms (symmetric I_3^-). However, when the distance between extreme atoms is greater, there will be two minima, one nearer an extreme atom and another nearer

the other extreme atom, as if a diatomic molecule and ion were being formed (asymmetric I_3^-) (Figure 2.1).

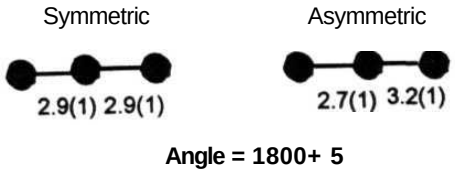

Figure 2.1 The two most commonly occuring geometries of the I_3^- ion (Ref. 4i).

Bonding in polyiodide ions I_3^-, I_5^-, I_8^{2-} has also been studied, using modified Huckel theory.[15] The calculated charges, bond order and energies were found to be in good agreement with experimental NQR results, bond lengths, stabilities and spectroscopy.

Recent studies include the *ab initio* calculations of ground electronic states of polyiodide anions, I_3^- and I_5^-.[16] The equilibrium geometries, harmonic frequencies and IR and Raman intensities were determined for I3" and I5" using coupled cluster and density functional methods.[16a] for the I_5^- ion the linear ($D_{\infty h}$) structure is obtained as a low energy transition state lying only about 0.1-0.2 eV above the C_{2v} global minimum-energy structure.

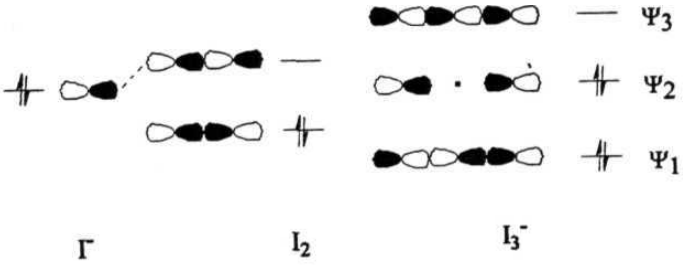

Figure 2.2 Rundle-Pimentel scheme of delocalised 3-center 0 bonding in I_3^-.

The nature of the bonding in symmetric trihalides (X_3^-), has been analysed **sing** both qualitative MO theory and density functional theory.[17] It was shown **that bonding in** all such anions can be explained based on the electron-rich 3-**center bonding** scheme of Rundle-Pimentel (Figure 2.2).[18] The equivalence of the donor-acceptor (I^- attack at the two possible sites of I-I) and hypervalent bonding views of these molecules were also inferred. The largest contributors to the **HOMO were** found to be terminal I atoms in I_3^-. Due to electron-electron **repulsion the** energy levels will be stabilised when the negative charge is delocalised over three atoms in I_3^- (Figure 2.3).

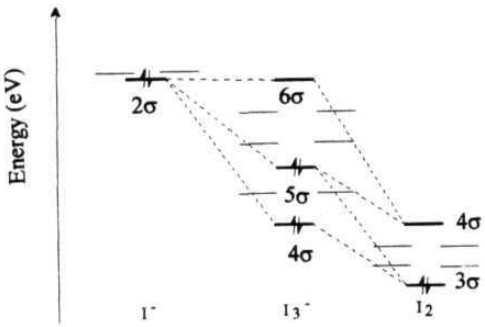

Figure 2.3 Fragment molecular orbital interaction diagram for I_3^- (The symmetry labels correspond to $C_{\infty v}$ symmetry; thicker lines denote a bonding energy levels.) (Ref. 17).

The asymmetry in bond lengths of I_3^- observed in polyiodide crystals, has been studied **in** detail.[4h,4i,19] A comparison of the degree of asymmetry of I_3^- in **two** sets is **done,** one containing H-bonded I_3^- anions and another without any H-bonded I_3^- anions. Based on the correlation and regression graphs it was concluded **that H-bonding** is a factor affecting the I_3^- symmetry but it is not a preferential factor (Figure 2.4).

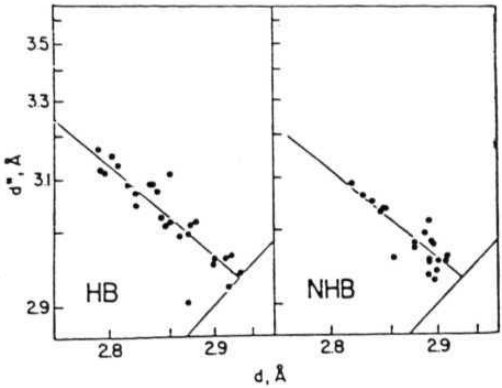

Figure **2.4** Rectified correlation of *d*(I-I) and rf*(I-I) in I_3^-, showing regression lines. HB set: I_3^- in structures containing N-H...I bonds; NHB set: I_3^- in structures without N-H...I bonds (Ref. 4i).

Recent *ab initio* Hartree-Fock crystal orbital calculations on two polyiodide systems, one with no true polyiodide chains (tetrathiofulvaleniumI_3) and another with polyiodide chains (dipyridiniumI_{10}), show that crystalline organic iodides with polyiodide chains could, in principle, be quasi-one-dimensional semi-conductors.[20] A polyiodide chain could be a carrier of semiconductivity only when it is formed by fully charged iodide anions with no charge transfer from the chains.

2.4 Spectroscopic and Conductivity Studies.

2.4.1 IR and Raman Studies

The far-infrared and Raman (Resonance-Raman) studies of the polyiodides have been useful in determining the nature of the polyiodide unit. The vibrational studies are particularly useful for both non-crystalline and crystalline salts and also polyiodide systems doped in polymeric matrices. The far-IR and Raman spectra of I_3^-, I_5^-, I_7^- and I_9^- have been studied in detail and vibrational assignments are

made based on I-I bond distances.[4e-g,21] In some cases, it has been observed that the laser excitation source in the Raman experiment results in the decomposition of the polyiodide species. Hence, the FT-Raman technique which operates under milder conditions, is preferred.

The higher polyiodides are classified into I", I_2 and I_3^- components from the structural information available and correlated to the vibrational bands observed in far-IR and Raman spectra (Figure 2.5, Figure 2.6). Thus, the Raman spectrum of a polyiodide species containing I_2 components show bands in the 170-190 cm^{-1} range, in agreement with the Raman bands observed in solid I_2 (180 and 190 cm^{-1}). Similarly, the I_3^- units have strong IR and Raman bands between 100 and 120 cm^{-1}, corresponding to the symmetric stretch.[4e-g,21] A discrete polyiodide unit shows a characterstic Raman pattern which can be used to identify unknown systems. The combination of far-IR and Raman spectra helps in determining the symmetry of the polyiodide unit, based on the IR and Raman active vibrations. The selection rules for I_3^- in some commonly occuring point group symmetries are as follows:

Point group symmetry	No. of modes	IR	Raman	Polarized band	Coincidences
$D_{\infty h}$	3*	2	1	1	0
$C_{\infty v}$	3*	3	3	1	3
C_{2v}	3	3	3	2	3
	3	3	3	3	3

* one mode is doubly degenerate

$D_{\infty h}$ (linear, centrosymmetric); $C_{\infty v}$ (linear non-centrosymmetric); C_{2v} (bent, symmetrical); C_s (bent, unsymmetrical)

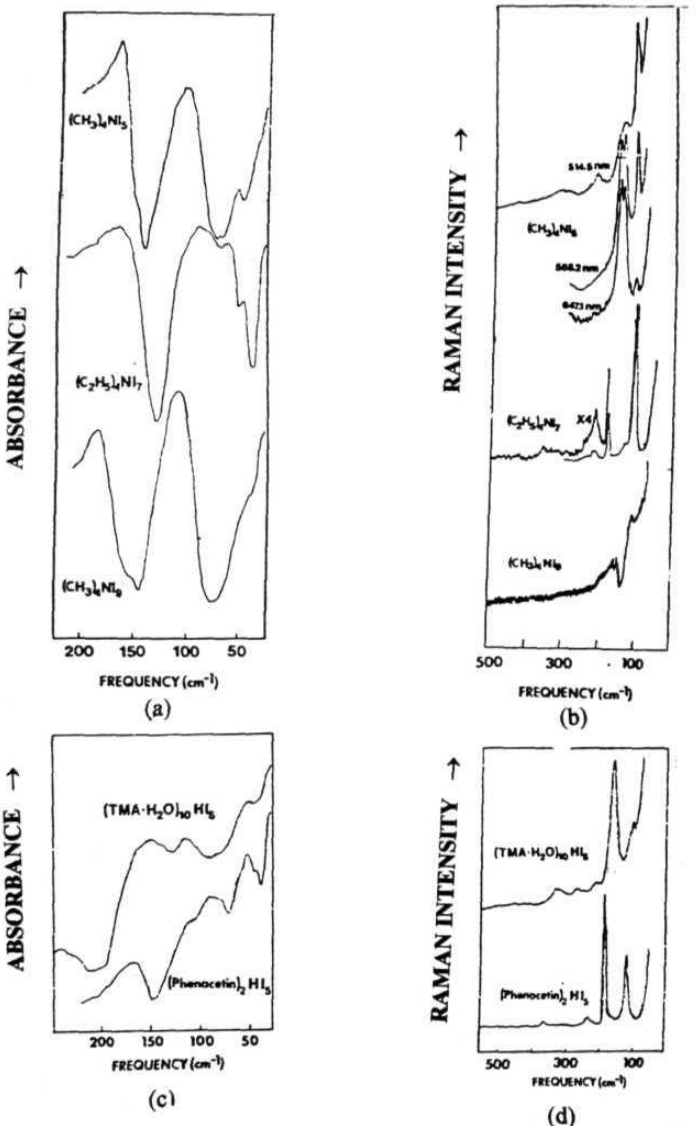

Figure 2.5 Far-IR and Raman spectra of some of the reported polyiodide compounds (Ref. 21): (a) Far-IR, (b) Raman spectra of $[Me_4N]I_5$, $[Me_4N]I_7$ and $[Me_4N]I_9$; (c) Far-IR, (d) Raman spectra of $(TMA.H_2O)_{10}HI_5$ (linear $(I_5^-)_n$) and $(phena)_2HI_5$ (zig-zag $(I_5^-)_n$).

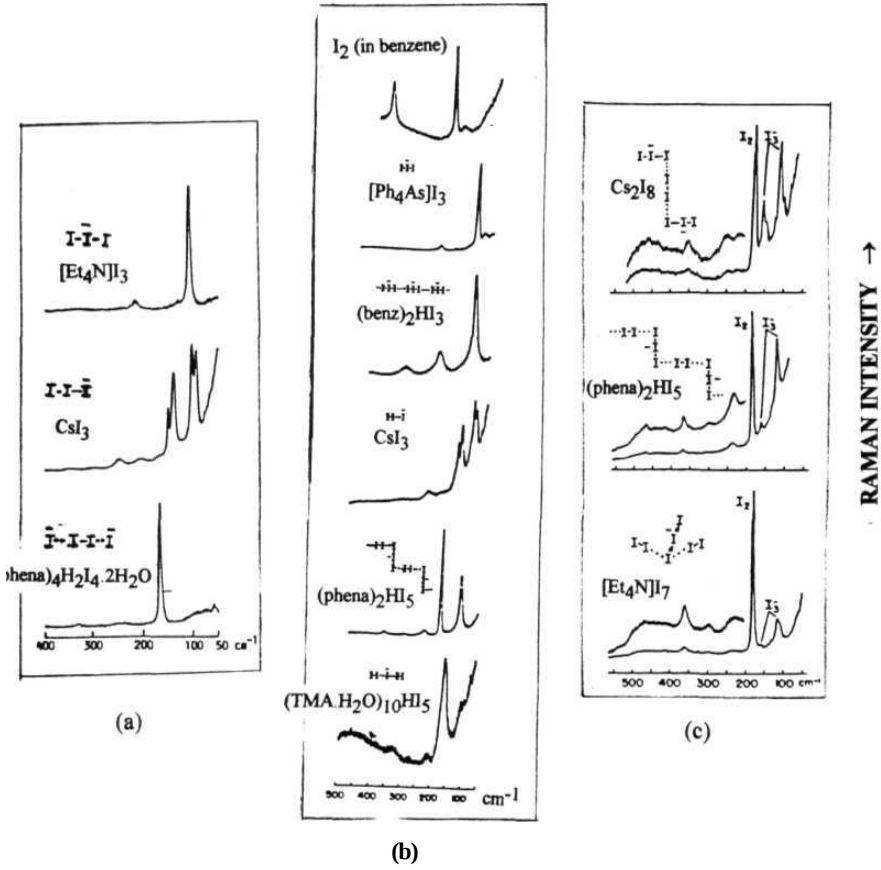

Figure 2.6 Comparison of Resonance Raman spectra of some of the reported polyiodide compounds (Ref. 22, 4f): (a) $[Et_4N]I_3$, CsI_3 and $(phena)_4H_2I_4.2H_2O$ (488.0 nm excitation), (b) I_2 (in benzene), $[Ph_4As]I_3$, $(benz)_2HI_3$, CsI_3, $(phena)_2HI_5$ and $(TMA.H_2O)_{10}HI_5$ (514.5 nm excitation) and (c) Cs_2I_8, $(phena)_2HI_5$, $[Et_4N]I_7$ (514.5 nm excitation).

The crystal interactions, such as site symmetry lowering causes removal of degeneracy and splitting of ν_1 vibration which make it appear in both IR and Raman.

A summary of these studies for various polyiodide units are presented in Table 2.1.

Table **2.1** Far-IR and Raman bands observed in different types of polyiodide salts (Numbers printed in bold refer to intense bands).

SNo.	Molecular formula	**Polyiodide unit**	Structure	**IR bands (cm^{-1})**	**Raman bands (cm^{-1})**	Ref.
1.	I_2(solid)		bond distance 2.72 A	-	425, 368, 214, **190, 180**	4f
2.	$(D_2I)I_3$	I_3^- (discrete) 2 types	linear symmetric ($D_{\infty h}$)		**121,** 207	23
3.	$(Me_4As)I_3$	I_3^- (discrete) 2 types	linear symmetric ($D_{\infty h}$)		**108**	24
4.	$[(EtNH_2)dt]I_3$	I_3^- (discrete)	linear asymmetric ($C_{\infty v}$)		**167**	4j
5.	$(n\text{-}Bu)_4NI_3$	I_3^- (chains)	nearly linear asymmetric		**108**	25

6.	(Caf)$H_2O(HI_3)$	I_3 (chains)	disordered		166,108	25
7.	(benz)HI_3	I_3^- (chains)	linear symmetric		333, 224, **112**	4f
8.	CsI_3		linear asymmetric		243, 157, **148, 137,** 102, 93	4f
9.	$[Ph_4As]I_3$	I_3^-	linear symmetric		235, 187, **118,** 94, 73	4f
10.	$(phena)_4H_2I_4$ $.2H_2O$	(discrete)	linear		168	22
11.	$(Me_4N)I_5$	I_5^- (discrete)	bent (C_{2v})	155, **145,** 83,76	158, 147, **113**	21
12.	$[Mn(mod)_3]I_5$	Is" (discrete)	bent (C_{2v})		**165, 143**	4j
13.	$[moH]I_5$	Is" (discrete)	L-shaped ($I_3^-.I_2$)		**164,** 135, 106	4j
14.	$(TMA.H_2O)HI_5$	$(I_5^-)_n$ (chain)	linear ($D\infty h$)	210, 198, 128, 90, 83,45	327, 270, 210, **163,** 105	21
15.	$(\alpha\text{-CD})_2LiI_3.I_2$	I_5^- (chain)	disordered ($I_3.I_2$)		**161, 107**	25
16.	$(phena)_2HI_5$	I_5^- (chain)	zig-zag chains	**146,** 108, 70, 44, 37	368, 301, 235, **184,** 115	21

17.	$[PPh_4]I_7$	I_7^- (discrete)	branched (C_s) (I_3).($2I_2$)	**175,** 166, 139, **113, 110,** 70	178, 166, 152, **118,** 74	26
18.	$[Et_4N]I_7$	I_7^- (discrete)	branched (C_s) (I_3).($2I_2$)	**132,** 72, 54	360, 217, **182,** 134, **108**	21
19.	$[(bntMe)_2I]I_7$	I_7^- (discrete)	branched (C_{3v}) (DPI,)		317, 175, **157**	23
20.	$[Ag(aneS6)]I_7$	I_7^- (discrete)	symmetrical (D_{3d}) (I).($3I_2$)		179, **165**	4j
21.	Cs_2I_8	I_8^{2-} (discrete)	Z-shaped		350, 280, 240, **171,** 147, 139, 117, **105,** 95	7f
22.	$(Me_4Sb)_3I_8$	I_8^{3-} (chains)	linear		no lines observed	24
23.	$[Me_4N]I_9$	***V*** (discrete)	(I_5^-).2(I_2); (I_5^-:C_{2v})	**157, 147,** 78,40	190, 157, 145, 108, 79	21, 27
24.	$[K(aneO5)_2]I_9$	I_9^- (network)			**180, 131,** 109	4j
25.	$[Pd(aneS4)_2I](I_5)I$	I_{11}^{3-} (rings)	2(I_5^-).(I^-);		**157,** 149	**4j**
26.	$[Ag_2(aneS5)]I_{12}$	I_{12}^{2-}	2(I^-) .5(I_2)		**172**	**4j**

27.	$[Cu(dafone)_3]I_{12}$		planar, branched	235, 137, 84		10
28.	$[morH]_2I_{16}$		nearly planar		**174,** 161, 139, 112	**4j**
29.	$(Cp_2Fe)_3I_{29}$			**139, 133, 106,** 87	428, 213, 172, 115, 74	8b

The higher polyiodide species are regarded as adducts of the type $[I^-.(I_2)_n]$ or $[I_3^-.(I_2)_n]$ and their Raman spectra shows characteristic peaks due to perturbed I_2 and symmetric or slightly asymmetric I_3^- for $[I_3^-.(I_2)_n]$. Therefore except for symmetric I_3^-, bent I_5^-, linear I_5^-, the IR and Raman techniques are unable to differentiate between different types of polyiodides. However, the vibrational spectrum can give valuable information on the extent of lengthening of I-I bond (in I_2 and I_3^-) and whether the bond is due to interaction with neutral I_2 or I", etc. These techniques are thus advantageous only for discrete polyiodide systems and for systems with extended networks, but they cannot identify the structure beyond the basic unit formed from I", I_2 and I_3^- fragments.[4].)

2.4.2 Electronic Spectroscopy

The electronic structure of the polyiodide ions can be best understood by first considering the solution absorption spectra of iodide, iodine and triiodide species. The iodide ion shows two peaks in the 50 kK region with a doublet structure due to the splitting of the ^2P state of iodine atom by spin orbit coupling.[25] The spectrum of I_2 consists of a single peak at around 20kK (Figure 2.7(a)). The spectrum of I_3^- consists of two strong absorption bands at 28kK and

35kK, attributed to spin-orbit splitting in the $\sigma_g \rightarrow \sigma_u^*$ transition (Figure 2.7(b)). Earlier on the basis of an empirical calculation, Gabes *et al* have suggested that two transitions, namely, $\sigma_g \rightarrow \sigma_u^*$ and $rc_g \rightarrow \sigma_u^*$, symmetry and spin allowed, could be expected in the 30,000 cm"[1] region of the electronic spectra of symmetric I_3^- ions.[28] But Mizuno *et al* have ascribed both the bands to the $\sigma_g \rightarrow \sigma_u^*$ transition split into $^2P_{3/2}$ and $^2P_{1/2}$ states of iodine based on the polarisation character of both the bands.[25] The I_3^- bands can also be seen as weak absorptions in the spectra of iodine solutions.

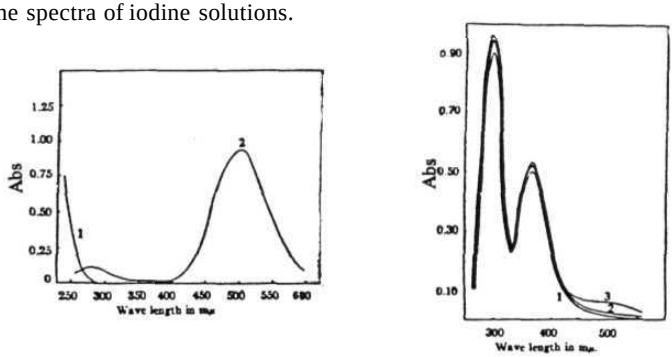

(a) (b)

Figure 2.7 Absorption spectra of (a) $(Me_4N)I$ (1) and I_2 (2); (b) $(Me_4N)I_3$ (1), $(Me_4N)I_5$ (2) and $(Me_4N)I_9$ (3) in ethylene chloride (Ref. 29).

It has been observed that higher polyiodides undergo progressive dissociation into iodine and the triiodide species on dilution (Figure 2.7(b)).[29] At infinite dilution the polyiodides dissociate completely to stable I3" and I_2 species. The electronic absorption spectra of the complexes in different solvents are similar, but are considerably different from the solid state spectra. It is also known that the polyiodides undergo structural reorganization in solution. Hence solid state diffuse reflectance spectra are used to distinguish the polyiodide species. The

molecular levels of symmetric and asymmetric I_3^- are assigned as follows based on the symmetry $D_{\infty h}$ and $C_{\infty v}$ (Figure 2.8).[28]

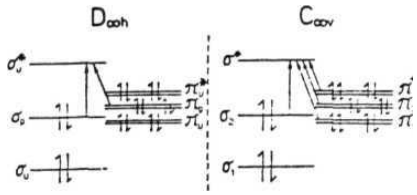

Figure 2.8 Molecular orbitals in symmetrical and asymmetrical linear I_3^- ions.

The reflectance spectra for linear triiodide, pentaiodide and other polyiodide chain complexes were studied and the optical bands were assigned on the above basis (Figure 2.9).[28] The polarized reflectance spectra of isolated symmetric and asymmetric triiodide crystals show broad bands at around 27.0 and 33.0 kK with subbands, due to spin-orbit splitting while the linear chain triiodides show bands at 22.0 and 30.5 kK.

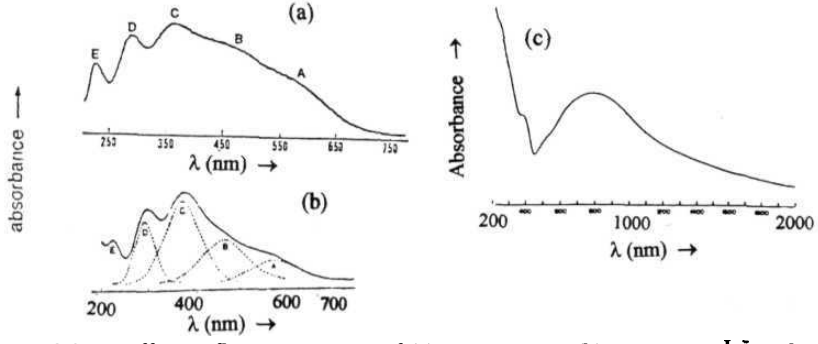

Figure 2.9 Diffuse reflectance spectra of (a) asymmetric, (b) symmetric I_3^- and (c) $(I_5^-)_n$ (Ref.28,4f).

The reflectance spectrum for chains of I_8^{3-} show a plateau with little structure covering the entire measurement range upto 800 nm due to electron delocalisation, while the isolated I_3^- shows a spectrum with a maximum at 570nm and a sloping edge upto 750nm.[24] Featureless absorption was also reported for a polyiodide containing planar I_{12}^{2-} unit and extensive I..I contacts.[10] The disordered chains of higher polyiodides show an additional band around 17.0 kK.25

A series of studies on I_2 adduct compounds with $[ML_3]$ complexes (where L= anionic bidentate ligand, M = Cr^{3+}, Mn^{4+}, Fe^{3+}, Co^{3+}) have been reported.[30] There has also been absorption studies of charge transfer complexes in PPBQ films which show a red-shifted I_3^- band.[13] The reason for the macrocycle tbp to be more readily oxidised than pc, is explained on the basis of the difference in energy levels of p-π orbitals of Co(tbp)I and Co(pc)I, based on the in plane and out-of plane polarised reflectance spectra.[11]

2.4.3 Conductivity Studies

The chemistry of mixed-valence donor-acceptor materials has drawn considerable interest due to the unusual electrical properties.[4e-g] The I_2 acts as an acceptor and fits into the crystal lattice of these materials by occupying one dimensional channels within the stacks of the partially oxidized donor molecules (Figure 2.10).

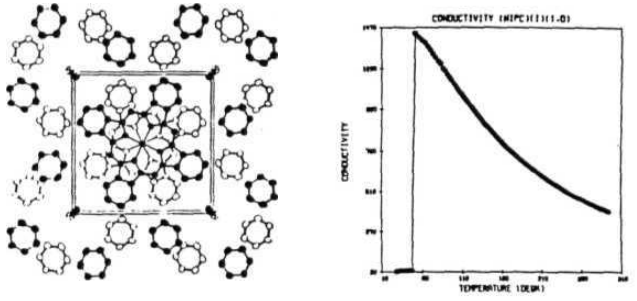

(a) (b)

Figure 2.10 (a) Crystal structure Ni(pc)I viewed along the c-axis, the linear polyiodide chain direction; (b) Electrical conductivity of a Ni(pc)I crystal measured in the *c* direction as a function of temperature (Ref. 4f).

A complete review on highly conductive halogenated low dimensional materials[4f] has classified these systems into various categories. These are the polycyclic aromatic hydrocarbons, the organo nitrogen systems, organo chalcogenide systems, stacked metallo-organic systems, 16-π electron tetraazaannulenes, 22-π electron metallo-macrocycles, porphyrin, other tetraazaanulenes, polyacetylenes etc. Out of these, the stacked metallo-macrocyclic systems have been studied in detail over the past few years. The anisotropic conductivities of these systems show a large variation from semi-conducting to super conducting, by just varying the metal ion or the ligand. A brief summary of the single crystal conductivities of [M(L)]I (stacked metallo-macrocyclic systems) is presented in Table 2.2.

Table 2.2 Single crystal conductivities along the polyiodide chain direction in iodine doped stacked metal lo-macrocyclic systems, [M(L)]I. (p = resistivity)

S No.	**Molecular Formula**	**Conductivity along axis (S cm"^{1})**	**Temperature (K)**	**Comments**	**Ref.**
1.	[Ni(pc)]I	260-750	300 **(RT)**	Molecular metal; $\rho \sim T^{1.9}$ upto 55 K	31
2.	[Ni(tbp)]I	330-600	300 **to 95**	Doubly mixed-valence molecular conductor	32
3.	[Ni(tbp)]I	300-1200	300 **to** 30	Ring-oxidized molecular metal; p $\sim T^{1}$, no double-mixed-valence conductor	33
4.	[Ni(tmp)]I	110	300 to 150	molecular conductor	34
5.	[Co(pc)]I	50	300 **(RT)**	comparable to metal-spine conductor	35
6.	**[Co(tbp)]I**	no measurable magneto-conductance		oxidation of the macrocycle	11

7.	[Cu(pc)]I	1000	300 (RT)	Molecular metal in Fermi Sea	36
8.	[Cu(tatbp)]I	100-500	300 to 150	Metallic conductor in Fermi Sea	37
9.	$[H_2(tbp)]I$	300-1200	300 to 35	Metallic conductor	33

It has been found that polyiodides play a minor role in charge transport, while the π-systems of the ligand columns are pathways for electrical conduction. It has been recently proposed based on crystal orbital calculations, that fully charged polyiodide anion chain could be a carrier of semi-conductivity along the chain direction, provided there is no charge transfer from the chain.[20]

The conductivity value for $[Sb(CH_3)_4]_3I_8$ which has ordered (but not aligned) iodine chains, is in the semi-conducting range, 1×10^{-6} to 10^{-8} Scm^{-1}.[24] Weakly interacting chains of I_7^- show very low conductivity of 2 x 10^{-10} S cm^{-1}.[30] The poly(ethyleneoxide)-NaI systems are found to be better electronic conductors at room temperature than the polyiodides of quarternary ammonium ions.[22] The high conductivity is correlated with the presence of a strong peak at 171 cm^{-1} in the resonance Raman spectra which may be due to higher polyiodide. The electrons from the ITO (indium tin oxide) glass and holes from the polyiodide valence band are responsible for the charge transport in poly(ethyleneoxide) systems.

The synthetic metals "$(ET)_2I_3$" are also popular for their ambient pressure superconductivity with T_c=1.4-1.5 K. Depending on the crystalline phases the conductivity varies as metallic to insulating, to superconducting.[38] The

$(ET)_2(I_3)(I_5)$ and $(ET)_2(I_3)(I_8)_{0.5}$ also show metallic properties due to presence of anionic vacancies producing slightly non-stoichiometric crystals.[39]

2.5 Detailed Structural Reports.

2.5.1 Classification based on the Cations

The polyiodide anions are generally synthesised by using certain types of cations and studied by varying their charge, size and symmetry. These can be broadly divided into few categories. They are the polyiodide salts of

(i) Big alkali cations

(ii) Complex cations

The complex cations are metal atoms coordinated to various types of ligands like ammine, pyridine, imidazole, bidentate ligands, cyclopentadienes, macrocycles or even solvent molecules.

(iii) Quaternary ammonium cations

(iv) Quarternary phosphonium cations

(v) N-containing organic cations

(vi) S-containing organic cations

(vii) Polymeric donor matrices

A table containing the polyiodides based on this classification is presented along with the comments on each compound (Table 2.3).

Table 2.3 Classification of polyiodide anions based on the cation type.

(i) Big alkali cations

SNo.	Molecular Formula	Polyiodide anion(s) involved	Shape of the anion bond distance in Å	Comments	Ref.
1.	CsI_3	I_3^-	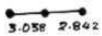	linear asymmetric (T = 113K)	40
2.	RbI_3	I_3^-	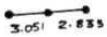	linear asymmetric	41
3.	TlI_3	I_3^-	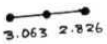	linear asymmetric	41
4.	Cs_2I_8	I_8^{2-}	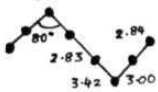	nearly-planar, Z-shaped (centrosym.)	42
5.	$K(H_2O)I_3$	I_3^-	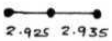	linear nearly symmetric	43

(ii) Complex cations

(a) $[ML_n]^2$

SNo.	Molecular Formula	Polyiodide anion(s) involved	Shape of the anion	Comments	Ref.
1.	$[Zn(NH_3)_4](I_3)_2$	I_3^-	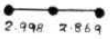	linear asymmetric	44
2.	$[Cu(NH_3)_4(I_2)_2]$	I_4^{2-}		linear coordinated (centrosym.)	45, 46
3.	$[Cu(NH_3)_4I_3)]I_3$	I_3^-	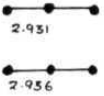	linear coordinated, (centrosym.)	46
4.	$[Cd(NH_3)_4(I_2)_2]$	I_4^{2-}	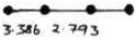	linear coordinated (centosym.)	47
5.	$[Cd(NH_3)_4(I_3)_2]$	$(I_2.I^-)_n$ nearly linear	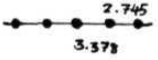	infinite parallel coordinated linear chains	47
6.	$[Pd(NH_3)_4]I_8$	I_8^{2-}	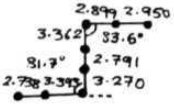	planar Z-shaped ribbons	48

7.	$[Co(NH_3)_4]I_7$	I_3^-, I_4^{2-}	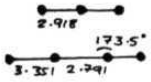	linear symm. I_3^- and slightly bent symm. I_4^{2-}	49
8.	$[Ni(NH_3)_6](I_3)_2$	I_3^-	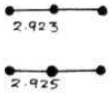	linear symmetric (centrosym.)	50
9.	$[Ni(NH_3)_6](I_5)_2$	I_5^-	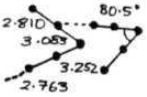	asymmetric V-shaped chain	50
10.	$[Pd(py)_2I_6]$	$[I^-.I_2]_n$	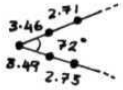	coordinated screw- and zig-zag chains	51
11.	$[Pd(py)_4]I_6$	I_3^-	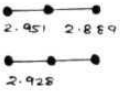	asymmetric linear and symmetric	51
12.	$[Cu(Meimd)_4](I_3)_2$	I_3^-	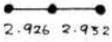	linear sym. having contacts with metal	52
13.	$[Ni(Meimd)_6](I_3)_2$	I_3^-	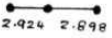	slightly asymmetric	53

14.	$[Ca(H_2O)_7](I_5)_2$	I_5^- 2 types	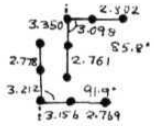	V-shaped planar linear chains formed by one arm	54
15.	$[Mg(H_2O)_6]I_8$	I_8^{2-}	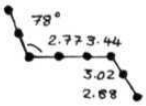	Z-shaped planar	55
16.	$[V(CH_3CN)_6]I_4$	I_4^{2-} discrete		linear more like $(I_3^-.I^-)$	56

(b) $[MA^{\frown}A)_2]^{2+}$, $[M(A^{\frown}A)_3]^{2+}$, $[M(A^{\frown}A^-)_3]^+$

SNo.	Molecular Formula	Polyiodide anion(s) involved	Shape of the anion	Comments	Ref.
17.	$[Ni(en)_2](I_3)_2$	$(I^-.I_2)_n$	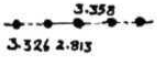	zig-zag chains, non-linear	57
18.	$[Mn(mod)_3]I_5.$ CH_2Cl_2	I_5^- 2 types	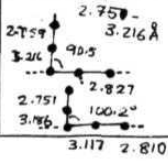	V-shaped chains forming 2-dim. network	30d

19.	$[Cu(dafone)_3]I_{12}$	I_{12}^{2-} discrete	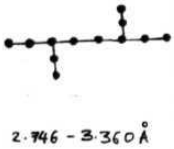	centrosym. planar (channel forming network)	10

(c) $[Fe(Cp)_2]^+$ and related cations

SNo.	Molecular Formula	Polyiodide anion(s) involved	Shape of the anion	Comments	Ref.
20.	$[Fe(Cp)_2]I_3$	I_3^-		linear symmetric (centrosym.)	58
21.	$[Fe(Cp)_2]I_7$	$(I_7^-)_n$		parallel chains formed from I_5^- and I_2; rope-like ribbons	59
22.	$[Fe(Cp)_2]_2I_{16}$	$(I_{16}^{2-})_n$		I_{16}^{2-} nets forming 34-membered ring-channels	60

23.	$[Fe(Cp)_2]_3I_{29}$	I_{29}^{3-}	*complex network*	3-dim. network $[(I_5^-).(I_{12}^{2-})]_{1/2}.3I_2$	8b
24.	$[Fe(Me_2Cp)_2]I_3$	I_3^-	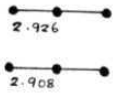	symmetric linear	61
25.	$[Fe(Me_2Cp)_2]I_5$	$(I_5^-)_n$		concatenated I_5^-, $(I_3^-.I_2)$ chains with alternating planar and helical regions	61
26.	$[Fe(Me_5Cp)_2]I_3$	I_3^- discrete		linear symmetric	62
27.	$[Fe(Me_5Cp)_2]I_5$	I_5^- discrete	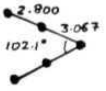	opened-out I_5^- ions	62
28.	$[Fe(Me_5Cp)_2]_4I_{26}$	I_{26}^{4-}	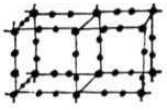	anionic channels, grating derived from cubic lattice	62

29.	$[Fe_2^{II,III}(Cp)_2(Cp_2Se)]I_5.CH_2Cl_2$	$(I_5^-)_n$		zig-zag chains of $I_3^-.I_2$	63
30.	$[Fe_2^{II,III}(Cp)_2(Br\text{-}PhCp)_2]I_5$	$(I_5^-)_n$	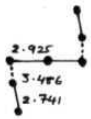	zig-zag chains of alternating $I_3^-.I_2$	64
31.	$[Fe_2^{II,III}(Cp)_2(naph\text{-}MeCp)_2]I_3$	I_3^- discrete 2 diff. crystals	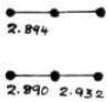	one linear sym., other slightly asym.	65
32.	$[Cr_2^{II,II}(Cp)_2I_3]_2I_{16}$	I_{16}^{2-}		spindle-shaped I_2 linked 3-dim. network	66

(d) Macrocycles and cryptates, $[M(Mac)]^{1+/2+}$ and related cations

SNo.	Molecular Formula	Polyiodide anion(s) involved	Shape of the anion	Comments	Ref.
33.	$[Ni(TAAB)](I_3)_2$	I_3^- 2 types	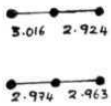	nearly symmetric I_3^- ions	67

34.	$[Pd(TAAB)]I_8$	I_8^{2-}	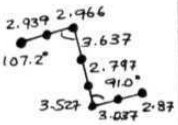	Z-shaped non-planar chains of $I_3^-.I_2.I_3^-$	67
35.	$[Pt(TAAB)]I_8$	I_8^{2-}	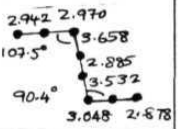	Z-shaped non-planar chains	68
36.	$[Ni(TAAB)]I_8$	I_8^{2-}		isostructural to $[Pd(TAAB)]I_8$	67
37.	$[Ag(aneS3)_2]I_5$	I_5^- discrete	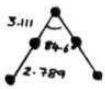	V-shaped	4j
38.	$[Ni(aneS3)_2](I_3)_2$	I_3^-		isolated I_3^-	4j
39.	$[Co(aneS3)_2](I_3)_2$	I_3^-		isolated I_3^-	4j
40.	$[Pd(aneS3)_2](I_3)_2$	I_3^-		isolated I_3^-	4j
41.	$[Pd(aneS4)](I_3)_2$	I_3^-		isolated I_3^-	4j

42.	$[Pd_2(aneS4)_2I]I_{11}$	I_{11}^{3-}	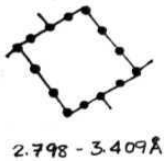	L-shaped I_5^- and I^- forming 14-membered rings	4j
43.	$[Pt_2(aneS4)_2I]I_{11}$	I_{11}^{3-}	*same as above*	infinite polycyclic ribbon	4j
44.	$[Rh(aneS4)Cl_2]I_7$	I_5^-, I_2	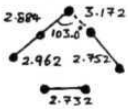	3-dim. matrix made of I_5^- and elongated I_2	4j
45.	$[Ag(aneS5)]_2I_{12}$	I_{12}^{2-} $\{(I_4^{2-})$ $.(4I_2)\}$	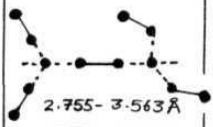	twisted H configuration	4j
46.	$[Ag(aneS6)]I_3$	I_3^-	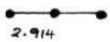	linear symmetric	4j
47.	$[Ag(aneS6)]I_7$	$(I_7^-)n$	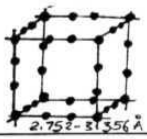	3-dim. matrix, distorted cubic lattice	4j
48.	$[Ni(aneN4)(CH_3CN)_2](I_3)_2$	I_3^-		isolated I_3^-	4j
49.	$[Pd(aneN4)](I_3)_2$	I_3^-		isolated I_3^-	4j

50.	$[Pd_2Cl_2(aneN2S4)](I_3)_2$	I_3^-	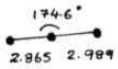	slightly asymmetric I_3^-	4j
51.	$[Pd_2Cl_2(aneN2S4)]_{1.5}(I_5)(I_3)_2$	I_5^-, I_3^-	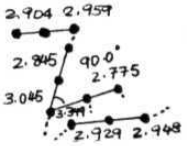	2-dim. layers of linked I_3^- form alternating fused ribbons	4j
52.	$[K(aneO5)]I_9$	$(I_9^-)_n$		3-dim. matrix, puckered cube-like cages	4j
53.	$[KCryp(2.2)]I_3$	I_3^-	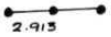	linear symmetric (centrosym.)	69
54.	$[KCryp(2.2.2)]_2I_{12}$	I_{12}^{2-} discrete		I_{12}^{2-} from $2I_5^-$ bridged to an I_2; (centrosym.)	70
55.	$[K(18\text{-}C\text{-}6)]_2I_{12}$	I_{12}^{2-} discrete	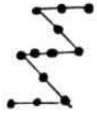	long fragment of $(I_3.I_2)$ chain (centrosym.)	71
56.	$[Cu(OETPP^{\bar{\cdot}})I_7$	I_7^-		discrete $(I^-).(3I_2)$	72

57.	[Cs(18-C-6)]I_3	I_3^-	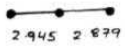	asymmetric isolated	73
58.	[Pb(18-C-6)]I_3	I_3^-	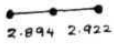	linear asymmetric isolated	73

(e) Partially oxidized (mixed valent) systems

SNo.	Molecular Formula	Polyiodide anion(s) involved	Shape of the anion	Comments	Ref.
59.	[Ni(pc)]I	$(I_3^-)_n$ I-I 3.00 Å, I..I 3.72 Å	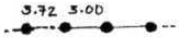	disordered iodine chains along 4-fold axis	31
60.	[Ni(tbp)]I	$(I_3^-)_n$	*all SNo.s 60-65 have similar shape as above*	disordered chains	32
61.	[Ni(tmp)]I	$(I_3^-)_n$		disordered chains	34
62.	[Co(pc)]I	$(I_3^-)_n$		disodered chains	35

63.	[Co(tbp)]I	$(I_3^-)_n$		disordered chains	11
64.	[Cu(pc)]I	$(I_3^-)_n$		disordered chains	36
65.	[Cu(tatbp)]I	$(I_3^-)_n$		disordered chains	37

(iii) $[ER_4]^+$, $[ER_2]^{2+}$

SNo.	Molecular Formula	Polyiodide anion(s) involved	Shape of the anion	Comments	Ref.
1.	$[NH_4]I_3$	I_3^-	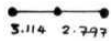	linear asymmetric	74
2.	$[(PPh_3)_2NH]I_3$	I_3^-	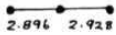	slightly asymmetric and isolated	75
3.	$[(Et)_4N]I_7$	$(I_7^-)_n$	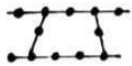	at R.T. and L.T.; zig-zag chains	76, 77
4.	$[(Et)_2(Me)(Ph)]I_3$	I_3^-	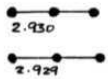	linear symmetric	77

5.	$[(Me)_2(Ph)_2N]I_3$	I_3^-		nearly linear symmetric	78
6.	$[(Me)_2(Ph)_2N]_3I_{13}$	I_{13}^{3-}	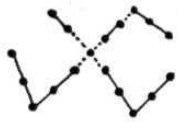	zig-zag chains of I^- and I_2 connected to 2 I_5^-	78
7.	$[(Me)_2(Ph)_2N]_2I_{12}$	I_{12}^{2-}	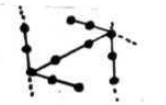	$2I_5^-$ bridged to an I_2; secondary bonds forming double chains	78
8.	$[(Me)_2(Ph)_2N]_2I_{16}$	I_{16}^{2-}	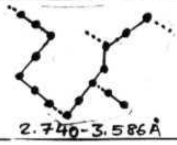	layers of 2 I_7^- and one I_2	78
9.	$[(nPr)_4N]I_3$	I_3^- 2 types		linear symmetric (centrosym.)	79
10.	$[(nPr)_4N]I_5$	$(I_5^-)_n$ 12-mem. meshes		slightly puckered square nets	79
11.	$[(nPr)_4N]I_7$	$(I_7^-)_n$	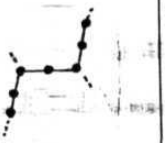	Z-shaped (centrosym.) twisted rope-ladders	79

12.	$[(nBu)_4N]I_3$	I_3^- 2 types	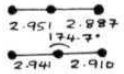	slightly asymmetric	80
13.	$[(Me)_4N]I_3$	I_3^-	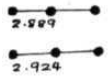	linear symmetric	4h
14.	$[(Me)_2NH_2]I_3$	I_3^-	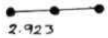	nearly linear symmetric	4i
15.	$[(Me)_4P]I_3$	I_3^- 3 types		2 sym. and one slightly asym.	4h
16.	$[(Me)(Ph)_3P]_2I_8$	I_8^{2-}	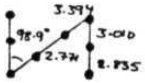	Z-shaped nearly planar	73
17.	$[(Me)(Ph)_3P]_4I_{22}$	I_{22}^{4-}	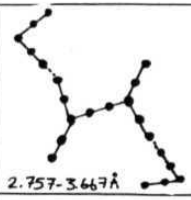	one I_{12}^{2-} end-on bonded to 2 I_5^- (centrosym.)	8a
18.	$[(Et)(Ph)_3P]I_3$	I_3^-	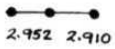	slightly asym. and bent; isolated	7b
19.	$[(Et)(Ph)_3P]I_5$	$(I_5^-)_n$		rope-ladder like iodine ribbons	7b

20.	$[(Et)(Ph)_3P]I_7$	$(I_7^-)_n$		I_5^- and I_2 connected to form puckered layers	7b
21.	$[(Ph)_4P]I_7$	I_7^- (discrete)		extended 3-dim. structure I..I 3.605 Å	25
22.	$[Me_4As]I_3$	I_3^- 2 types		linear symmetric	24
23.	$[Me_4Sb]_3I_8$	$(I_8^{3-})_n$		infinite linear chains	24
24.	$[(Me)_2TeI(I_3)]$	$(I^-.I_2)_n$	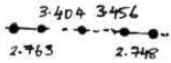	coordinated zig-zag chains, non-linear	81
25.	$[UrH]I_3$	I_3^-		slightly distorted with end-to-end contacts	82
26.	$[Ur\text{-}Me]I_3$	I_3^- 2types	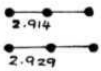	linear symmetric	83

27.	[Ur-Et]I_3	I_3^-	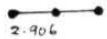	linear symmetric	83
28.	[Ur-nPr]I_3	I_3^- 3 types		all slightly asymmetric and distorted	83
29.	[Ur-nPr]I_5	I_5^- 2 types		V-shaped I_5^- pairs with long contacts	84
30.	[Ur-nPr]I_7	$(I_7^-)_n$		2-dim. network	84
31.	[Ur-nBu]I_3	I_3^-	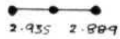	linear asymmetric	83
32.	[BenzamideH]I_3	$(I_3^-)_n$	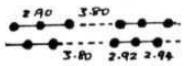	1-dim. nearly linear disordered chains	85
33.	[QuinuclidineH]I_5	$(I_5^-)_n$	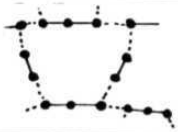	2-dim. rope-ladder network	86
34.	$[(py)_2I]I_7$	$(I_7^-)_n$		coarse-meshed network	87

35.	$[Me\text{-}N4\text{-}Adam]_2I_8$	I_8^{2-}	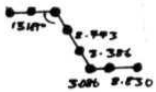	out-stretched Z-shaped planar	88
36.	$[Me_4\text{-}1,2Etham](I_3)_2$	I_3^-	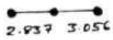	linear asymmetric	4i
37.	$[Me_4\text{-}1,3Propam](I_3)_2$	I_3^- 4 types	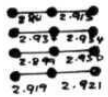	2 sym. and other 2 slightly asym.	4i
38.	$[Tropanium]I_3$	I_3^-	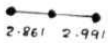	slightly asymmetric and bent	4i
39.	$[Me\text{-}Piper](I_3)_2$	I_3^- 2 types	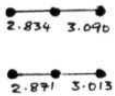	nearly linear asymmetric	4i
40.	$[Me_2\text{-}Piper](I_3)_2$	I_3^-	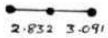	linear asymmetric short contacts	4i
41.	$[Quinuclidinium]I_3$	I_3^- 2 types	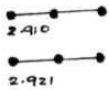	linear symmetric	4i
42.	$[1\text{-}azo\text{-}prop]I_3$	I_3^- 7 types	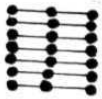	all nearly linear and symmetric	4i

43.	$[DabcoH_2](I_3)_2$	I_3^- 2 types	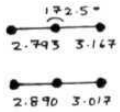	both asymmetric and one linear	4i
44.	$[\beta\text{-Naphtham}]I_5$	$(I_5^-)_n$		zig-zag chains	89
45.	$[phenaH]_2I_4.2H_2O$	I_4^{2-}		linear $I^-.I_2.I^-$	90
46.	$[ThreobromineH]_2I_{16}$	I_{16}^{4-}	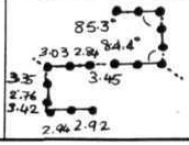	S-shaped planar (centrosym.)	91

(iv) $[ArNH]^+$ and related cations

SNo.	Molecular Formula	Polyiodide anion(s) involved	Shape of the anion	Comments	Ref.
1.	$[bpyH]I_3$	I_3^-	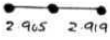	nearly sym. and linear isolated	7a

2.	[bpyH]I_5	$(I_5^-)_n$		I_3^- to 2 I_2's in a trigonal planar way forming zig-zag chains	7a
3.	[bpyH]I_7	$(I_7^-)_n$		V-shaped I_5^- to I_2 in a trigonal pyramidal way forming zig-zag chains	7a
4.	[(i-Pr)Taz]I_3	I_3^- 2 types	2.910 2.910	linear asymmetric alternating	92
5.	[(i-Pr)Taz]I_5	I_5^-		V-shaped isolated	92
6.	[(t-Bu)Taz]I_3	I_3^-	2.923 2.906	linear symmetric	92
7.	[(t-Bu)Taz]I_5	I_5^-		I_3^- and I_2 form zig-zag chains	92
8.	[(t-Bu)Taz]I_7	$(I_7^-)_n$		3-dim. network of alternating pyramidal and Z-shaped I_7^-	92

9.	[(Et)Taz]I_3	I_3^- 2 types	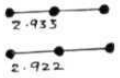	linear symmetric alternating	92
10.	[PyrazineH]$_2I_{10}$	$(I_7^-)_n$ and $(I_3^-)_n$	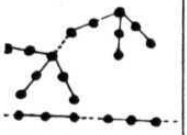	2 distinct moieties; sheets of I_7^- and zig-zag chains of I_3^-	93
11.	[(Me)$_4$PyrazineH]I_3	I_3^-		linear asymmetric	94
12.	[(Me)$_4$PyrazineH]I_5	$(I_5^-)_n$		branched chains inter-woven to form sheet-structure	94
13.	[pyH]I_5	$(I_5^-)_n$	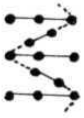	pyramidal tri-coordinated branched chains	89
14.	[n-Me-γ-pico]I_7	$(I_7^-)_n$	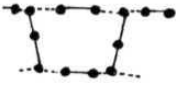	twisted ladder-like networks, I_3^- forming bridges	89

(v) Organic S-containing cations

SNo.	Molecular Formula	Polyiodide anion(s) involved	Shape of the anion	Comments	Ref.
1.	$[EOST]_2I_3$	I_3^-		linear symmetric filled in between the EOST stacks	6
2.	$[morH]_2I_{16}$	I_{16}^{4-}	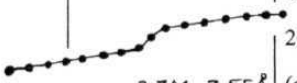	nearly linear $2(I_8^{2-})$ (centrosym.)	95
3.	$[tetrazole]I_3$	I_3^-	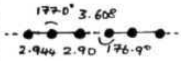	linear chains	96
4.	$[D_2I]I_3$	I_3^- (2 types)	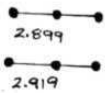	linear symmetric	23
5.	$[(bntMe)_2I]I_7$	I_7^- (discrete) $(I^-).(3I_2)$	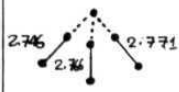	contact of 3.507 Å between anions	23

6.	$[ET]_2I_3$	I_3^-		chains of I_3^-	38
7.	$[ET]_2(I_3)(I_5)$	I_3^-, I_5^-	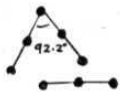	V-shaped planar I_5^- and linear I_3^-	39
8.	$[ET]_2(I_3)(I_8)_{0.5}$	I_3^-, I_8^{2-}		Z-shaped planar I_8^{2-} and linear I_3^-	39

(vi) Other Organic cations

SNo.	Molecular Formula	Polyiodide anion(s) involved	Shape of the anion	Comments	Ref.
1.	$[(18\text{-}C\text{-}6).H_3O]I_7$	$(I_7^-)_n$	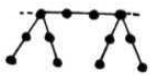	infinite saw-horse	97
2.	$[Ph_2I]I_3$	I_3^-	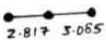	asymmetric and slightly bent	4i

(vii) Polymeric donor matrices (partially oxidised systems)

SNo.	Polymeric system	Polyiodide anion(s) involved	Shape of the anion	Comments	Ref.
1.	Poly(ethyleneoxide)-NaI	$(I_3^-)_n$		based on res-Raman and diffuse reflectance	22
2.	Poly(vinylalcohol); (PVA)	$(I_3^-)_n$, $(I_5^-)_n$	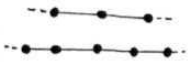	intermixed I_5^- and I_3^- chains	12
3.	Poly(cyclophosphazene-benzoquinone); (PPBQ)	$(I_3^-)_n$, $(I_5^-)_n$	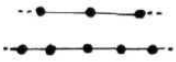	1-dim. chains	98
4.	Poly(acetylene)	$(I_3^-)_n$, $(I_5^-)_n$	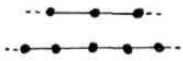	linear I_5^- or asymmetric bent I_3^-	99

2.5.2 Commonly occuring Polyiodide Anions.

The commonly occuring polyiodide ions are the I_3^-, I_4 ", I_5^-, I_7^-, I_8^{2-}, I_9^- and the I_{16}^{4-}. These ions are briefly described in a systematic way, based on the data in Table 2.3.

I_3^- : A discrete triiodide anion (a combination of I_2 and I"), is the most commonly occuring polyiodide species which is linear or nearly linear in all cases.

It may be symmetric[69] with equal I-I distances and asymmetric[40] with one long and another short distance closer to I-I distance in solid I_2. The sum of the two distances is always equal to a constant value of 5.8(1) A. Besides discrete I_3^- ion, there are also compounds wherein the I_3^- ions are connected to one another via van der Waals contacts. These occur as infinite linear chains mostly in combination with stacked metal complex cations and are often disordered.[31] (scheme 1)

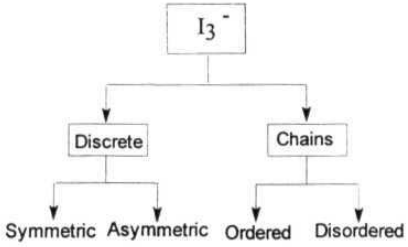

Scheme 1

I_4^{2-} : The anion I_4^{2-} is a linear ion and is formed by interaction of $2I^-$ with one I_2[47] or one I" with an asymmetric I_3^-.[56] (scheme 2)

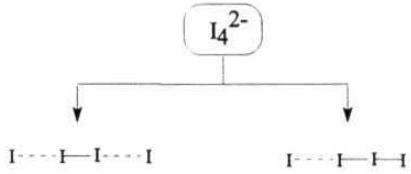

Scheme 2

I_5^- : The pentaiodide species as a discrete ion is made of two I_2 molecules bridged to an I" ion forming a V-shaped ion (angle 90°±10).[4j] It also occurs as L-

shaped zig-zag networks (formed from I_3^- and I_2 interactions)[64,94] and in some cases as linear chains.[21] (scheme 3)

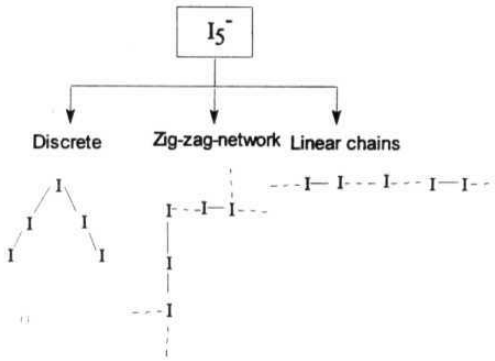

Scheme 3

I_7^- : The I_7^- ion exists as a branched ion, either in discrete form or as networks. The discrete ion has a 3-pronged structure and is made up of a central I" interacting equally with 3 I_2 molecules[23,72] or an I_3^- ion with 2 I_2 molecules[25] or an I_5^- ion with one I_2 molecule (scheme 4).[7a] An infinite network is formed from the above ions interconnected to each other by long bonds, < 3.50 A. In a few cases, the I_7^- forms very symmetric anionic lattice such as cubic cages in $[Ag(aneS6)]I_7$.[4j]

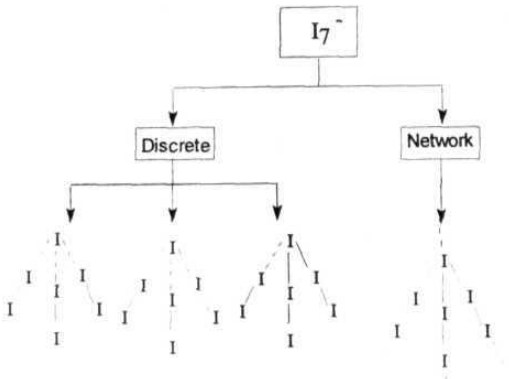

Scheme 4

I_8^{2-} : A discrete I_8^{2-} ion is formed when an I_2 is bridged between 2 I_3^- ions. The interaction is such that the ion is always Z-shaped[42] or has an out-stretched Z-shape.[88] The Z-shaped I_8^{2-} ion is mostly planar and only in few cases it is non-planar with dihedral angles of ~ 90° between the two halves.[68] The I_8^{2-} also occurs in dimeric form as I_{16}^{4-}, with a planar S-shape[91] or nearly linear chain.[95] Some of the I_8^{2-} ions are completely isolated ones while others have van der Waals' contacts with other units at the two arms of the ions. (scheme 5)

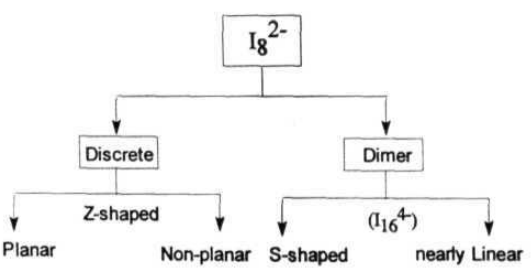

Scheme 5

I_9^- : A discrete I_9^- ion, like I_7^-, is a branched ion made from smaller fragments of an I_5^- and 2 I_2 molecules.[100] The I_9^- is not so commonly occuring as I_3^-, I_5^- and I_7^-, which are often obtained easily with the same cation by varying the amount of I_2. This ion also generally forms networks containing numerous I-I long bonds and contacts between the I_9^- ions.[4j] (scheme 6)

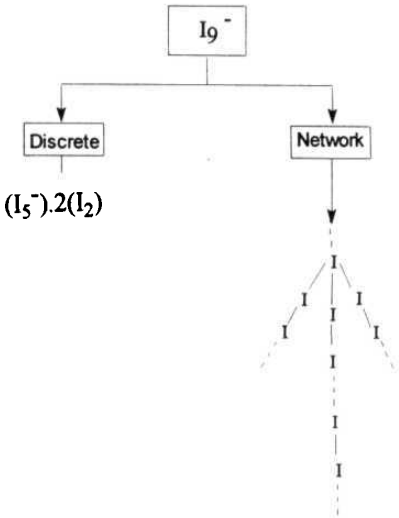

Scheme 6

2.5.3 New-type of Polyiodide Anions.

The new type of anions are mostly formed as networks, rather than discrete ones. The discrete I_{12}^{2-} unit, though discovered recently, is found to form with many types of cations and has a branched structure in most cases. The new anions are generally the ones with high iodine content and are less stable at room temperature.

In the case of infinite chains and networks, it may not be always possible to identify poly iodide units such as I_{2n-1}^- or I_{2n}^{2-}. It is sometimes useful to indicate the formula of such compounds in the form of I_p^-. The highest value of p, so far known, is 9.67, found in $[Cp_2Fe]_3I_{29}$.[4i]

I_8^{3-} / ($I_{2.67}^-$) : These species were found to occur as infinite linear non-aligned chains. It is difficult to split the species into smaller fragments, as each one of the I atoms are separated by 3.3 A from its adjacent atom (Figure 2.11).[24]

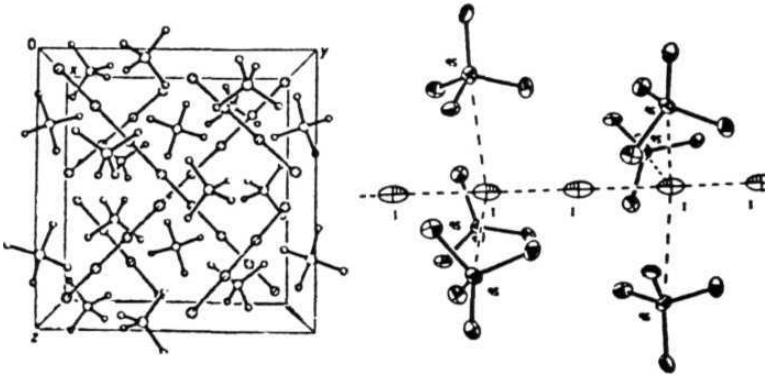

(a) **(b)**

Figure 2.11 (a), (b) Structure of $[Me_4Sb]_3I_8$ showing linear iodine chains of the type $(I_8^{3-})_n$ (Ref. 24).

I_{11}^{3-} : The I_{11}^{3-} is also a rare species, formed as counter-ion for the cation $[M_2(aneS4)_2I]^{3+}$ (M=Pd/Pt). The smaller units of I_5^- and I" can be identified from this species which combine to form infinite arrays of 14-membered rings (Figure 2.12).[4j]

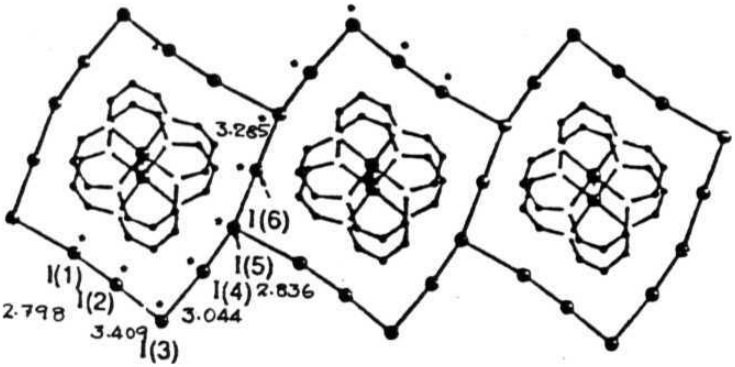

Figure 2.12 View of $[Pd_2(aneS4)_2I]I_{11}$ showing 14-membered polyiodide rings fused to give an infinite polycyclic ribbon (Ref. 4j).

I_{12}^{2-} : As mentioned earlier, the I_{12}^{2-} ion has been very recently found to occur with many types of cations. It is generally formed from an interaction of an I_2 bridged between 2 I_5^- ions, which results in a discrete branched structure (Figure 2.13).[70,10,4j,71,78,101]

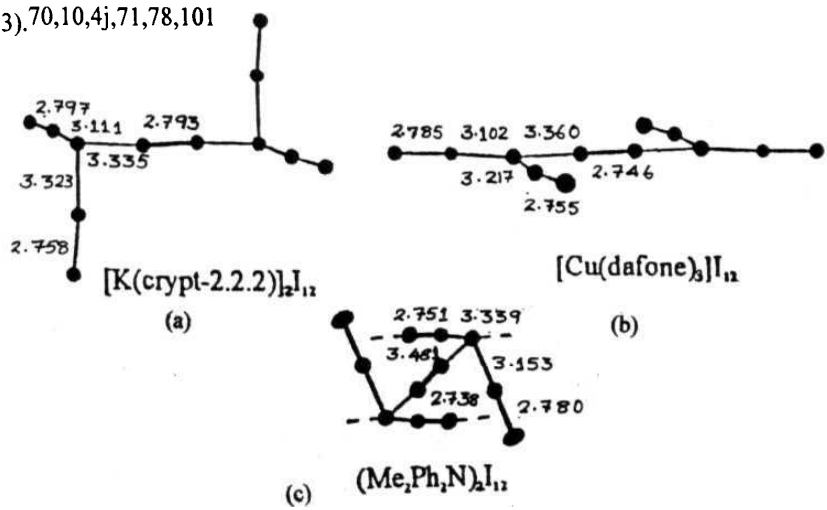

Figure 2.13 Different shapes of I_{12}^{2-} ion known: (a) discrete branched non-planar, (b) discrete branched planar, (c) branched non-planar network

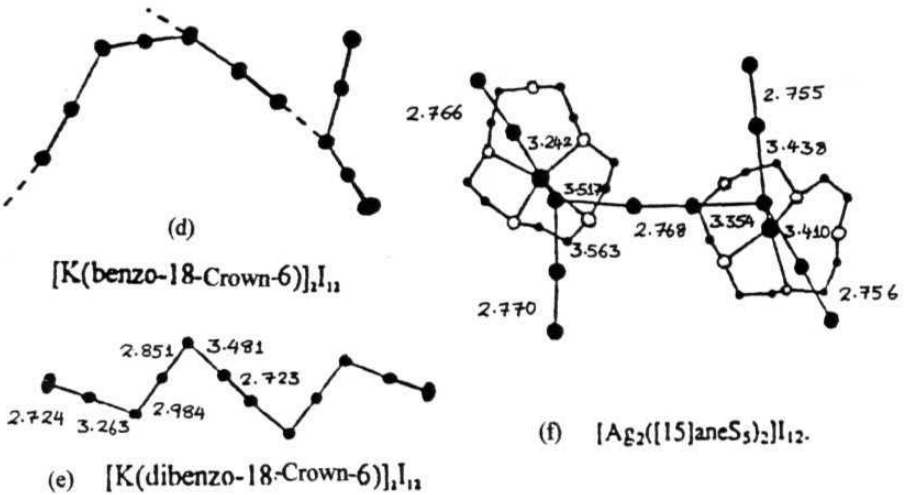

Figure 2.13 (cont'd) Different shapes of I_{12}^{2-} ion known: (d) network, (e) zig-zag ribbon and (f) discrete twisted H shape

I_{13}^{3-} : Only one species of I_{13}^{3-} has been isolated in the compound $[Me_2Ph_2N]_3I_{13}$, which is formed from zig-zag chains of I_2 and I" weakly coordinated to 2 I_5^- ions (Figure 2.14).[78]

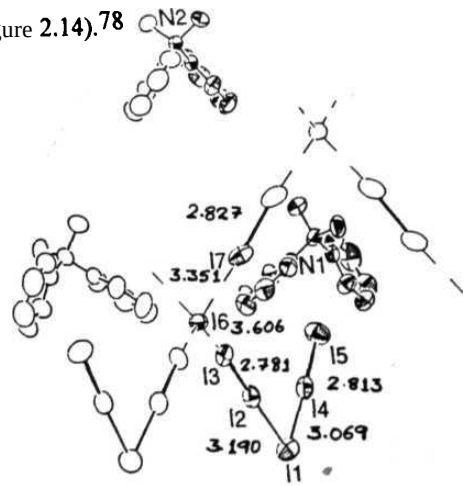

Figure 2.14 Structure of $[Me_2Ph_2N]_3I_{13}$(Ref. 78)

I_{16}^{2-} Earlier, the I_{16}^{2-} ion was found to occur as spindle shaped anion in $[Cp_2CrI_3]I_{16}$.[66] Recently the ion has been found in two other complexes but with different shapes (Figure 2.15).[60,78] In $[Fe(Cp)_2]_2I_{16}$, nets of I_{16}^{2-} ions formed from two symmetric I5" ions bridged by I_2 units, assemble to form large channels filled with cations. The I_2 unit distances vary from 2.721 to 2.778 A and the bridging distances are in 3.480 to 3.544 A range. Whereas in $[Me_2Ph_2N]_2I_{16}$, two Z-shaped I_7^- ions and an I_2 molecule bond to each other at distances of 3.445 to 3.586 A to form layers of I_{16}^{2-} ions.

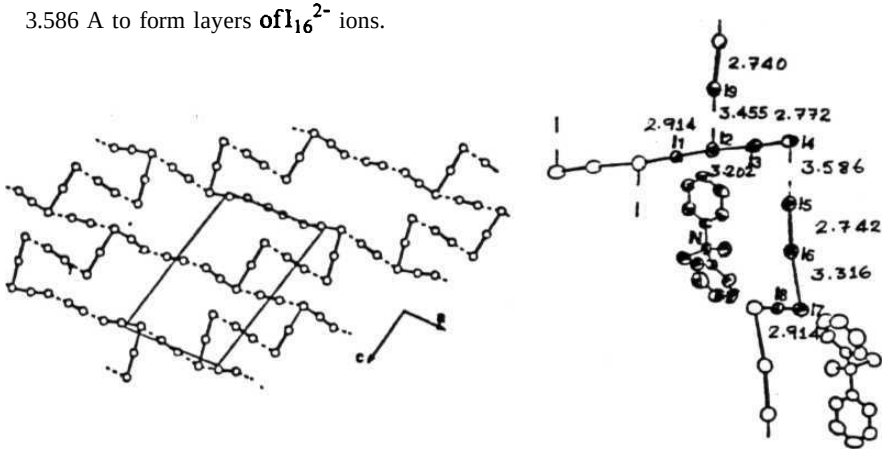

(a) (b)

Figure 2.15 Two different shapes of I_{16}^{2-} ion in (a) $[Fe(Cp)_2]_2I_{16}$ and (b) $[Me_2Ph_2N]_2I_{16}$.

I_{22}^{4-} : The large I_{22}^{4-} species is made up of a central I_{12}^{2-} ion interacting with 2 I_5^- ions on both the sides (Figure 2.16).[8a]

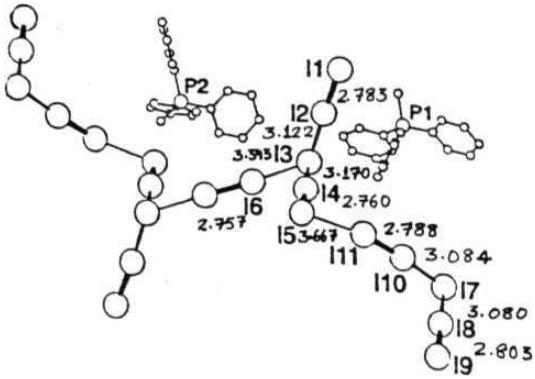

Figure **2.16** Structure of I_{22}^{4-} ion in $[MePh_3P]_4I_{22}$ (Ref. 8a).

I_{26}^{4-} / ($I_{6.5}^{-}$) :This polyiodide forms anionic channels made up of I_2 and I" ions. The anionic grating is derived from a primitive cubic lattice (Figure 2.17).[62] There are two types of I" ions, one with a coordination of six I_2 units around it and another with five I_2 units, bonded at distances in the range of 3.232 to 3.641 A. The bridging I_2 units have bond distances in the range of 2.732 to 2.768 A.

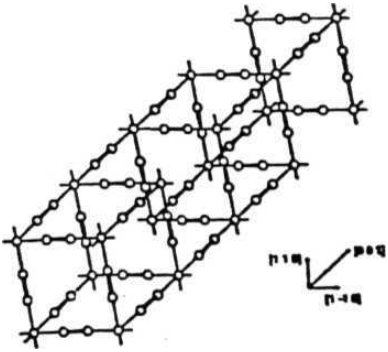

Figure 2.17 Structure of I_{26} " ion showing iodine atoms placed on a cubic-like lattice in $[Fe(MeCp)_2]_4I_{26}$ (Ref. 62).

I_{29}^{3-} / ($I_{9.67}^{-}$) : The most iodine-rich compound yet known is the $[Cp_2Fe]_3I_{29}$ with $I_{9.67}^{-}$ per cation. The I_{29}^{3-} anion is a complex network formed by bands of I_{12}^{2-} ions and chains of I_5^{-} ions that are bridged by I_2 molecules (Figure 2.18).[8b]

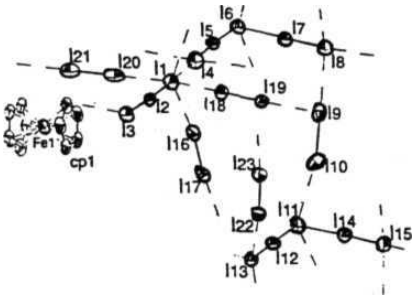

Figure 2.18 Part of the complex network of I_{29}^{3-} ion (Ref. 8b).

2.5.4 Polyiodide Doped Systems.

Polymeric matrices such as poly(vinyl)alcohol, form dark blue complex with aqueous I_2 in presence of KI, similar to the starch-iodine or the amylose-iodine complex. The polyiodides in these complexes are believed to be quasi-one-dimensional and composed mainly of I3" and I_5^{-} chains. In thin film form these iodine doped complexes are high-quality optical polarizers.[12] The incorporation of iodine in the polymer host, the nature of the interaction between the polyiodide chains and the host and the structure of polyiodides in the complex has been studied extensively. The structure and its relationship to the electronic and vibrational properties of these aggregates using resonance Raman and UV/Vis spectroscopy as the main tools is an active field of investigation.

References

(1) N. N. Greenwood and A. Earnshaw in *Chemistry of the Elements,* Pergamon Press, Oxford (United Kingdom), 1985, p.920.

(2) J. Passmore, P. Taylor, T. Whidden and P. S. White *Can. J. Chem.* 1979, *57,* 968.

(3) F. H. Herbstein and W. Schwotzer *Angew. Chem. Int. Ed. Engl.* 1982 *21,* 219.

(4) (a) A. I. Popov in *Halogen Chemistry,* Ed. V. Gutmann, Academic Press, London (United Kingdom), 1967, vol. 1, p.225. (b) A. J. Downs and C. J. Adams in *Comprehensive Inorganic Chemistry,* Eds. J. C. Bailer, H. J. Emeléus, R. Nyholm and A. F. Trotman-Dickenson, Pergamon Press, Oxford (United Kingdom), 1973, vol. 3, p. 1476. (c) E. H. Wiebenga, E. E. Havinga and K. H. Boswijk in *Adv. Inorg. Chem. Radiochem.*, Academic Press, New York (USA), **1961,** vol.3, p. 133. (d) K. -F. Tebbe in *Homoatomic Rings, Chains and Macromolecules of Main-group Elements,* Ed. A. L. Rheingold, Elsevier, Amsterdam (The Netherlands), 1977, p.551. (e) P. Coppens in *Extended Linear Chain Compounds,* Ed. J. S. Miller, Plenum, New York (USA) **1982,** vol. 1, p.333. (0 T. J. Marks and D. W. Kalina in *Extended Linear Chain Compounds,* Ed. J. S. Miller, Plenum, New York (USA) 1982, vol.1, p. 197. (g) J. R. Ferraro *Coord. Chem. Rev.* **1982,** *43,* 205. (h) P. K. Bakshi, M. A. James, T. S. Cameron and O. Knop *Can. J. Chem.* 1996, *74,* 559. (i) K. N. Robertson, T. S. Cameron and O. Knop *Can. J. Chem.* **1996,** *74,* 1572. 0) A. J. Blake, F. A. Devillanova, R. O. Gould, W. -S. Li, V. Lippolis, S. Parsons, C. Radek and M. Schroder *Chem. Soc. Rev.* **1998,** *27,* 195

(5) A. I. Popov and R. E. Buckles in *Inorganic Syntheses,* McGraw-Hill, New York (USA), **1957,** vol. 5, p. 167.

(6) T. Naito, A. Tateno, T. Udagawa, H. Kobayashi, R. Kato, A. Kobayashi and T. Nogami *J. Chem. Soc, Faraday Trans.* **1994,** *90,* 763.

(7) (a) K. -F. Tebbe and M. Bittner *Z. anorg. allg. Chem.* **1995,** *621,* 218. (b) K. -F. Tebbe and T. Farida Z *Naturforsch.* **1995,** *50b,* 1685.

(8) (a) K. -F. Tebbe and T. Farida Z *Naturforsch.* **1995,** *50b,* 1440. (b) K. -F. Tebbe and R. Buchem *Angew. Chem. Int. Ed. Engl.* **1997,** *36,* 1345.

(9) A. J. Blake, R. O. Gould, S. Parsons, C. Radek and M. Schroder *Angew. Chem. Int, Ed. Engl.* **1995,** *34,* 2374.

(10) (a) S. Menon and M. V. Rajasekharan *Inorg. Chem.* **1997,** *36,* 4983. (b) S. Menon, Ph.D. Thesis, University of Hyderabad, Hyderabad, India, 1996.

(11) K. Liou, T. P. Newcomb, M. D. Heagy, J. A. Thompson, W. B. Heuer, R. L. Musselman, C. S. Jacobsen, B. M. Hoffman and J. A. Ibers *Inorg. Chem.* 1992,57,4517.

(12) A. Sengupta, E. L. Quitevis and M. W. Holtz *J. Phys. Chem.B* **1997,** *101,* 11092.

(13) M. Josowicz, J. Li, C. F. Windisch Jr., G. J. Exarhos, D. R. Baer, W. D. Samuels and M. D. Ulmen *Chem. Mater.* **1997,** *9,* 1285.

(14) J. C. Slater *Acta Crystallogr.* **1959**, *12*, 197.

(15) E. H. Wiebenga nd D. Kracht *Inorg. Chem.* **1969,** *8,* 738.

(16) (a) S. B. Sharp and G. I. Gellene *J. Phys. Chem. A* **1997,** *101,* 2192. (b) A. D. Becke *J. Chem. Phys.* **1993,** *98,* 5648. (c) Z. Lin and M. B. Hall *Polyhedron* **1993** *12,* 1499.

(17) G. A. Landrum, N. Goldberg and R. Hoffmann *J. Chem. Soc, Dalton Trans.* **1997,** 3605.

(18) (a) G. C. Pimentel *J. Chem. Phys.* **1951,** *19,* 446. (b) R. J. Hach and R. E. Rundle *J. Am. Chem. Soc.* **1951,** *73,* 4321.

(19) H.-B. Bürgi *Angew. Chem. Int. Ed. Engl.* **1975,** *14,* 460.

(20) E. B. Starikov *Int. J. Quant. Chem.* **1997,** *64,* 473.

(21) E. M. Nour, L. H. Chen and J. Laane *J. Phys. Chem.* **1986,** *90,* 2841.

(22) L. C. Hardy and D. F. Shriver *J. Am. Chem. Soc.* **1986,** *108,* 2887.

(23) F. Demartin, P. Deplano, F. A. Devillanova, F. Isaia, V. Lippolis and G. Verani *Inorg. Chem.* **1993,** *32,* 3694.

(24) U. Behrens, H. J. Breunig, M. Denker and K. H. Ebert *Angew. Chem. Int. Ed. Engl.* **1994,** *33,* 987.

(25) M. Mizuno, J. Tanaka and I. Harada *J. Phys. Chem.* **1981,** 55, 1789.

(26) R. Poli, J. C. Gordon, R. K. Khanna and P. E. Fanwick *Inorg. Chem.* **1992, 57,3165.**

(27) P. Deplano, F. A. Devillanova, J. R. Ferraro, J. R. Mercuri, L. Maria, V. Lippolis and E. F. Trogu *Appl. Spectrosc.* **1994,** *48,* 1236. *(Chem. Abstr.* **1995,** 41233j.)

(28) W. Gabes and D. J. Stufkens *Spectrochim. Acta* **1974,** *30A,* 1835.

(29) R. E. Buckles, J. P. Yuk and A. I. Popov *J. Am. Chem. Soc.* **1952,** *74,* 4379.

(30) (a) G.Crisponi, P. Deplano and E. F. Trogu *Inorg. Chim. Acta* **1983,** *75,* 135. (b) G. Crisponi, P. Deplano, V. Nurchi and E. F. Trogu *Polyhedron* **1984,** *13,* 1241. (c) G. Crisponi, P. Deplano and E. F. Trogu *J. Chem. Soc, Dalton Trans.* **1986,** 365. (d) P. Deplano, E. F. Trogu, F. Bigoli and M. A. Pellinghelli *J. Chem. Soc, Dalton Trans.* **1987,** 2407.

(31) C. Schramm, R. P. Scaringe, D. R. Stojakovic, B. M. Hoffman, J. A. Ibers and T. J. Marks *J. Am. Chem. Soc.* **1980,** *102,* 6702.

(32) J. Martinsen, L. J. Pace, T. E. Phillips, B. M. Hoffinan and J. A. Ibers *J. Am. Chem. Soc.* **1982,** *104,* 83.

(33) K. Murata, K. Liou, J. A. Thompson, E. M. McGhee, D. E. Rende, D. E. Ellis, R. L. Musselman, B. M. Hoffman and J. A. Ibers *Inorg. Chem.* **1997,** *36,* 3363.

(34) L. J. Pace, J. Martinsen, A. Ulman, B. M. Hoffinan and J. A. Ibers *J. Am. Chem. Soc.* **1983,***105,* 2612.

(35) J. Martinsen, J. L. Stanton, R. L. Greene, J. Tanaka, B. M. Hoffinan and J. A. Ibers J. *Am. Chem. Soc.* **1985,** *107,* 6915.

(36) M. Y. Ogawa, J. Martinsen, S. M. Palmer, J. L. Stanton, J. Tanaka, R. L. Greene, B. M. Hoffinan and J. A. Ibers J. *Am. Chem. Soc.* **1987,** *109,* 1115.

(37) K. Liou, M. Y. Ogawa, T. P. Newcomb, G. Quirion, M. Lee, M. Poirier, W. P. Halperin, B. M. Hoffinan and J. A. Ibers *Inorg. Chem.* **1989,** *28,* 3889.

(38) J. M. Williams, T. J. Emge, H. H. Wang, M. A. Beno, P. T. Copps, L. N. Hall, K. D. Carlson and G. W. Crabtree *Inorg. Chem.* **1984,** *23,* 2558.

(39) M. A. Beno, U. Geiser, K. L. Kostka, H. H. Wang, K. S. Webb, M. A. Firestone, K. D. Carlson, L. Nuñez, M. -H. Whangbo and J. M. Williams *Inorg. Chem.* **1987,** *26,* 1912.

(40) J. Runsink, S. S. Walstra and T. Migchelsen *Acta Crystallogr.* **1972,** *B28,* 1331.

(41) K. -F. Tebbe and U. Georgy *Acta Crystallogr.* **1986,** *C42,* 1675.

(42) E. E. Havinga, K. H. Boswijk and E. H. Wiebenga *Acta Crystallogr.* **1954,** *7,* 487.

(43) R. Thomas and F. H. Moore *Acta Crystallogr.* **1980,** *B36,* 2869.

(44) K. -F. Tebbe Z *Kristallogr.* **1980,** *153,* 297.

(45) E. Dubler and L. Linowsky *Helv. Chim. Acta* **1975,** *58,* 2604.

(46) K. -F. Tebbe Z *anorg. allg. Chem.* **1982,** *489,* 93.

(47) K. -F. Tebbe and M. Plewa Z *anorg. allg. Chem.* **1982,** *489,* 111.

(48) K. -F. Tebbe and B. Freckmann Z *Naturforsch.* **1982,** *37B,* 542.

(49) K. -F. Tebbe *Ada Crystallogr.* **1983,** *C39,* **154.**

(50) K. -F. Tebbe, T. Gilles and B. Radke *Z. Naturforsch.* **1998,** *53B,* 87.

(51) K. -F. Tebbe, A. G. Kavoosian and B. Freckmann Z. *Naturforsch.* **1996,** *51B,* 999.

(52) K. -F. Tebbe and S. Nafepour *Ada Crystallogr.* **1994,** *C50,* **171.**

(53) K. -F. Tebbe and S. Nafepour *Acta Crystallogr.* **1994,** *C50,* **1566.**

(54) R. Thomas and F. H. Moore *Ada Crystallogr.* **1981,** *B3* 7, 2156.

(55) R. Thomas and F. H. Moore *Ada Crystallogr.* **1981,** *B37,* 2153.

(56) P. B. Hitchcock, D. L. Hughes, G. J. Leigh, J. R. Sanders, J. de Souza, C. J. McGarry and L. F. Larkworthy *J. Chem. Soc.,Dalton Trans.* **1994,** 3683.

(57) H. U. Diiker, B. Freckmann, H. Niebuhr, M. Plewa and K. -F. Tebbe Z. *Kristallogr.* **1979,** *149,* 131.

(58) T. Bernstein and F. H. Herbstein *Ada Crystallogr.* **1968,** *B24,* **1640.**

(59) K. -F. Tebbe and R. Buchem Z. *Kristallogr.* **1995,** *210,* 438.

(60) K. -F. Tebbe and R. Buchem Z. *Kristallogr.* **1996,** *211,* **689.**

(61) K. -F. Tebbe and R. Buchem Z. *anorg. allg. Chem.* **1998,** *624,* 679.

(62) K. -F. Tebbe and R. Buchem Z *anorg. allg. Chem.* **1998,** *624,* 671.

(63) J. A. Kramer, F. H. Herbstein and D. N. Hendrickson *J. Am. Chem. Soc.* **1980,** *102,* 2293.

(64) T. -Y. Dong, M. -Y. Hwang, C. -C. Schei, S. -M. Peng and S. -K. Yeh *J. Organomet. Chem.* **1989,** *369,* C33.

(65) T. -Y. Dong, X. -Q. Lai, Z. -W. Lin and K. -J. Lin *Angew. Chem. Int. Ed. Engl.* **1997,** *36,* 2002.

(66) D. B. Morse, T. B. Rauchfuss and S. R. Wilson *J. Am. Chem. Soc.* **1990,** *112,* **1860.**

(67) A. J. Jircitano and K. B. Mertes *Inorg. Chem.* **1983,** *22,* **1828.**

(68) A. J. Jircitano, M. C. Colton and K. B. Mertes *Inorg. Chem.* **1981,** *20,* **890.**

(69) K. -F. Tebbe and A. Kavoosian *Acta Crystallogr.* **1995,** *C51,* 562.

(70) K. -¥. Tebbe and A. Kavoosian Z *Naturforsch.* **1993,** *48B,* 438.

(71) K. -F. Tebbe and M. E. Essawi *Z. anorg. allg. Chem.* **1998,** *624,* (in press).

(72) M. W. Renner, K. M. Barkigia, Y. Zhang, C. J. Medforth, K. M. Smith and J. Fajer *J. Am. Chem. Soc.* **1994,** *116,* 8582.

(73) K. -F. Tebbe, M. E. Essawi and S. A. E. Khalik Z *Naturforsch.* **1995,** *50B,* 1429.

(74) K. -F. Tebbe, B. Freckmann, M. Hörner, W. Hiller and J. Strahle *Acta Crystallogr.* **1985,** *C41,* 660.

(75) K. -F. Tebbe and N. Krauss *Acta Crystallogr.* **1990,** *C46,* 878.

(76) K. -F. Tebbe and T. Gilles *Acta Crystallogr.* **1993,** *C49,* 2042.

(77) K. -F. Tebbe and W. Lindenthal Z *anorg. allg. Chem.* **1993,** *619,* 1483.

(78) K. -F. Tebbe and T. Gilles Z *anorg. allg. Chem.* **1996,** *622,* **138.**

(79) K. -F. Tebbe and T. Gilles Z *anorg. allg. Chem.* **1996,** *622,* 1587.

(80) J. R. Ferraro *J. Phys. Chem. Sol.* **1986,** *47,* 301.

(81) H. Pritzkow *Inorg. Chem.* **1979,** 75, 311.

(82) K. -F. Tebbe and K. Nagel Z *anorg. allg. Chem.* **1995,** *621,* 225.

(83) K. -F. Tebbe, T. Farida, H. Stegemann and H. Fiillbier Z *anorg. allg. Chem.* **1996,** *622,* 525.

(84) K. -F. Tebbe and K. Nagel Z *anorg. allg. Chem.* **1996,** *622,* 1323.

(85) J. M. Reddy, K. Knox and M. B. Robin *J. Chem. Phys.* **1964,** *40,* 1082.

(86) J. Jander, H. Pritzkow and K. -U. Trommsdorff Z *Naturforsch.* **1975,** *30B,* 720.

(87) O. Hassel and H. Hope *Acta Chem. Scand.* **1961,** *15,* 407.

(88) P. K. Hon, T. C. W. Mak and J. Trotter *Inorg. Chem.* **1979,** *18,* 2916.

(89) F. H. Herbstein, G. M. Reisner and W. Schwotzer *J. Incl. Phen.* **1985,** *3,* **173.**

(90) F. H. Herbstein, M. Kapon and W. Schwotzer *Helv. Chim. Ada* **1983,** *66,* 35.

(91) F. H. Herbstein and M. Kapon *J. Chem. Soc, Chem. Commun.* **1975,** 677.

(92) H. Stegemann, A. Oprea, K. Nagel and K. -F. Tebbe Z *anorg. allg. Chem.* **1997,** *623,* 89.

(93) T. L. Hendrixson, M. A. T. Horst and R. A. Jacobson *Ada Crystallogr.* **1991,** *C47,* 2141.

(94) R. D. Bailey and W. T. Pennington *Ada Crystallogr.* **1995,** *B51,* 810.

(95) F. Bigoli, M. A. Pellinghelli, G. Crisponi, P. Deplano and E. F. Trogu *J. Chem. Soc, Dalton Trans.* **1985,** 1349.

(96) F. H. Herbstein and W. Schwotzer *J. Chem. Soc, Perkin Trans. II* **1984,** 1917.

(97) P. C. Junk, L. R. MacGillivray, M. T. May, K. D. Robinson and J. L. Atwood *Inorg. Chem.* **1995,** *34,* 5395.

(98) T. Yokoyama, K. Kaneyuki, H. Sato, H. Hamamatsu and T. Ohta *Bull. Chem. Soc, Jpn.* **1995,** *68,* 469.

(99) S. L. H. Su, A. J. Signorelli, G. P. Pez and R. H. Baughman *J. Chem. Phys.* **1978,** *69,* 106.

(100) W. J. James, R. J. Hach, D. French and R. E. Rundle *Ada Crystallogr.* **1955,** *8,* **814.**

(101) M. El Essawi, I. Dombrowski, T. Gilles, A. Kavoosian and K. -F. Tebbe Z *Kristallogr. Suppl.* **1998,** *15,* 61.

CHAPTER 3

Polyiodide Salts of Metal Complex Cations: Part 1. Polyiodide Anions with Normal Iodine Content

Synthesis, Crystal Structure and Conductivity Studies of $[Mn(phen)_3](I_3)_2$, $[Mn(bpy)_3](I_3)_{1.5}(I_8)_{0.25}$ and $[Ni(phen)_3](I_3)_2 \cdot CH_3CN$

The syntheses, crystal structures of three polyiodide complexes, *viz.*, $[Mn(phen)_3](I_3)_2$ (1) and $[Mn(bpy)_3](I_3)_{1.5}(I_8)_{0.25}$ (2) and $[Ni(phen)_3](I_3)_2 \cdot CH_3CN$ (3) and spectral and conductivity properties of 1 and 2 are discussed in this chapter. While 1 and 3 contain discrete I_3^- ions, 2 contains I_3^- ions as well as linear polyiodide chains. The structure of the cation of the complex 1 has not been reported so far, and that of 2 and 3 are compared with the reported ones.'

3.1 Experimental

3.1.1 Syntheses

3.1.1 (a) $[Mn(phen)_3](I_3)_2$ (1). To a solution of $Mn(OAc)_2 \cdot 4H_2O$ (0.500 g, 2.04 mmol) and 1,10-phenanthroline hydrate (1.270 g, 6.41 mmol) in water (10 mL), a solution of I_2 (1.0 g, 3.9 mmol) in dichloromethane (25 mL) and solid KI (0.66 g, 4.0 mmol) were added. Dil. sulfuric acid (1 M, 1 mL) was then added to the two phase reaction mixture, and the mixture was stirred for 10 min. The deep brown colored organic layer was separated by extraction with an additional amount of

dichloromethane (50 mL), and dried over Na_2SO_4. The brown crystalline product that formed after the filtrate was allowed to stand at room temperature for 3 d was separated, and recrystallized from acetonitrile as large deep brown triangular prismatic crystals. Yield: 1.770 g (1.30 mmol, 64%). Anal. Calcd for $C_{36}H_{24}N_6MnI_6$ (MW 1357.0): C, 31.86; H, 1.78; N, 6.19. Found: C, 31.61; H, 1.72; N, 6.16. Characteristic IR bands (cm^{-1}): 1589(w), 1519(s), 1424(s), 1340(w), 1139(s), 1101(s), 866(w), 834(s), 774(w), 761(w), 721(s), 639(w), 420(w).

3.1.1 (b) $[Mn(bpy)_3](I_3)_{1.5}(I_8)_{0.25}$ (2). The complex was synthesized by a procedure similar to 3.2.1 (a) described above using bpy instead of phen. To a solution of $Mn(OAc)_2 \cdot 4H_2O$ (0.500 g, 2.04 mmol) and 2,2'-bipyridine (1.00 g, 6.40 mmol) in water (10 mL), a solution of I_2 (1.0 g, 3.9 mmol) in dichloromethane (25 mL) and solid KI (0.66 g, 4.0 mmol) were added. Dil. sulfuric acid (1 M, 1 mL) was then added to the two phase reaction mixture, and the mixture was stirred for 10 min. The deep brown colored organic layer was separated by extraction with an additional amount of dichloromethane (50 mL), and dried over Na_2SO_4. In this case, the dichloromethane extract was allowed to stand at 10 °C for 3 d. Recrystallization of the crude product from acetonitrile solvent yielded deep brown rectangular plate like crystals. The crystals have been observed to lose I_2 slowly over a period of several days at room temperature. Yield: 1.050 g (0.78mmol, 39%). Anal. Calcd for $C_{30}H_{24}N_6MnI_{65}$ (MW 1348.3): C, 26.72; H, 1.79; N, 6.23. Found; C, 27.85; H, 1.75; N, 5.97. Characteristic IR bands (cm^{-1}): 1591(s), 1487(w), 1468(w), 1433(s), 1310(w), 1152(w), 1101(w), 1012(s), 760(s), 735(w), 650(w), 627(w), 409(w).

3.1.1 **(c)** **$[Ni(phen)_3](I_3)_2 \cdot CH_3CN$ (3).** The complex was prepared following a procedure similar to 3.2.1(a), using a solution of $Ni(OAc)_2 \cdot 4H_2O$ (0.500 g, 1.96 mmol) and 1,10-phenanthroline hydrate (1.250 g, 6.31 mmol) in water (10 mL), to which a solution of I_2 (1.0 g, 3.9 mmol) in dichloromethane (25 mL) and solid KI (0.66 g, 4.0 mmol) were added. Dil. sulfuric acid (1 M, 1 mL) was then added to the two phase reaction mixture, and the mixture was stirred for 10 min. The deep brown colored organic layer was separated by extraction with an additional amount of dichloromethane (50 mL). The dichloromethane extract was allowed to stand at room temperature for 3 d and the brown crystals that formed were separated. Yield: 1.630g (1.12mmol, 61%). Anal. Calcd for $C_{36}H_{24}N_6NiI_6$ (MW 1360.8): C, 31.78; H, 1.78; N, 6.18. Found: C, 31.14; H, 1.95; N, 6.39. The crystalline compound was again recrystallized from acetonitrile as large deep brown rectangular crystals. Yield: 1.520 g (1.08mmol, 55%). Anal. Calcd for $C_{38}H_{27}N_7NiI_6$ (MW 1401.8): C, 32.56; H, 1.94; N, 6.99. Found: C, 32.90; H, 1.98; N, 7.00. Characteristic IR bands (cm^{-1}): 2361(w), 2255(w), 1780(w), 1624(w), 1582(w), 1514(s), 1493(w), 1424(s), 1339(w), 1221(w), 1140(w), 1101.5(w), 868(w), 841(s), 768(w), 721(s), 642(w), 422.5(w).

3.1.1 (d) **$[Cu(phen)_3](I_3)_2 \cdot CH_3CN$** (4). The complex was prepared in a similar way as 3.2.1(c) using a solution of $Cu(OAc)_2 \cdot 4H_2O$ (0.500 g, 1.93 mmol) and 1,10-phenanthroline hydrate (1.250 g, 6.31 mmol) in water (10 mL), to which a solution of I_2 (1.0 g, 3.9 mmol) in dichloromethane (25 mL) and solid KI (0.66 g, 4.0 mmol) were added. Dil. sulfuric acid (1 M, 1 mL) was then added to the two phase reaction mixture, and the mixture was stirred for 10 min. The deep brown colored organic layer was separated by extraction with an additional amount of dichloromethane (50 mL). The dichloromethane extract was allowed to stand at room temperature for 3 d to yield brown crystalline product. Recrystallization of

the crystalline product from acetonitrile yielded deep brown rectangular crystals. Yield: 1.50 g (1.05 mmol, 54%). Anal. Calcd for $C_{38}H_{27}N_7CuI_6$ (MW 1406.7): C, 32.45; H, 1.93; N, 6.97. Found: C, 32.09; H, 1.75; N, 6.78. Characteristic IR bands (cm"^{1}): 1622(w), 1580(w), 1514(s), 1422(s), 1339(w), 11263.5(w), 1138(s), 1099.5(w), 864(w), 837(vs), 762(w), 719.5(vs), 644(w), 417(w).

3.1.1 (e) $[Co(phen)_3](I_3)_2 \cdot CH_3CN$ (5). This complex was synthesised in the same way as above, using a solution of $Co(OAc)_2 \cdot 4H_2O$ (0.500 g, 1.96 mmol) and 1,10-phenanthroline hydrate (1.250 g, 6.31 mmol) in water (10 mL), to which a solution of I_2 (1.0 g, 3.9 mmol) in dichloromethane (25 mL) and solid KI (0.66 g, 4.0 mmol) were added. Dil. sulfuric acid (1 M, 1 mL) was then added to the two phase reaction mixture, and the mixture was stirred for 10 min. The deep brown colored organic layer was separated by extraction with an additional amount of dichloromethane (50 mL). The dichloromethane extract was allowed to stand at room temperature for 3 d to yield brown crystalline product. Recrystallization of the crystalline product from acetonitrile yielded deep brown needle-like crystals. Yield: 1.65 g (1.18 mmol, 59%). Anal. Calcd for $C_{38}H_{27}N_7CoI_6$ (MW 1402.0): C, 32.55; H, 1.94; N, 6.99. Found: C, 31.96; H, 1.59; N, 6.96. Characteristic IR bands (cm"^{1}): 1622(w), 1578(w), 1512(s), 1493(w), 1422(s), 1337(w), 1302(w), 1219(w), 1138(w), 1099.5(w), 839(s), 764(w), 721(vs), 639(w), 448(w), 422.5(w).

3.1.2 Physical Measurements. The elemental analyses were performed on a Perkin-Elmer 240C elemental analyzer. Room temperature magnetic data were obtained on a Cahn-3000 microbalance using the Faraday method. $Hg[Co(CNS)_4]$ was used as the primary standard. Diamagnetic corrections were applied using Pascal's constants.2 The EPR spectra were recorded for frozen solution, powder,

and single crystal samples on a JEOL FE-3X spectrometer equipped with a JEOL NM-7700 temperature controller using DPPH as the internal standard. Resistivity measurements were obtained for single crystals of the complexes at room temperature by a two-probe method using contacts made of silver paint. A constant current source (Keithly Model 224) was used for the measurement, and the voltage was measured using a multimeter (Keithly Model 175). The currents were in the range 0.01-0.04 μA, while the voltage varied between 50 and 400 mV for each measurement. An average of 3 measurements (which agreed within 8%) was taken as the resistivity of the crystal. Specific conductivities were calculated from the resistivity values.

3.1.3 X-ray Crystallography. For each complex, a suitable single crystal was mounted on a glass fiber with epoxy resin. The X-ray data were collected at ambient temperature on an Enraf-Nonius CAD4 Diffractometer for 1 and 3 and on a Siemens SMART CCD Diffractometer for 2 (at 213 K) using graphite monochromated MoKα radiation. A (partial) data set was also collected at 130 K for 1 on a Siemens P4 diffractometer (at University of Canterbury, New Zealand). The intensities of three standard reflections monitored for every 100 reflections during the respective data collections indicated negligible crystal decomposition. The crystallographic data for the three complexes are presented in Table 3.1, 3.3 and 3.5 respectively. The data were corrected for Lorentz-polarization effects and absorption.[3] The structures were solved by direct methods or Patterson method and refined by least-squares techniques; the programs used were SHELXS-86 and SHELXL-93 for 1 and 3, and SHELXTL and SHELXL-97 for 2.[4,5] Individual details are given below.

3.1.3 (a) $[Mn(phen)_3](I_3)_2$ (1). The complex crystallizes in the hexagonal space group Rl with 6 mononuclear cations in the unit cell. A total of 3790 reflections (2384 unique, 1981 with F > 4σF) were collected in the 2θ range, 4-50°, with indices -19 < *h* ≤ 16, 0 < *k* < 19, 0 < / < 30. The non-hydrogen atoms were refined anisotropically over F^2, while the hydrogen atoms were included in calculated positions (C-H = 0.96 A) using a riding model. The final values of the conventional and weighted agreement R factors were, R_1 = 0.0365 and wR_2 = 0.0782. The maximum residual electron density is 1.663 eA"^{3}, close to I(4). Important bond distances and angles are presented in Table 3.2. Full crystallographic data and positional parameters are listed in Appendix D.

Table 3.1

Crystallographic data for $[Mn(phen)_3](I_3)_2$ (1).

formula	$C_{36}H_{24}I_6MnN_6$	Z	6
formula weight	1356.96	space group	R 3 (No. 148)
a	16.456(2) A	T	293(2) K
b	16.456(3) A	*X*	0.71073 A
c	25.864(4) A	p(obsd)	2.37 Mg/m^3
a	90°	p(calcd)	2.229 Mg/m^3
P	90°	μ	4.941 mm^{-1}
y	120°	Rl	0.0365
V	6066(2) A^3	wR2	0.0782

$R1 = \Sigma||F_o| - |F_c||/\Sigma|F_o|$

$wR2 = [\Sigma\{w(F_o^2 - F_c^2)^2\}/\Sigma(wF_o^4)]^{1/2}$

$w^{-1} = [\sigma^2(F_o^2) + (0.0248P)^2 + 50.8570P]$, $P = (F_o^2 + 2F_c^2)/3$

Table 3.2

Selected bond distances (A) and angles (°) for 1

I(1)-I(2)	2.9116(6)	I(3)-I(4)	2.828(1)
Mn(l)-N(l)	2.254(5)	Mn(1)-N(2)	2.263(4)
I(1)-I(2)-I(1)#1	180.0	I(4)-I(3)-I(4)#2	180.0
N(1)-Mn(1)-N(2)	73.7(2)		

Intermolecular contacts :

(a) No I...I contacts :

(b) I...ring contacts

Distances:

I(2)...N(2)#3	3.769(5)	I(2)...N(2)#4	3.769(5)
I(2)...N(1)#5	3.830(5)	I(2)...N(1)#6	3.830(5)
I(1)...H(9)#7	3.176(8)	I(4)...H(1)#8	3.185(7)
I(4)...H(1)#9	3.185(7)		

Angles:

I(l)-H(9)-C(9)#7	136.7(9)	I(4)-H(1)-C(1)#8	120.9(7)

Symmetry transformations used to generate equivalent atoms:

#1: -x, -y+1, -z; #2:-x, -y, -z; #3 -x+y, -x+1, z; #4 x-y, x,-z; #5 x-1, y, z; #6-x+1,-y+l,-z; #7 -y+0.667, x-y+0.333, 0.333+z; #8 -x+0.667, -y+0.333, -z+0.333; #9 x-y-0.333, x-0.667, -z+0.333;

3.1.3 (b) $[Mn(bpy)_3](I_3)_{1.5}(I_8)_{0.25}$ (2). The complex crystallizes in the monoclinic space group C2/c with 8 mononuclear cations in the unit cell. A total of 15,592 reflections (5394 unique, 4192 with F > $4\sigma F$) were collected in the 2θ range, 4-47°, with indices -26 < $h \leq$ 32, -14 $\leq k \leq$ 14,-25 < / $\leq$ 25. The non-hydrogen atoms were refined anisotropically over F^2, while the hydrogen atoms were included in calculated positions (C-H = 0.96 A) using a riding model. Four iodine atoms (I(4), I(5), I(6), I(7)) show serious disorder. The disorder was modelled as follows: I(4) and I(5) were each split into two sites about the crystallographic inversion centre. I(6) and I(7) which form an infinite chain, were each split into four sites with equal occupation factors in such a way, that the disordered sites are situated very nearly along the chain propagation direction. This model led to a significant drop in R from 0.064 to 0.054 and much more reasonable thermal parameters. The final values of the conventional and weighted agreement R factors were R_1 = 0.0536 and wR_2 = 0.1310. The maximum residual electron density is 1.317 $eÅ^{-3}$, close to I(5B). Selected bond distances and angles are presented in Table 3.4. Full crystallographic data and positional parameters are listed in Appendix E.

Table 3.3

Crystallographic data for $[Mn(bpy)_3](I_3)_{1.5}(I_8)_{0.25}$ (2).

formula	$C_{30}H_{24}I_{6.50}MnN_6$	Z	8
formula weight	1348.34	space group	C2/c (No.15)
a	29.3213(11) A	T	213 K
b	12.9177(4) A	*X*	0.71073 A
c	23.2863(4) A	p(obsd)	2.43 Mg/m^3
a	90°	p(calcd)	2.368 Mg/m^3

p	120.950(2)°	μ	5.684 mm^{-1}
y	90°	Rl	0.0536
V	7564.2(5) A^3	wR2	0.1310

R1 - $\Sigma||F_o| - |F_c||/\Sigma|F_o|$

wR2 = $[\Sigma\{w(F_o^2 - F_c^2)^2\}/\Sigma(wF_o^4)]^{1/2}$

$w^{-1} = [\sigma^2(F_o^2) + (0.0732P)^2 + 184.1418P]$, $P = (F_o^2 + 2F_c^2)/3$

Table 3.4

Selected bond distances (A) and angles (°) for 2

I(l)-I(2)	2.8833(7)	I(1)-I(3)	2.9676(7)
I(4A)-1(5A)#1	2.897(2)	I(4A)-I(5B)	2.900(2)
I(4B)-I(5A)	2.731(6)	I(4B)-I(5B)#1	3.066(6)
I(5A)-I(4A)#1	2.897(2)	I(5B)-I(4B)#1	3.066(6)
I(6A)-I(7A)	2.920(4)	I(6A)-I(6D)#2	2.953(3)
I(6B)-I(7B)	2.949(4)	I(6B)-I(6C)#2	2.982(4)
I(6C)-I(7C)	2.923(4)	I(6C)-I(6B)#2	2.982(4)
1(6D)-I(7D)	2.909(4)	I(6D)-I(6A)#2	2.953(3)
I(7A)-I(7D)#3	2.910(4)	I(7B)-I(7C)#3	2.838(5)
I(7C)-I(7B)#3	2.838(5)	I(7D)-I(7A)#3	2.910(4)
Mn(l)-N(4)	2.223(6)	Mn(1)-N(6)	2.245(6)
Mn(l)-N(2)	2.245(5)	Mn(1)-N(1)	2.253(4)
Mn(l)-N(5)	2.255(5)	Mn(1)-N(3)	2.266(5)

I(2)-I(l)-I(3)	178.48(2)	I(5A)#1-I(4A)-I(5B)	177.74(11)
I(5A)-I(4B)-I(5B)#1	179.3(3)	I(7 A)-I(6A)-I(6D)#2	177.25(11)
I(7B)-I(6B)-I(6C)#2	173.64(10)	I(7C)-I(6C)-I(6B)#2	171.92(9)

I(7D)-I(6D)-I(6A)#2	170.69(10)	I(7D)#3-I(7A)-I(6A)	169.15(11)
I(7C)#3-I(7B)-I(6B)	171.15(11)	I(7B)#3-I(7C)-I(6C)	174.05(11)
I(6D)-I(7D)-I(7A)#3	176.44(12)	N(2)-Mn(l)-N(l)	73.67(18)
N(4)-Mn(l)-N(3)	73.6(2)	N(6)-Mn(l)-N(5)	73.0(2)

Intermolecular contacts :

(a) I...I contacts :

Distances:

I(1)...I(5B)#4	4.145(2)	I(2)...I(7A)#5	3.960(3)
I(2)...I(7B)#5	3.961(3)	I(2)...I(6D)#5	4.080(3)
I(2)...I(6C)#5	4.277(3)		

Angles:

I(1)-I(5B)#4-I(4A)#4	120.71(8)	I(1)-I(2)-I(7B)#5	169.71(5)
I(2)-I(7B)#5-I(6B)#4	82.11(8)		

(b) I...ring contacts :

Distances:

I(2)...H(3A)#6	3.183(2)	I(2)...H(8A)#7	3.1860(6)
I(3)...H(29A)#8	3.1435(6)	I(6A)...H(27A)#9	3.205(2)
I(6B)...H(4A)#10	3.179(2)	I(6C)...H(24A)#9	3.156(2)
I(6D)...H(24A)#9	3.158(2)	I(7A)...H(17A)#11	3.130(2)
I(7B)...H(17A)#11	3.168(3)		

Angles:

I(2)-H(3A)#6-C(3)#6	128.9(5)	I(2)-H(8A)#7-C(8)#7	131.9(4)
I(3)-H(29A)#8-C(29)#8	134.9(5)	I(6A)-H(27A)#9-C(27)#9	154.5(5)
I(6B)-H(4A)#10-C(4)#10	151.3(4)	I(6C)-H(24A)#9-C(24)#9	162.5(5)
I(6D)-H(24A)#9-C(24)#9	149.8(5)	I(7 A)-H(17 A)# 11 -C(17)# 11	161.7(5)

I(7B)-H(17A)#11-C(17)#11 151.1(5)

Symmetry transformations used to generate equivalent atoms:

#1 -x+1, y, -z+3/2; #2 -x, -y, -z+1; #3 -x, y, -z+1/2; #4 -x+1/2, -y+1/2, -z+1; #5 x, y+1, z; #6 -x+1/2, -y+3/2, -z+1; #7 -x+1/2, y+1/2, -z+1/2; #8 -x+1/2, y-1/2, -z+1/2; #9 -x, y-1,-z+1/2; #10x-l/2, y-1/2, z; #11 -x, y -z+1/2

3.1.3 (c) $[Ni(phen)_3](I_3)_2 \cdot CH_3CN$ (3). The complex crystallizes in the triclinic space group $P\bar{1}$ with 2 mononuclear cations in the unit cell. A total of 7507 reflections (7057 unique, 4569 with F > 4σF) were collected in the 2θ range, 4-50° , with the data gathered having indices $0 < h < 10$, $-13 < k < 14$, $-21 < / < 21$. The non-hydrogen atoms were refined anisotropically over F^2, while the hydrogen atoms were included in calculated positions (C-H • 0.96 A) using a riding model. A disordered molecule of CH_3CN was located from the difference electron density map. The site occupancy factor was found to be best fitting to a value of 0.30. The C-C and the C-N distances were fixed due to severe distortions in bond length during refinement. The final values of the conventional and weighted agreement R factors were, R_1 = 0.0609 and wR_2 = 0.1395. The maximum residual electron density is 1.907 $eÅ^{-3}$, close to I(5). Selected bond distances and angles are presented in Table 3.6. Full crystallographic data and positional parameters are listed in Appendix F.

Table 3.5

Crystallographic Data for $[Ni(phen)_3](I_3)_2 \cdot CH_3CN$ (3)

formula	$C_{38}H_{27}I_6N_7Ni$	Z	2
formula weight	1401.78	space group	P F (No. 2)

a	10.01(2) A	T	293(2) K
b	12.581(4) A	λ	0.71073 A
c	18.003(2) A	ρ(calcd	2.266 Mg/m^3
a	78.78(2)°	μ	5.016 mm^{1}
β	86.63(4)°	R1	0.0609
γ	67.59(5)°	wR2	0.1395
V	2055(3) A^3		

$R1 = \Sigma||F_o| - |F_c||/\Sigma|F_o|$

$wR2 = [\Sigma\{w(F_o^2 - F_c^2)^2\}/\Sigma(wF_o^4)]^{1/2}$

$w^{-1} = [\sigma^2(F_o^2) + (0.0785P)^2 + 9.4097P]$, $P = (F_o^2 + 2F_c^2)/3$

Table 3.6

Selected bond lengths [A] and angles [deg] for 3.

Bond distances :

Ni-N(5)	2.084(7)	Ni-N(6)	2.086(7)
Ni-N(4)	2.089(7)	Ni-N(3)	2.094(7)
Ni-N(2)	2.096(6)	Ni-N(l)	2.098(7)
I(l)-I(2)	2.891(4)	I(2)-I(3)	2.928(3)
I(4)-I(5)	2.882(2)	I(5)-I(6)	2.925(2)

Bond angles :

N(5)-Ni-N(6)	79.8(3)	N(4)-Ni-N(3)	79.5(3)
N(2)-Ni-N(l)	79.2(2)	I(1)-I(2)-I(3)	176.24(3)
I(4)-I(5)-I(6)	174.87(4)		

Intermolecular contacts :

(a) I...I contacts :

Distances:

I(1)...I(1)#1	4.134(3)	I(3)...I(4)	4.077(2)

Angles:

I(2)-I(1)-I(1)#1	122.40(3)	127.61(4)

(b) I...ring contacts :

Distances:

I(6)...N(1)#2	3.881(9)	I(5)...N(7)#3	3.58(1)
I(1)...H(3)#4	3.162(9)	I(2)...H(10)	3.186(8)
I(4)...H(2)#5	3.130(9)	I(5)...H(32)	3.013(10)

Angles:

I(5)-N(7)#3-C(37)#3	116.9(7)	I(1)-H(3)#4-C(3)#4	154.9(9)
I(2)-H(10)-C(10)	134.2(9)	I(4)-H(2)#5-C(2)#5	137.6(9)
I(5)-H(32)-C(32)	160.2(12)		

Symmetry transformations used to generate equivalent atoms:

#1 -x, -y+l,-z; #2-x+l,-y+l,-z+l; #3 -x+1, -y, -z+1; #4 x, y-1, z; #5 x+1, y-1, z;

3.1.3 (d) **$[Cu(phen)_3](I_3)_2 \cdot CH_3CN$** (4). The complex crystallizes in the triclinic space group $P\bar{1}$ with similar unit cell parameters as 3, i.e. *a* = 9.9904(7) A, *b* = 12.67(1) A, *c* = 18.095(9) A, α = 78.54(6)°, p = 86.17(5)°, y = 67.72(7)° and V = 2059(3). These cell parameters suggested 4 to be isostructural to complex 3.

3.2 Results and Discussion

3.2.1. Syntheses. The formation of complexes 1 and 2 were accidentally detected while performing equivalent weight determination for some high valence manganese complexes of phen and bpy by the iodometry method in water-acetonitrile medium. During the iodometry experiments which involve reduction by excess potassium iodide, brown crystalline products that were soluble in dichloromethane were isolated in *ca.* 20% yield. In fact, as early as 1966, Goodwin and Sylva[6] had noticed the formation of "highly insoluble $Mn(base)_3(I_3)_2$", when iodide is added to a "preparative solution" containing $KMnO_4$, conc. HC1, and bpy/phen, but they have not been further described. The present structural studies *(vide supra)* revealed the presence of novel triiodide and polyiodide anions in the crystals. Subsequently a more efficient procedure has been developed for the synthesis of these complexes from manganese(II) acetate tetrahydrate, the respective ligand (phen or bpy), potassium iodide, and iodine as described above. The compounds obtained this way are identical to the ones obtained during iodometry. The new method uses a dichloromethane/water two-phase procedure, whereas the known general procedures for the synthesis of polyiodides either involve a reaction between solid iodide salts and gaseous iodine, or use methanol or acetic acid as the solvent.[7] The two phase method has also been used by us for the preparation of $[Cu(dafone)_3]I_{12}$, where dafone is 4,5-diazafluoren-9-one.[8] This method was extended for other metal acetate salts and a series of compounds were prepared. In the complexes, $[Ni(phen)_3](I_3)_2 \cdot CH_3CN$, $[Cu(phen)_3](I_3)_2$ CH_3CN and $[Co(phen)_3](I_3)_2 \cdot CH_3CN$, the solvent used for recrytallization gets accommodated in the crystal lattice. The IR and elemental analysis of $[Ni(phen)_3](I_3)_2$, before and after recrystallization confirms presence of CH_3CN in the recrystallized product.

3.2.2 (a) Structure of 1. The structure consists of $[Mn(phen)_3]^{2+}$ cations, and I_3^- anions. Views of the cation and the anions are shown in Figure 3.1.

The cation has an exact C_3 symmetry as the manganese atom is sitting on a crystallographic three-fold axis and approximates D_3 symmetry very closely. There are two types of I_3^- anions in the crystal. Although both I_3^- anions are linear and symmetric, they differ from each other on the basis of their apparent I-I distances. One of them possesses the shortest I-I distance (2.828(1) A) yet known in symmetrical I_3^- ions,[9] whereas the other possesses the normal I-I distance of 2.912(1) A.

a

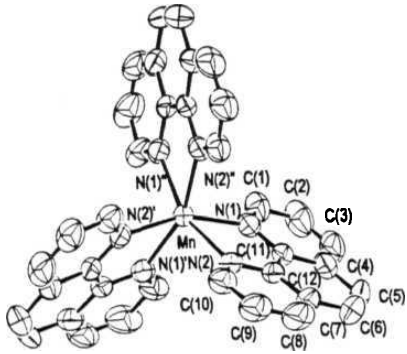

1)

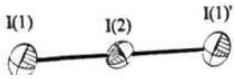

c

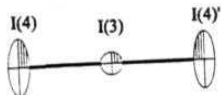

Figure 3.1 Views of the cation and anions of 1 (50% probability ellipsoids). (a) $[Mn(phen)_3]^{2+}$ viewed along the *c*-axis. (b) "normal" I_3^- (': *-x, 1-y, -z).* (c) "short" I_3^- (': *-x, -y, -z).*

The large apparent libration associated with the terminal iodine atoms of the "short" I_3^- ions might well suggest that this observed shortening could be an artifact due to some disorder along the molecular axis. The relatively large thermal parameters for the terminal iodine I(4) ($U_{11} = U_{22}$ - 0.271(1) A^2, U_{33} = 0.043(1) A^2, U_{12} = 0.136(3) A^2), may imply disorder about the inversion centre, however, the analysis of the anisotropic parameters did not suggest splitting of the atomic position. Refinement of a partial low temperature data set showed considerable reduction in the thermal parameters, but no disorder : T = 130 K, *a* = 16.248(2) A, *c* = 25.757(5) A, R_1 = 0.0539, wR_2 = 0.1325 for 1247 reflections (having indices 0 < h < 8, -19 < k < 0, 0 < 1 < 30), I(l)-I(2) =2.9077(9) A, I(3)-I(4) = 2.844(2) A, $U_{11} = U_{22}$ = 0.130(2) A^2, U_{33} = 0.019(1) A^2, U_{12} = 0.065(l)A^2 for I(4). Tables and figures are in Appendix G .

It is noteworthy that the anion is pinched between two $[Mn(phen)_3]^{2+}$ cations along the three-fold symmetry axis as shown in Figure 3.2(a) with the distance between the I_3^- ion and the phen ligand (I(4)···C(1)) being 3.75 A. Thus, while disorder cannot be ruled out, the observed shortening of the I-I bonds may be a real effect of steric crowding, the strain being reflected in the highly distorted nature of the anisotropic vibration ellipsoids of the terminal iodine atoms as can be seen in Figure 3.1(c). The "normal" I_3^- ions also make lateral contacts with the ligand carbon and nitrogen atoms (I(2)···C(10), I(2)···N(2), 3.77 A) forming a hexagonal network of the cations as shown in Figure 3.2(b). Thus, the crystal can be thought of as a supermolecule formed by the stacking of the layers of the hexagonal network, with the "short" I_3^- ions bridging successive pairs of the layers. It appears likely that the network is stabilized by the sharing of each of the "normal" I_3^- ions by two adjacent cations, and the stacking of the layers is stabilized by the sharing of the "short" I_3^- ions by two cations in successive layers.

The stoichiometry of the repeating motif is best described as: $\{Mn(phen)_3(I_3)_{1.5}\}_2(I_3)$, where the I_3^- ions inside the curly brackets are of the "normal" type and that outside is of the "short" type. This kind of packing leads to the formation of microchannels with a van der Waal's diameter of 1.2 A along the c-axis as shown in Figure 3.2(c).

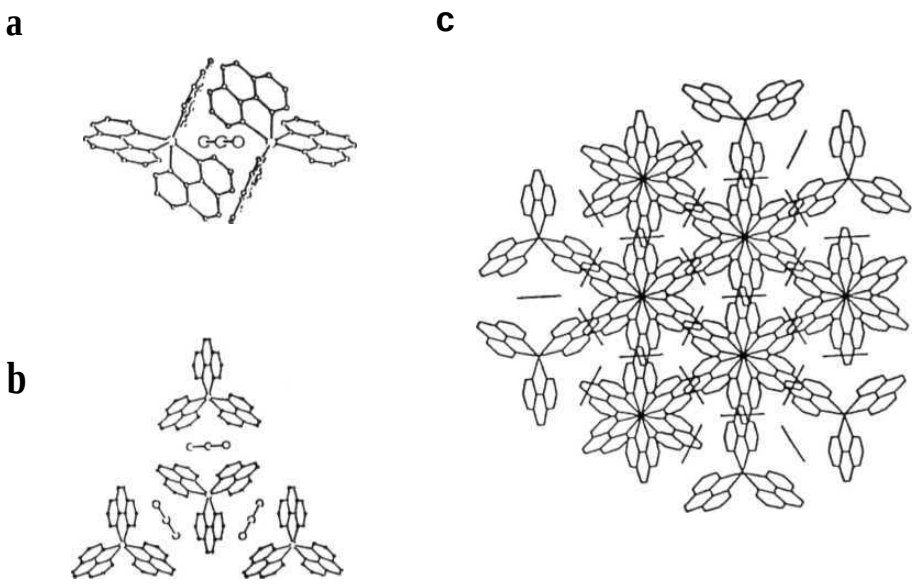

Figure 3.2 Illustration of some aspects of packing in 1. (a) the "short" I_3^- pinched between two cations from adjacent layers. (b) lateral sharing of the "normal" I_3^- by adjacent cations in a layer. (c) packing viewed along the *c*-axis. The "short" I_3^- ions which are along the c-axis are not visible in this view, but they hold together the snow-flake like dimeric units of $[Mn(phen)_3]^{2+}$.

The coordination geometry of the manganese atom in the $[Mn(phen)_3]^{2+}$ cation is trigonally distorted octahedral (approximate D_3 symmetry). The N(l)-Mn(l)-N(2) bond angle (73.7°) and the average Mn-N bond distance (2.258 A) are consistent with a previously observed correlation between these parameters.[10]

3.2.2 (b) Structure of 2. The structure consists of $[Mn(bpy)_3]^{2+}$ cations, I_3^- anions, and infinite polyiodide chains $[(I_8^{2-})_n]$ (Figure 3.3). A packing diagram is shown in Figure 3.4.

In this crystal also there are two types of I_3^- ions. One of the ions, I(2)-I(l)-I(3), is slightly bent and unsymmetric with the I-I distances of 2.883(1) and 2.968(1) A and the I-I-I angle of 178.48(2)°. The other I_3^- ion, is disordered about a crystallographic two fold axis. More significant is the presence of a linear polyiodide chain built from I(6) and I(7) atoms, running nearly parallel to the crystallographic c-axis. The I(6) and I(7) are both disordered along the c-axis in 4 different positions (I(6A), I(6B), I(6C), I(6D) and I(7A), I(7B), I(7C), I(7D)) respectively.

A room temperature data set was initially collected for 2 on a Nicolet R3m/V diffractometer and refined (Mn and I atoms anisotropic, the rest isotropic) : a - 29.374(6) A, b =12.980(3) A, c = 23.368(5) A, β = 121.05(3)°, R =0.0938, R_w = 0.1893 for 6694 observed reflections (Tables and figures are in Appendix H). The two I atoms which form a chain in the lattice had very large thermal parameters and appeared to be disordered. It has not been possible to model the disorder due to insufficient number of observed reflections. The data collected at 213 K on a different crystal improved the data / parameter ratio considerably and

allowed a full anisotropic refinement as well as modelling of the disordered atoms, starting with the room temperature coordinates.

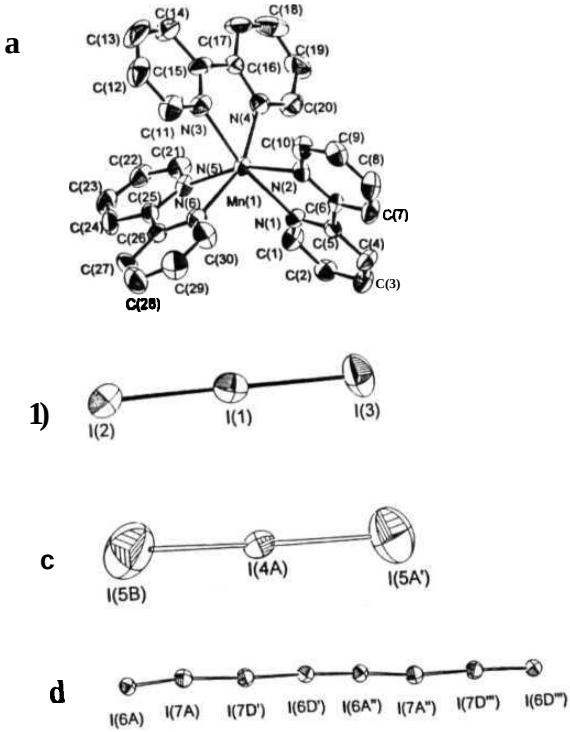

Figure 3.3 Views of the cation and anions in 2 (50% probability ellipsoids). (a) $[Mn(bpy)_3]^{2+}$ viewed along the c-axis which is close (within 5°) to the (pseudo) 3-fold axis of the (nominally) trigonally distorted octahedron. (b), (c) the two crystallographically inequivalent I_3^- ions (': *]-x, y,* 1½-*z*). (d) repeating unit of the $(I_8^{2-})_n$. (': -*x*, tt ½-*z*; ": *x*, -*y*, -½+*z*; ": -*x*, -*y*, -*z*;)• In (c), (d) only one member of the disordered set of ions is shown. (Additional drawings are in Appendix E.)

The I(6)-I(7) vector makes an angle of 3° with the c-axis and the chains are separated from the cation and the I_3^- anions, with the latter ions at distances varying between 4.08 A (from I(6D) of the chain) and 3.96 A (from I(7B) of the chain). The chain can be thought of as formally built by an endless repetition of linear I_8^{2-} units. Isolated I_8^{2-} ions usually have Z-type or outstretched Z-type structures[11] while isolated I_{16}^{4-} ions have S-type or chair type structures,[12] and I-I distances in these ions are consistent with interacting I_3^- and I_2 units. Linear iodine chains are expected to have alternating I-I distances based on the multicenter bonding model, and also require additional stabilization from other structural factors to prevent cleavage into separate I_3^- ions.[13] The stabilization is usually provided by coordinative bonds to the cations in the lattice.[14] Since there is no coordinative bonding interaction between the polyiodide chain and the $[Mn(bpy)_3]^{2+}$ cation, no such stabilization is possible in 2. Therefore, we assume that the stability results at least in part from weak interactions of the linear chain with the I_3^- ions in the lattice.

The iodine chains shown in the packing diagram (Figure 3.4) conform to two types of bond distance sequences, *viz.*, ·2.92-2.91-2.91-2.95-2.92-2.91-2.91··, and 2.95-2.84-2.92-2.98-2.95-2.84-2.92··.However, due to the presence of disorder, these sequences are somewhat arbitrary. What seems certain is that the present chain in 2 is more compact with an average I-I distance of 2.92 A than those in $[Sb(CH_3)_4]I_8$[14] and $[Cd(NH_3)_4]I_6$[13] which have average I-I distances of 3.29 and 3.17 A, respectively. This arrangement does not appear to be particularly stable, as demonstrated by the observation *(vide supra)* of the slow loss of I_2 from the crystals of 2 at ambient temperature. The unsymmetric I_3^- make lateral contacts with the ring carbons at a distance of about 3.8 A (I(3)-C(29), I(2)-C(3), **I(2)-C(8)).**

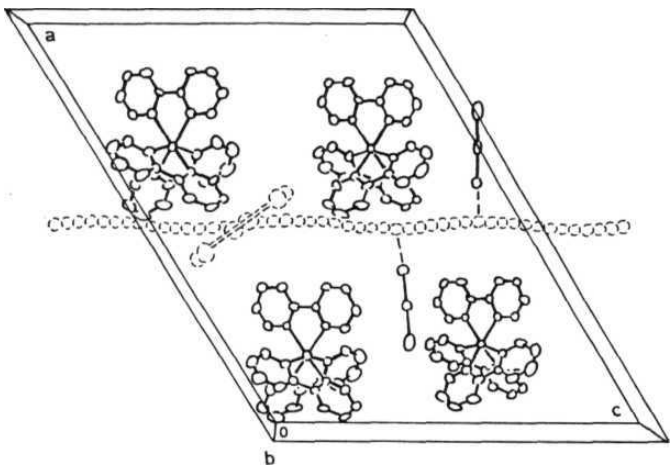

Figure 3.4 Packing diagram for 2. The disordered linear iodine chains run nearly parallel (within 3°) to the *c*-axis. All the disordered atoms of the chain are shown with dotted boundary. The disordered I_3^- is represented by dotted atoms and dotted hollow bonds. The chains are well isolated and aligned and make only weak contacts with I_3^- ions in the lattice. Two of the symmetry generated I_3^- are removed from the figure for clarity.

The geometry of the manganese center is pseudo-octahedral, with three bpy ligands binding to the manganese atom. The observed Mn-N bond distances and N-Mn-N bond angles (Table 3.4) are comparable to the same cation in $[Mn(bpy)_3](ClO_4)_2 \cdot 0.5H_2O$.[1a]

3.2.2 (c) Structure of 3. The structure consists of $[Ni(phen)_3]^{2+}$ cations, and two unsymmetrical slightly bent I_3^- anions. Views of the cation and I_3^- ions are shown in Figure 3.5. Selected bond distances and bond angles are listed in Table 3.6. The complex crystallises in the triclinic space group $P\bar{1}$, unlike the Mn analogue which crystallizes in a more symmetric space group, $R\bar{3}$. There has been a report of the formation of $[Ni(phen)_3](I_3)_2$, which crystallises in the monoclinic space group $P2_1/c$.[15] This could be the crystalline compound that was obtained before recrystallisation from CH_3CN in our synthesis.

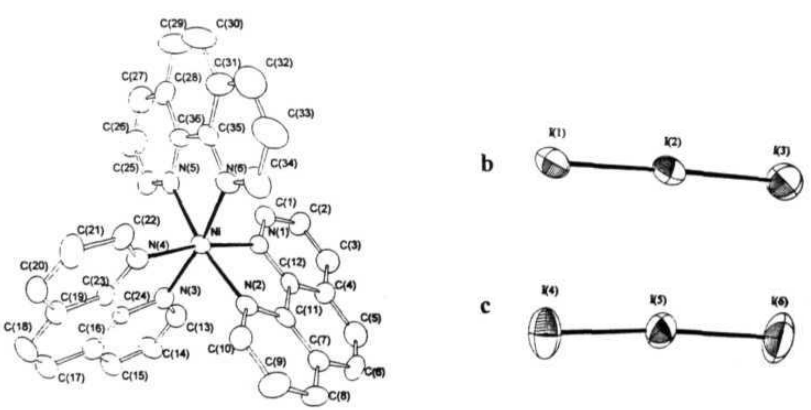

Figure 3.5 Views of the cation and anions of 3 (50% probability ellipsoids):(a) $[Ni(phen)_3]^{2+}$ cation (b), (c) the two asymmetric I_3^- anions.

The I-I distances for one of the I_3^- are 2.891 and 2.928 A **(I-I-I** angle of 176.240), **while** for the other are 2.882 and 2.925 A **(I-I-I** angle of **174.87°).** The Ni-N distances are in the range of 2.084 to 2.098 A, appreciably shorter than the Mn-N distances in 1 and 2. The N-Ni-N bite angles are correspondingly larger (average, 79.5°). These parameters are comparable to the reported structure of the **cation .**[1b] The two I_3^- ions have van der **waals'** contacts of 4.08 A (between **I(3)** and **I(4))** and 4.13 A (between **I(1)** and **I(1)' (':** -x, **1-y,** -z)) (Figure 3.6(a)). These result in a loosely connected S-shaped I_{12}^{4-} unit. Two such units are assembled in a displaced "head to tail" fashion around the cations resulting in contacts of 3.85 A between the ring carbons and iodines (I(4)-C(2); **I(5)···C(32)).**

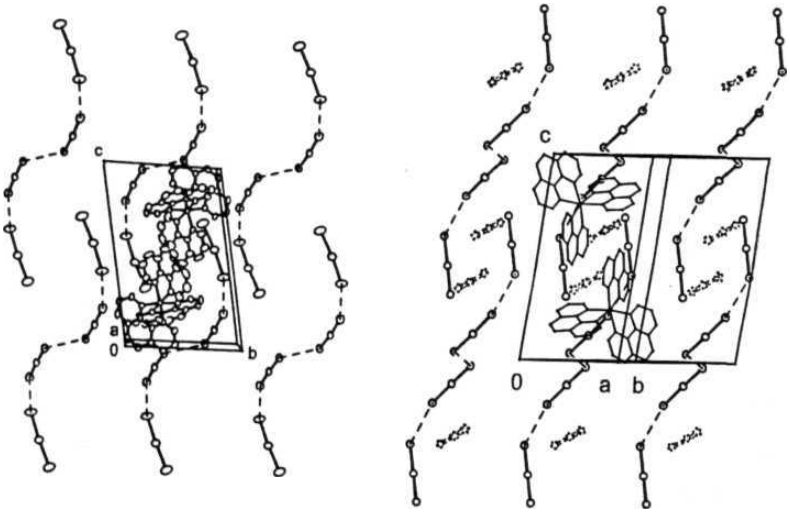

(a) (b)

Figure 3.6 Packing diagram for 3. (a) Viewed nearly along a-axis. (b) View showing the disordered CH3CN molecules (represented by dotted atoms and dotted hollow bonds).

There are also disordered CH_3CN molecules sitting in the cavities formed by the packing of the anions and cation. Only one-third of electron density corresponding to CH_3CN could be located from the difference fourier map. (Figure 3.6(b)).

3.2.3 EPR Spectra, Magnetic Studies and Conductivity of 1 and 2. Polycrystalline samples of 1 and 2 gave EPR spectra with broad features associated with transitions among the zero field split levels of the A_{1g} state. In frozen acetonitrile and dimethylformamide glassy solutions only the g = 2 signal is seen with hyperfine splitting (90 G). The other signals are probably broadened out due to strain in the glassy medium. Single crystals of both complexes gave five broad signals at several orientations but hyperfine splitting was not resolved. Since 1 has an exact trigonal symmetry, measurement with field along the hexagonal crystal axis will give the zero-field splitting (D). The spectrum along this axis is shown in Figure 3.7(a), from which a value of 0.154 cm^{-1} (g = 2.06) is calculated for D. In case of 2, the symmetry is close to trigonal, the normals to the planes defined by N(l), N(3), N(5), and N(2), N(4), N(6), respectively, being collinear within 2°. If one takes this as the (pseudo) trigonal axis of the cation, then the two magnetically equivalent sites of the monoclinic cell are found to be aligned with each other and also with the crystal c-axis within 5°. As a result, only one magnetic site is seen in the **EPR** spectra in all planes. Figure 3.7(b) shows the **EPR** spectrum along a direction close to the c-axis from which a D value of 0.066 cm^{-1} (g = 2.03) is estimated **for** 2.

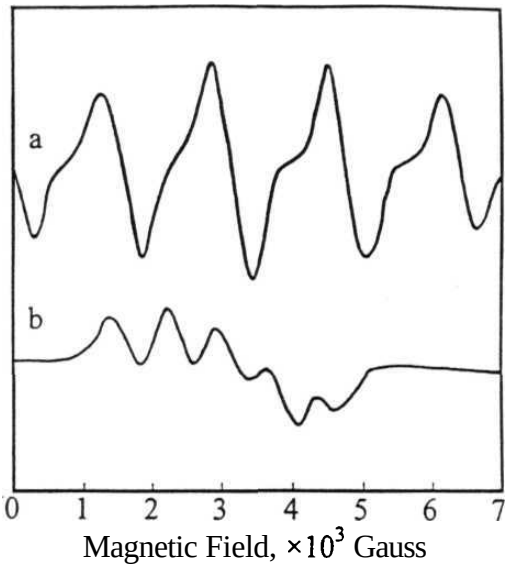

Figure 3.7 Single crystal EPR spectra measured at X-band (300 K) with the magnetic field along (a) the trigonal axis of $[Mn(phen)_3]^{2+}$ in 1 and (b) the (pseudo) trigonal axis of $[Mn(bpy)_3]^{2+}$ in 2.

The observed room temperature magnetic moment values of 5.85 and 6.05 μ_B for 1 and 2, respectively, are consistent with the expected spin only magnetic moment for S = 5/2, high spin d^5 manganese(II) complexes.

Room temperature resistivity measurements of single crystals of 1 and 2 revealed that 1 is an insulator, while 2 is an anisotropic semiconductor with a conductivity value in the range, 1-3 × 10^{-6} Scm^{-1}, for several crystals along directions close to the c-axis. The conductivity dropped to < 10^{-9} Scm^{-1}, when measured along a direction perpendicular to the c-axis. The measured conductivity value is comparable to that reported for $[Sb(CH_3)_4]_3I_8$ which has ordered (but not aligned) iodine chains.[14]

3.3 Conclusions

The formation of some unusual polyiodide anions has been observed during the synthesis of the present set of complexes, that involve slight differences in the size and shape of the cations (ligand and metal ion), which have greatly influenced the structure and packing of polyiodide anions. The polyiodide salts of tris-chelate complex cations belong to a completely new category of cations which have not been studied earlier. Such studies will be useful in achieving polyiodide species with special physical properties arising from charge transfer electronic transitions and low dimensional solid state structures of polyiodide anions. The above tris-phenanthroline complexes of M(II) (where M = Mn, Ni, Cu, Co) and the $[Mn(bpy)_3]^{2+}$ cation prefer to form polyiodide salts with normal iodine content, i.e., I ~ 3 per anionic charge. The crystal structure of 1 reveals an unusual kind of packing and the presence of microchannels in the crystals. It also has a symmetrical I_3^- with shortest I-I distance known. The presence of linear iodine chains is the most important feature of the crystal structure of 2. The linear iodine chains exhibit very different structural features in comparison to other previously reported polyiodide species. The crystal structure of 3 also shows presence of two I_3^- anions as in the case of 1, but both are slightly distorted and pack in a completely different manner with van der Waals' contacts between four units and also accommodating disordered solvent molecules in the empty cavities. The observed magnetic moments and EPR spectral patterns for the complexes 1 and 2, are consistent with those expected for high-spin d^5 manganese(II) complexes. Significantly, 2 exhibits anisotropic conductivity properties, quite unlike 1, but very similar to $[Sb(CH_3)_4]_3I_8$, which contains linear iodine chains, suggesting that this conductivity must be arising from the presence of linear iodine chains in the crystals.

References

(1) (a) X. -M. Chen, R. -Q. Wang, and Z. -T. Xu *Acta Crystallogr.* **1995, *C51,*** 820. (b) K. **R.** Butler and M. R. Snow J. *Chem. Soc Sec.A* **1971,** 565.

(2) R. L. Datta and A. Syamal *Elements of Magnetochemistry*, S. Chand Co. Ltd., New Delhi (India), **1982.**

(3) A. C. T. North, D. C. Phillips and F. S. Mathews *Acta Crystallogr.* **1968, *A24*, 351.**

(4) (a) G. **M.** Sheldrick, *SHELXS86. Acta Crystallogr.* **1990,** *A46,* 467. (b) G. M. Sheldrick, *SHELXL93*, University of Gottingen, Gottingen, **1993.**

(5) (a) G. M. Sheldrick, (1995) *SHELXTL Crystallographic System,* v. 5.03, Siemens Analytical X-ray Instruments, Inc.: Madison, WI, USA. (b) G. M. Sheldrick, *SHELXL97,* University of Gottingen, Gottingen, **1997.**

(6) H. A. Goodwin and R. N. Sylva *Aust. J. Chem.* **1965,***18,* 1743.

(7) A. **I.** Popov and R. E. Buckles *Inorganic Syntheses,* McGraw-Hill, New York (USA), **1957,** vol. 5, p. 167.

(8) S. Menon and M. V. Rajasekharan *Inorg. Chem.* **1997,** *36,* 4983.

(9) (a) K. Toman, J. Honzl and J. Jecny *Acta Crystallogr.* **1965,** *18,* 673. (b) T. Bernstein and F. H. Herbstein *Acta Crystallogr.* **1968,** *B24,* 1640. (c) Y. S. Sohn, S. W. Albert and D. N. Hendrickson *Inorg. Chem.* **1974,** *13,* 301 (d) M. G. Drew and J. D. Wilkins *J. Chem. Soc, Dalton Trans.* **1973,** 2664. (e) J. W. Bats, J. J. de Boer and D. Bright *Inorg. Chim. Acta* **1971,** *5,* 605. (f) F. Demartin, P. Deplano, F. A. Devillanova, F. Isaia, V. Lippolis and G. Verani *Inorg. Chem.* **1993,** *32,* 3694.

(10) (a) A. F. Bertram and J. A. Ibers *Inorg. Chem.* **1972,** *11,* 1109. (b) O. P. Anderson, *J. Chem. Soc, Dalton Trans.* **1973,** 1237. (c) D. Boys, C. Escobar and O. Wittke *Acta Crystallogr.* **1984,** *C40,* 1359. (d) J. Baker, L.

M. Engelhardt, B. N. Figgis and A. H. White *J. Chem. Soc, Dalton Trans.* **1975,** 530. (e) L. L. Koh, Y. Xu, A. K. Hsieh, B. Song, F. Wu and L. Ji *Acta Crystallogr.* **1994,** *C50,* 884.

(11) (a) E. E. Havinga, K. H. Boswijk and E. H. Wiebenga *Acta Crystallogr.* **1954,** 7, 487. **(b) P.** K. Hon, T. C. W. Mak and J. Trotter *Inorg. Chem.* **1979,** *8*, 2916. (c) A. J. Jircitano, M. C. Colton and K. B. Mertes *Inorg. Chem.* **1981,** *20,* 890. (d) B. Freckmann and K. -F. Tebbe Z. *Kristallogr.* **1981,** *154,*27 *A.*

(12) (a) F. H. Herbstein and M. Kapon *J. Chem. Soc, Chem. Commun.* 1975, 677. (b) F. Bigoli, M. A. Pellinghelli, G. Crisponi, P. Deplano and E. F. Trogu *J. Chem. Soc, Dalton Trans.* **1985,** 1349.

(13) K. -F. Tebbe in *Homoatomic Rings, Chains and Macromolecules of Main-group Elements,* Ed. A. L. Rheingold, Elsevier, Amsterdam (The Netherlands), **1977,** p.551.

(14) U. Behrens, H. J. Breunig, M. Denker and K. H. Ebert *Angew. Chem. Int. Ed Engl.* **1994,** *33,* 987.

(15) **B.** Freckmann and K. -F. Tebbe *Acta Crystallogr.* **1981,** *A37,* C228.

CHAPTER 4

Polyiodide Salts of Metal Complex Cations : Part 2. Polyiodide Anions with Higher Iodine Content

Syntheses and Crystal Structures of $[Cu(bpy)_3]I_8 \cdot CH_2Cl_2$, $[Fe(bpy)_3]I_9$, $[Zn(bpy)_3]I_{12}$ and $[Zn(phen)_3]I_{12}$

The polyiodide species formed with metal complex cations are very sensitive to the metal ion involved and also on the size, shape and rigidity of the ligand. An ion having empirical formula, I_p^-, with $p > 4$ can be considered as a polyiodide with higher iodine content. A large number of compounds have been synthesised that have p varying from 4 to 9.67. These contain anionic units of I_8^{2-}, I_{16}^{4-}, I_{18}^{4-}, I_5^-, I_{22}^{4-}, I_{12}^{2-}, I_{26}^{4-}, I_7^-, I_{16}^{2-}, I_9^- and I_{29}^{3-}.[1-4] As can be seen in the previous chapter, the complex cations of Mn^{2+} and other metal tris chelates of 1,10-phenanthroline, prefer I_3^- ions as counter-anions. But under the same reaction conditions, i.e. ratio of iodine to iodide remaining the same, most of the 2,2'-bipyridine tris-chelate cations crystallize out as polyiodides with $p > 4$, i.e. I_8^{2-}, I_{18}^{4-} or I_{12}^{2-}. The same has been observed earlier in the case of $[Cu(dafone)_3]I_{12}$.[2b]

In this chapter, synthesis and structural characterization of four such complexes, $[Cu(bpy)_3]I_8 \cdot CH_2Cl_2$, $[Fe(bpy)_3]I_9$, $[Zn(bpy)_3]I_{12}$ and $[Zn(phen)_3]I_{12}$ will be discussed, along with attempted synthesis of polyiodide salts of

$[Al(bpy)_3]^{3+}$ and $[Co(bpy)_3]^{2+}$, which resulted in the isolation of $[bpyH]I_5$ and $[bpyH]I_7$ respectively.

4.1 Synthesis and Crystal Structure of $[Cu(bpy)_3]I_8 \cdot CH_2Cl_2$

4.1.1 Experimental

4.1.1 (a) Synthesis. $[Cu(bpy)_3]I_8 \cdot CH_2Cl_2$ (6) To a solution of $Cu(OAc)_2 \cdot 4H_2O$ (0.500 g, 1.93 mmol) and 2,2'-bipyridine (1.00 g, 6.40 mmol) in water (10 mL), a solution of I_2 (1.0 g, 3.9 mmol) in dichloromethane (25 mL) and solid KI (0.66 g, 4.0 mmol) were added. Dil. sulphuric acid (1 M, 1 mL) was then added to the two phase reaction mixture, and the mixture stirred for 10 min. The deep brown coloured organic layer was separated by extraction with an additional amount of dichloromethane (50 mL), and dried over Na_2SO_4. After filtering the organic solution and allowing the filtrate to stand at low temperature (~10°C) for 3-4 d, dark shining rectangular crystals formed. The crystals were seen to lose I_2 and the shine slowly over a period of several days at room temperature. Yield: 1.370 g (0.84 mmol, 63%, based on I_2). Anal. Calcd for $C_{31}H_{26}N_6Cl_2CuI_8$ (MW 1632.3): C, 22.81; H, 1.61; N, 5.15. Found: C, 22.57; H, 1.80; N, 5.45. Characteristic IR bands (cm^{-1}): 1590(s), 1563(s), 1485(w), 1468(s), 1436(s), 1308(s), 1246(w), 1152(w), 1098(s), 1057(w), 1019(w), 885(w), 756(vs), 733(s), 648(w), 623(w), 511(vw), 430(s), 413(s).

$[Ni(bpy)_3]I_8$. (7) The complex was prepared following a similar procedure, using $Ni(OAc)_2 \cdot 4H_2O$ (0.500 g, 1.96 mmol). The dark shining triangular shape crystals formed after allowing the filtrate to stand at low temperature (~ 10°C) for 3 to 4 days. The crystals were found to lose I_2 over a period of time, when stored at room temperature. Yield: 1.52 g (0.99 mmol, 74% based on I_2). Anal. Calcd for

$C_{30}H_{24}N_6NiI_8$: (MW 1542.5) C, 23.36; H, 1.57; N, 5.45. Found: C, 23.39; H, 1.42; N, 5.22. Characteristic IR bands (cm^{-1}): 1593(w), 1468(w), 1435(w), 1308(w), 1152(w), 1101.5(w), 1017(w), 768(s), 733(w), 650(w), 631(w), 415(w).

4.4.1 (b) X-ray Crystallography Data for a dark brown rectangular crystal were collected at 298 K on a CAD4 diffractometer using graphite monochromated Mo-K_α radiation. The data were corrected for Lorentz-polarization effects and absorption.[5] A linear decay correction was also applied as the crystal showed a 15% decay of the intensities of the standard reflections. The structure was solved by a combination of Patterson and direct methods (SHELXS) and refined (over F^2) by least squares techniques (SHELXL).[6]

The complex crystallises in the monoclinic system, space group C2/c, with 4 molecules in the unit cell. A total of 4273 reflections (3908 unique, 2660 with F > 4σF) were collected in the 26 range 4.1 to 50°, with indices -21 < h < 21, 0 < k < 23, 0 < 1 < 14. Non-hydrogen atoms except the solvent atoms were refined anisotropically and all ring and solvent hydrogen atoms were included in calculated positions using a riding model. The atoms of the solvent CH_2Cl_2 were located from the difference fourier map and bond length constraints were applied. The final cycle of full matrix least squares refinement on F^2 converged with unweighted and weighted agreement factors of R1 = 0.0497 and wR2 = 0.1375. The goodness of fit was S = 0.883 with 2660 observations, 216 parameters and 4 restraints. The maximum and minimum peaks on the final difference fourier map corresponded to 1.586 and -0.992 e/A^3 respectively. Crystallographic data and selected bond angles and bond distances are listed in Table 4.1 and Table 4.2 respectively. Full crystallographic data and other positional parameters are listed in Appendix I.

Table 4.1

Crystallographic Data for $[Cu(bpy)_3]I_8 \cdot CH_2Cl_2$ (6)

formula	$C_{15.50}H_{13}ClCu_{0.50}I_4N_3$	z	8
formula weight	816.11	space group	C2/c(No. 15)
a	18.4452(16) A	T	293(2) K
b	19.9512(11) A	*X*	0.71073 A
c	12.4287(10) A	p(calcd)	2.431 Mg/m^3
a	90°	μ	6.178 mm^{-1}
β	102.873(7)°	R1	0.0497
y	90°	wR2	0.1375
V	4458.9(6) A^3		

R1 = $\Sigma||F_o| - |F_c||/\Sigma|F_o|$

wR2 = $[\Sigma\{w(F_o^2 - F_c^2)^2\}/\Sigma(wF_o^4)]^{1/2}$

$w^{-1} = [\sigma^2(F_o^2) + (0.0982P)^2 + 47.9340P]$, $P = (F_o^2 + 2F_c^2)/3$

Table 4.2

Selected bond lengths [A] and angles [deg] for 6.

Bond distances :

I(1)-I(2)	2.8663(11)	I(2)-I(3)	2.9703(10)
I(3)-I(4)	3.3919(10)	I(4)-I(4)#l	2.7827(13)
Cu-N(3)	2.031(6)	Cu-N(2)	2.041(6)
Cu-N(l)	2.327(6)		

Bond angles :

I(1)-I(2)-I(3)	177.61(3)	I(2)-I(3)-I(4)	86.04(2)
I(4)#1-I(4)-I(3)	172.20(2)	N(3)-Cu-N(3)#2	80.3(3)

N(2)-Cu-N(l) 76.2(2)

Intermolecular contacts :

(a) I...I contacts :

Distances:

I(3)...I(3)#3 4.048(1)

Angles:

I(2)-I(3)-I(3)#3 150.26(3)

(b) I...ring contacts :

Distances:

I(1)...H(7)#4	3.199(1)	I(3)...H(8)#5	3.117(1)
I(3)...H(11)#6	3.188(1)	I(4)...H(14)#7	3.182(1)
I(1)-Cl1(1)	3.815(8)		

Angles:

I(l)-H(7)#4-C(7)#4	148.9(6)	I(3)-H(8)#5-C(8)#5	142.6(5)
I(3)-H(11)#6-C(11)#6	130.8(5)	I(4)-H(14)#7-C(14)#7	164.0(5)
1(2)-1(1)-C1(1)	68.3(1)		

Symmetry transformations used to generate equivalent atoms:

#1 -x+l,y,-z+l/2; #2 -x,y,-z+3/2; #3 -x+1/2, y-1/2, -z+1; #4 -x+1/2, -y-1/2, -z+1; #5 x, y z-1; x,-y,-1/2; #6 -x+1/2, y-1/2,-z+3/2; #7 -x+1/2, -y+1/2, -z+1;

4.1.2 Results and Discussion

4.1.2 (a) Structure. The structure of 6 consists of $[Cu(bpy)_3]^{2+}$ cation, I_8^{2-} anion and disordered CH_2Cl_2 solvent molecules. Views of the cation and I_8^{2-} anion are shown in Figure 4.1

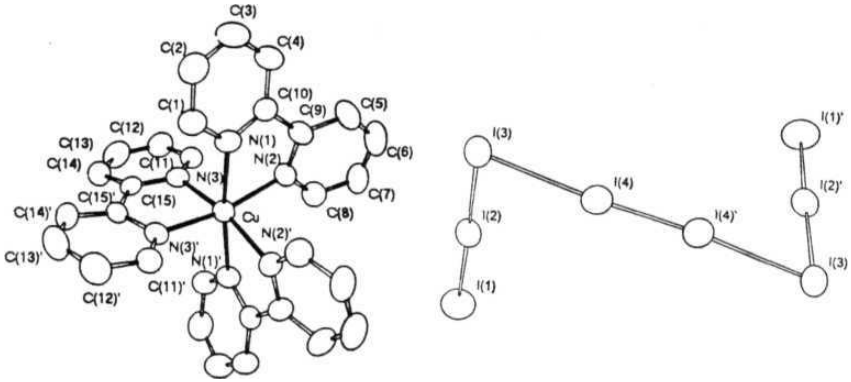

(a) (b)

Figure 4.1 Views of the cation and anion of 6 (40% probability ellipsoids) : (a) $[Cu(bpy)_3]^{2+}$ (' = -x, y, -z+3/2), (b) I_8^{2-} (' = -x+1, y, -z+1/2).

The cation has a site symmetry of 2, with the Cu atom sitting on a crystallographic 2-fold axis and having a tetragonally elongated geometry.

The I_8 anion similarly has a 2-fold axis passing through the centre of the I(4)-I(4)' bond. The I_8^{2-} ion is formed from an I_2 molecule bridged between two I_3^- ions ($I_3^-.I_2.I_3^-$) at a distance of 3.392 A and at an angle of 86.04°. The I_3^- is slightly asymmetric with bond distances of 2.866 and 2.970 A and an angle of 177.6°. The I_2 is slightly elongated to a bond length of 2.783 A (I-I bond distance of 2.70 A in crystalline I_2 [7]), due to the interaction with I_3^- ions on both sides. The bond distances and angles are similar to the other reported centrosymmetric Z-shaped planar I_8^{2-} structures.[1] However, the I_8^{2-}, here, is anti-planar with a torsion angle of 93.21° between I(1)-I(3)-I(3)'-I(1)'. There are two other discrete

I_8^{2-} described in literature which have anti-planar geometry, but these ions have longer $I_3^-..I_2$ contacts (> 3.50 Å).[1g,h] A list of all the reported I_8^{2-} anions are compared in Table 4.1. The I_8^{2-} ions are nearly isolated except for van der Waals' contacts 4.048 A between the I(3) atoms of adjacent ions.

(a)

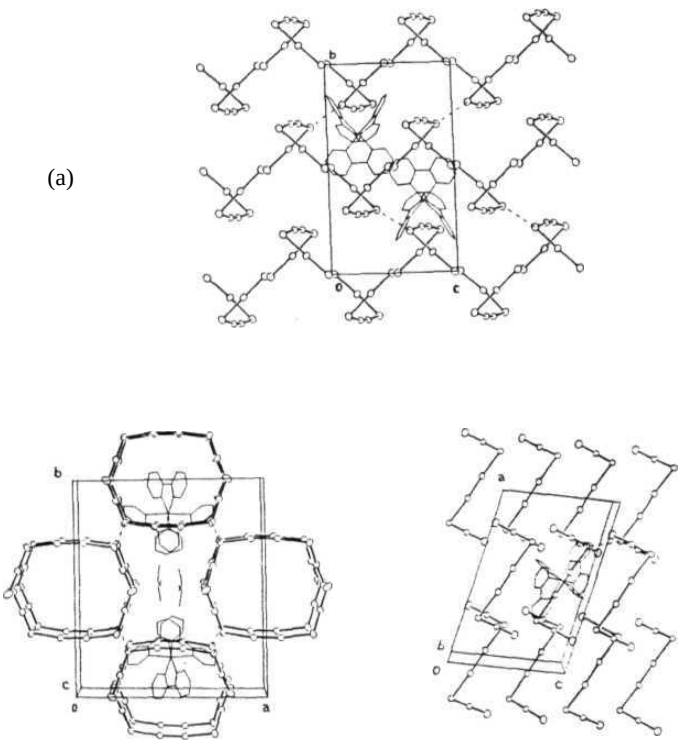

(b) (c)

Figure 4.2 Views of the packing in 6, viewed normal to (a) bc, (b) ab and (c) ac planes. The cations occupy the channels along *a*-axis while the disordered CH_2Cl_2 molecules occupy the channels along *c*-axis. (All cations ans solvent molecules are not shown.)

Table 4.1 Comparison of structural parameters in I_8^{2-} anions.

Compound	Structure	Type	Torsion angle (1-3-6-8)	I..I Contact distance	Ref.
Cs_2I_8		isolated centrosym	180°	>3.90 Å	1a
$[Adam]_2I_8$	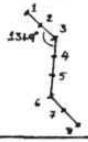	isolated centrosym	180°	>4.28 Å	1b
$[Mg(H_2O)_6]I_8$	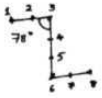	isolated centrosym	180°	>3.84 Å	1c
$[MePh_3P]_2I_8$	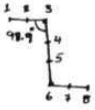	isolated centrosym	180°	>4.56 Å	1d
$[Cu(phen)_2X]_2I_8$*	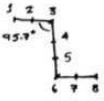	isolated centrosym	180°	>4.50 Å	1e
$[Cu(bpy)_3]I_8$		isolated centrosym	93.21°	>4.04 Å	this work

$[Pd(NH_3)_4]I_8$	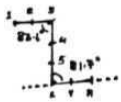	discrete (chains 3.641 A)	180°	>4.03 Å	1e
$[Pd(TAAB)]I_8$	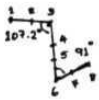	isolated discrete	105.8°	>4.07 Å	1f
$[Pt(TAAB)]I_8$	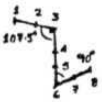	isolated discrete	106.1°	>4.07 Å	1f
$(phen)_3.H_2I_8$*	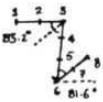	discrete	-110.2°	>3.74 Å	1e
$[Threo]_2I_{16}$	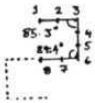	centrosym (dimer 3.45 Å)	5.9°	>3.84 Å	1g
$[moH]_2I_{16}$	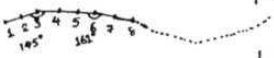	centrosym (dimer 3.55 Å)	-	-	1h

structure not reported in detail.

The anion also makes contacts of 3.9 to 4.0 A with ligand carbons (I(1)..C(7), I(3)..C(8), I(4)..C(14)). The cation and anions pack in layers forming channels along c-axis direction. These channels are filled with disordered solvent molecules (CH_2Cl_2). The I_8^{2-} with its unique I..I contact forms infinite networks resulting in channels along a-axis direction that are filled with ordered cations of $[Cu(bpy)_3]^{2+}$ (Figure 4.2).

The coordination geometry of Cu atom is tetragonally distorted octahedron with two equal long axial bonds (2.327 A) and four nearly equal equatorial bonds (average 2.036 A), due to static Jahn-Teller distortion of the Cu^{2+} complex ion. Similar geometry was observed in $[Cu(phen)_3](ClO_4)_2$,[8a] while $[Cu(bpy)_3](ClO_4)_2$[8b] exhibits two unequal axial bonds. The $[Cu(en)_3]^{2+}$ [8b] and $[Cu(dafone)_3]^{2+}$ ions,[2b] other tris- chelates of Cu^{2+}, show trigonal distortion and tetrahedral distortions, respectively.

The N-Cu-N chelate bite angles are 80.3° for the bpy ligand with twO-fold symmetry axis and 76.2° for the other two ligands. The angle between the mean planes of the two pyridine rings in the bpy ligands are 22.1° and 15.0° respectively. Similar non-coplanarity of the bpy ligand was also observed in the complex $[Cu(bpy)_3](ClO_4)_2$.[8]

4.1.2 (b) **EPR.** The X-band EPR spectra of the microcrystalline sample of 6 at 300 K and 153 K show a strong signal at g = 2.09 with anisotropy, but no hyperfine features. The frozen CH_3CN solution (153 K) also shows a broad spectrum with parallel components of the hyperfine splitting barely resolved. (Figure 4.3(a)(3)).

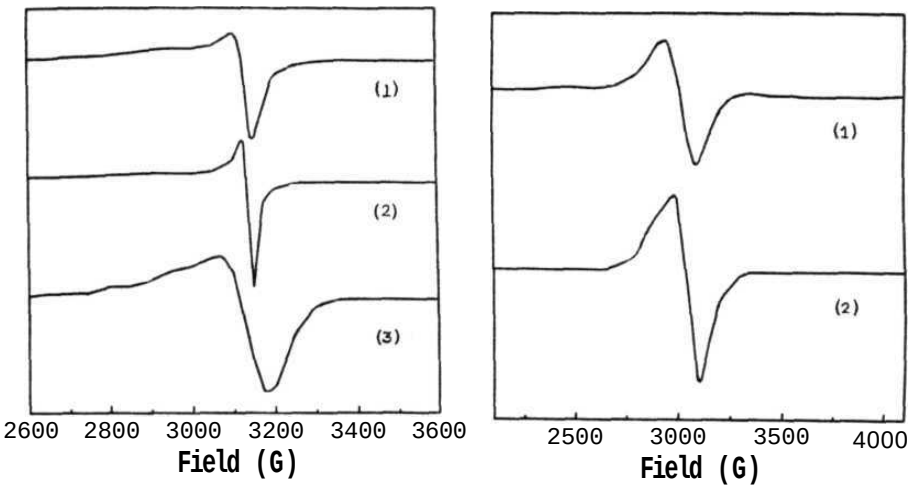

(a) **(b)**

Figure 4.3 EPR spectra of 6 and 4 : (a) microcrystalline sample of 6 at 300K, v = 9.170 GHz (1), 153 K, v = 9.170 GHz (2) and CH_3CN glass, v = 9.150 GHz (3); (b) microcrystalline sample of 4 at 300K, v = 9.165 GHz (1) and 153 K, v = 9.168 GHz (2).

The EPR spectra of microcrystalline sample of $[Cu(phen)_3](I_3)_2 \cdot CH_3CN$ (4), shows a single absorption at g = 2.15 at 300 K as well as 153 K (Figure 4.3(b)). The frozen CH_3CN solution (153 K) of 4 also shows a single absorption at g = 2.11 and no hyperfine features. The **EPR** spectra of the nitrate salts of $[Cu(bpy)_3]^{2+}$ and $[Cu(phen)_3]^{2+}$ were previously reported. They have an isotropic spectrum (>263 K) and anisotropic spectra (77 K to 263 K), indicating a dynamic Jahn-Teller distortions above 263 K.[9]

4.2 Synthesis and Crystal Structure of $[Fe(bpy)_3]I_9$

4.2.1 Experimental

4.2.1 (a) Synthesis. $[Fe(bpy)_3]I_9$. (8) The complex was prepared using $Fe_2(SO_4)\cdot 7H_2O$ (0.500 g, 1.78 mmol) and 2,2'-bipyridine (1.00 g, 6.40 mmol) in water (10 mL), a solution of I_2 (1.0 g, 3.9 mmol) in dichloromethane (25 mL) and solid KI (0.66 g, 4.0 mmol) were added. Dil. sulphuric acid (1 M, 1 mL) was then added to the two phase reaction mixture, and the mixture stirred for 10 min. The deep brown coloured organic layer was separated by extraction with an additional amount of dichloromethane (50 mL), and dried over Na_2SO_4. After filtering the organic solution and allowing the filtrate to stand at low temperature (~10°C) for 3-4 d, dark shining (with a greenish tinge) rhombic shaped crystals formed. The crystals have been observed to lose I_2 and the shine slowly over a period of several days at room temperature. Yield: 1.123 g (0.674 mmol, 59%, based on I_2). Anal. Calcd for $C_{30}H_{24}N_6FeI_9$ (MW 1666.5): C, 21.62; H, 1.45; N, 5.04. Found: C, 21.75; H, 1.41; N, 5.02. Characteristic IR bands (cm^{-1}): 2920.5(vw), 1601(w), 1462(w), 1439(s), 1385(s), 1310(w), 1238(w), 1152(w), 876(w), 754(vs), 727(s), 413(w).

4.2.1 (b) X-ray Crystallography. Data for a dark greenish-shining rectangular rod-like crystal were collected at 298 K on a CAD4 diffractometer using graphite monochromated Mo-K_α radiation. The data were corrected for Lorentz-polarization effects and absorption.[5] The structure was solved using a combination of Patterson and direct methods (SHELXS) and refined (over F^2) by least squares techniques (SHELXL).[6]

The complex crystallises in the monoclinic system, space group $P2_1/c$, with 4 molecules in the unit cell. A total of 6542 reflections (6094 unique, 4222 with F > 4σF) were collected in the 2θ range 4 to 50°, with indices 0 < h < 10, 0 < k < 26, -18 < 1 < 17. The complete data with h index upto 14 could not be collected as the crystal showed a decay of 50%. Hence the structure solution and refinement was done with about 90% of the required data after applying a linear decay correction. All non-hydrogen atoms were refined anisotropically and all ring hydrogen atoms were included in calculated positions using a riding model. The final cycle of full matrix least squares refinement on F^2 converged with unweighted and weighted agreement factors of R1 = 0.0629 and wR2 = 0.1266. The goodness of fit was S = 1.140 with 4222 observations and 450 parameters. The maximum and minimum peaks on the final fourier map corresponded to 1.683 and -1.277 e/A^3 respectively. Crystallographic data and selected bond angles and bond distances are listed in Table 4.3 and Table 4.5 respectively. Full crystallographic data and other positional parameters are listed in Appendix J.

Table 4.3

Crystallographic Data for $[Fe(bpy)_3]I_9$ (8)

formula	$C_{30}H_{24}FeI_9N_6$	*I*	4
formula weight	1666.50	space group	P 2_1/c (No. 14)
	12.237(4) A	T	293(2) K
b	22.496(4) A	*X*	0.71073 A
c	15.779(5) A	p(calcd)	2.711 Mg/m^3
a	90°	μ	7.204 mm^{-1}
p	109.94(3)°	R1	0.0629
γ	90°	wR2	0.1266

V 4083(2) A^3

$R1 = \Sigma||F_o| - |F_c||/\Sigma|F_o|$

$wR2 = [\Sigma\{w(F_o^2 - F_c^2)^2\}/\Sigma(wF_o^4)]^{1/2}$

$w^{-1} = [\sigma^2(F_o^2) + (0.0361P)^2 + 91.6184P]$, $P = (F_o^2 + 2F_c^2)/3$

Table 4.4

Selected bond lengths [A] and angles [deg] for 8.

Bond distances :

I(1)-I(2)	2.8585(14)	I(2)-I(3)	3.0232(14)
I(3)-I(4)	3.509(2)	I(4)-I(5)	2.752(2)
I(5)-I(6)	3.408(2)	I(6)-I(9A)	3.019(3)
I(6)-I(7)	3.277(2)	I(7)-I(8)	2.729(2)
I(8)-I(9B)#1	3.507(3)	I(9A)-I(9B)#2	2.817(4)
I(9A)-I(9A)#2	3.531(5)	I(9B)-I(9A)#2	2.817(4)
Fe-N(6)	1.950(8)	Fe-N(2)	1.956(8)
Fe-N(l)	1.960(9)	Fe-N(5)	1.961(9)
Fe-N(3)	1.966(9)	Fe-N(4)	1.974(9)

Bond angles :

I(1)-I(2)-I(3)	173.59(4)	I(2)-I(3)-I(4)	178.88(4)
I(5)-I(4)-I(3)	170.71(5)	I(4)-I(5)-I(6)	176.29(4)
I(9A)-I(6)-I(7)	111.37(6)	I(9A)-I(6)-I(5)	115.26(6)
I(7)-I(6)-I(5)	84.77(4)	I(8)-I(7)-I(6)	174.77(5)
I(7)-I(8)-I(9B)#1	169.48(6)	I(9B)#2-I(9A)-I(6)	173.50(9)
I(6)-I(9A)-I(9A)#2	177.65(12)	N(2)-Fe-N(l)	81.5(4)
N(6)-Fe-N(5)	81.6(4)	N(3)-Fe-N(4)	81.9(4)

Intermolecular contacts :

(a) I...I contacts :

Distances:

1(1)...I(1)#3	3.832(2)	I(6)...I(9B)	3.757(3)
I(8)...I(9A)#1	3.571(3)		

Angles:

I(2)-I(l)-I(l)#3	161.35(5)	I(6)-I(9B)-I(9A)#2	170.0(1)
I(7)-I(8)-I(9A)#1	157.04(6)		

(b) I...ring contacts :

Distances:

I(5)...H(13)#4	3.185(12)	I(6)...H(27)#5	3.142(14)
I(7)...H(8)#6	3.033(11)	I(9A)...H(18)#7	3.016(16)
I(9B)...H(18)#8	3.132(16)		

Angles:

I(5)-H(13)#4-C(13)#4	132.2(12)	I(6)-H(27)#5-C(27)#5	159.3(13)
I(7)-H(8)#6-C(8)#6	131.8(11)	I(9A)-H(18)#7-C(18)#7	124.2(14)
I(9B)-H(18)#8-C(18)#8	133.5(14)		

Symmetry transformations used to generate equivalent atoms:

#1 -x+1, -y+1, -z+2; #2 -x+2, -y+1, -z+2; #3 -x, -y, -z; #4 -x, -y, -z; #5 -x, y+1/2, -z+1/2; #6 -x+1, -y+1, -z+1; #7 x+1, y, z+1; #8 x+1,-y+1/2, z+1/2;

4.2.2 Results and Discussion

4.2.2 (a) Structure. The structure consists of $[Fe(bpy)_3]^{2+}$ cation and network forming centrosymmetric I_{18}^{4-} anion. Views of the cation and the anion are shown in Figure 4.4(a), (b).

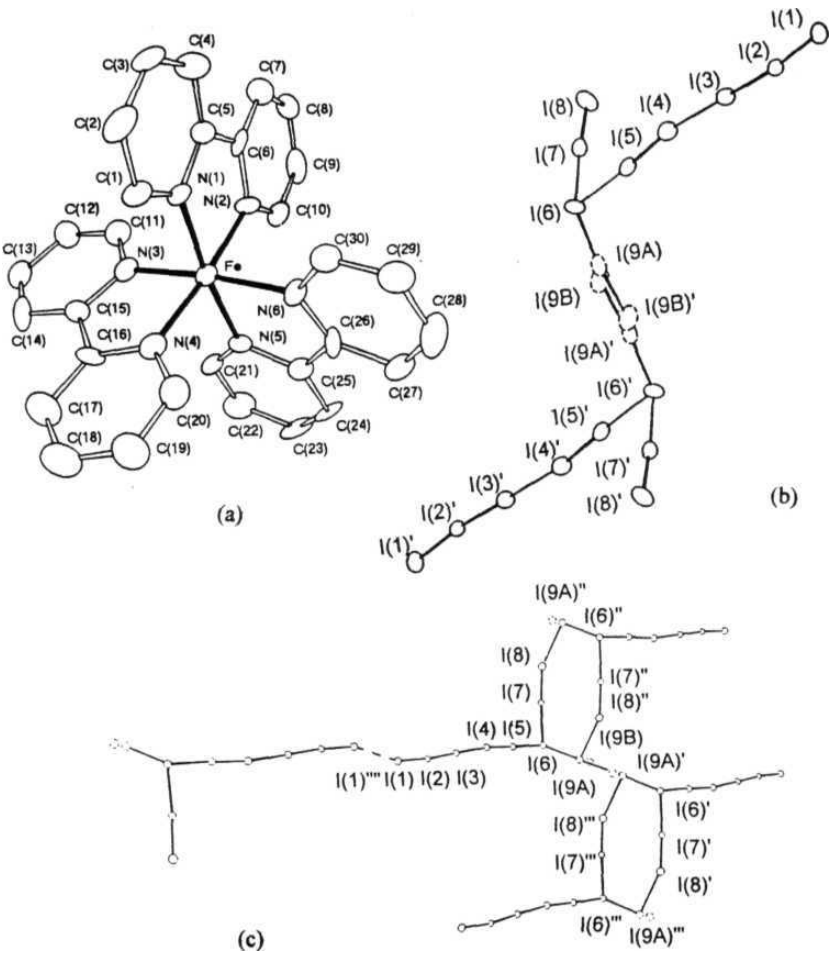

Figure 4.4 Views of the cation and anion of 8 (40% probability ellipsoids for a, b) : (a) $[Fe(bpy)_3]^{2+}$ cation, (b) the I_{18}^{4-} unit consisting of an iodine disordered in two positions (I(9A), I(9B)) (' = -x+2, -y+1, -z+2), (c) the $(I_9^{2-})_n$ repeating unit forming 8-membered bridged rings along ***a*-axis.** The linear I_5^- branches above and below the ring planes are also shown (' = -x+2, -y+1, -z+2; " = -x+1, -y+1, -z+2;''' = x+1, y, z; "" - -x, **-y,-z**).

The anion I_{18}^{4-} is a new polyiodide species which forms infinite networks running along *a*-axis direction. The asymmetric unit consists of nine iodine atoms, one of them is disordered in two positions (I(9A) and I(9B) with equal occupation factors). Based on the bond distances (Figure 4.4(b)), the polyiodide unit can be thus divided into smaller fragments of I_3^-, I_2 that are connected by longer bonds. The repeating unit can be described to form infinite chains of 8-member planar rings {I(9A)-I(6)-I(7)-I(8)-I(9A)"-I(6)"-I(7)"-I(8)"}, (deviations from the mean plane range from 0.02 A for I(7) to 0.12 A for I(8)) bridged via I_3^- ions, running parallel to *a*-axis. These rings are connected to linear branches of the type $I_3^-.I_2$ at I(6) position, inclined above and below the ring. The I(1) makes van der Waals' contact of 3.832 A with the I(1)"' of the adjacent I_{18}^{4-} unit (Figure 4.4(c)). The I_{18}^{4-} repeating unit can also be described as parallel zig-zag chains of iodine atoms running diagonally across the bc plane, linked through the I_2 units of I(7)-I(8) (Figure 4.5(a)). There has been a recent report of discrete I_{18}^{4-} anion in the complex, $[SnI_2(mbit)_2](I_3)_2.2/3I_2$, [3] in which two I_8^{2-} units related by a symmetry centre are held together by a disordered diiodine molecule through an interaction across a distance of 3.55 A.

The anionic network of I_{18}^{4-}, assembles to form channels along both a- and b- axis directions, which are filled with $[Fe(bpy)_3]^{2+}$ cations (Figure 4.5(a),(b)). The cations and anionic network pack in layers along c-axis direction (Figure 4.5(c)). The channels hold the cations with planar 8-membered rings on one side and perpendicular linear $I_3^-.I_2$ units along the other side. The anion also makes contacts of 3.6 to 4.0 A with the ligand rings (I(5)..C(13), I(7)..C(27), I(7)..C(8), I(9A)..C(18)).

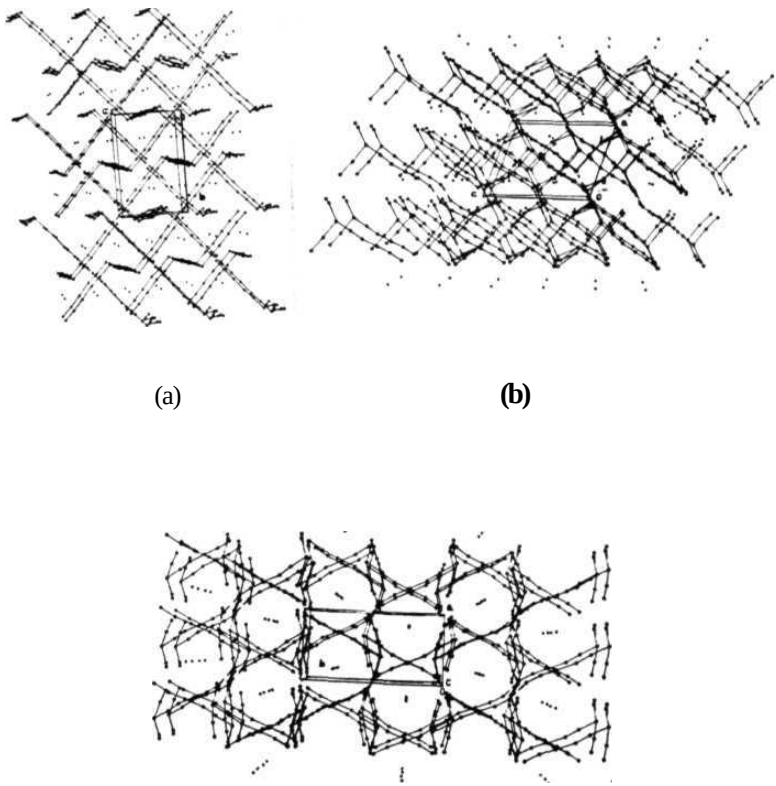

(a) **(b)**

(c)

Figure 4.5 Views of packing of anion in 8 (a) **bc** plane, (b) ac plane and (c) ab plane (**Fe^{2+}** atoms are shown as small circles. The ligands are omitted.).

The coordination geometry of the Fe atom is pseudo-octahedral with nearly equal Fe-N bond distances (average 1.96 A) and N-Fe-N chelate bite angles

(81.7°). These are consistent with the literature values reported for $[Fe(bpy)_3]^{2+}$ [10a] as well as $[Fe(bpy)_3]^{3+}$ cation.[10b] The bpy ligands are nearly planar having angles of 7.2°, 1.5° and 5.4° respectively, between the mean planes of the two pyridine rings.

4.3 Syntheses and Crystal Structures of $[Zn(bpy)_3]I_{12}$ and $[Zn(phen)_3]I_{12}$

4.3.1 Experimental

4.3.1 (a) Synthesis. $[Zn(bpy)_3]I_{12}$ (9) The complex was prepared using $Zn(OAc)_2{\cdot}4H_2O$ (0.500 g, 1.91 mmol) and 2,2'-bipyridine (1.00 g, 6.40 mmol) in water (10 mL), a solution of I_2 (1.0 g, 3.9 mmol) in dichloromethane (25 mL) and solid KI (0.66 g, 4.0 mmol) were added. Dil. sulphuric acid (1 M, 1 mL) was then added to the two phase reaction mixture, and the mixture stirred for 10 min. The deep brown coloured organic layer was separated by extraction with an additional amount of dichloromethane (50 mL), and dried over Na_2SO_4. After filtering the organic solution and allowing the filtrate to stand at low temperature (~10°C) for 3-4 d, dark shining rectangular shaped crystals formed. The crystals have been observed to lose I_2 and the shine slowly over a period of several days at room temperature. Yield: 1.175 g (0.57 mmol, 71% based on I_2). Anal. Calcd for $C_{30}H_{24}N_6ZnI_{12}$ (MW 2056.8): C, 17.52; H, 1.18; N. 4.09. Found: C. 17.25; H. 1.15; N, 4.05. Characteristic IR bands (cm^{-1}): 1593(s), 1562.5(w), 1470(s), 1435(s), 1310(w), 1244(w), 1153.5(w), 1099.5(w), 1057(w), 1017(s), 887(w), 754(vs), 733(s), 648(w), 627(w), 430(w), 409(w).

$[Zn(phen)_3]I_{12}$ (10) The complex was prepared following a similar procedure as for (a), by using $Zn(OAc)_2{\cdot}4H_2O$ (0.500 g, 1.91 mmol) and 1,10-

phenanthroline(1.250g, 6.2 mmol). The dark shining rhombic shaped crystals formed after allowing the filtrate to stand at ~ 10°C for 3 to 4 days. These crystals also lose I_2 and the shine slowly over a period of several days at room temperature. Yield: 1.205 g (0.57 mmol, 71% based on I_2). Anal. Calcd for $C_{36}H_{24}N_6ZnI_{12}$ (MW 2128.9): C, 20.31: H, 1.14: N, 3.95. Found: C, 20.65; H, 1.10; N, 3.95. Characteristic IR bands (cm^{-1}): 1578(w), 1512(s), 1422(s), 1138(w), 1099.5(w), 864(w), 839(s), 760(s), 721(s), 638.5(w), 606(w), 552(w), 476.5(w).

4.3.1 (b) X-ray Crystallography. Data for a lustrous rectangular crystals (9 black, 10 dark brown) were collected at 298 K on a CAD4 diffractometer using graphite monochromated Mo-K_α radiation. The data were corrected for Lorentz-polarization effects and absorption.[5] The structure was solved by a combination of Patterson and direct methods (SHELXS) and refined (over F^2) by least squares techniques (SHELXL).[6]

9 crystallises in the monoclinic system, space group $P2_1/c$, with 4 molecules in the unit cell. A total of 6375 reflections (6375 unique, 4117 with $F > 4\sigma F$) were collected in the 2θ range 3.3 to 45°, with indices $-13 < h < 13$, $0 < k < 18$, $0 < 1 < 24$. Non-hydrogen atoms were refined anisotropically and all ring hydrogen atoms were included in calculated positions using a riding model. The final cycle of full matrix least squares refinement on F^2 converged with unweighted and weighted agreement factors of R1 = 0.0475 and wR2 = 0.1131. The goodness of fit was S = 0.996 with 4117 observations and 442 parameters. The maximum and minimum peaks on the final fourier map corresponded to 1.456 and -1.421 e/A^3 respectively. Crystallographic data and selected bond angles and bond distances are listed in Table 4.5 and Table 4.6 respectively. Full crystallographic data and other positional parameters are listed in Appendix K.

Table 4.5

Crystallographic Data for $[Zn(bpy)_3]I_{12}$ (9)

formula	$C_{30}H_{24}I_{12}N_6Zn$	Z	4
formula weight	2056.76	space group	P 2,/c (No. 14)
a	12.515(4) A	T	293(2) K
b	17.388(1) A	A	0.71073 A
c	22.589(1) A	p(calcd)	2.783 Mg/m^3
a	90°	μ	8.074 mm^{-1}
p	92.950(9)°	R1	0.0475
1	90°	wR2	0.1131
V	4909(1) A^3		

$R1 = \Sigma||F_o| - |F_c||/\Sigma|F_o|$

$wR2 = [\Sigma\{w(F_o^2 - F_c^2)^2\}/\Sigma(wF_o^4)]^{1/2}$

$w^{-1} = [\sigma^2(F_o^2) + (0.0627P)^2 + 31.1543P]$, $P = (F_o^2 + 2F_c^2)/3$

Table 4.6

Selected bond lengths [A] and angles [deg] for 9.

<u>Bond distances</u> :

I(l)-I(2)	2.788(2)	I(2)-I(3)	3.074(2)
I(3)-I(9)	3.123(2)	1(3)-1(4)	3.374(2)
I(4)-I(5)	2.7681(19)	1(5)-I(6)	3.244(2)
I(6)-I(7)	3.1442(18)	I(6)-I(11)	3.3152(17)
I(7)-I(8)	2.7405(17)	I(9)-I(10)	2.7822(19)
I(11)-I(12)	2.7222(16)	Zn-N(l)	2.136(10)
Zn-N(6)	2.137(11)	Zn-N(4)	2.140(11)
Zn-N(3)	2.162(12)	Zn-N(2)	2.164(10)

Zn-N(5)	2.188(11)

Bond angles :

I(l)-I(2)-I(3)	175.39(6)	I(2)-I(3)-I(9)	104.29(5)
I(2)-I(3)-I(4)	88.73(5)	I(9)-I(3)-I(4)	145.11(6)
I(5)-I(4)-I(3)	179.06(5)	I(4)-I(5)-I(6)	179.93(6)
I(7)-I(6)-I(5)	86.80(4)	I(7)-I(6)-I(ll)	85.20(4)
I(5)-I(6)-I(11)	134.37(7)	I(8)-I(7)-I(6)	174.75(6)
I(10)-I(9)-I(3)	178.94(6)	I(12)-I(11)-I(6)	173.57(6)
N(4)-Zn-N(3)	75.8(5)	N(1)-Zn-N(2)	76.3(4)
N(6)-Zn-N(5)	76.5(4)		

Intermolecular contacts :

(a) I...I contacts :

Distances:

I(l)...I(10)#l	4.149(2)	I(10)...I(l)#2	4.149(2)
I(3)...I(11)#3	4.184(2)	I(11)...I(3)#4	4.184(2)
I(9)...I(8)#5	3.903(2)	I(8)...I(9)#5	3.903(2)
I(6)...I(10)#6	3.547(2)	I(10)...I(6)#7	3.547(2)
I(10)...I(12)#8	3.876(2)	I(12)...I(10)#9	3.876(2)
I(9)...I(12)#8	4.049(2)	I(12)...I(9)#9	4.049(2)

Angles:

I(2)-I(1)-I(10)#1	**164.12(7)**	I(10)-I(9)-I(8)#5	**91.61(4)**
I(7)-I(8)-I(9)#5	**143.61(6)**	I(5)-I(6)-I(10)#6	**132.24(6)**
I(9)-I(10)-I(6)#7	**165.84(6)**	I(9)-I(10)-I(12)#8	**72.83(4)**
I(11)-I(12)-I(10)#9	175.07(5)		

(b) I...ring contacts :

Distances:

I(1)...H(28)	3.164(2)	I(9)...H(18)#10	3.177(1)
I(4)..H(7)#11	3.191(1)	I(5)...H(4)#11	3.205(1)

Angles:

I(1)-H(28)-C(28)	136.6(11)	I(9)-H(18)#10-C(18)#10	149.1(3)
I(4)-H(7)#11-C(7)#11	159.4(10)	I(5)-H(4)#11-C(4)#11	158.5(10)

Symmetry transformations used to generate equivalent atoms:

#1 -x+1, y+1/2, -z+1/2; #2 -x+1, y-1/2, -z+1/2; #3 -x, -y+1/2, z-1/2; #4 x, -y+1/2, z+1/2; #5-x+1,-y+1,-z+l; #6 x+1,-y+1/2, z+1/2; #7 x-1, -y+1/2, z-1/2 #8 -x+1, y-1/2, -z+3/2; #9 -x+1, y+1/2, -z+3/2; #10 -x+2, y-1/2,-z+1/2; #11 -x+2, y+1/2,-z+1/2;

10 crystallises in the triclinic system, space group P1, with 2 molecules in the unit cell. A total of 8948 reflections (8856 unique, 5478 with F > 4σF) were collected in the 2θ range 3.6 to 50°, with indices -14 < h < 15, -16 < k < 16, 0 < 1 < 18. Non-hydrogen atoms were refined anisotropically and all ring hydrogen atoms were included in calculated positions using a riding model. The refinement showed an improvement on reducing the site occupancy factor of two adjacent iodines to 0.75. This means that an I_2 site is partially occupied. The intensity of the standard did not show any decay during the measurement. The final cycle of full matrix least squares refinement on F^2 converged with unweighted and weighted agreement factors of R1 = 0.0565 and wR2 = 0.1410. The goodness of fit was S = 0.970 with 5478 observations and 496 parameters. The maximum and minimum peaks on the final fourier map corresponded to 1.664 and -1.843 e/A^3 respectively. Crystallographic data and selected bond angles and bond distances are listed in Table 4.7 and Table 4.8 respectively. Full crystallographic data and other positional parameters are listed in Appendix L.

Table 4.7

Crystallographic Data for $[Zn(phen)_3]I_{12}$ **(10)**

formula	$C_{36}H_{24}I_{12}N_6Zn$	Z	2
formula weight	2128.78	space group	P T (No. 2)
a	12.867(2) A	T	293(2) K
b	14.047(2) A		0.71073 A
c	15.832(2) A	p(calcd)	2.790 Mg/m^3
a	85.34(1)°	μ	7.826 mm^{-1}
p	76.53(1)°	R1	0.0565
y	65.61(1)°	wR2	0.1410
V	2534.1(6) $Å^3$		

R1 = $\Sigma||F_o| - |F_c||/\Sigma|F_o|$

wR2 = $[\Sigma\{w(F_o^2 - F_c^2)^2\}/\Sigma(wF_o^4)]^{1/2}$

$w^{-1} = [\sigma^2(F_o^2) + (0.0857P)2 + 20.9707P]$, $P = (F_o^2 + 2F_c^2)/3$

Table 4.8

Selected bond lengths [A] and angles [deg] for 10.

Bond distances :

I(l)-I(2)	2.8029(15)	I(2)-I(3)	3.0472(16)
I(3)-I(4)	3.0263(18)	I(4)-I(5)	2.8504(18)
I(5)-I(6)	3.419(2)	I(6)-I(7)	2.743(2)
I(7)-I(8)	3.534(2)	I(8)-I(9)	2.914(2)
I(9)-I(10)	2.920(2)	I(10)-I(11)	3.240(2)
I(11)-I(12)	2.722(2)	Zn(1)-N(6)	2.144(11)

Zn(1)-N(1)	2.147(10)	Zn(l)-N(5)	2.174(10)
Zn(1)-N(3)	2.181(9)	Zn(1)-N(4)	2.187(9)
Zn(l)-N(2)	2.188(9)		

Bond angles :

I(1)-I(2)-I(3)	178.02(5)	I(4)-I(3)-I(2)	94.04(4)
I(5)-I(4)-I(3)	175.71(5)	I(4)-I(5)-I(6)	103.29(5)
I(7)-I(6)-I(5)	176.45(5)	I(6)-I(7)-I(8)	172.81(5)
I(9)-I(8)-I(7)	107.67(5)	I(8)-I(9)-I(10)	179.17(6)
I(9)-I(10)-I(11)	101.30(6)	I(12)-I(11)-I(10)	163.20(8)
N(6)-Zn(1)-N(5)	77.2(4)	N(3)-Zn(1)-N(4)	76.8(3)
N(1)-Zn(1)-N(2)	76.8(4)		

Intermolecular contacts :

(a) I...I contacts :

Distances:

I(1)...I(12)#1	3.592(2)	I(12)...I(1)#1	3.592(2)
I(5)...I(8)#2	3.985(2)	I(8)...I(5)#2	3.985(2)
I(6)...I(6)#2	4.081(2)		

Angles:

I(2)-I(1)-I(12)#1	139.64(5)	I(11)#1-I(12)#-I(1)	150.02(7)
I(4)-l(5)-I(8)#2	138.11(6)	I(6)-I(5)-I(8)#2	118.60(5)
I(7)-l(6)-I(6)#2	76.42(4)	I(5)-I(6)-I(6)#2	102.68(4)

(b) I...ring contacts :

Distances:

I(1)...H(21)#3	3.084(1)	I(7)...H(6)#4	3.214(2)

I(10)...H(5)	3.159(1)	I(12)...H(15)#5	3.133(2)

Angles:

I(1)-H(21)#3-C(21)#3	143.3(9)	I(7)-H(6)#4-C(6)#4	154.9(11)
I(10)-H(5)-C(5)	145.0(10)	I(12)-H(15)#5-C(15)#5	159.6(9)

Symmetry transformations used to generate equivalent atoms:

#1 -x-1, -y+2, -z+2; #2 -x+1, -y+1, -z+2; #3 -x, -y+1, -z+1; #4 -x, -y+1, -z+2; #5 x-1, y, z+1;

4.3.2 Results and Discussion

4.3.2 (a) Structure of 9 The structure consists of $[Zn(bpy)_3]^{2+}$ cations and I_{12}^{2-} anions. Views of cation and anions are shown in Figure 4.6.

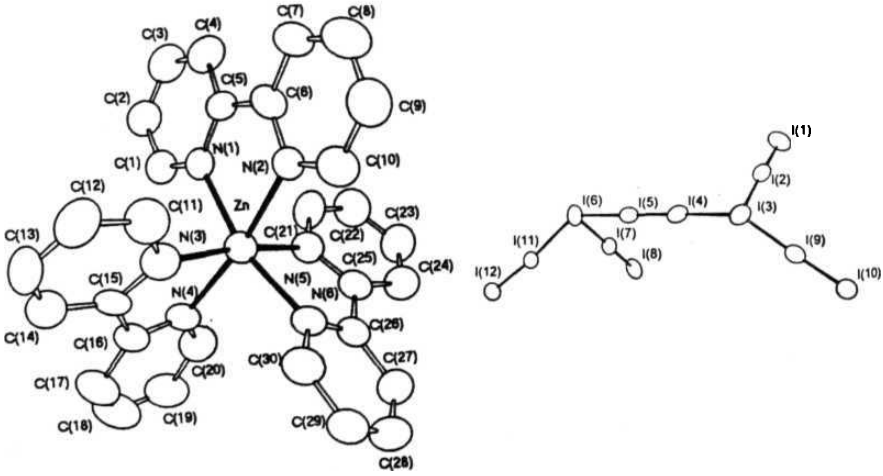

(a) (b)

Figure 4.6 Views of the cation and anion of 9 (40% probability ellipsoids) : (a) the cation $[Zn(bpy)_3]^{2+}$ and (b) the I_{12}^{2-} anion.

The I_{12}^{2-} ion is different from the previously reported centrosymmetric I_{12}^{2-} anions.[1,15] The I_{12}^{2}anionconsists of an I_2 molecule bridged between two I_5^- anions as observed in other cases. The bridging I_2 unit has a bond distance of 2.768 A, indicating the interactions on both sides. Among the I_5^- anions, one is symmetrical (I(1), I(2), I(3), I(9) and I(10)) while the other is unsymmetrical (1(8), I(7), I(6), I(11) and I(12)) with a slightly longer bond of 3.315 between the I" and one of the I_2. The shape of the I_{12}^{2-} anion is different from the other three reported I_{12}^{2-}. A planar I_{12}^{2-} in $[Cu(dafone)_3]I_{12}$,[2b] is obtained by increasing the $I_5^-.I_2$ bond angle to 180° from 90° as in the non-planar anion of $[K(crypt)]_2I_{12}$.[2a] In both cases the angle between the two I_5^- units is - 0° or 180°, i.e. both the I_5^- units are parallel to each other. But in this case the two I_5^- units are perpendicular to each other making an angle of 81.8° between the planes. In other words, this non-planar I_{12}^{2-} anion is obtained by increasing the $I_5^-.I_2$ angle (the angles I(9)-I(3)-I(4) and I(5)-I(6)-I(11), here) to ~ 140° from 90° as observed in $[K(crypt)_2]I_{12}$ or decreasing to ~140° from 180°, found in $[Cu(dafone)_3]I_{12}$. Thus, this discrete non-planar I_{12}^{2-} unit is an intermediate of the two reported centrosymmetric I_{12}^{2-} anions.

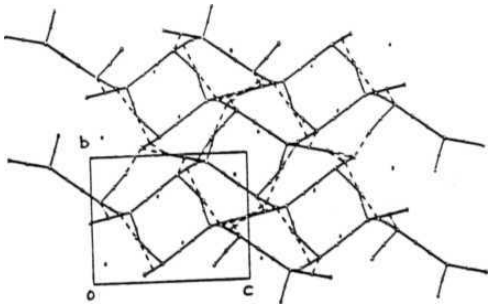

Figure 4.7 Views of packing of anion in 9. bc plane projection showing the network of I_{12}^{2-} ions. (the Zn^{2+} atoms are shown as small circles. Ligand molecules are omitted.) Other figures are in Appendix L.

Unlike the other I_{12}^{2-} which are nearly isolated, the anion here forms networks of branched chains aligned at parallel as well as perpendicular angles with respect to each other. The contact distance of 3.547 A between I(6) of a unit and I(10) of another is almost same as the non-bonded I..I distance of 3.55 A observed in crystalline I_2.[7] The four contacts at the I(6) atom position could be the reason for the I_5^- unit to be unsymmetrical due to steric crowding. The branched chains of $(I_{12}^{2-})_n$ pack in mutually perpendicular directions forming a close network of iodine atoms (Figure 4.7). The $[Zn(bpy)_3]^{2+}$ cations are embedded inside the polyiodide cages. A polyiodide anionic unit forms numerous I..I van der Waals' contacts in the range of 3.8 to 4.0 A with the adjacent units, that leads to a close network of iodine atoms. The cation placed inside the iodine cages make contacts of 3.9 to 4.0 A between I(1)..C(28), I(9)..C(18), I(4)..C(7) and I(5)..C(4).

The coordination geometry of Zn atom is pseudo-octahedral with nearly equal Zn-N bond distances (average 2.15 A) and N-Zn-N bond angles (average 76.2°) as also observed in $[Zn(bpy)_3](ClO_4)_2$.[11] Each ligand is bound to the Zn using one long (average 2.17Å) and one short bond (average 2.14 A). The angle between the mean planes of the two pyridine rings in the bpy ligands are 8.3°, 13.4° and 15.1° respectively.

4.3.2 (b) Structure of 10 The structure consists of $[Zn(phen)_3]^{2+}$ cations and unbranched nearly planar I_{12}^{2-} anions. Views of the cation and anion are shown in Figure 4.8.

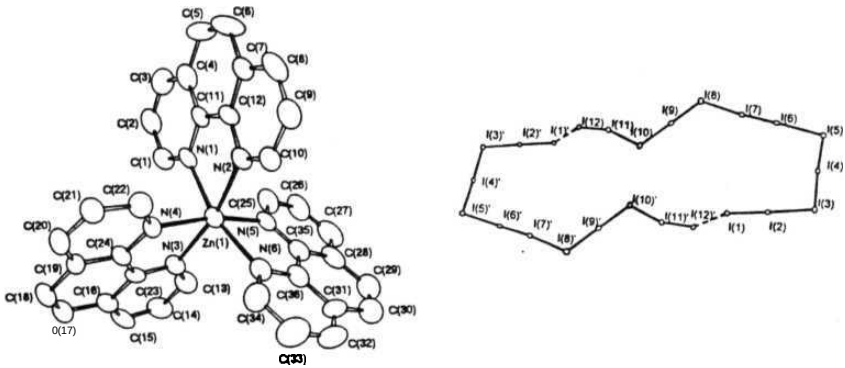

(a) (b)

Figure 4.8 Views of the cation and anion of 10 (40% probability ellipsoids): (a) the cation $[Zn(phen)_3]^{2+}$, (b) the dimeric I_{24}^{4-} anion (' = -x-1, -y+2, -z+2).

The I_{12}^{2-} anion here, has a new structure, unlike the branched shape of I_2 bridged between two I_5^-. It is now assembled as a dimeric I_{24}^{4-} nearly planar ring. This is assumed by considering the I(12)-I(l)' and I(l)-I(12)' distance of 3.59 A, as a long bond. The bond distances for the I_{12}^{2-} unit are 2.803, 3.047, 3.026, 2.850, 3.419, 2.743, 3.534, 2.914, 2.920, 3.240 and 2.722 A. The anion can thus be divided into smaller fragments of $\{I_5^-.I_2.I_3^-.I_2\}$, out of which the I_5^- and I_3^- are both symmetrical. The 24-membered nearly planar ring is mainly deviated off the plane due to the I_2 unit of I(11)-I(12). The structural solution suggested loss of some amount of I_2 from this unit in the crystal, refining well to a site occupancy factor of 0.75 for both atoms. The crystals have been observed to lose I_2 at ambient temperature as confirmed by the elemental analysis of freshly prepared crystals, and the same after standind at room temperature for a few days.

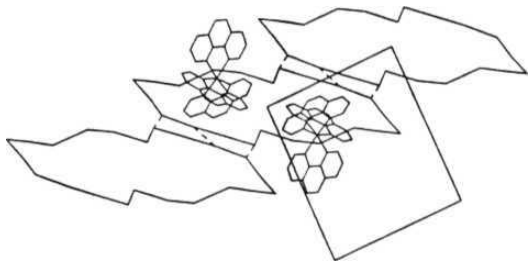

Figure 4.9 View of packing in 10 showing interconnected 24-membered rings (Other figures are in Appendix L).

The I_{24}^{4-} makes contacts with the adjoining rings at a distance of - 4.0 A (Figure 4.9). Each ring accommodates two cations, each inside the I_{12}^{2-} pocket and that are held firmly with iodine - ring contacts of 3.9 to 4.0 A (I(1)..C(21), I(7)..C(6), I(10)..C(5) and I(12)..C(15)).

The anion formed here does not prefer a branched unit as in the case of $[Zn(bpy)_3]I_{12}$, but unbranched unit that is formed by splitting one of the I_5^- units into $I_3^-.I_2$ and making bonds with the central I_2 at edges rather than the middle of I_5^-.

The coordination geometry around the Zn^{2+} is again pseudo-octahedral as $[Zn(bpy)_3]^{2+}$, with nearly equal Zn-N bond distances of average 2.17 A and N-Zn-N chelate angles of average 76.9°. A closer observation reveals two slightly short axial bonds of 2.145 A and 4 nearly equal equatorial bonds of 2.18 A. The structure of the cation has not been reported in literature.

4.3.2 (c) Comparison. A comparison of the I_{12}^{2-} anions reported in literature is summarised in Table 4.2.

Table 4.2 Comparison of structure in I_{12}^{2-} anions .

Compound	Structure	Type	Bond angles			angle betn. I_5^- planes	Ref.
			1	2	3		
$[K(cryp)]_2I_{12}$	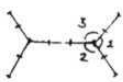	centrosym isolated	101.6	98.5	89.7	~180°	2a
$[Cu(dafone)_3]I_{12}$	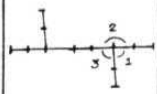	centrosym planar isolated	110.4	174.1	93.0	~0°	2b
$[Me_2Ph_2N]_2I_{12}$	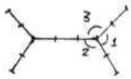	centrosym isolated	100.2	111.0	83.9	~180°	2c
$[MePh_3P]_4I_{22}$	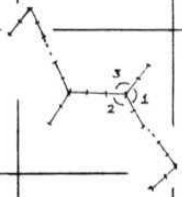	centrosym isolated	92.3	121.6	78.1	~180°	2d
$[Zn(bpy)_3]I_{12}$	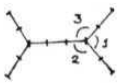	networks	104.3 85.2	145.1 134.4	88.7 86.8	82°	this work

$[Ag_2(aneS5)_2]I_{12}$	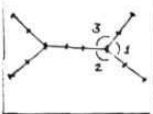	isolated	146.6 153.9	128.0 120.6	84.4 85.4	40°	2e
$[K(db18\text{-}C\text{-}6)]_2I_{12}$		centrosym isolated	102.8	87.6	174.4		2f
$[K(b18\text{-}C\text{-}6)]_2I_{12}$*		network	-	-	-		2g
$[Zn(phen)_3]I_{12}$	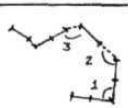	ring forming dimer	94.0	103.3	107.7	14°	this work

structure not reported in detail.

The I_{12}^{2-} shows a wide range of structural diversity depending on the cation. The shape of the anion is very sensitive to the metal atom and the ligand in complex cations. The assembly of smaller fragments of I_5^-, I3", I_2 and I" to a I_{12}^{2-} unit can lead to many possible shapes, some of which have been characterised. The anion which was quite unknown till recently, has emerged with many shapes for the discrete unit.

4.4 Synthesis and Crystal Structure of $[bpyH]I_5$ and $[bpyH]I_7$ obtained in an Attempted Synthesis of $[Al(bpy)_3]I_x$ and $[Co(bpy)_3]I_y$

4.4.1 Experimental

4.4.1 (a) Synthesis. $[bpyH]I_5$ (11) The complex was prepared following a similar procedure as others, using $Al(NO_3)_3 \cdot 9H_2O$ (0.700 g, 1.87 mmol) and 2,2'-bipyridine (1.00g, 6.4 mmol) and a solution of I_2 (1.5 g, 6.0mmol) in dichloromethane (40 mL) and solid KI (1.00 g, 6.0 mmol). Dil. sulphuric acid (1 M, 1 mL) was then added to the two phase reaction mixture, and the mixture stirred for 10 min. The deep brown coloured organic layer was separated by extraction with an additional amount of dichloromethane (50 mL), and dried over Na_2SO_4. The organic solution was filtered and dark shining plate-like crystals formed after allowing the filtrate to stand at ~ 10°C for 3 to 4 days. The crystals have been observed to be unstable losing I_2 slowly over a period of several days at room temperature. Yield: 1.550 g (1.96 mmol, 65%, based on I_2). Anal. Calcd for $C_{10}H_9N_2I_5$ (MW 791.7): C, 15.17; H, 1.15; N, 3.54. Characteristic IR bands (cm^{-1}): 3142(w), 3081(w), 2926(w), 1580(s), 1524(s), 1427.5(s), 1321(w), 1152(w), 991.5(w), 912(w), 754(vs).

$[bpyH]I_7$ (12) The complex was prepared following a similar procedure as followed for other preparations, using $Co(OAc)_2 \cdot 4H_2O$ (0.500 g, 1.96 mmol) and 2,2'-bipyridine (l.OOg, 6.40 mmol) in water (10 mL), a solution of I_2 (1.0 g, 3.9 mmol) in dichloromethane (25 mL) and solid KI (0.66 g, 4.0 mmol) were added. Dil. sulphuric acid (1 M, 1 mL) was then added to the two phase reaction mixture, and the mixture stirred for 10 min. The deep brown coloured organic layer was separated by extraction with an additional amount of dichloromethane (50 mL), and dried over Na_2SO_4. After filtering the organic solution and allowing the

filtrate to stand at ~10°C for 3-4 d, dark shining rectangular crystals formed. These crystals have also been observed to be unstable losing I_2 slowly over a period of several days at room temperature. Yield: 0.930 g (0.89 mmol, 67% based on I_2). Anal. Calcd for $C_{10}H_9N_2I_7$ (MW 1045.5): C, 11.49; H, 0.87; N, 2.80. Found: C. 11.61; H, 0.79; N, 2.71. Characteristic IR bands (cm^{-1}): 1580(w), 1524(w), 1427.5(w), 1319(w), 1211(w), 1167(w), 1152(w), 1082(w), 914(w), 864(w), 754(s), 540(w), 442(w).

4.4.1 (b) X-ray Crystallography Data for a dark rectangular plate-like crystals were collected at 298 K on a CAD4 diffractometer using graphite monochromated Mo-K_α radiation. The data were corrected for Lorentz-polarization effects and absorption.[12] The structure was solved by direct methods (SHELXS) and refined (over F^2) by least squares techniques (SHELXL).[6]

11 crystallises in the monoclinic system, space group $P2_1/a$, with 4 molecules in the unit cell. A total of 3367 reflections (3138 unique, 1543 with $F > 4\sigma F$) were collected in the 2θ range 4.8 to 50°, with indices $0 < h < 9$, $0 < k < 30$, $-10 < 1 < 10$. All iodine atoms were refined anisotropically and all ring nitrogen and carbon atoms were left isotropic. The hydrogen atoms were included in calculated positions using a riding model. The final cycle of full matrix least squares refinement on F^2 converged with a high unweighted and weighted agreement factors of R1 = 0.1108 and wR2 = 0.2790. The goodness of fit was S = 0.936 with 1543 observations and 104 parameters. The maximum and minimum peaks on the final fourier map corresponded to 4.42 and -3.30 e/A^3 respectively. Crystallographic data and selected bond angles and bond distances are listed in Appendix M.

12 crystallises in the triclinic system, space group $P\bar{1}$, with 2 molecules in the unit cell. A total of 2838 reflections (2799 unique, **1831** with $F > 4\sigma F$) were collected in the 2θ range 4.1 to 50°, with indices $-8 < h < 8$, $-11 \leq k \leq 11$, $0 \leq l \leq 17$. All iodine atoms were refined anisotropically and all ring nitrogen and carbon atoms were left isotropic. The hydrogen atoms were included in calculated positions using a riding model. The final cycle of full matrix least squares refinement on F^2 converged with a high unweighted and weighted agreement factors of $R1 = 0.1095$ and $wR2 = 0.3396$. The goodness of fit was $S = 1.635$ with 1831 observations and 113 parameters. The maximum and minimum peaks on the final fourier map corresponded to 3.61 and -3.31 e/A^3 respectively. Crystallographic data and selected bond angles and bond distances are listed in Appendix M.

4.4.2 Results and Discussion

4.4.2 (a) Synthesis. $[bpyH]I_5$ (11) and $[bpyH]I_7$ (12) An attempted synthesis of polyiodides of Al^{3+} tris chelates was unsuccessful. The Al^{3+} did not form a tris chelate with bpy or phen, and on the other hand, a polyiodide of protonated bpy, i.e. $[bpyH]^+I_5^-$ (11) formed. This was confirmed by separate synthesis, involving only bpy ligand, under same conditions. The phen did not form good crystalline quality compound; hence it was not analysed further. Similarly, Co^{2+} also did not form the tris-chelate with bpy, instead $[bpyH]^+I_7^-$ (12) was formed that was extracted in dichloromethane layer and recrystallised. The synthesis of polyiodides of $[Al(bpy)_3]^{3+}$ and $[Co(bpy)_3]^{2+}$, thus require a new method of preparation.

4.4.2 (b) Structure. **[bpyH]I_5** (11) and **[bpyH]I_7** (12) The structure of **11** and 12 were confirmed by solving the single crystal x-ray data. The structures have been reported earlier.[13] The repeating unit I_5^- , consists of trigonally planar branched chains of $I_3^-.I_2$, in **11** (Figure 4.10(a)) and trigonally pyramidal branched chains of $I_5^-.I_2$ in 12 (Figure 4.10(b)). The $bpyH^+$ cations sit inside the channels formed by the anionic chain network in both **11** and 12. In case of **11,** it is difficult to differentiate N atoms from carbons, based on the ring angles. Due to mono-protonation of the ligand, it is assumed that the bpy ligand has a cis-planar structure (H could not be located from the difference fourier map).[14]

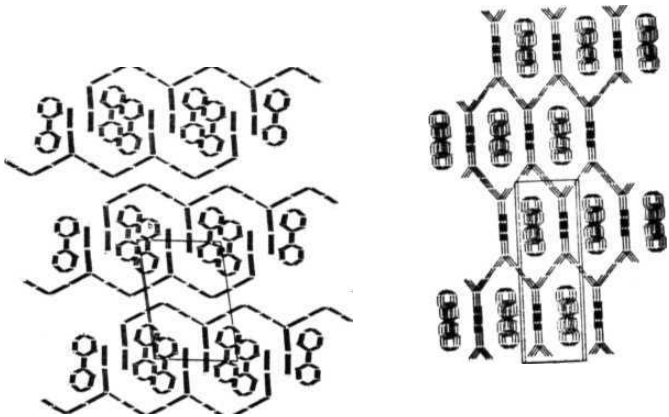

(a) (b)

Figure 4.10 Polyiodide network formed by (a) I_5^- repeating unit in **11** and (b) I_7 repeating unit in 12.

4.5 Conclusions

The iodine content for the complex cations $[Cu(bpy)_3]^{2+}$, $[Ni(bpy)_3]^{2+}$, $[Fe(bpy)_3]^{2+}$, $[Zn(bpy)_3]^{2+}$ and $[Zn(phen)_3]^{2+}$ has been found to be greater than the normal 6 iodines. This leads to the suggestion that the $[M(bpy)_3]^{2+}$ cations generally form polyiodide anions with higher nuclearity compared to $[M(phen)_3]^{2+}$, with the exception of $[Zn(phen)_3]^{2+}$.

$[Cu(bpy)_3]I_8 \cdot CH_2Cl_2$ contains I_8^{2-} anions packed in layers with the cations to form channels along c-axis direction, which are filled with disordered solvent molecules.

In $[Fe(bpy)_3]I_9$, polyiodide networks are formed by a new centrosymmetric I_{18}^{4-} repeating unit with the cations sitting inside the channels formed by the anion.

The structure of $[Zn(bpy)_3]I_{12}$ and $[Zn(phen)_3]I_{12}$ shows two different types of I_{12}^{2-} units. The $[Zn(bpy)_3]^{2+}$ forms a branched anionic network formed from $\{I_5^-.I_2.I_5^-\}$ fragments, while the $[Zn(phen)_3]^{2+}$ cations prefer a new unbranched 24-member, nearly planar dimeric ring.

References

(1) (a) E. E. Havinga, K. H. Boswijk and E. H. Wiebenga *Acta Crystallogr.* **1954,** 7, 487. (b) P. K. Hon, T. C. W. Mak and J. Trotter *Inorg. Chem.* **1979,** *18,* 2916. (c) R. Thomas and F. H. Moore *Acta Crystallogr.* **1981,** *B37,* 2153. (d) K. -F. Tebbe, M. E. Essawi and S. A. E. Khalik Z *Naturforsch.* **1995,** *SOB,* 1429. (e) K. -F. Tebbe and B. Freckmann Z *Naturforsch.* **1982,** *37B*, 542. (f) A. J. Jircitano, M. C. Colton and K. B. Mertes *Inorg. Chem.* **1981,** *20,* 890. (g) F. H. Herbstein and M. Kapon *J. Chem. Soc, Chem. Commun.* 1975, 677. (h) F. Bigoli, M. A. Pellinghelli, G. Crisponi, P. Deplano and E. F. Trogu *J. Chem. Soc, Dalton Trans.* **1985,** 1349. (i) A. J. Jircitano and K. B. Mertes *Inorg. Chem.* **1983,** *22,* 1828.

(2) (a) K. -F. Tebbe, A. Kavoosian, Z *Naturforsch, B: Chem. Sci.* **1993,** *48,* 438. (b) S. Menon and M. V. Rajasekharan, *Inorg. Chem.* **1997,** *36,* 4983. (c) K. -F. Tebbe and T. Gilles Z *anorg. allg. Chem.* **1996,** *622,* 138. (d) K. -F. Tebbe and T. Farida Z. *Naturforsch.* **1995,** *50b,* **1440.** (e) A. J. Blake, R. O. Gould, W. -S. Li, V. Lippolis, S. Parsons, C. Radek and M. Schroder *Inorg. Chem.* **1998,** *37,* 5070. (0 K. -F. Tebbe and M. E. Essawi Z *anorg. allg. Chem.* **1998,** *624,* (in press). (g) M. El Essawi, I. Dombrowski, T. Gilles, A. Kavoosian and K. -F. Tebbe Z *Kristallogr. Suppl.* **1998,** *15,* 61.

(3) (a) F. Bigoli, P. Deplano, F. A. Devillanova, V. Lippolis, M. L. Mercuri, M. A. Pellinghelli and E. F. Trogu *Inorg. Chim. Ada* **1998,** *267,* 115.

(4) (a) A. J. Blake, F. A. Devillanova, R. O. Gould, W. -S. Li, V. Lippolis, S. Parsons, C. Radek and M. Schroder *Chem. Soc. Rev.* **1998,** *27,* 195. (b) K. -F. Tebbe and R. Buchem Z *anorg. allg. Chem.* **1998,** *624,* 671. (c) F. Demartin, P. Deplano, F. A. Devillanova, F. Isaia, V. Lippolis and G.

Verani *Inorg. Chem.* **1993,** *32,* 3694. (d) D. B. Morse, T. B. Rauchfuss and S. R. Wilson *J. Am. Chem. Soc.* **1990,** *112,* 1860. (e) K. -F. Tebbe and R. Buchem *Angew. Chem. Int. Ed. Engl.* **1997,** *36,* 1345.

(5) N. Walker and D. Stuart *Acta Crystallogr.* **1983,** *A39,* 153.

(6) G. M. Sheldrick, *SHELX-97,* University of Gottingen, Gottingen, 1997.

(7) (a) A. I. Kitaigorodskii, T. L. Khotsyanova and Yu. T. Struchkov, *Zh. Fa. Khim. 1953, 27,* 780. (b) F. V. Bolhius, P. P. Koster and T. Michelsen, *Acta Crystallogr.* **1967,** *23,* 90.

(8) (a) O. P. Anderson, *J. Chem. Soc, Dalton Trans.* **1973,** 1237. (b) O. P. Anderson, *J. Chem. Soc, Dalton Trans.* **1972,** 2597. (c) D. L. Cullen and E. C. Lingafelter *Inorg. Chem.* **1970,** *9,* 1858.

(9) (a) H. C. Allen Jr., G. F. Kokoszka and R. G. Inskeep *J. Am. Chem. Soc.* **1964,** *86,* 1023. (b) B. J. Hathaway, P. G. Hodgson and P. C. Power *Inorg. Chem.* **1974,** *13,* 2009.

(10) (a) B. N. Figgis, B. W. Skelton and A. H. White *Aust. J. Chem.* 1978, *31,* 57. (b) S. Decurtins, H. W. Schmalle, P. Schneuwly, J. Ensling and P. Gütlich *J. Am. Chem. Soc.* **1994,** *116,* 9521.

(11) X. -M. Chen, R. -Q. Wang, and Z. -T. Xu, *Acta Crystallogr.* **1995,** *C51,* 1545.

(12) A. C. T. North, D. C. Phillips and F. S. Mathews, *Acta Crystallogr.* **1968,** *A24,* 351.

(13) K. -F. Tebbe and M. Bittner *Z. anorg. allg. Chem.* **1995,** *621,* 218.

(14) (a) L. L. Merritt and E. D. Schroeder *Acta Crystallogr.* **1956,** *9,* 801. (b) B. -C. Wang and A. W. Cordes *Inorg. Chem.* **1970,** *9,* 1643.

CHAPTER 5

Polyiodide Salts of Metal Complex Cations : Part 3. Far-IR, Raman and Electronic Absorption Spectroscopy of the Polyiodide Salts

5.1 Introduction

Vibrational and electronic spectroscopy have been used for identifying the polyiodide species present and to estimate the extent of electronic charge transfer from donor to acceptor in certain polyiodide salts.[1] These techniques are particularly useful for non-crystalline or severely disordered crystalline polymeric materials where x-ray structural determination is hampered. Based on the spectral patterns for polyiodide salts with known structures, the spectroscopic information for unknown structures can be reliably correlated to a large extent. The solution state studies have not yielded much information about the stability of the polyiodide species. It has only been stated[1a] that polyiodides higher than I_3^-, exist only in highly concentrated solutions and undergo progressive dissociation to smaller fragments, finally dissociating completely to I_3^- and I_2 at infinite dilution.

In this chapter the far-IR, Raman, electronic absorption and diffuse reflectance spectroscopy of the polyiodide salts of complex cations synthesised and structurally characterised in the earlier two chapters (3 and 4), are presented and correlated to the structure of the polyiodide anions present in these compounds.

5.2 Experimental

5.2.1 Physical Measurements. Far-IR spectra were recorded as polyethylene pellets on a Bruker IFS 66v FT-IR spectrometer in the range of 450-50 cm^{-1}.

The Raman experiment was conducted at University of Bern, Switzerland, by assembly of the following optical components: Ar laser line of wavelength 514.5 nm, Czerny - Turner Spex 1402 double monochromator with gratings blazed at 500nm (1220 groves/mm), 0.150 mm slits, cooled RCA C31034 photomultiplier tube, Spex DM302 amplifier discriminator, Standard Research SR400 photon counting system. The microcrystalline sample was used in pressed pellet form, glued to a black metal strip with rubber cement, which was tied to the sample holder by wire and inserted into the He gas flow tube maintained at 20 K. The output vibrational frequencies were plotted after monochromator calibration correction of 0.376 nm.

Electronic spectra were recorded in dichloromethane solvent in the range, 300-1100 nm on a JASCO 7800 spectrophotometer using quartz cells of 1 cm path length. Powder diffuse reflectance spectra were recorded in the range of 350-750 nm on a Cary 17 UV/VIS/NIR spectrophotometer with an integrating sphere by coating the sample on the inside of the cell with grease. The absorbance spectra were recalculated using Kubelka-Munk function.[2]

5.3 Results and Discussion

5.3.1 Vibrational Spectroscopy : Far-IR Spectroscopy and Raman Spectroscopy

5.3.1 (a) IK and Raman Studies

The far-infrared and Raman spectra of discrete polyiodides such as I_3^-, I_5^-, I_7^-, I_9^- , etc. and extended networks of polyiodide anions have been studied in detail and vibrational assignments have been made based on I-I bond distances in the basic unit formed from I", I_2 and I_3^- fragments.3 The vibrational spectrum can also give information on the extent of lengthening of I-I bond (in I_2 and I_3^-) and long bonds formed due to interaction of smaller fragments in these systems.

The Raman spectrum of a polyiodide species containing I_2 component is expected to show bands in the 170-190 cm^{-1} range (the Raman bands in solid I_2 are observed at 180 and 190 cm^{-1}). The I_3^- units show strong IR and Raman bands in 100-120 cm^{-1} range (corresponding to the symmetric stretch ν_1) and in 130-155 cm^{-1} range (corresponding to antisymmetric stretch ν_3).[1,3] Similarly, discrete I_5^- units show strong Raman bands at around 145, 160 cm^{-1} and also at 105 cm^{-1}. Based on the x-ray structures the I_3^- ions are classified as linear symmetric ($D_{\infty h}$), linear asymmetric ($C_{\infty v}$), slightly bent symmetric (C_{2v}) and slightly bent asymmetric (C_s). Out of these the last three types have common IR and Raman active vibrational modes. In the $D_{\infty h}$ symmetry the symmetric stretching modes are exclusively Raman active and the antisymmetric stretching modes are exclusively IR active.

A summary of these studies for various polyiodide units are presented in Table 5.1 and the far-IR and Raman plots are presented in Figures 5.1, 5.2, 5.3, 5.4.

Table 5.1 Far-IR and Raman bands observed in different types of polyiodide salts of metal complex cations and few other cations. (Numbers printed in bold refer to relatively intense bands and numbers underlined refer to bands due to metal-N (ligand) stretching).

SNo.	Molecular formula	Polyiodide unit	Structure	IR bands (cm^{-1}) at 300 K	Raman bands (cm^{-1}) at 20 K	Ref.
1.	I_2(solid)		bond distance 2.72 Å	-	425, 368, 214, **190**, **180**	1
2.	$[Mn(phen)_3](I_3)_2$ (**1**)	I_3^-, 2 types	linear symmetric (centrosym.) ($D_{\infty h}$)	420, 275, 251, 237, <u>**214**</u>, 160, **149**, **130**, 110, 81	335, **167**, 142, **113**	*
3.	$[Mn(bpy)_3](I_3)_{1.5}(I_8)_{0.25}$ (**2**)	I_3^-, 2 types $(I_8^{2-})_n$ chains	nearly linear asymmetric I_3^-; disordered I_3^-, I_8^{2-}	**410**, 354, **248**, **237**, <u>208</u>, *196*, **139**, **120**, 95	219, 130, **104**	*

4.	$[Ni(phen)_3](I_3)_2 \cdot CH_3CN$ (3)	I_3 , 2 types	nearly linear asymmetric	**439, 299,** 249. 235, 181, **140, 135,** 115	328, 231, 165, **156,** 142, 132, **112.5**	
5.	$[Cu(phen)_3](I_3)_2 \cdot CH_3CN$ (4)	***V* (?)**	structure not determined		165, **138, 111,86**	*
6.	Cs_2I_8		Z-shaped, planar;		350, 280, 240, **171,** 147, 139, 117, **105, 95**	1
7.	$[Ni(bpy)_3](I_8)$ (7)	I_8^{2-} **(?)**	structure not determined		431, 331, 221, **159, 108, 99**	*
8.	$[Fe(bpy)_3](I_9)$ (8)	(centrosym.)	network of I_{18}^{4-} formed by I_3^- .and I_2. units	415, 380, 363, 197, 172, 160, **128.5**, **93,** 69	**165,** 136, 106.5	*
9.	$[Ag_2(aneS5)]I_{12}$	I_{12}^{2-}	$2(I^-)$.$5(I_2)$		172	1
10.	$[Cu(dafone)_3]I_{12}$	I_{12}^{2-}	planar, branched (centrosym.)	427, 397, 277. 232, 155, **138, 84**		4

11.	$[Zn(bpy)_3](I_{12})$ (9)	$(I_{12}^{2-})_n$	branched, network; $2(I_5^-).(I_2)$		327, 218, 181, 133, 106.5	*
12.	$[Zn(phen)_3](I_{12})$ (10)	$(I_{12}^{2-})_2$	dimeric ring, of $[(I_5^-).(I_2).(I_3^-).(I_2)]_2$	420, 287, 240, 205, 193, 176, 140, 136, 98, 75, 54	340, 225, 176.5, 169, 144, 109.5	*
13.	$[bpyH]I_5$ (11)	$(I_5^-)_n$	$(I_3^-).(I_2)$ branched chains		343, 221, 172, 117, 108	*

* this work

The far-IR spectra at room temperature and Raman spectra at low temperature (~20 K) of the polyiodide salts of metal complex cations are interpreted based on the structural results.

Complex 1 consists of 2 types of symmetric linear I_3^- ions differing in I-I distances. At room temperature the distances are 2.912 and 2.828 A while at 130 K the shorter I_3^- elongates to 2.844 A and the normal I_3^- shortens to 2.908 A. Thus, the far-IR bands (Figure 5.1a) at 149 and 130 cm"^{1} correspond to the antisymmetric stretches of the two different I_3^- while the Raman bands (Figure 5.1b) at 142 and 113 cm"^{1} probably correspond to the symmetric stretches of the two I_3^- ions at low temperature. The vibrational spectra of 2 (Figure 5.1c,d) is difficult to interpret as the structure at room temperature as well as at 213 K reveal two types of I_3^- ions (one of them asymmetric and the other I_3^- disordered) as well as disordered chains of $(I_8^{2-})_\infty$. The absence of the strong band at ~ 170 cm*^{1}

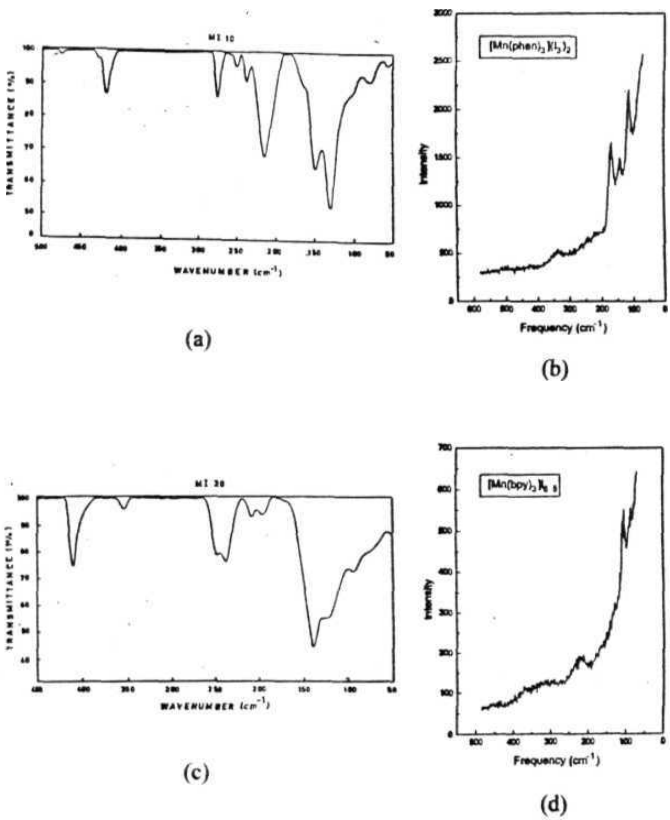

Figure 5.1 **Far-IR** (at 300 **K)** and Raman spectra (at 20 K, λ_o = 514.5 nm) of polyiodide salts of metal complex cations: (a) far-IR spectrum, (b) Raman spectrum of **$[Mn(phen)_3](I_3)_2$ (1);** (c) **far-IR** spectrum, (d) Raman spectrum of $[Mn(bpy)_3](I_3)_{1.5}(I_8)_{0.25}$ **(2)**

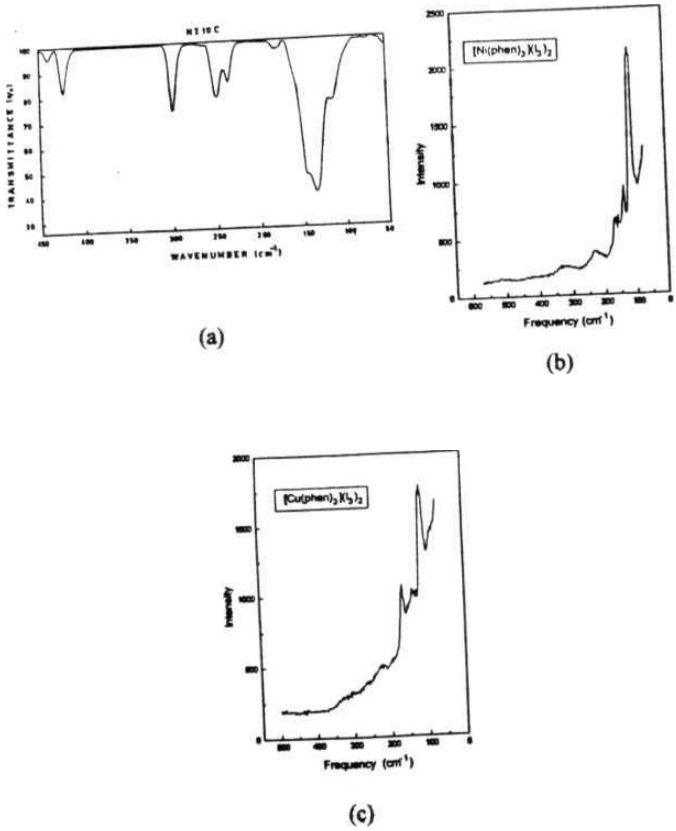

Figure 5.2 Far-IR (at 300 K) and Raman spectra (at 20 K, λ_o = 514.5 nm) of polyiodide salts of metal complex cations: (a) far-ER spectrum, (b) Raman spectrum of of $[Ni(phen)_3](I_3)_2 \cdot (CH_3CN)$ (3); (c) Raman spetrum of $[Cu(phen)_3](I_3)_2 \cdot CH_3CN$ (4).

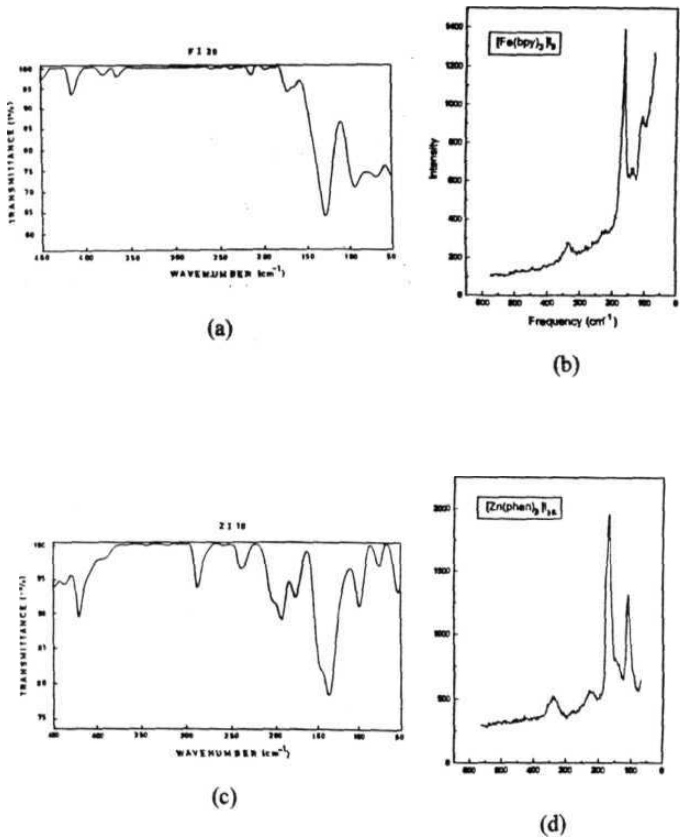

Figure 5.3 Far-IR (at 300 K) and Raman spectra (at 20 K, $\lambda_0 = 514.5$ nm) of polyiodide salts of metal complex cations: (a) far-IR spectrum, (b) Raman spectrum of $[Fe(bpy)_3](I_9)$ (8) (c) far-IR spectrum, (d) Raman spectrum of of $[Zn(phen)_3](I_{12})$ **(10)**

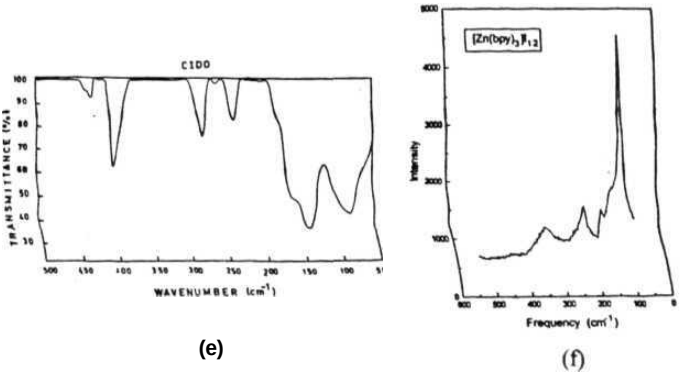

Figure 5.3 (cont'd): (e) far-IR spectrum of $[Cu(dafone)_3](I_{12})$, (Ref. 4); (f) Raman spectrum of $[Zn(bpy)_3](I_{12})$ **(9)**

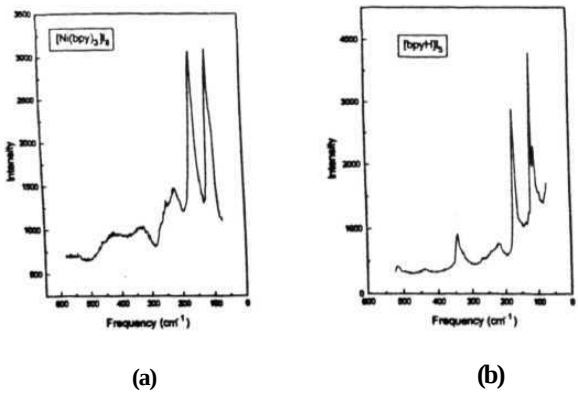

Figure 5.4 Raman spectra (at 20 K, λ_o = 514.5 nm) of polyiodide salts of metal complex cation and $[bpyH]^+$: (a) $[Ni(bpy)_3](I_8)$ **(7);(b)** $[bpyH](I_5)$ **(11)**

corresponding to I_2 molecules is consistent with the interpretation of disorder in the crystal. Complex 3 has two asymmetric slightly bent I_3^- with similar bond distances. The Raman spectrum of 3 (Figure 5.2b) shows a strong peak (possibly a doublet) at 112.5 cnr' followed by several weaker bands at higher energy. The Raman spectrum of 4 (Figure 5.2c) which is expected to be isostructural to 3, has a similar pattern with slight differences in frequencies due to probable variation of bond distances in the complex.

The far-IR spectrum of 8 shows a strong band at 128.5 cnr' corresponding to the I_3^- sub-unit of I_{18}^{4-} anionic network (Figure 5.3a). The Raman spectrum has strong bands at 165 and 106.5 cnr' corresponding to I_2 and I_3^- fragments respectively (Figure 5.3b). The far-IR and Raman spectra of 10 show a wide range of bands from 176.5 to 98 cm^{-1} (Figure 5.3c,d). These are consistent with the I_{12}^{2-} structure that is made up of I_5^-, I_3^- and I_2 fragments. The far-IR spectra of another I_{12}^{2-} which has a planar branched structure shows strong bands at ~155 and 138 and 84 cm'[1] corresponding to the I_5^- fragments (Figure 5.3e).[4] The complex 9, however, has non-planar branched I_{12}^{2-} with an I_2 bridged between a symmetric I_5^- and another asymmetric I_5^-. The Raman spectrum thus shows bands at 133 and 106.5 cm^{-1} due to I_5^- unit and at 181 cm^{-1} due the bridging I_2 unit (Figure 5.3f).

The Raman spectrum of 7 (Figure 5.4a), shows strong bands 159 cm^{-1} and 108 cm^{-1} with a shoulder at 99 cm"'. The crystal structure of this compound has not been determined. The absence of a peak corresponding to I_2 implies that the I_8^{2-} unit is made up of discrete I_5^- and I_3^-, or it could be an infinite iodine chain as in 2. Finally, the Raman spectrum of 11 (Figure 5.4b), shows bands corresponding to I_3^- (117, 108 cm"') and I_2 (172 cnr') units, consistent with the $(I_5^-)_n$ structure.

5.3.2 Electronic Spectroscopy: Solution Absorption and Powder Diffuse Reflectance Spectroscopy

The optical absorption spectra of I_2 in non-aqueous solvents show a single peak at around 500nm (20kK) while the spectrum of I_3^- consists of two strong absorption bands at around 360nm (28kK) and 290nm (35kK), attributed to spin-orbit splitting in the $\sigma_g \rightarrow \sigma_u^*$ transition. The studies on higher polyiodides have shown that in solution the polyiodides undergo structural reorganization and progressively dissociate into stable I_2 and I_3^- species upon dilution.[5] Therefore, diffuse reflectance spectra are more useful to distinguish the polyiodide species in the solid state. The polarized reflectance studies of isolated symmetric and asymmetric I_3^- crystals show spectra with broad bands at around 27.0 and 33.0 kK with subbands, due to spin-orbit splitting while the linear chains $(I_3^-)_n$, show spectra with bands at 22.0 and 30.5 kK.[5] The disordered chains of higher polyiodides show an additional band around 17.0 kK.

5.3.2 (a) Optical Absorption Spectra

All complexes were insoluble in water, but soluble in organic solvents such as dichloromethane and acetonitrile forming dark brown coloured solutions. The electronic absorption spectra pattern of the complexes in dichloromethane or acetonitrile were similar, but with very different molar extinction coefficients.

A summary of the optical absorption studies for various polyiodide units are presented in Table 5.2 along with the interpretation of the plots shown in Figures 5.5-5.8.

The electronic spectrum of I_2 in CH_2Cl_2 shows a band at 505 nm with a molar extinction coefficient (e) of 780 M^{-1} cm^{-1} and weak absorptions at 365 nm and 295 nm indicating the presence of small amounts of I_3^- at a dilution of 10^{-5} M.

The solution spectrum of I_3^- in CH_2Cl_2 shows the spin-orbit split bands at 365 nm and 295 nm with molar extinction coefficients (ε) of 25,000 M^{-1} cm^{-1} and 48,000 M^{-1} cm^{-1} respectively. Based on these values, the amount of I_3^- and I_2 present in the solution spectra of the various polyiodide salts of metal complex cations are estimated.

In agreement with the crystal structure, the electronic spectrum of 1 and 3 in solution confirm 2 moles of I_3^- in solution (Figure 5.5a,c). However, the electronic spectrum of 4 (Figure 5.5d), shows presence of 1.5 moles of I_3^- in solution instead of the expected 2 moles of I_3^-. The solution spectrum of 2 also agrees well with the solid state, showing 1.5 moles of I_3^- ions in solution (Figure 5.5b). The presence of chains of I_8^{2-} ions in solution was not easily detectable in the spectrum.

In case of the polyiodides anions with higher iodine content, the I_2 band at 505 nm appears as a shoulder to the very strong 362 nm band of I_3^-. The molar extinction coefficients of the 505 nm band are thus not very accurate and are more than the expected values in most cases. The electronic spectrum of 6 which has I_8^{2-} in solid state shows partial dissociation of the anion into I_3^- and I_2 fragments (Figure 5.6a). The spectrum of 7, which probably has I_8^{2-} anions in solid state, shows similar break-up into I_3^- and I_2 units (Figure 5.6b). The solution spectrum of 8 indicates nearly complete dissociation of I_{18}^{4-} anion into I_3^- and I_2 . This is evident from the presence of 2 moles of I_3^- present in the solution spectrum. The I_2 peak, here, is masked by the two $[Fe(bpy)_3]^{2+}$ charge-transfer bands (523 and 487 nm), of much higher extinction coefficients (Figure 5.6c).

Table 5.2 Electronic bands observed in different types of polyiodide salts of metal complex cations and **bpyH$^+$** in **CH_2Cl_2** as solvent. (The wavelengths are printed in italics and the corresponding molar extinction coefficient is given in the bracket; the bands due to metal **complex** cations are underlined.)

SNo.	Molecular formula	Polyiodide unit(s)	Electronic bands, **nm** (molar extinction coefficient, **M^{-1}** cm^{-1})	Comments
1.	**$[Mn(phen)_3](I_3)_2$** (1)	**I_3^-**	***534*sh(789),** 566(43,374), 292(95,869), 275(1,02,693)	bands corresponding to ~2 moles of **I_3^-** observed.
2.	**$[Mn(bpy)_3](I_3)_{1.5}(I_8)_{0.25}$** (2)	**I_3^-, $(I_8^{2-})_n$**	***535*sh(403), *366*(40,201),** 505(48,985)	bands corresponding to **~1.5** moles of **I_3^-** and another polyiodide species(?) observed.
3.	**$[Ni(phen)_3](I_3)_2 \cdot CH_3CN$ (3)**	I3"	566(47,942), ***281*sh(1,75,133),** 275(1,88,497)	bands corresponding to ~2 moles of **I_3^-** and another intense band also observed.

4.	$[Cu(phen)_3](I_3)_2 \cdot CH_3CN$ (4)	I_3^- (?)	757(453)t, 362(34,891), *289*sh(75,818), 277.5(89,166)	bands corresponding to ~1.5 moles of I_3^- observed.
5.	$[Cu(bpy)_3](I_8) \cdot CH_2Cl_2$ (6)	I_8^{2-}	*770*(896)†, *505*sh(2,591), 365(33,663), 294.5(85,610)	bands corresponding to I_2 and I_3^- observed showing partial dissociation of I_8^{2-}.
6.	$[Ni(bpy)_3](I_8)$ (7)	I_8^{2-} (?)	505sh(2,8O8), 366(36,597), *305.5*sh(56,908), *298.5*(61,962)	bands corresponding to I_2, I_3^- and another polyiodide species(?) observed.
7.	$[Fe(bpy)_3](I_9)$ (8)	$(I_{18}^{4-})_n$	*523*(8,809)‡, *487*(8,095)‡, 363(46,743), **295(1,11024)**	bands corresponding to I_3^- observed; the I_2 band may have got overlapped with the Fe^{2+} bands.

8.	$[Cu(dafone)_3]I_{12}$*	I_{12}^{2-}	505(1,918), *359*(1,782), 5/5(7,633), 505(8,610)	bands corresponding to mainly I_2 observed. Spectrum unique to I_{12} anion.
9.	$[Zn(bpy)_3](I_{12})$ (9)	$(I_{12}^{2-})_n$	*515*sh(1,848), 566(49,504), 5/6(38,951)	bands corresponding to I_2, I_3^- and another polyiodide species observed.
10.	$[Zn(phen)_3](I_{12})$ (10)	$(I_{12}^{2-})_2$	*505*sh(3,826), *365*(46,434), *295.5*(67,846), 275.5(63,650)	bands corresponding to I_2 and I_3^- observed.
11.	$[bpyH]I_5$ (11)	$(I_5^-)_n$	505sh(786), *365*(28,271), 299(50,865)	bands corresponding to 1 mole of I_2 and I_3^- observed.
12.	$[bpyH]I_7$ (12)	$(I_7^-)_n$	505sh(2,025), 565(28,715), 296.5(61,922)	bands corresponding to I_2 and I3' observed.

* Ref. 4; t d-d transition in Cu^{2+} ion; *t* MLCT band.

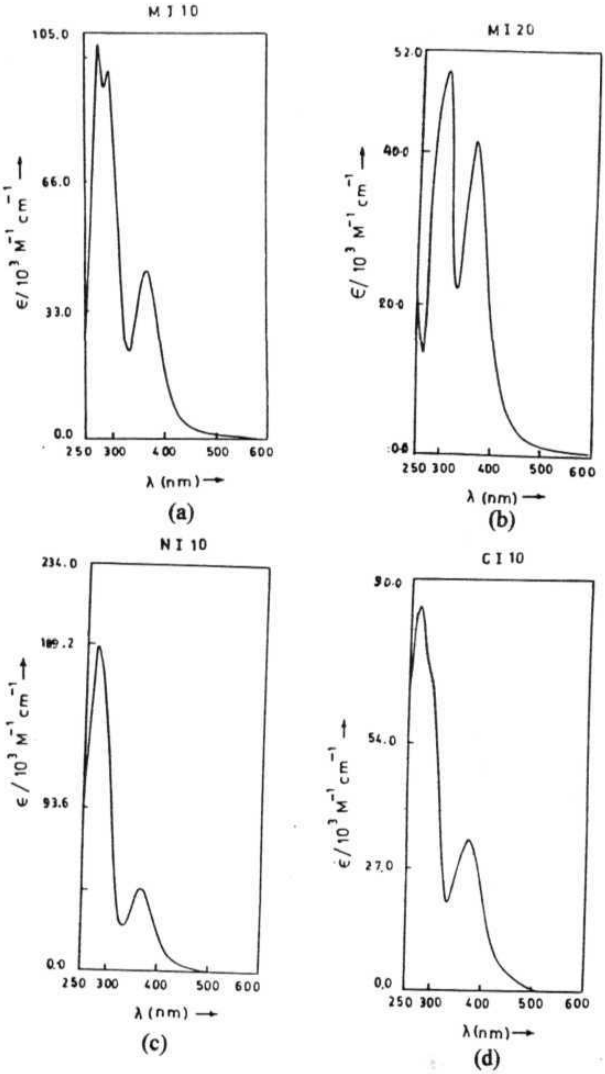

Figure 5.5 Electronic spectra of polyiodide salts of metal complex cations in CH_2Cl_2 as solvent : (a) $[Mn(phen)_3](I_3)_2$ (1). (b) $[Mn(bpy)_3](I_3)_{1.5}(I_8)_{0.25}$ (2); (c) $[Ni(phen)_3](I_3)_2 \cdot CH_3CN$ (3), (d) $[Cu(phen)_3](I_3)_2 \cdot CH_3CN$ (4)

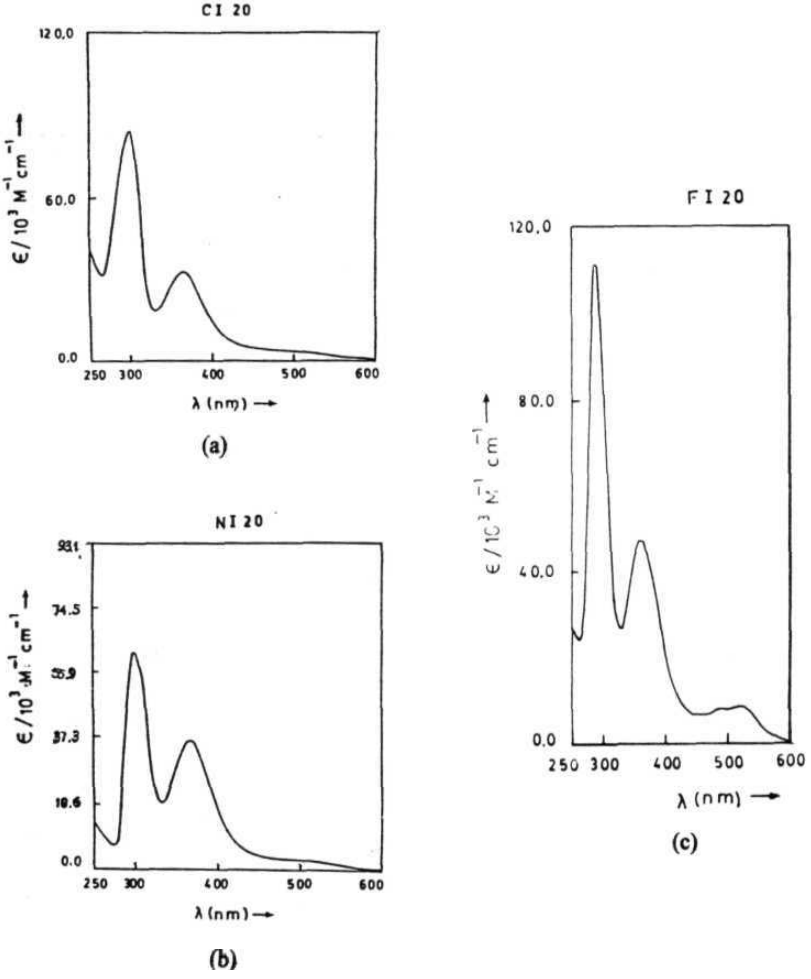

Figure 5.6 Electronic spectra of polyiodide salts of metal complex cations in CH_2Cl_2 as solvent : (a) $[Cu(bpy)_3](I_8)\cdot CH_2Cl_2$ (6), (b) $[Ni(bpy)_3](I_8)$ (7), (c) $[Fe(bpy)_3](I_9)$ **(8)**

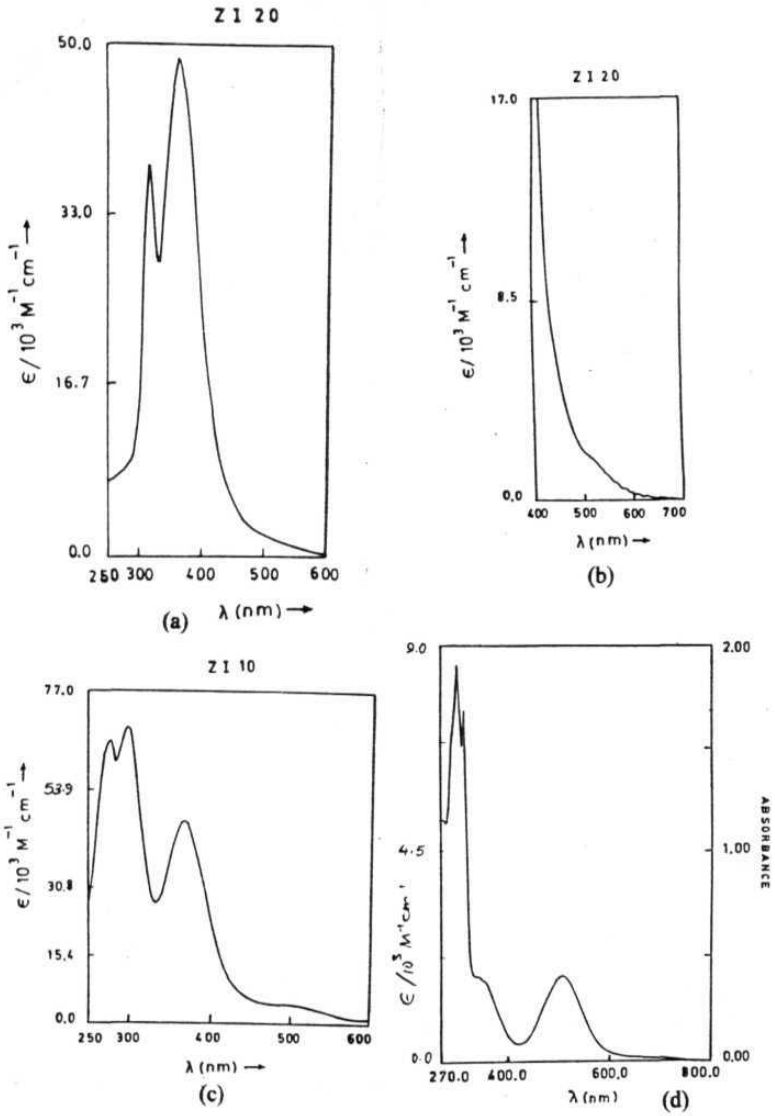

Figure 5.7 Electronic spectra of polyiodide salts of metal complex cations in CH_2Cl_2 as solvent : (a), (b) $[Zn(bpy)_3](I_{12})$ (9); (c) $[Zn(phen)_3](I_{12})$ (10); (d) $[Cu(dafone)_3](I_{12})$ (Ref.4)

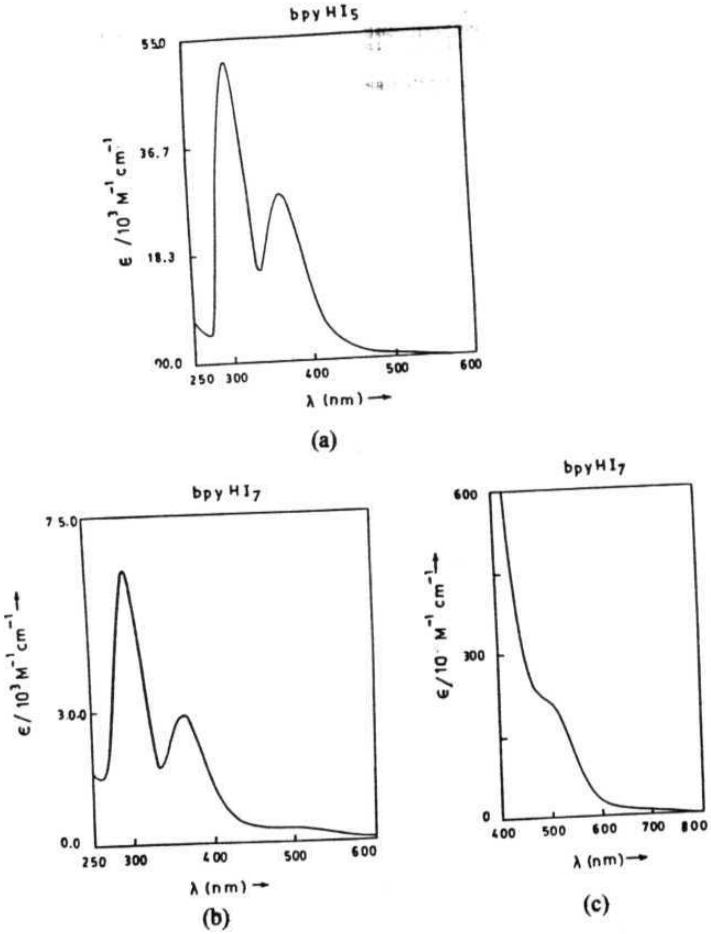

Figure 5.8 Electronic spectra of poly iodide salts of $[bpyH]^+$ in CH_2Cl_2 as solvent : (a) $[bpyH](I_5)$ **(11),** (b), (c) $[bpyH](I_7)$ (12) .

The electronic spectra of 9 shows presence of ~2 moles of I_3^- ions in the solution and also I_2 peak, indicating the near-complete dissociation of I_{12}^{2-} anion in solution (Figure 5.7a,b). The electronic spectrum of 10 is quite different from 9, which also has I_{12}^{2-} anions in solid state and solution spectrum indicating complete break-up into I_3^- and I_2 ions (Figure 5.8c). The electronic spectrum reported[4] for $[Cu(dafone)_3]I_{12}$, shows mainly I_2 band and does not have any prominent I_3^- bands (Figure 5.7d). It appears that in CH_2Cl_2 solution the I_3^- is getting oxidized by the Cu(II) complex ion.

The electronic spectrum of 11 shows a clear break-up of the $(I_5^-)_n$ chain into one mole of I_3^- and I_2. The spectrum of 12 also confirms the presence of one mole of I_3^- and slight excess of I_2 in solution (Figure 5.8).

5.3.2 (b) Powder Diffuse Reflectance Spectra

The powder diffuse reflectance spectra of the two complexes 1 and 2 measured were found to be similar to each other and exhibit features at 23.0, 20.8, 18.5, 17.2 kK (Figure 5.9a,b). Since there are no spin allowed d-d transitions for the S Mn(II) ion, the features must be associated with the polyiodide ions. The observed close similarity of the two spectra implies that the presence of a linear iodine chain in 2 has practically no influence on its solid state spectrum.

This is in striking contrast to the marked difference observed in the diffuse reflectance spectra of $[Sb(CH_3)_4]_3I_8$ and $[As(CH_3)_4]I_3$.[6] The antimony compound, which has chains of $(I_8^{3-})_n$ but no I_3^- ion, is described as having a metallic luster, its spectrum being a featureless plateau with little structure covering the entire measurement range upto 800 nm due to electron delocalisation, while the isolated I_3^- shows a spectrum with a maximum at 570nm and a sloping edge upto 750nm. Featureless absorption was also reported for the complex $[Cu(dafone)_3]I_{12}$, containing planar I_{12}^{2-} unit and extensive I..I contacts (Figure 5.9c).[4] The spectra

of 1 and 2, on the other hand, are very similar to the reported description of the spectrum of the arsenic compound, which contains only I_3^- ions.

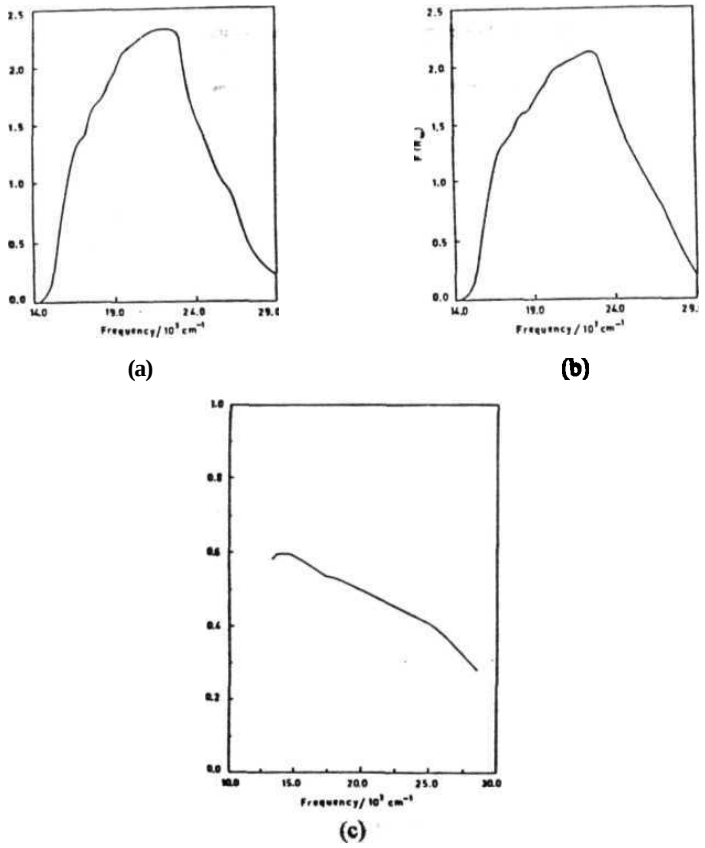

Figure 5.9 Powdered diffuse reflectance spectra of poly iodide salts of metal complex cations: (a) $[Mn(phen)_3](I_3)_2$ (1); (b) $[Mn(bpy)_3](I_3)_{1.5}(I_8)_{0.25}$ (2) and (c) $[Cu(dafone)_3](I_{12})$, (Ref.4).

The close similarity of the diffuse reflectance spectra of the two complexes 1 and 2, inspite of the different structural features is thus, not fully understood. It

appears **that** the optical spectrum of 2 is mainly due to the I_3^- ions with a little contribution from the (disordered) iodine chain. This would mean the electronic delocalisation implied by a flat absorption curve is hampered in 2 either by the disorder in the chain or by contacts with isolated I_3^- ions in the lattice.

5.4 Conclusions

The vibrational spectra of polyiodide salts of metal complex cations have been correlated with the structural data. A detailed interpretation of the solid state vibrational spectra may often require consideration of site symmetry effects on the selection rules and degeneracies of a free molecule or ion. However, certain qualitative conclusions regarding the nature of the polyiodide can be drawn without a detailed analysis. The most useful fact is that a strong Raman band in the range of 165 cm^{-1} - 180 cm^{-1} is a signature of 'free' I_2 molecule. The least perturbed I_2 molecules will be at the higher energy end of this range. The absence of such a peak in $[Ni(bpy)_3]I_8$ (7), the structure of which is not known, indicates that the I_8^{2-} is not the Z-shaped ion containing a weakly perturbed I_2 molecule. It probably has infinite iodine chains containing strongly perturbed I_2 molecules. Alternatively, it may contain I_5^- and I_3^- ions.

Coming to electronic spectroscopy, it is sometimes possible to derive the ratio, $[I_3^-]:[I_2]$ in the polyiodide by measuring the UV-visible absorption spectrum of a dilute solution. However, the presence of absorption due to the ligands, and possible redox reactions involving the cation or solvent limit the utility of this method.

Diffuse reflectance spectra is sometimes useful in identifying polyiodides having extended electronic delocalisation. However, the diffuse reflectance spectrum of 2 is mainly due to the I_3^- ions with little contribution from the (disordered) iodine chain.

References

(1) (a) A. I. Popov in *Halogen Chemistry*, Ed. V. Gutmann, Academic Press, London (United Kingdom), **1967,** vol. 1, p.225. (b) P. Coppens in *Extended Linear Chain Compounds,* Ed. J. S. Miller, Plenum, New York (USA) **1982,** vol. 1, p.333. (c) T. J. Marks and D. W. Kalina in *Extended Linear Chain Compounds,* Ed. J. S. Miller, Plenum, New York (USA) **1982,** vol.1, p. 197. (d) J. R. Ferraro *Coord. Chem. Rev.* **1982,** *43,* 205.

(2) G. Kortüm, *Reflectance Spectroscopy,* Springer-Verlag, New York (United States of America), **1969,** p. 106.

(3) (a) M. Mizuno, J. Tanaka and I. Harada, *J. Phys. Chem.* **1981,** 55, 1789. (b) E. M. Nour, L. H. Chen and J. Laane *J. Phys. Chem.* **1986,** *90,* 2841. (c) L. C. Hardy and D. F. Shriver *J. Am. Chem. Soc.* **1986,** *108,* 2887. (d) A. J. Blake, F. A. Devillanova, R. O. Gould, W. -S. Li, V. Lippolis, S. Parsons, C. Radek and M. Schroder *Chem. Soc. Rev.* **1998,** *27,* 195

(4) (a) S. Menon and M. V. Rajasekharan *Inorg. Chem.* **1997,** *36,* 4983. (b) S. Menon, Ph.D. Thesis, University of Hyderabad, Hyderabad, India, **1996.**

(5) (a) W. Gabes and M. A. M. Nijiman-Meester, *Inorg. Chem.* **1973,** *12,* 589. (b) W. Gabes and D. J. Stufkens, *Spectrochim. Acta Part A* **1974,** *30,* 1835. (c) A. I. Popov and R. F. Swensen, *J. Am. Chem. Soc.* **1955,** *77,* 3724. **(d)** R. E. Buckles, J. P. Yuk and A. I. Popov, *J. Am. Chem. Soc.* **1952,** *74,* 4379.

(6) U. Behrens, H. J. Breunig, M. Denker, K. H. Ebert, *Angew. Chem. Int. Ed. Engl.* **1994,** *33,* 987.

CHAPTER 6

Polyiodide Salts of Metal Complex Cations : Part 4. Structural Comparisons.

This chapter presents a comparison of the structures of all the polyiodides and tris-chelates reported in this thesis. A brief description of the different types of polyiodide anions formed, based on bond distances, angles and I..I contacts is given. Finally, the cation-anion packing in these complexes is discussed and comparisons are drawn.

6.1 Comparison of the Tris-Chelate Cations

A plot of metal-nitrogen (M-N) distances vs. N-M-N chelate angles for a series of such complexes is shown in Figure 6.1. The structural data are tabulated in Table 6.1. A correlation between increasing M-N distances and decreasing N-M-N angles is observed considering the average values. A large variation in M-N distances and N-M-N angles is observed in Cu^{2+} complexes due to the statically Jahn-Teller distorted d^9 cation. The non-bonded N..N bite in these complexes is found to be nearly constant in the range of 2.6-2.7 A. The M-N distance varies because of the changing covalent radius of the metal ion forcing the N-M-N angle to alter in order to compensate for the inflexibility of the ligand bite (phen/bpy). Similar results were obtained for a series of phen complexes of transition metal ions studied earlier.[1]

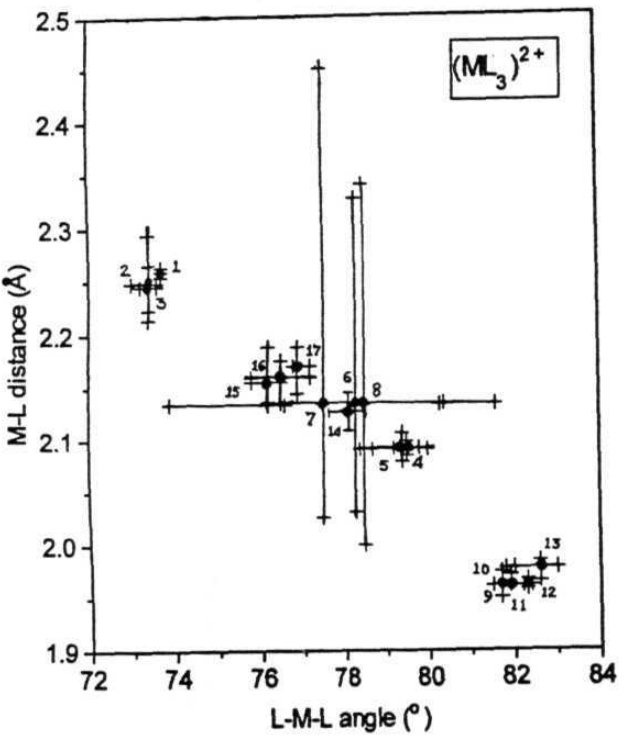

Figure 6.1 Plot of the metal - N (ligand) bond distances and bite angles (N-M-N) for the tris-chelates formed by bpy and phen. The symbols ++ and ‡ denote the observed ranges of bond distances and angles for a given ion, with the intersection corresponding to the average values. Numbers refer to serial numbers in Table **6.1**.

Table 6.1 Structural data of the transition metal tris-chelate cations studied (* this work).

SNo	Complex	M-N distances (A), α‡	N-M-N angles (°)	Average valuest	Ref.
1.	$[Mn(phen)_3](I_3)_2$ (1)	2.254, 2.263;	73.7	2.259(3,6) Å, 73.7° (2,2)	*
2.	$[Mn(bpy)_3](I_3)_{1.5}(I_8)_{0.25}$ (2)	2.253, 2.245;(4°) 2.266, 2.223;(4°) 2.255, 2.245; (4°)	73.7, 73.6, 73.0	2.248(2,14) A, 73.4° (1,4)	•
3.	$[Mn(bpy)_3](ClO_4)_2 \cdot 0.5H_2O$	2.294,2.219; 2.230, 2.280; 2.233,2.214; (13-25°)	73.4, 73.2, 73.6	2.245 A, 73.4°	2
4.	$[Ni(phen)_3](I_3)_2 \cdot CH_3CN$ (3)	2.098, 2.096; 2.094, 2.089; 2.084, 2.086;	79.2, 79.5, 79.8	2.091(3,6) A, 79.5° (2,3)	*
5.	$[Ni(phen)_3][Mn(CO)_5]$	2.078, 2.090; 2.093, 2.078; 2.095,2.106;	80.0, 79.4, 78.7	2.090 A, 79.4°	1
6.	$[Cu(bpy)_3]I_8 \cdot CH_2Cl_2$ (6)	2.327, 2.041;(22°) 2.031 x 2; (15°)	76.2, 80.3	2.133(4,168) A, 78.3° (1,25)	*
7.	$[Cu(bpy)_3](ClO_4)_2$	2.450, 2.026;(31°) 2.034, 2.035;(11°) 2.030, 2.226;(14°)	73.9, 80.4, 78.2	2.134 A, 77.5°	3
8.	$[Cu(phen)_3](ClO_4)_2$	2.34, 2.02; 2.06, 2.06; 2.32, 2.00;	76.6, 81.6, 77.2	2.13 A, 78.5°	4
9.	$[Fe(bpy)_3]I_9$ (8)	1.960, 1.956;(7°) 1.966, 1.974;(2°) 1.961, 1.950;(5°)	81.5, 81.9, 81.4	1.961(4,10) A, 81.7° (2,2)	*
10.	$[Fe(bpy)_3][NaFe(ox)_3]$	1.977, 1.977;(9°)	81.8	1.977, 81.8°	5
11.	$[Fe(bpy)_3][LiCr(ox)_3]$	1.971, 1.972;(9°)	81.9	1.972 A. 81.9°	5

12.	$[bpyH][Fe^{III}(bpy)_3](ClO_4)_4$	1.958, 1.959; 1.960, 1.960; 1.964, 1.967; (<6°)	**82.2, 82.3, 82.4**	1.961 A, 82.3°	6
13.	$[Fe(phen)_3](ClO_4)_2 \cdot 0.5H_2O$	1.973,1.982; 1.980, 1.981; 1.984, 1.965;	82.8, 83.0, 82.0	1.978 A, 82.6°	7
14.	$[Co(phen)_3](ClO_4)_2 \cdot H_2O$	2.124, 2.138; 2.109,2.138; 2.111,2.142;	**78.1, 78.5, 77.8**	2.127 A, 78.1°	8
15.	$[Zn(bpy)_3]I_{12}$ (9)	2.136, 2.164;(8°) 2.162, 2.140;(13°) 2.188, 2.137;(15°)	76.3, 75.8, 76.5	2.155(4,21) A, 76.2° (3,4)	•
16.	$[Zn(bpy)_3](ClO_4)_2$	2.172, 2.166; 2.135 x 2;(17°)	75.8, 77.2	2.159A, 76.5°	9
17.	$[Zn(phen)_3]I_{12}$ (10)	2.147,2.188; 2.181,2.187; 2.174,2.144;	**76.8,** 76.8, 77.2	2.170(4,20) A, 76.9° (2,2)	*

‡ : The two M-N distances formed with each ligand (bpy/phen) are grouped. The twist angle a, observed for bpy ligand is given in paranthesis. † : The two standard deviations in paranthesis are calculated as: $\sigma 2[f(p1..)] = \Sigma(\partial f/\partial pi)2si2$ and $\sigma 2mean \cdot \Sigma(xi-x)2/(n-1)$, respectively.

While phen is a rigid planar ligand, coordinated bpy shows considerable deviation from planarity, with interplanar angle between the two pyridine rings (a) ranging from 0 to 22°. Both the ligands coordinate in a symmetrical fashion with the two Mn-N bond distances equal within about 0.02 A. However, Cu(II) complexes are exceptional in this regard. Due to Jahn-Teller distortion, two of the three ligand molecules in a tris-chelate adopt highly unsymmetrical coordination mode with Cu-N bond distances differing by as much as 0.4 A. The Cu(II) complex ion in 6 has a C_2 symmetry while the Mn(II), Ni(II) and Fe(II) complex ions (in 1, 2, 3 and 8) closely approach D_3 symmetry. The Zn(II) complexes in 9 and 10 deviate more strongly from trigonal symmetry (the Zn-N bond length differences = 0.02 - 0.05 A for 9, 0.01 - 0.04 A, for 10, a = 8 - 15° for 9.).

6.2 Structure and Bonding in the Polyiodide Anions

The structures of polyiodide anions formed with tris-chelate cations are collected in Figure 6.2. The cations $[Mn(phen)_3]^{2+}$, $[Ni(phen)_3]^{2+}$ and $[Mn(bpy)_3]^{2+}$ prefer I_3^- as the counter-anion (Figure 6.2a,b,c). In the highly symmetrical complex, $[Mn(phen)_3](I_3)_2$ (1), the two triiodide anions occur in linear and symmetric form, having two different I-I distances and no I..I contacts between them. But in $[Ni(phen)_3](I_3)_2 \cdot CH_3CN$ (3), the change of metal atom and the slight decrease in the metallic radius results in the change of anion shapes to slightly bent and unsymmetrical triiodides and also having end-to-end van der Waals contacts between four anions. Similarly, the change of ligand from phen to less rigid bpy in 1, resulted in complex 2, $[Mn(bpy)_3](I_3)_{15}(I_8)_{025}$, which also has two types of triiodides. One of them is linear asymmetrical, while the other is disordered about the inversion centre. The rest of the charge is balanced by linear infinite polyiodide chains of the type $(I_8)^{2-}$. The chain is disordered and is difficult to divide into smaller fragments of I_3^- and I_2 based on bond distances, as can be done in other cases. Although infinite chains of I_8^{2-} are not known yet, the occurance of a nearly linear dimer of I_8^{2-} (I_{16}^{4-}) has been reported once.[10]

In $[Cu(bpy)_3](I_8) \cdot CH_2Cl_2$ (6), the anion I_8^{2-} has a commonly occuring centrosymmetric Z-shape of the type $I_3^-.I_2.I_3^-$. But the difference here is that the unit is non-planar (Figure 6.2d). Non-planar $Ig^{2''}$ have been reported in a few examples wherein, the anion is forced to become non-planar by the cationic environment, resulting in the elongation and distortion of one of the I_3^--I_2 bonds. In 6, there is no elongation of the bond and there is a uniform distortion making the two I_3^- arms nearly orthogonal. The anions have weak van der Waals contacts between I_8^{2-} units at the $I_3^-.I_2$ junction, leading to formation of a loose network of the anions.

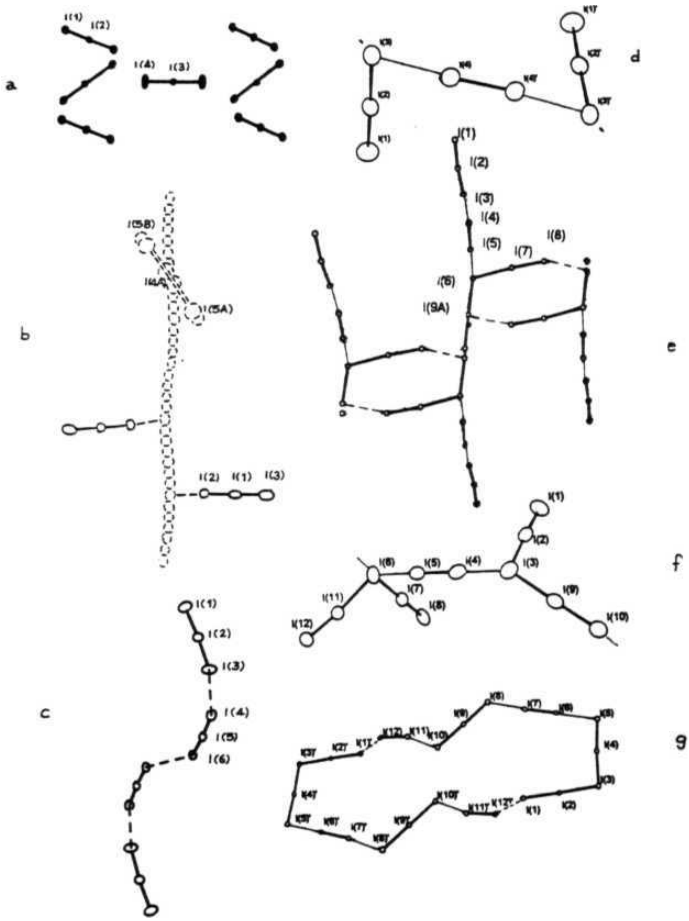

Figure 6.2 Polyiodide anions formed with transition metal tris-chelate cations: (a) I_3^- in 1; (b) I_3^-, $(I_8^{2-})_n$ in 2; (c) I_3^- in 3; (d) I_8^{2-} in 6; (e) $(I_{18}^{4-})_n$ in 8; (f) I_{12}^{2-} in 9 and (g) I_{24}^{4-} in 10.

The network forming centrosymmetric I_{18}^{4-} (Figure 6.2e) made up of I_3^- and I_2 molecules, is a new anion occuring in $[Fe(bpy)_3]I_9$ (8). The I_{12}^{2-} anion in 9 is formed by an I_2 unit bridged between two bent I_5^- units. One of the I_5^- here is symmetrical $(I_2 \cdot I^- \cdot I_2)$, while the other is asymmetrical $(I_3^- \cdot I_2)$ (Figure 6.2f). The I..I contacts lead to the formation of a close network.

The I_{12}^{2-} anion in $[Zn(phen)_3]I_{12}$ (10), has a new shape, that of a dimeric 24-membered ring formed by end-to-end connection of two I_{12}^{2-} units (Figure 6.2g). The shape of the ring is like the number '8', so as to fit two $[Zn(phen)_3]^{2+}$ cations inside the ring. These rings are connected to each other by I..I contacts at three adjacent iodines on the ring.

6.3 Cation - Anion Packing

6.3 (a) Cationic arrangement. An interesting study of these polyiodide salts of metal complex cations, is the arrangement of the divalent cations in the crystal lattice. A careful look at the packing in all the complexes, revealed similarities in the packing of some of the cations.

The $[Mn(bpy)_3]^{2+}$ cations in 2, are arranged in a nearly-planar hexagonal-like layers stacked parallel to form hexagonal-like (honey-comb) channels along the c-axis. These channels are filled with infinite chains of I_8^{2-}. Just as hexagonal layers of carbon stack as layers of *abab*.. type in graphite, the planar hexagonal layers of cations of 1, form *abcabc*... stacking layers along c-axis direction (Figure 6.3).

The cations of $[Ni(phen)_3](I_3)_2 \cdot CH_3CN$ (3) and $[Zn(phen)_3]I_{12}$ (10) also adopt a packing similar to 2, forming parallel stacked roughly planar hexagonal-like layers (Figure 6.4).

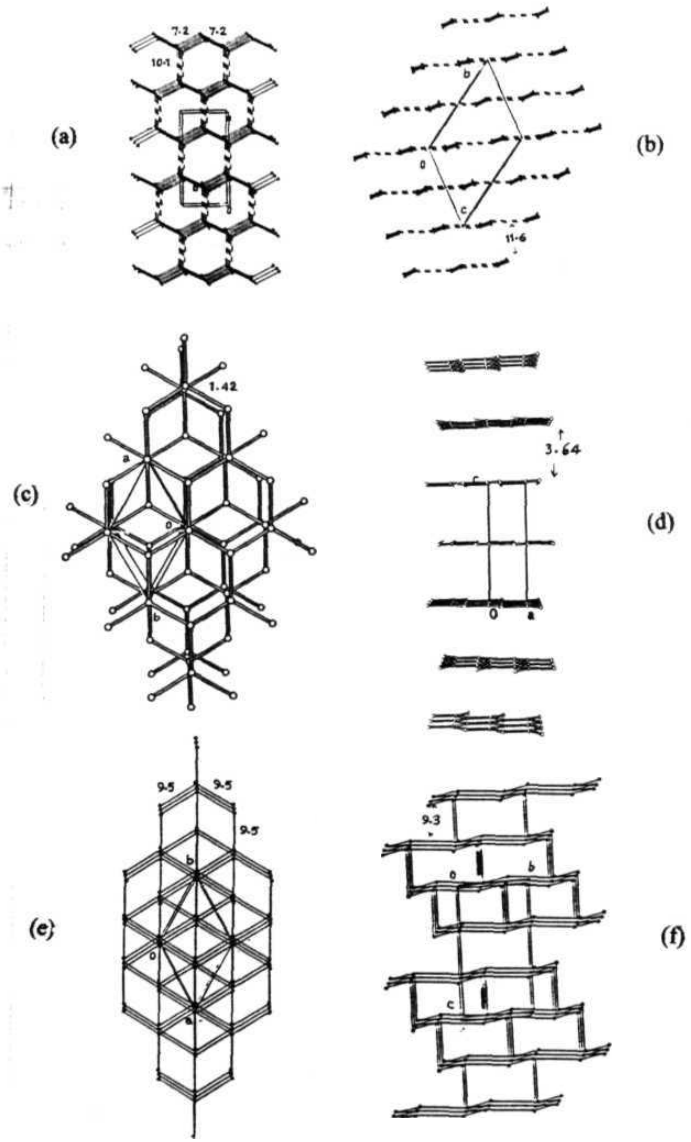

Figure 6.3 Two views of the packing of metal ions: (a), (b) in 2; (c), (d) in graphite (coordinates taken from ORTEX program examples); (e), (f) in 1. (distances between atoms are given in A.)

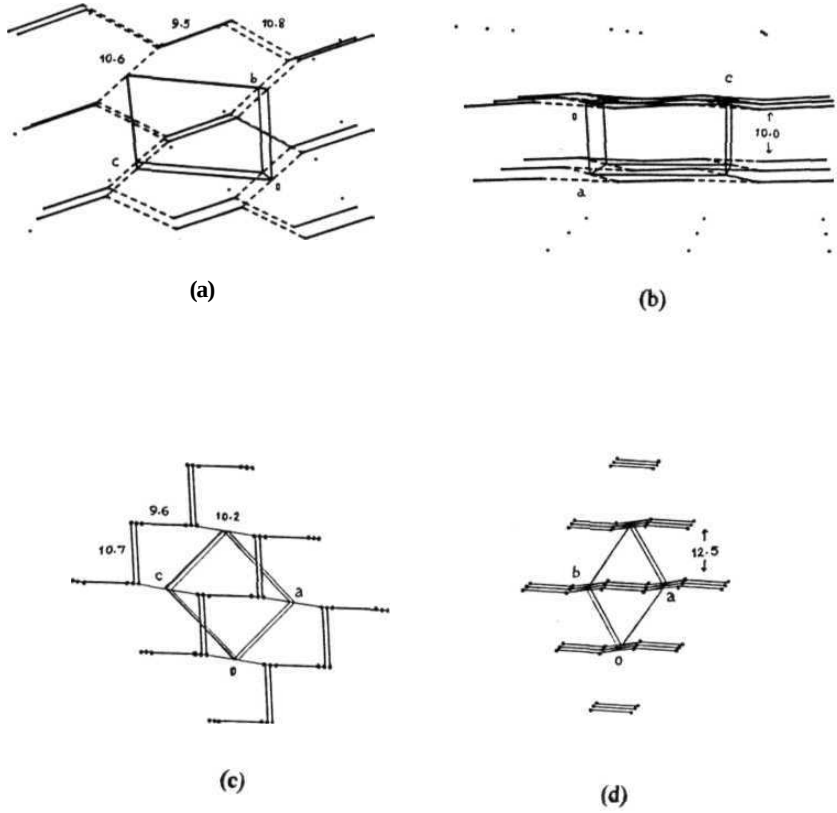

Figure 6.4 Two views of the packing of metal ions: (a), (b) in 3; (c), (d) in 10. (distances between atoms are given in A.)

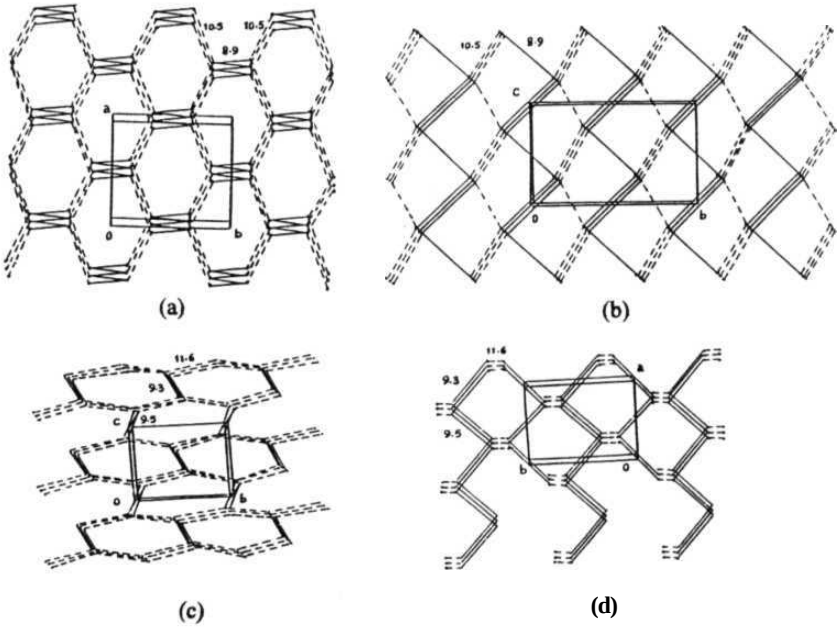

Figure 6.5 Two views of **the** packing of metal ions : (a), (b) in 6; (c), (d) in 9. (distances between atoms are given in A.)

The $[Cu(bpy)_3]I_8$ (6) and $[Zn(bpy)_3]I_{12}$ (9) however, form 6-membered non-planar rings packed in layers (Figure 6.5).

The cations in $[Fe(bpy)_3]I_9$ (8) are aligned linear along c-axis direction. These aligned cations are parallel to the adjacent chains of cations forming a rhombic pattern when viewed normal to the ab-plane (Figure 6.6). Such aligned cations were also observed in $[Cu(dafone)_3]I_{12}$.[11].

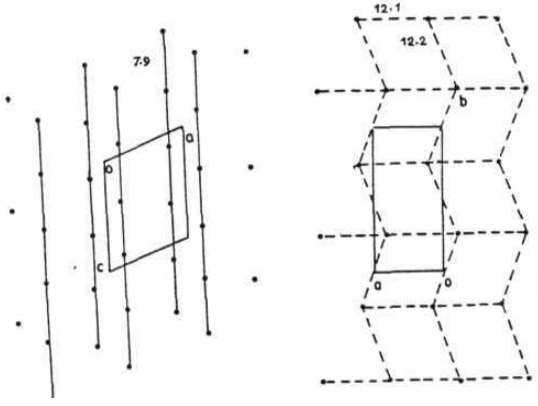

(a) (b)

Figure 6.6 Two views of the packing of metal ions in 8. (distances between atoms are given in A.)

6.3 (b) Crystal packing. After a study of the cationic arrangement it is easier to understand the cation-anion packing in the polyiodide.

In $[Mn(phen)_3](I_3)_2$(**1**), $[Mn(bpy)_3](I_3)_{1.5}(I_8)_{0.25}$ (**2**), $[Ni(phen)_3](I_3)_2.CH_3CN$ (3) and $[Cu(bpy)_3](I_8).CH_2Cl_2$ (6), a layered packing of cations and anions are observed (Figure 6.7, 6.8).

In the Mn^{2+} complexes 1 and 2, the cations pack in a more symmetric way, forcing the I_3^- to become linear and symmetric in 1, and forming hexagonal-like channels filled with polyiodide chains in 2 (Figure 6.7). The packing is less rigid in 3, leading to $I_3^-..I_3^-$ contacts and also formation of empty cavities. These cavities are occupied by disordered molecules of the solvent, CH_3CN, used for recrystallisation of complex. In 6, layered packing of cation and anion along with loose network of centrosymmetric I_8^{2-} anions, leads to formation of large channels along c-axis direction. These channels are filled with disordered solvent molecules of CH_2Cl_2. Thus, in complexes 3 and 6, there is an 'equal influence' of cation and anion on the crystal lattice formation.

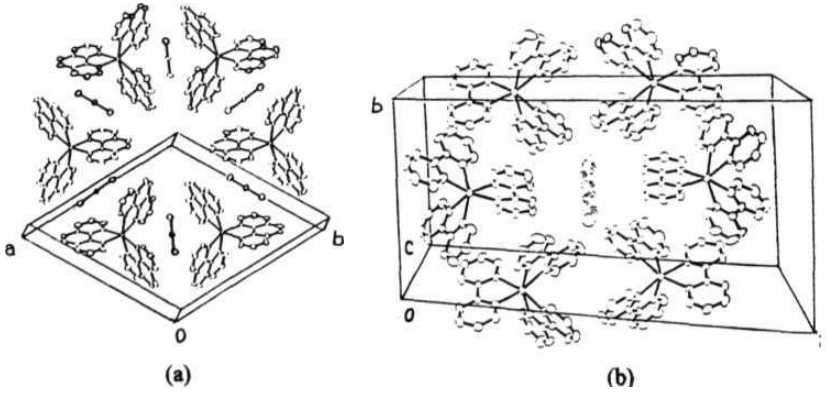

Figure 6.7 Cation-anion packing in polyiodides salts of metal complex cations: layered packing in (a) 1; (b) 2.

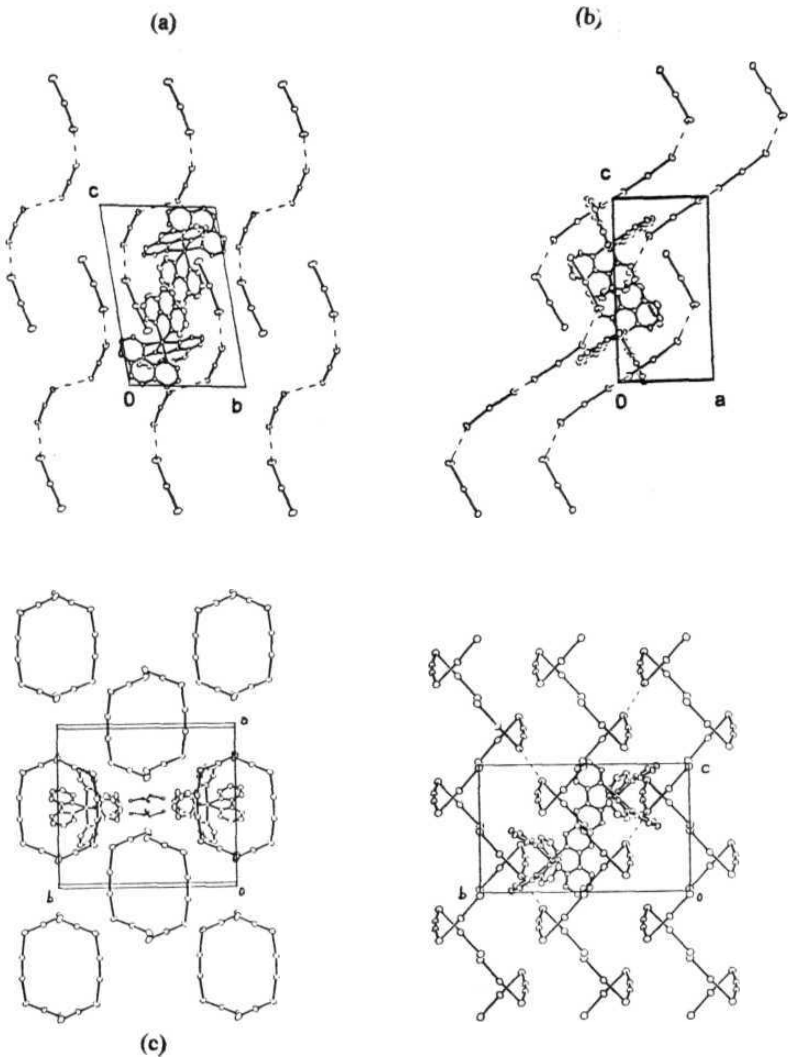

Figure 6.8 Cation-anion packing in polyiodides salts of metal complex cations: (a), (b) in 3; (c), (d) in 6.

The anionic networks are more dominating in the higher iodine content complexes of $[Fe(bpy)_3]I_9$ (8), $[Zn(bpy)_3]I_{12}$ (9) and $[Zn(phen)_3]I_{12}$ (10). In these, the cations are either sitting inside the compact anionic channels (8), or trapped inside thick anionic cages (9), or anionic rings (10) (Figure 6.9). Thus, the anionic network dominates over the cation packing arrangement in these complexes.

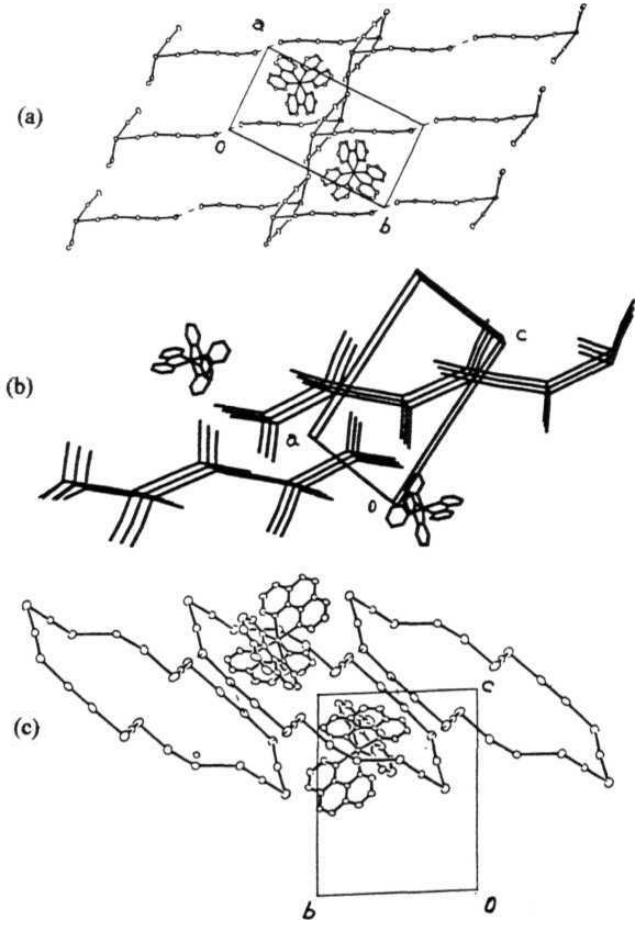

Figure 6.9 Cation-anion packing in **polyiodides** salts of **metal** complex cations: (a) in 8; (b) in 9; (c) in 10.

This is also reflected in their high crystal densities which range from 2.71 to 2.79 g ml^{-1}, while the other polyiodides have (1, 2, 3, 6) have densities ranging from 2.23 to 2.43 g ml^{-1}.

6.4 Conclusions

The polyiodide salts of Mn^{2+} complex cations can be considered as symmetrical arrangement of cations accomodating counter-anions like I_3^- in between the layers (See back cover).

The polyiodide salts of Fe^{2+} and Zn^{2+} , on the other hand, are tris-chelate cations trapped inside the anionic polyiodide networks (See back cover).

The complexes $[Ni(phen)_3](I_3)_2 \cdot CH_3CN$ and $[Cu(bpy)_3]I_8 \cdot CH_2Cl_2$ lie in between the above two categories. The uniform cation-anion interactions leads to a nullification of lattice dominance and neutral solvent molecules fill the empty interstices.

References

(1) A. F. Bertram and J. A. Ibers, *Inorg. Chem.* **1972,** //, 1109.

(2) X. -M. Chen, R. -Q. Wang, and Z. -T. Xu *Ada Crystallogr.* **1995,** *C51,* 820.

(3) O. P. Anderson *J. Chem. Soc, Dalton Trans.* **1972,** 2537.

(4) O. P. Anderson *J. Chem. Soc, Dalton Trans.* **1973**, 1237.

(5) S. Decurtins, H. W. Schmalle, P. Schneuwly, J. Ensling and P. Gutlich *J. Am. Chem. Soc.* **1994,** *116*, 9521.

(6) B. N. Figgis, B. W. Skelton and A. H. White ***Aust.*** *J. Chem.* **1978,** *31,* 57.

(7) L. L. Koh, Y. Xu, A. K. Hsieh, B. Song, F. Wu and L. Ji *Acta Crystallogr.* **1994,** *C50,* 884.

(8) D. Boys, C. Escobar and O. Wittke *Acta Crystallogr.* **1984,** *C40,* 1359.

(9) X. -M. Chen, R. -Q. Wang, and Z. -T. Xu, *Ada Crystallogr.* **1995,** *C51,* 1545.

(10) F. Bigoli, M. A. Pellinghelli, G. Crisponi, P. Deplano and E. F. Trogu *J. Chem. Soc, Dalton Trans.* **1985,** 1349.

(11) S. Menon and M. V. Rajasekharan *Inorg. Chem.* **1997,** *36,* 4983.

APPENDICES (A-N)

APPENDIX **A.** Crystallographic tables for $[Mn_2O_2(bpy)_4]Ce(NO_3)_6 \cdot 5H_2O$ (**1**).

Table A1.
Crystal data and structure refinement for $[Mn_2O_2(bpy)_4]Ce(NO_3)_6 \cdot 5H_2O$ (1).

Crystal Data :		
Systematic name	Tetrakis(2,2'-bipyridine)di-μoxo-dimanganese(III,IV)hexanitratocerate(III) pentahydrate	
Structural formula	$[Mn_2O_2(bpy)_4]Ce(NO_3)_6 \cdot 5H_2O$	
Empirical formula	$C_{40}H_{42}CeMn_2N_{14}O_{25}$	
Formula weight	1368.88	
Temperature	132(2) K	
Crystal system	monoclinic	
Space group	C2/c (No. 15)	
Unit cell dimensions	a = 12.940(3) Å	$\alpha = 90^o$
	b = 18.060(2) Å	$\beta = 96.29(2)^o$
	c = 22.544(11) Å	$\gamma = 90^o$
Volume	5237(3) $Å^3$	
Z	4	
Crystal shape	rectangular	
Crystal colour	black	
Density (measured)	1.74 Mg/m^3	
Density measurement method	floatation	
Density (calculated)	1.736 Mg/m^3	
Absorption coefficient	1.429 mm^{-1}	
F(000)	2752	
Crystal size	0.35 x 0.30 x 0.26 mm	
Data Collection :		
Diffractometer	Siemens P4	
Radiation type	Mo-Kα	
Wavelength	0.71073 Å	
Radiation source	fine focus sealed tube	
Monochromator	graphite	
Measurement method	ω-2θ	
Standard reflns.	3 measured every 100 reflections.	
θ range for data collection	2.07 to 27.50^o	
Index ranges	$-16 \le h \le 0$, $0 \le k \le 23$, $-28 \le l \le 29$	
Reflections collected	6034	
Independent reflections	6021 [R(int) = 0.0281]	
Mean intensity/sigma	29.07	
No. reflns.I > 2 σ(I)	4877	
+Absorption correction	semiempirical	
Max.& min. transmission	.327 and .257	
Solution and Refinement :		
Atom sites soln. - primary	direct/Patterson	
Atom sites soln. - secondary	difference fourier	

Atom sites some - hydrogens	geometrical
Treatment of hydrogen atoms	riding model
Refinement method	Full-matrix least-squares on F^2
Data / restraints / parameters	5645 / 12 / 409
Goodness-of-fit(S)[I >2σ(I)]	1.134
Goodness-of-fit(S)(all data)	1.224
Final R indices [I >2σ(I)]	R1 = 0.0358 wR2 = 0.0783
R indices (all data)	Rl = 0.0539 wR2 = 0.0947
Maximum shifVesd	-0.157 for HW3A
Mean shift/esd	0.006
Largest diff. peak and hole	0.925 and -0.589 e. A"^{3}

Computer Programs :

Data collection	Siemens 1990-4 system
Cell refinement	Siemens 1990-4 system
Data reduction	Siemens 1990-4 system
Structure solution	SHELXS-86
Structure refinement	SHELXL-93
Molecular graphics	ORTEP
Publication material	SHELXL-93

$R1 = \Sigma||F_o| - |F_c||/\Sigma|F_o|$

$wR2 - [\Sigma\{w(F_o^2 - F_c^2)^2\}/\Sigma(wF_o^4)]^{1/2}$

$w^{-1} = [\sigma^2(F^2) + (0.0342P)^2 + 13.2986P]$, $P = (F_o^2 + 2F_c^2)/3$

$S = [\Sigma\{w(F_o^2 - F_c^2)^2\}/(n-p)]^{1/2}$

Table A2.
Atomic coordinates (x 10^4) and equivalent isotropic displacement parameters (A^2 x 10^3) for 1. U(eq) is defined as one third of the trace of the orthogonalized Uij tensor.

	x	y	z	U(eq)
Mn	1021(1)	-3112(1)	2721(1)	19(1)
O(1)	0	-3779(1)	2500	24(1)
O(2)	0	-2449(1)	2500	23(1)
N(l)	1644(2)	-2955(1)	1899(1)	24(1)
N(2)	2151(2)	-3940(1)	2739(1)	22(1)
N(3)	2023(2)	-2329(1)	3159(1)	25(1)
N(4)	801(2)	-3264(1)	3637(1)	28(1)
C(l)	1366(2)	-2413(2)	1508(1)	29(1)
C(2)	1768(2)	-2361(2)	962(1)	34(1)
C(3)	2476(2)	-2889(2)	819(1)	37(1)
C(4)	2766(2)	-3455(2)	1223(1)	31(1)
C(5)	3286(2)	-4612(2)	2159(1)	33(1)
C(6)	3474(2)	-5126(2)	2613(1)	37(1)
C(7)	2997(2)	-5039(2)	3128(1)	33(1)
C(8)	2352(2)	-4442(2)	3178(1)	27(1)
C(9)	2615(2)	-4029(1)	2231(1)	23(1)
C(10)	2340(2)	-3470(1)	1765(1)	23(1)
C(11)	2668(2)	-1883(2)	2891(1)	32(1)

C(12)	3204(2)	-1306(2)	3185(1)	36(1)
0(13)	3070(2)	-1175(2)	3770(1)	34(1)
C(14)	2419(2)	-1634(2)	4056(1)	30(1)
C(15)	1064(2)	-2737(2)	4612(1)	34(1)
C(16)	441(2)	-3279(2)	4828(2)	41(1)
C(17)	18(2)	-3818(2)	4439(2)	39(1)
C(18)	210(2)	-3794(2)	3851(1)	34(1)
C(19)	1242(2)	-2745(1)	4015(1)	26(1)
C(20)	1917(2)	-2214(2)	3745(1)	25(1)
Ce	0	0	0	20(1)
N(5)	230(2)	734(1)	-1188(1)	24(1)
O(3)	136(1)	35(1)	-1142(1)	26(1)
0(4)	321(2)	1032(1)	-1670(1)	31(1)
0(5)	221(1)	1108(1)	-713(1)	26(1)
N(6)	-2367(2)	299(1)	-147(1)	29(1)
CX6)	-1968(1)	-9(1)	319(1)	33(1)
0(7)	-3317(2)	358(2)	-264(1)	51(1)
0(8)	-1763(1)	559(1)	-504(1)	31(1)
N(7)	548(2)	1438(1)	682(1)	31(1)
0(9)	-374(2)	1292(1)	479(1)	31(1)
0(10)	757(2)	1987(1)	1000(1)	53(1)
O(11)	1252(1)	1012(1)	539(1)	32(1)
OW1	0	-5288(1)	2500	43(1)
OW2	-493(2)	2640(1)	1917(1)	65(1)
OW3(.611)*	-4372(2)	877(2)	-1390(1)	57(1)
OW4(.389)*	-3942(2)	1105(2)	-1537(1)	69(3)

*The site occupation factors of disordered sites are given after the respective atom labels.

Table A3. Anisotropic displacement parameters (A^2 x 10^3) for 1. The anisotropic displacement factor exponent takes the form: -2 n^2 [h^2 a^{*2} U11 + ... + 2 h k a* b* U12]

	U11	U22	U33	U23	U13	UI2
Mn	18(1)	20(1)	19(1)	-1(1)	7(1)	0(1)
0(1)	24(1)	18(1)	29(1)	0	3(1)	0
0(2)	25(1)	18(1)	29(1)	0	12(1)	0
N(l)	27(1)	22(1)	23(1)	-2(1)	4(1)	3(1)
N(2)	18(1)	25(1)	23(1)	-2(1)	4(1)	0(1)
N(3)	18(1)	24(1)	32(1)	-1(1)	6(1)	-1(1)
N(4)	24(1)	22(1)	40(1)	-3(1)	12(1)	1(1)
C(l)	31(1)	23(1)	32(1)	0(1)	2(1)	0(1)
C(2)	39(2)	29(1)	34(2)	9(1)	4(1)	1(1)
C(3)	42(2)	42(2)	28(1)	7(1)	14(1)	4(1)
C(4)	30(1)	37(2)	28(1)	2(1)	12(1)	4(1)
C(5)	36(1)	38(2)	27(1)	1(1)	10(1)	14(1)
C(6)	35(1)	42(2)	34(1)	4(1)	5(1)	18(1)
C(7)	29(1)	39(1)	29(1)	6(1)	2(1)	8(1)
C(8)	24(1)	35(1)	23(1)	2(1)	4(1)	2(1)
C(9)	22(1)	27(1)	21(1)	-2(1)	5(1)	1(1)

C(10)	22(1)	24(1)	24(1)	-1(1)	3(1)	-KD
C(ll)	29(1)	31(1)	38(2)	-4(1)	11(1)	-5(1)
C(12)	31(1)	34(2)	45(2)	1(1)	9(1)	-10(1)
C(13)	27(1)	29(1)	44(2)	-6(1)	-1(1)	-6(1)
C(14)	25(1)	32(1)	32(1)	-6(1)	4(1)	3d)
C(15)	31(1)	39(2)	34(2)	3d)	7(1)	7(1)
C(16)	34(2)	48(2)	43(2)	13(1)	13(1)	7(1)
C(17)	32(1)	35(2)	52(2)	16(1)	16(1)	1(1)
C(18)	26(1)	27(1)	51(2)	0(1)	12(1)	-1(1)
C(19)	20(1)	25(1)	34(1)	1(1)	6(1)	5(1)
C(20)	17(1)	27(1)	30(1)	-3(1)	5(1)	3(1)
Ce	21(1)	20(1)	21(1)	0(1)	8(1)	KD
N(5)	22(1)	26(1)	24(1)	2(1)	6(1)	0(1)
O(3)	33(1)	23(1)	25(1)	-2(1)	8(1)	-1(1)
O(4)	34(1)	35(1)	24(1)	6(1)	7(1)	-3(1)
O(5)	33(1)	24(1)	23(1)	-1(1)	10(1)	-1(1)
N(6)	26(1)	33(1)	29(1)	-6(1)	6(1)	3(1)
O(6)	32(1)	39(1)	29(1)	2(1)	12(1)	2(1)
O(7)	23(1)	71(2)	59(2)	-4(1)	7(1)	6(1)
O(8)	29(1)	34(1)	32(1)	4(1)	9(1)	5(1)
N(7)	37(1)	28(1)	31(1)	-2(1)	12(1)	-6(1)
0(9)	32(1)	28(1)	35(1)	-3(1)	14(1)	2(1)
0(10)	66(2)	41(1)	56(1)	-26(1)	22(1)	-16(1)
0(11)	29(1)	35(1)	34(1)	-4(1)	9(1)	-2(1)
OW1	49(2)	25(1)	55(2)	0	0(2)	0
0W2	58(2)	79(2)	60(2)	-30(1)	19(1)	-16(1)
OW3	52(3)	64(3)	52(3)	0(2)	-7(2)	9(2)
OW4	76(5)	64(5)	61(5)	-21(4)	-22(4)	18(4)

Table A4. Hydrogen coordinates (x 10^4) and isotropic displacement parameters ($Å^2$ x 10^{-3}) for 1.

	x	y	z	U(eq)
H(1)	880(2)	-2052(2)	1607(1)	43
H(2)	1561(2)	-1971(2)	692(1)	51
H(3)	2761(2)	-2865(2)	449(1)	55
H(4)	3246(2)	-3824(2)	1131(1)	46
H(5)	3612(2)	-4658(2)	1804(1)	50
H(6)	3924(2)	-5534(2)	2572(1)	55
H(7)	3113(2)	-5388(2)	3443(1)	49
H(8)	2036(2)	-4382(2)	3536(1)	41
H(ll)	2757(2)	-1969(2)	2484(1)	48
H(12)	3658(2)	-1005(2)	2985(1)	54
H(13)	3418(2)	-773(2)	3979(1)	51
H(14)	2320(2)	-1550(2)	4462(1)	44
H(15)	1368(2)	-2362(2)	4871(1)	52
H(16)	309(2)	-3278(2)	5234(2)	61
H(17)	-400(2)	-4201(2)	4576(2)	58

H(18)	-84(2)	-4165(2)	3586(1)	51
HW1A	0	-4751(1)	2500	145(32)
HW1B	317(5)	-5428(2)	2894(1)	49(20)
HW2A	73(3)	2598(5)	2234(1)	237(40)
HW2B	-247(5)	2394(5)	1577(2)	125(20)
HW3A	-3956(6)	1252(3)	-1167(2)	85
HW3B	-4166(7)	899(5)	-1791(2)	85
HW4A	-4479(3)	1469(2)	-1491(3)	104
HW4B	-3888(9)	815(4)	-1172(2)	104

Hydrogen atoms are labelled according to the atom to which they are attached. AU hydrogens except HW1A, HW1B, HW2A, HW2B, HW3A, HW3B, HW4A and HW4B were refined using the riding model (the positional parameters of the riding atoms have same e.s.ds as the atom on which they ride). Bond length constraints were applied to HW1A, HW1B, HW2A, HW2B, HW3A, HW3B, HW4A and HW4B (0.97 A) All hydrogens except HWl A, HW1B, HW2A and HW2B were assigned fixed U(iso) values (= 1.5 x U(iso) of the atom to which they are attached.)

APPENDIX B.Crystallographic tables for $[Mn_2O(OA$

Table **B1.**
Crystal data and structure refinement for $[Mn_2O(OAc)_2(bpy)_2(H_2O)_2](NO_3)_2 \cdot 5H_2O$ (3).

Crystal Data :		
Structural formula	$[Mn_2O(OAc)_2(bpy)_2(H_2O)_2](NO_3)_2 \cdot 5H_2O$	
Empirical formula	$C_{24}H_{36}Mn_2N_6O_{18}$	
Formula weight	806.47	
Temperature	293(2) K	
Crystal system	Monoclinic	
Space group	$P\ 2_1/n$ (No.14)	
Unit cell dimensions	a =18.252(4) A	a = 90 deg.
	b = 9.968(3) A	β = 99.33(1) deg.
	c = 19.157(3) A	γ = 90 deg.
Volume	3439(1) A^3	
Z	4	
No. reflns. used for cell	25	
Cell measurement theta min/max	5.5/12.28	
Crystal shape	Rectangular	
Crystal colour	Brown	
Density (calculated)	1.557 Mg/m^3	
Absorption coefficient	0.819 mm^{-1}	
F(000)	1664	
Crystal size	.45 x .23 x .20 mm	
Data Collection :		
Diffractometer	Enraf Nonius CAD-4	
Radiation type	MoK_α	
Wavelength	0.71073 A	
Radiation source	Fine focus sealed tube	
Monochromator	Graphite	
Measurement method	Omega-2theta	
Standard reflns.	2 measured every 90 min	
Theta range for data collection	1.68 to 24.99 deg.	
Index ranges	$0 \le h \le 21$, $-4 \le k \le 11$, $-22 \le l \le 22$	
Reflections collected	6306	
Independent reflections	6039 [R(int) = 0.0172]	
Mean intensity/sigma	11.51	
No. reflns. [F > 4 sigma(F)]	3014	
Absorption correction	None	
Solution and Refinement :		
Atom sites soln. - primary	Patterson	
Atom sites soln. - secondary	Difference fourier	
Atom sites soln. - hydrogens	Geometrical	
Treatment of hydrogen atoms	Riding model	
Refinement method	Full-matrix least-squares on F^2	
Data / restraints / parameters	6039/21/503	

Goodness-of-fit (S) [F>4sigma(F)]	0.951
Goodness-of-fit (S) (all data)	0.949
Final R indices [F>4sigma(F)]	R1 = 0.0569 wR2 = 0.1358
R indices (all data)	Rl =0.1460 wR2 = 0.1609
Maximum shift/esd 0.315 for H W6A	
Mean shift/esd	0.014
Largest difl peak and hole	0.476 and -351 e.Å^{-3}

Computer Programs :

Data collection	CAD-4 system
Cell refinement	CAD-4 system
Data reduction	CAD-4 system
Structure solution	SHELXS-97
Structure refinement	SHELXL-97
Molecular graphics	ORTEP
Publication material	SHELXL-97

$R1 = \Sigma||F_o| - |F_c||/\Sigma|F_o|$

$wR_2 = [\Sigma\{w(F_o^2 - F_c^2)^2\}/\Sigma(wF_o^4)]^{1/2}$

$w^{-1} = [\sigma^2(F_o^2) + (0.0847P)^2 + 0.000P]$, $P = (F_o^2 + 2F_c^2)/3$

$S = [\Sigma\{w(F_o^2 - F_c^2)^2\}/(n-p)]^{1/2}$

Table B2. Atomic coordinates (x 10^4) and equivalent isotropic displacement parameters (Å^2 x 10^3) for 3. U(eq) is defined as one third of the trace of the orthogonalized Uij tensor.

	x	y	z	U(eq)
Mn(l)	5695(1)	2273(1)	3321(1)	39(1)
Mn(2)	5145(1)	2803(1)	1708(1)	44(1)
O(1)	5465(2)	3373(3)	2587(1)	46(1)
N(l)	5895(2)	1251(3)	4274(2)	42(1)
N(2)	4986(2)	3222(4)	3905(2)	50(1)
N(3)	5848(2)	4077(4)	1287(2)	48(1)
N(4)	4899(2)	2343(4)	640(2)	46(1)
C(l)	6387(2)	259(4)	4417(2)	53(1)
C(2)	6533(3)	-343(5)	5072(2)	68(2)
C(3)	6167(3)	109(6)	5586(3)	76(2)
C(4)	5666(3)	1124(6)	5455(2)	67(2)
C(5)	4525(3)	3303(5)	4995(3)	65(1)
C(6)	4041(3)	4263(6)	4728(3)	78(2)
C(7)	4017(3)	4720(6)	4061(3)	83(2)
C(8)	4499(3)	4163(5)	3643(3)	68(2)
C(9)	5000(2)	2770(5)	4575(2)	49(1)
C(10)	5527(2)	1704(5)	4785(2)	47(1)
C(ll)	6291(3)	4986(5)	1652(2)	57(1)
C(12)	6725(2)	5848(5)	1337(3)	64(2)
C(13)	6700(3)	5782(5)	625(3)	70(2)
C(14)	6256(2)	4849(5)	235(2)	64(2)
C(15)	5245(2)	2683(5)	-495(2)	62(1)
C(16)	4731(3)	1716(6)	-771(2)	71(2)

C(17)	4306(3)	1078(5)	-341(2)	69(2)
C(18)	4397(3)	1437(5)	360(2)	58(1)
C(19)	5309(2)	2975(4)	217(2)	47(1)
C(20)	5825(2)	3994(5)	576(2)	47(1)
0(2)	4777(2)	856(3)	2982(1)	52(1)
0(3)	4362(2)	1610(3)	1898(1)	54(1)
0(4)	5911(2)	1141(3)	1771(1)	58(1)
0(5)	6356(2)	1072(3)	2922(1)	53(1)
C(21)	4313(2)	865(4)	2425(2)	45(1)
C(22)	3650(3)	-21(5)	2354(2)	68(2)
C(23)	6343(2)	674(5)	2289(2)	50(1)
C(24)	6871(3)	-440(6)	2186(3)	87(2)
OW1	4279(1)	4407(2)	1496(1)	62(1)
OW2	6635(2)	3524(2)	3795(1)	64(1)
N(5)	2629(3)	3106(5)	1825(3)	96(2)
0(6)	2817(2)	3551(6)	1268(2)	126(2)
O(7A) (0.50)	2948(7)	3758(16)	2327(8)	165(6)
O(7B) (0.50)	2922(5)	3355(11)	2452(5)	78(3)
O(8)	2122(3)	2254(5)	1786(3)	130(2)
N(6)	7046(4)	6825(6)	3762(3)	133(3)
O(9)	6537(4)	6334(7)	3343(3)	185(3)
0(10)	7555(4)	6162(8)	4136(3)	208(3)
O(11)	7184(6)	7887(6)	3844(5)	279(5)
OW3	2641(2)	7036(4)	1444(1)	165(2)
OW4	7382(2)	3406(2)	5164(1)	90(1)
OW5	8036(2)	5983(3)	5500(1)	130(2)
OW6	5383(3)	7929(2)	3170(1)	158(2)
OW7	4249(1)	6570(2)	2310(2)	194(3)

* The site occupation factors of disordered sites are given after the respective atom 'abels

Table B3. Anisotropic displacement parameters (A^2 - 10^3) for 3

	U11	U22	U33	U23	U13	U12
Mn(l)	44(1)	43(1)	30(1)	2(1)	4(1)	KD
Mn(2)	48(1)	50(1)	30(1)	5(1)	-1(1)	-6(1)
O(1)	57(2)	46(2)	33(1)	2(1)	1(1)	-4(2)
N(l)	40(2)	45(2)	38(2)	5(2)	1(2)	-7(2)
N(2)	46(2)	52(2)	50(2)	-4(2)	0(2)	3(2)
N(3)	48(2)	59(2)	37(2)	6(2)	2(2)	0(2)
N(4)	45(2)	55(2)	36(2)	4(2)	-2(2)	-1(2)
C(l)	54(3)	50(3)	51(3)	8(2)	0(2)	-5(2)
C(2)	73(3)	64(3)	60(3)	20(3)	-11(3)	-4(3)
C(3)	82(4)	90(4)	51(3)	29(3)	-7(3)	-19(3)
C(4)	73(3)	94(4)	37(2)	8(3)	13(2)	-25(3)
C(5)	66(3)	73(3)	59(3)	-9(3)	20(2)	-10(3)
C(6)	71(3)	95(4)	73(3)	-26(3)	30(3)	-5(3)
C(7)	62(3)	89(4)	98(4)	-25(4)	10(3)	20(3)

C(8)	69(3)	74(4)	59(3)	-9(3)	1(3)	9(3)
C(9)	46(2)	62(3)	40(2)	-6(2)	13(2)	-16(2)
C(10)	42(2)	58(3)	38(2)	4(2)	0(2)	-17(2)
C(ll)	57(3)	59(3)	51(3)	8(2)	-6(2)	-12(3)
C(12)	47(3)	54(3)	84(3)	24(3)	-9(2)	-7(2)
C(13)	46(3)	87(4)	77(3)	36(3)	6(2)	-6(3)
C(14)	48(3)	84(4)	58(3)	31(3)	5(2)	3(3)
C(15)	53(3)	89(4)	42(2)	12(3)	5(2)	13(3)
C(16)	76(3)	93(4)	41(3)	-9(3)	-3(2)	16(3)
C(17)	73(3)	75(4)	52(3)	-10(3)	-14(3)	2(3)
C(18)	56(3)	65(3)	47(3)	-2(2)	-7(2)	-6(3)
C(19)	47(2)	57(3)	34(2)	11(2)	0(2)	11(2)
C(20)	40(2)	57(3)	44(2)	13(2)	0(2)	3(2)
0(2)	55(2)	52(2)	46(2)	5(1)	-2(1)	-11(2)
0(3)	50(2)	63(2)	45(2)	7(2)	1(1)	-14(2)
0(4)	65(2)	68(2)	37(2)	-8(2)	-KD	15(2)
0(5)	54(2)	66(2)	36(2)	-5(1)	1(1)	16(2)
C(21)	42(2)	44(3)	46(2)	-7(2)	3(2)	-1(2)
C(22)	65(3).	69(3)	66(3)	8(3)	-1(3)	-24(3)
C(23)	38(2)	59(3)	51(3)	-6(2)	5(2)	-3(2)
C(24)	74(3)	110(4)	68(3)	-35(3)	-13(3)	42(3)
O'W1	65(2)	64(2)	54(2)	8(2)	-2(2)	10(2)
OW2	68(2)	66(2)	52(2)	1(2)	-5(2)	-23(2)
N(5)	52(3)	99(4)	130(4)	-16(4)	-9(3)	25(3)
0(6)	77(3)	178(5)	111(4)	23(3)	-20(3)	-4(3)
0(7A)	138(10)	191(13)	180(11)	-72(10)	68(8)	-14(9)
O(7B)	48(5)	107(7)	73(5)	-23(5)	-9(4)	-12(5)
O(8)	104(3)	104(3)	170(5)	-26(3)	-9(3)	-8(3)
N(6)	203(7)	79(4)	112(5)	13(3)	11(5)	49(4)
O(9)	188(6)	168(6)	176(6)	-26(5)	-37(5)	-24(5)
0(10)	249(8)	214(7)	155(6)	-11(5)	16(5)	39(6)
0(11)	407(13)	80(4)	332(11)	-24(6)	4(9)	25(7)
OW3	188(5)	161(5)	153(5)	-41(4)	48(4)	-40(5)
OW4	87(3)	114(3)	65(2)	-15(2)	-2(2)	11(2)
0W5	129(4)	125(4)	134(4)	-11(3)	12(3)	17(3)
OW6	198(5)	119(4)	165(5)	-24(4)	52(4)	-25(4)
OW7	279(7)	78(3)	193(6)	-45(4)	-58(5)	36(4)

The anisotropic displacement factor exponent takes the form:
$-2\pi\ [h\ a^*\ U11 + \ldots + 2hka^*b^*U12]$

Table B4. Hydrogen coordinates (× 10) and isotropic displacement parameters (A × 10) for 3

	x	y	z	U(eq)
H(l)	6641	-35	4062	79
H(2)	6873	-1041	5158	102
H(3)	6260	-278	6033	114
H(4)	5417	1429	5811	101
H(5)	4540	3003	5456	97

H(6)	3718	4618	5008	117
H(7)	3686	5393	3883	125
H(8)	4479	4451	3178	102
H(ll)	6305	5038	2139	86
H(12)	7031	6466	1606	96
H(13)	6984	6369	401	105
H(14)	6244	4788	-251	96
H(15)	5537	3120	-780	93
H(16)	4675	1497	-1248	107
H(17)	3965	421	-520	104
H(18)	4099	1035	651	86
H(22A)	3673	-667	1986	102
H(22B)	3209	511	2236	102
H(22C)	3639	-478	2793	102
H(24A)	7116	-751	2638	130
H(24B)	7234	-114	1917	130
H(24C)	6601	-1167	1936	130
HW1A	4338(2)	4982(4)	1909(2)	111(5)
HW1B	3788(2)	4019(6)	1467(4)	111(5)
HW2A	6933(4)	3457(4)	4261(2)	111(5)
HW2B	6673(8)	4455(3)	3658(3)	111(5)
HW3A	2900(2)	6697(6)	1891(2)	111(5)
HW3B	2239(2)	7577(7)	1566(4)	111(5)
HW4A	7662(2)	3893(6)	4857(2)	111(5)
HW4B	7287(4)	4054(5)	5516(3)	111(5)
HW5A	7947(5)	6375(7)	5031(1)	111(5)
HW5B	7872(5)	6656(7)	5807(2)	111(5)
HW6A	5265(4)	8788(4)	3362(2)	111(5)
HW6B	5431(6)	8111(7)	2682(2)	111(5)
HW7A	4644(1)	7051(6)	2136(3)	111(5)
HW7B	4004(3)	7233(6)	2562(4)	111(5)

Hydrogen atoms are labelled according to the atom to which they are attached. All hydrogens except HW1A, HW1B, HW2A, HW2B, HW3A, HW3B, HW4A, HW4B, HW5A, HW5B, HW6A, HW6B, HW7A and HW7B, were refined using the riding model (the positional parameters of the riding atoms have same e.s.ds as the atom on which they ride). Bond length constraints (0.97 A) were applied to all the water hydrogens. All hydrogens except HW1A, HW1B, HW2A, HW2B, HW3A, HW3B, HW4A, HW4B, HW5A, HW5B, HW6A, HW6B, HW7A and HW7B (these were fixed to a common U(iso) value), were fixed to U(iso) values (=1 2xU(iso) of the atom to which they are attached).

APPENDIX C. Table C1. Selected crystallographic data for $[Mn_3O_4(phen)_4(H_2O)_2](ClO_4)(NO_3)_3 \cdot 2(CH_3OH) \cdot 2(H_2O)$ (4)

Table C1. Crystal data and structure refinement for $[Mn_3O_4(phen)_4(H_2O)_2](ClO_4)(NO_3)_3 \cdot 2(CH_3OH) \cdot 2(H_2O)$ (4)

Crystal Data :	
Structural formula	$[Mn_3O_4(phen)_4(H_2O)_2](ClO_4)(NO_3)_3 \cdot 2(CH_3OH) \cdot 2(H_2O)$
Empirical formula	$C_{50}H_{32}Cl_1Mn_3N_{11}O_{23}$
Formula weight	1355.14
Temperature	293(2) K
Crystal system	Triclinic
Space group	$P\bar{1}$ (NO. 2)
Unit cell dimensions	a = 12.708(5) Act = 108.673(16) deg.
	b = 13.4919(12) A β = 99.24(2) deg.
	c = 17.716(4) A γ = 91.610(18) deg.
Volume	2830.0(12) A^3
Z	2
No. reflns. used for cell	22
Cell measurement theta mm max	5.24/14.10
Crystal shape	Plate
Crystal colour	Dark-brown
Density (calculated)	1.590 Mg/m^3
Absorption coefficient	0.798 mm^{-1}
F(000)	1370
Crystal size	0.38 x 0.25 x 0.03 mm
Data Collection :	
Diffractometer	Enraf Nonius CAD-4
Radiation type	MoK_α
Wavelength	0.71073 A
Radiation source	fine focus sealed tube
Monochromator	graphite
Measurement method	omega-2theta
Standard reflns.	2 measured every 60 min.
Theta range for data collection	2.18 to 24.98 deg.
Index ranges	$0 \le h \le 13$, $-16 \le k \le 16$, $-20 \le l \le 20$
Reflections collected	8485 [R(int) = 0.0588]
Independent reflections	7996
Mean intensity/sigma	10.44
No. reflns., I > 2 sigma(I)	4204
Absorption correction	Semiempirical
Max. and min transmission	0.999 and 0.898
Solution and Refinement :	
Atom sites soln. - primary	Patterson
Atom sites soln. - secondary	difference fourier

Atom sites soln. - hydrogens	geometrical
Treatment of hydrogen atoms	riding model
Refinement method	Full-matrix least-squares on F^2
Data / restraints / parameters	79% / 0 / 703
Goodness-of-fit (S) [I>2sigma(I)]	1.097
Goodness-of-fit (S) (all data)	1.097
Final R indices [I>2sigma(I)]	R1 = 0.1067, wR2 = 0.2775
R indices (all data)	R1 = 0.1928, wR2 = 0.3308
Maximum shift/esd	-0.185 for y N11
Mean shift/esd	0.005
Largest diff. peak and hole	1.164 and -0.742 e. A"^{3}

Computer Programs :

Data collection	CAD-4 system
Cell refinement	CAD-4 system
Data reduction	CAD-4 system
Structure solution	SHELXS-86
Structure refinement	SHELXL-93
Molecular graphics	ORTEP
Publication material	SHELXL-93

$R1 = \Sigma||F_o| - |F_c||/\Sigma|F_o|$

$wR2 = [\Sigma\{w(F_o^2 - F_c^2)^2\}/\Sigma(wF_o^4)]^{1/2}$

$w^{-1} = [\sigma^2(F_o^2) + (0.1648P)^2 + 13.700P]$, $P = (F_o^2 + 2F_c^2)/3$

$S = [\Sigma\{w(F_o^2 - F_c^2)^2\}/(n-p)]^{1/2}$

Table C2. Selected bond lengths [A] and angles [deg] for 4.

Bond distances:

Mn(1)-O(2)	1.798(6)
Mn(1)-O(1)	1.813(6)
Mn(1)-O(4)	1.822(5)
Mn(1)-O(5)	2.016(6)
Mn(1)-N(1)	2.050(7)
Mn(1)-N(2)	2.076(7)
Mn(1)-Mn(2)	2.670(2)
Mn(1)-Mn(3)	3.234(2)
Mn(2)-O(2)	1.785(6)
Mn(2)-O(1)	1.807(6)
Mn(2)-O(3)	1.817(6)
Mn(2)-O(6)	2.010(6)
Mn(2)-N(3)	2.069(7)
Mn(2)-N(4)	2.076(7)
Mn(3)-O(4)	1.759(5)
Mn(3)-O(3)	1.769(6)
Mn(3)-N(8)	2.006(7)
Mn(3)-N(5)	2.029(8)
Mn(3)-N(7)	2.083(7)
Mn(3)-N(6)	2.104(7)

Bond angles:

O(1)-Mn(1)-O(5)	175.0(2)
N(1)-Mn(1)-N(2)	79.1(3)
O(2)-Mn(2)-O(6)	174.2(3)
N(3)-Mn(2)-N(4)	78.3(3)
O(4)-Mn(3)-O(3)	99.7(3)
N(5)-Mn(3)-N(7)	93.3(3)
N(5)-Mn(3)-N(6)	80.0(3)
Mn(2)-O(1)-Mn(1)	95.0(3)
Mn(2)-O(2)-Mn(1)	96.4(3)
Mn(3)-O(3)-Mn(2)	129.9(3)
Mn(3)-O(4)-Mn(1)	129.1(3)

APPENDIX D. Crystallographic tables for $[Mn(phen)_3](I_3)_2$ (1).

Table D1.
Crystal data and structure refinement for $[Mn(phen)_3](I_3)_2$ (1).

Crystal Data :			
Systematic name	Tris(phenanthroline)manganese(II)triiodide		
Structural formula	$[Mn(phen)_3](I_3)_2$		
Empirical formula	$C_{12}H_8I_2Mn_{0.33}N_2$		
Formula weight	452.32		
Melting point	555 K		
Temperature	293(2) K		
Crystal system	Hexagonal		
Space group	R 3 (No. 148)		
Unit cell dimensions	a = 16.456(2) A	b = 16.456(3) A	c = 25.864(4) A
	a = 90 deg.	β = 90 deg.	γ = 120 deg.
Volume	6066(2) A^3		
Z	18		
No. reflns. used for cell measurement	25		
Cell measurement theta min/max	6.3/11.6		
Crystal shape	Triangular prismatic		
Crystal colour	dark brown		
Density (measured)	2.37 Mg/m^3		
Density measurement method	Floatation		
Density (calculated)	2.229 Mg/m^3		
Absorption coefficient	4.941 mm^{-1}		
F(000)	3750		
Crystal size	76x .38 x .22 mm		

Data Collection :	
Diffractometer	Enraf Nonius CAD-4
Radiation type	MoK_α
Wavelength	0.71073 A
Radiation source	Fine focus sealed tube
Monochromator	Graphite
Measurement method	omega-2theta
Standard reflns.	2 measured every 60 min.
Theta range for data collectio	2.13 to 24.99 deg.
Index ranges	$-19 \le h \le 16$; $0 \le k \le 19$; $0 \le l \le 30$
Reflections collected	3790
Independent reflections	2384 [R(int) = 0.0282]
Mean intensity/sigma	36.63
No. reflns. $[F_o>4\sigma(F_o)]$	1981
Absorption correction	Semiempirical
Max. and min. transmission	0.973 and 0.702

Solution and Refinement :

Atom sites soln. - primary	Patterson	
Atom sites soln. - secondary	Difference fourier	
Atom sites soln. - hydrogens	Geometrical	
Treatment of hydrogen atoms	Riding model	
Refinement method	Full-matrix least-squares on F^2	
Data / restraints / parameters	2384/0/151	
Goodness-of-fit (S) $[F_o>4\sigma(F_o)]$	1.123	
Goodness-of-fit (S) (all data)	1.163	
Final R indices $[F_o>4\sigma(F_o)]$	R1 = 0.0365	wR2 = 0.0782
R indices (all data)	Rl = 0.0478	wR2 = 0.0833
Maximum shift/esd	0.004	
Mean shift/esd	0.000	

Largest diff. peak and hole 1.663 and -0.934 e. $Å^{-3}$

Computer Programs :

Data collection	CAD-4 system
Cell refinement	CAD-4 system
Data reduction	CAD-4 system
Structure solution	SHELXS-86
Structure refinement	SHELXL-93
Molecular graphics	ORTEP
Publication material	SHELXL-93

$Rl = \Sigma||F_o| - |F_c||/\Sigma|F_o|$

$wR_2 = [\Sigma\{w(F_o^2 - F_c^2)^2\}/\Sigma(wF_o^4)]^{1/2}$

$w^{-1} = [\sigma^2(F_o^2) + (0.0248P)^2 + 50.8570P], P = (F_o^2 + 2F_c^2)/3$

$S = [\Sigma\{w(F_o^2 - F_c^2)^2\}/(n-p)]^{1/2}$

Table D2.

Atomic coordinates (× 10) and equivalent isotropic displacement parameters (A × 10) for 1

	x	y	z	U(eq)
1(1)	-56(1)	3914(1)	902(1)	78(1)
I(2)	0	5000	0	54(1)
I(3)	0	0	0	46(1)
I(4)	0	0	1093(1)	195(1)
Mn(l)	6667	3333	122(1)	38(1)
N(1)	7688(3)	4593(3)	586(2)	49(1)
N(2)	6997(3)	4608(3)	-362(2)	47(1)
C(l)	8015(4)	4583(5)	1051(2)	64(2)
C(2)	8591(5)	5413(6)	1327(3)	86(2)
C(3)	8853(5)	6247(6)	1106(4)	85(2)
C(4)	8551(4)	6292(5)	610(3)	71(2)
C(5)	8812(5)	7148(5)	334(5)	95(3)
C(6)	8535(6)	7150(5)	-142(5)	96(3)
C(7)	7909(5)	6293(5)	-407(3)	74(2)

C(8)	7568(6)	6249(6)	-903(4)	88(3)
C(9)	6947(6)	5427(6)	-1114(3)	78(2)
C(10)	6662(5)	4611(5)	-828(2)	62(2)
C(11)	7610(4)	5439(4)	-146(2)	51(1)
C(12)	7952(4)	5440(4)	362(2)	52(1)

*The site occupation factors of disordered sites are given after the respective atom labels.
U(eq) is defined as one third of the trace of the orthogonalized U,j tensor.

Table D3.
Anisotropic displacement parameters (A × 10˘) for 1.

	U_{11}	U_{22}	U_{33}	U_{23}	U_{13}	U_{12}
I(1)	77(1)	86(1)	67(1)	2(1)	-12(1)	37(1)
I(2)	39(1)	65(1)	51(1)	-12(1)	-5(1)	21(1)
I(3)	43(1)	43(1)	53(1)	0	0	21(1)
I(4)	271(1)	271(1)	43(1)	0	0	136(1)
Mn(l)	37(1)	37(1)	41(1)	0	0	19(1)
N(l)	40(2)	49(3)	56(3)	-9(2)	-1(2)	21(2)
N(2)	48(3)	48(3)	55(3)	5(2)	7(2)	31(2)
C(l)	53(4)	66(4)	63(4)	-11(3)	-5(3)	21(3)
C(2)	63(4)	97(6)	78(5)	-33(5)	-19(4)	25(4)
C(3)	54(4)	65(5)	119(7)	•45(5)	-14(4)	18(4)
C(4)	39(3)	56(4)	114(6)	-25(4)	-5(4)	20(3)
C(5)	56(4)	34(4)	173(10)	-13(5)	5(5)	7(3)
C(6)	71(5)	43(4)	168(10)	20(5)	6(6)	24(4)
C(7)	56(4)	45(4)	124(7)	22(4)	21(4)	28(3)
C(8)	91(6)	77(5)	110(6)	54(5)	31(5)	53(5)
C(9)	89(5)	84(5)	78(5)	30(4)	16(4)	56(5)
C(10)	64(4)	71(4)	62(4)	18(3)	12(3)	42(4)
C(11)	43(3)	41(3)	76(4)	8(3)	14(3)	25(3)
C(12)	35(3)	41(3)	78(4)	-8(3)	6(3)	18(2)

The anisotropic displacement factor exponent takes the form:
$-2\pi^2$ [h $a^{*2}U11$ + ... + 2hka*b*U12]

Table D4.
Bond lengths (A) and angles (°) for 1.

I(1)-I(2)	2.9116(6)	I(2)-I(1)#1	2.9116(6)
I(3)-I(4)	2.8280(12)	I(3)-I(4)#2	2.8280(12)
Mn(1)-N(1)#3	2.254(5)		2.254(5)
Mn(1)-N(1)#4	2.254(5)	Mn(1)-N(2)#3	2.263(4)
Mn(1)-N(2)#4	2.263(4)	Mn(1)-N(2)	2.263(4)
N(1)-C(1)	1.321(8)	N(1)-C(12)	1.364(7)
N(2)-C(10)	1.326(7)	N(2)-C(11)	1.349(7)
C(1)-C(2)	1.407(9)	C(2)-C(3)	1.344(12)
C(3)-C(4)	1.391(11)	C(4)-C(12)	1.403(8)

C(4)-C(5)	1.438(11)	C(5)-C(6)	1.315(13)
C(6)-C(7)	1.438(12)	C(7)-C(8)	1.388(12)
C(7)-C(11)	1.409(8)	C(8)-C(9)	1.337(11)
C(9)-C(10)	1.392(9)	C(11)-C(12)	1.428(9)

I(1)-I(2)-I(1)#1	180.0	I(4)-I(3)-I(4)#2	180.0
N(1)#3-Mn(1)-N(1)	94.3(2)	N(1)#3-Mn(1)-N(1)#4	94.3(2)
N(l)-Mn(l)-N(l)#4	94.3(2)	N(1)#3-Mn(1)-N(2)#3	73.7(2)
N(1)-Mn(1)-N(2)#3	103.3(2)	N(1)#4-Mn(1)-N(2)#3	159.3(2)
N(1)#3-Mn(1)-N(2)#4	103.3(2)	N(1)-Mn(1)-N(2)#4	159.3(2)
N(1)#4-Mn(1)-N(2)#4	73.7(2)	N(2)#3-Mn(1)-N(2)#4	92.4(2)
N(1)#3-Mn(1)-N(2)	159.3(2)	N(1)-Mn(1)-N(2)	73.7(2)
N(1)#4-Mn(1)-N(2)	103.3(2)	N(2)#3-Mn(1)-N(2)	92.4(2)
N(2)#4-Mn(1)-N(2)	92.4(2)	C(1)-N(1)-C(12)	118.4(5)
C(1)-N(1)-Mn(1)	126.5(4)	C(12)-N(1)-Mn(1)	115.0(4)
C(10)-N(2)-C(11)	118.4(5)	C(10)-N(2)-Mn(1)	126.7(4)
C(11)-N(2)-Mn(1)	114.9(4)	N(1)-C(1)-C(2)	122.0(7)
C(3)-C(2)-C(1)	119.5(8)	C(2)-C(3)-C(4)	120.4(7)
C(3)-C(4)-C(12)	117.3(7)	C(3)-C(4)-C(5)	124.7(7)
C(12)-C(4)-C(5)	117.9(8)	C(6)-C(5)-C(4)	122.2(8)
C(5)-C(6)-C(7)	121.5(8)	C(8)-C(7)-C(11)	117.5(7)
C(8)-C(7)-C(6)	124.4(7)	C(11)-C(7)-C(6)	118.2(8)
C(9)-C(8)-C(7)	120.9(7)	C(8)-C(9)-C(10)	118.6(7)
N(2)-C(10)-C(9)	123.0(7)	N(2)-C(11)-C(7)	121.5(6)
N(2)-C(11)-C(12)	118.5(5)	C(7)-C(11)-C(12)	119.9(6)
N(1)-C(12)-C(4)	122.2(6)	N(1)-C(12)-C(11)	117.7(5)
C(4)-C(12)-C(11)	120.1(6)		

Symmetry transformations used to generate equivalent atoms:
#1 = -x, -y+1, -z; #2 = -x, -y, -z; #3 = -x+y+1, -x+1, z; #4 = -y+1, x-y, z

Table D5.
Hydrogen coordinates (× 10) and isotropic displacement parameters (A × 10) for 1.

	x	y	z	U(eq)
H(l)	7861(4)	4009(5)	1200(2)	90(8)
H(2)	8787(5)	5384(6)	1660(3)	90(8)
H(3)	9240(5)	6798(6)	1285(4)	90(8)
H(5)	9189(5)	7718(5)	499(5)	90(8)
H(6)	8749(6)	7720(5)	-312(5)	90(8)
H(8)	7774(6)	6799(6)	-1092(4)	90(8)
H(9)	6711(6)	5401(6)	-1444(3)	90(8)
H(10)	6216(5)	4042(5)	-971(2)	90(8)

Hydrogen atoms are labelled according to the atom to which they are attached. All hydrogens were refined using the riding model (the positional parameters of me riding atoms have same e.s ds as the atom on which they ride) All hydrogens were refined with a common U(iso) value (= 0.086 A^2).

APPENDIX E. Crystallographic tables and figures for $[Mn(bpy)_3](I_3)_{1.5}(I_8)_{0.25}$ (2).

Table E1.
Crystal data and structure refinement for $[Mn(bpy)_3](I_3)_{1.5}(I_8)_{0.25}$ (2).

Crystal Data :

Structural formula	$[Mn(bpy)_3](I_3)_{1.5}(I_8)_{0.25}$		
Empirical formula	$C_{30}H_{24}I_{6.50}MnN_6$		
Formula weight	1348.34		
Melting point	473 K		
Temperature	213 K		
Crystal system	Monoclinic		
Space group	C2/c(No.15)		
Unit cell dimensions	a = 29.3213(11) A	b= 12.9177(4) A	c = 23.2863(4) A
	α = 90 deg.	β = 120.950(2) deg.	γ = 90 deg.
Volume	7564.2(5) A^3		
Z	8		
No. reflns. used for cell measurement	23		
Crystal shape	Rectangular prism		
Crystal colour	Dark brown		
Density (measured)	2.43 Mg/m^3		
Density measurement method	Floatation		
Density (calculated)	2.368 Mg/m^3		
Absorption coefficient	5.684 mm^{-1}		
F(000)	4924		
Crystal size	.12 x .14 x .36 mm		

Data Collection ;

Diffractometer	Siemens SMART CCD
Radiation type	MoK_α
Wavelength	0.71073 A
Radiation source	Fine-focus sealed tube
Monochromator	Graphite
Measurement method	Omega-2theta
Theta range for data collection	1.83 to 23.26 deg.
Index ranges	$-26 \leq h \leq 32$
	$-14 \leq k \leq 14$
	$-25 \leq l \leq 25$
Reflections collected	15592
Independent reflections	5394 [R(int) = 0.0282]
Mean intensity/sigma	17.58
No. reflns. $[F_o>4\sigma(F_o)]$	4192
Absorption correction	SADABS

Solution and Refinement :

Atom sites soln. - primary	Patterson
Atom sites soln. - secondary	Difference fourier
Atom sites soln. - hydrogens	Geometrical

Treatment of hydrogen atoms	Riding model	
Refinement method	Full-matrix least-squares on F^2	
Data / restraints / parameters	5394/0/469	
Goodness-of-fit (S) $[F_o>4\sigma(F_o)]$	0.891	
Goodness-of-fit (S) (all data)	0.891	
Final R indices $[F_o>4\sigma(F_o)]$	R1 = 0.0536	wR2 = 0.1310
R indices (all data)	R1 = 0.0957	wR2 = 0.1708
Maximum shift/esd	-0.124 for U13 l(4A)	
Mean shift/esd	0.011	
Largest diff. peak and hole	1.317 and -1.295 e. A"^{3}	

Computer Programs :

Data collection	Siemens SAINT
Cell refinement	Siemens SAINT
Data reduction	SHELXTLv.5.03
Structure solution	SHELXS-97
Structure refinement	SHELXL-97
Molecular graphics	ORTEP
Publication material	SHELXL-97

$R1 = \Sigma||F_o| - |F_c||/\Sigma|F_o|$

$wR_2 - [\Sigma\{w(F_o^2 - F_c^2)^2\}/\Sigma(wF_o^4)]^{1/2}$

$w^{-1} = [\sigma^2(F_o^2) + (0.0732P)^2 + 184.1418P]$, $P = (F_o^2 + 2F_c^2)/3$

$S = [\Sigma\{w(F_o^2 - F_c^2)^2\}/(n-p)]^{1/2}$

Table E2.

Atomic coordinates (×10) and equivalent isotropic displacement parameters (A x 10) for 2.

	x	y	z	*U*(eq)
Mn(l)	1848(1)	4967(1)	2050(1)	28(1)
N(l)	2562(2)	5535(4)	3004(2)	32(1)
N(2)	2564(2)	4444(4)	2017(2)	29(1)
N(3)	1192(2)	4085(4)	1171(3)	40(2)
N(4)	1658(2)	3614(4)	2479(2)	35(1)
N(5)	1258(2)	5959(4)	2147(2)	32(1)
N(6)	1689(2)	6365(4)	1400(3)	37(1)
	2547(2)	6018(6)	3491(3)	40(2)
C(2)	2994(2)	6360(5)	4066(3)	42(2)
C(3)	3481(2)	6176(6)	4132(3)	44(2)
C(4)	3506(2)	5673(6)	3637(3)	41(2)
C(5)	3042(2)	5343(5)	3064(3)	28(2)
C(6)	3038(2)	4751(5)	2513(3)	30(2)
C(7)	3492(2)	4531(6)	2502(3)	45(2)
C(8)	3462(2)	3982(6)	1974(3)	44(2)
C(9)	2978(2)	3654(6)	1473(3)	45(2)
C(10)	2541(2)	3906(6)	1523(3)	40(2)

C(ll)	974(3)	4357(6)	536(3)	48(2)
C(12)	502(3)	3911(7)	32(4)	62(3)
C(13)	267(3)	3211(8)	195(5)	79(3)
C(14)	486(3)	2903(7)	859(4)	65(3)
C(15)	964(2)	3342(5)	1345(4)	45(2)
C(16)	1232(2)	3049(5)	2069(3)	35(2)
C(17)	1044(3)	2281(6)	2300(4)	57(2)
C(18)	1312(3)	2059(6)	2978(5)	73(3)
C(19)	1749(3)	2610(6)	3404(4)	58(2)
C(20)	1910(3)	3388(6)	3134(3)	50(2)
C(21)	1047(2)	5706(6)	2536(3)	40(2)
C(22)	644(2)	6256(6)	2527(3)	43(2)
C(23)	442(2)	7072(6)	2116(4)	48(2)
C(24)	650(2)	7361(6)	1706(3)	44(2)
C(25)	1065(2)	6781(5)	1745(3)	33(2)
C(26)	1313(2)	7039(5)	1346(3)	33(2)
C(27)	1178(2)	7890(5)	935(4)	45(2)
C(28)	1419(3)	8069(7)	570(4)	67(3)
C(29)	1790(3)	7382(7)	624(4)	61(2)
C(30)	1916(3)	6548(6)	1036(3)	49(2)
I(1)	1838(1)	6073(1)	4575(1)	48(1)
I(2)	1054(1)	7699(1)	4123(1)	50(1)
I(3)	2659(1)	4424(1)	5075(1)	71(1)
I(4A)(.25)	5054(1)	1373(1)	7635(1)	31(1)
I(4B)(.25)	4893(2)	1374(4)	7284(3)	148(3)
I(5A)(.50)	4234(1)	1590(2)	5933(1)	109(1)
I(5B)(.50)	4373(1)	1105(2)	6200(1)	128(1)
I(6AX25)	32(1)	-13(2)	4851(1)	52(1)
I(6B)(.25)	67(1)	-14(2)	4561(1)	47(1)
I(6C)(.25)	75(1)	25(2)	4260(1)	47(1)
I(6D)(.25)	83(1)	85(2)	3962(1)	50(1)
I(7A)(.25)	103(1)	130(2)	3648(1)	59(1)
I(7B)(.25)	88(1)	97(2)	3310(1)	58(1)
I(7C)(.25)	52(1)	69(2)	2989(1)	55(1)
I(7D)(.25)	15(1)	57(2)	2671(1)	60(1)

*The site occupation factors of disordered sites are given after the respective atom labels.
U(eq) is defined as one third of the trace of the orthogonalized Uij tensor.

Table E3.
Anisotropic displacement parameters (A × 10) for 2.

	U_{11}	U_{22}	U_{33}	U_{23}	U_{13}	U_{12}
Mn(l)	24(1)	32(1)	28(1)	-2(1)	13(1)	0(1)
N(l)	29(2)	35(3)	29(2)	-6(2)	14(2)	-4(2)
N(2)	30(2)	30(3)	26(2)	-3(2)	14(2)	6(2)
N(3)	35(2)	44(3)	41(3)	-13(2)	19(2)	-4(2)
N(4)	35(2)	35(3)	38(2)	-2(2)	20(2)	3(2)
N(5)	24(2)	41(3)	28(2)	-1(2)	13(2)	3(2)

N(6)	30(2)	39(3)	42(3)	1(2)	20(2)	0(2)
C(l)	32(3)	53(4)	37(3)	-9(3)	19(2)	-4(3)
C(2)	48(3)	40(4)	40(3)	-9(3)	25(3)	-2(3)
C(3)	32(3)	58(5)	5(3)	-9(3)	11(3)	-1(3)
C(4)	28(3)	50(4)	42(3)	-10(3)	16(2)	-6(3)
C(5)	28(2)	27(3)	26(3)	0(2)	13(2)	2(2)
C(6)	24(2)	31(3)	27(3)	1(3)	8(2)	3(3)
C(7)	25(3)	57(5)	49(4)	-7(3)	16(3)	4(3)
C(8)	36(3)	62(5)	43(3)	-2(3)	26(2)	14(3)
C(9)	55(3)	47(4)	41(3)	-2(3)	32(3)	12(3)
C(10)	38(3)	49(4)	29(3)	-6(3)	15(2)	5(3)
C(ll)	47(3)	60(5)	33(3)	-12(3)	18(3)	1(3)
C(12)	45(4)	76(6)	40(4)	-21(4)	5(3)	4(4)
C(13)	38(4)	91(7)	69(6)	-36(5)	2(4)	-23(5)
C(14)	37(4)	56(5)	82(5)	-20(4)	16(4)	-12(4)
C(15)	32(3)	36(4)	72(4)	-25(3)	30(3)	-11(3)
C(16)	35(3)	28(3)	43(3)	-3(3)	20(2)	1(3)
C(17)	51(3)	34(4)	83(5)	-11(4)	33(3)	-20(3)
C(18)	97(4)	41(5)	113(5)	-5(4)	76(4)	-22(4)
C(19)	73(4)	46(4)	58(4)	18(3)	34(3)	2(4)
C(20)	45(3)	56(5)	44(4)	6(3)	19(3)	-9(4)
C(21)	40(3)	45(4)	40(3)	-1(3)	25(2)	-4(3)
C(22)	34(3)	54(4)	44(3)	-13(3)	23(2)	-7(3)
C(23)	25(3)	60(5)	62(4)	-7(4)	26(2)	0(3)
C(24)	33(3)	45(4)	48(4)	6(3)	6(3)	4(3)
C(25)	29(3)	33(3)	30(3)	-3(3)	10(2)	5(3)
C(26)	31(3)	33(3)	30(3)	0(3)	13(2)	-4(3)
C(27)	44(3)	30(4)	70(4)	8(3)	36(3)	10(3)
C(28)	59(4)	54(5)	82(5)	29(4)	31(4)	9(4)
C(29)	56(3)	68(5)	71(4)	27(4)	43(3)	0(4)
C(30)	49(3)	56(5)	54(3)	11(3)	35(3)	12(3)
1(1)	62(1)	53(1)	37(1)	-5(1)	33(1)	-10(1)
I(2)	43(1)	69(1)	38(1)	-5(1)	21(1)	-4(1)
I(3)	115(1)	51(1)	72(1)	14(1)	67(1)	24(1)
I(4A)	39(1)	28(1)	33(1)	-9(1)	23(1)	-5(1)
1(4B)	112(3)	150(4)	85(6)	3(4)	78(3)	9(4)
1(5A)	89(1)	142(2)	97(1)	-19(1)	48(1)	-23(1)
I(5B)	142(1)	142(2)	101(1)	-31(1)	63(1)	-44(1)
1(6A)	39(1)	54(1)	53(2)	2(2)	17(1)	0(1)
I(6B)	41(1)	54(1)	46(1)	-1(1)	22(1)	-2(1)
1(6C)	45(1)	56(1)	45(1)	0(1)	26(1)	2(1)
1(6D)	46(1)	54(1)	55(1)	-1(1)	30(1)	3(1)
1(7A)	54(1)	63(1)	65(1)	2(1)	34(1)	13(1)
I(7B)	56(1)	62(1)	60(1)	4(1)	32(1)	13(1)
1(7C)	58(1)	60(1)	50(1)	0(1)	29(1)	6(1)
1(7D)	60(1)	60(1)	61(3)	0(1)	32(2)	5(1)

The anisotropic displacement factor exponent takes the form:
$-2\pi^2[h^2a^{*2}U11 + ... + 2hka^*b^*U12]$

Table E4.
Bond lengths (A) and angles (°) for 2.

Mn(1)-N(4)	2.223(6)	Mn(1)-N(6)	2.245(6)
Mn(l)-N(2)	2.245(5)	Mn(1)-N(1)	2.253(4)
Mn(1)-N(5)	2.255(5)	Mn(1)-N(3)	2.266(5)
N(1)-C(1)	1.315(9)	N(1)-C(5)	1.361(8)
N(2)-C(10)	1.315(8)	N(2)-C(6)	1.330(7)
N(3)-C(11)	1.322(9)	N(3)-C(15)	1.345(9)
N(4)-C(16)	1.333(7)	N(4)-C(20)	1.340(8)
N(5)-C(25)	1.334(8)	N(5)-C(21)	1.372(9)
N(6)-C(30)	1.342(10)	N(6)-C(26)	1.359(8)
C(l)-C(2)	1.378(8)	C(2)-C(3)	1.377(10)
C(3)-C(4)	1.356(10)	C(4)-C(5)	1.395(8)
C(5)-C(6)	1.489(9)	C(6)-C(7)	1.375(9)
C(7)-C(8)	1.382(10)	C(8)-C(9)	1.361(8)
C(9)-C(10)	1.385(10)	C(11)-C(12)	1.398(10)
C(12)-C(13)	1.307(14)	C(13)-C(14)	1.392(13)
C(14)-C(15)	1.392(9)	C(15)-C(16)	1.497(10)
C(16)-C(17)	1.372(11)	C(17)-C(18)	1.383(12)
C(18)-C(19)	1.352(11)	C(19)-C(20)	1.389(11)
C(21)-C(22)	1.370(10)	C(22)-C(23)	1.340(10)
C(23)-C(24)	1.423(11)	C(24)-C(25)	1.390(9)
C(25)-C(26)	1.483(10)	C(26)-C(27)	1.375(9)
C(27)-C(28)	1.377(13)	C(28)-C(29)	1.357(12)
C(29)-C(30)	1.360(11)	I(1)-I(2)	2.8833(7)
I(1)-I(3)	2.9676(7)	I(4A)-I(5A)#1	2.897(2)
I(4A)-I(5B)	2.900(2)	I(4B)-I(5A)	2.731(6)
I(4B)-I(5B)#1	3.066(6)	I(5A)-I(4A)#1	2.897(2)
I(5B)-I(4B)#1	3.066(6)	I(6A)-I(7A)	2.920(4)
I(6A)-I(6D)#2	2.953(3)	I(6B)-I(7B)	2.949(4)
I(6B)-I(6C)#2	2.982(4)	I(6C)-I(7C)	2.923(4)
I(6C)-I(6B)#2	2.982(4)	I(6D)-I(7D)	2.909(4)
I(6D)-I(6A)#2	2.953(3)	I(7A)-I(7D)#3	2.910(4)
I(7B)-I(7C)#3	2.838(5)	I(7C)-I(7B)#3	2.838(5)
I(7D)-I(7A)#3	2.910(4)		

N(4)-Mn(1)-N(6)	157.34(17)	N(4)-Mn(1)-N(2)	103.52(19)
N(6)-Mn(1)-N(2)	95.31(19)	N(4)-Mn(1)-N(1)	97.68(18)
N(6)-Mn(1)-N(1)	99.65(18)	N(2)-Mn(1)-N(1)	73.67(18)
N(4)-Mn(1)-N(5)	91.1(2)	N(6)-Mn(1)-N(5)	73.0(2)
N(2)-Mn(1)-N(5)	162.48(19)	N(1)-Mn(1)-N(5)	95.07(18)
N(4)-Mn(1)-N(3)	73.6(2)	N(6)-Mn(1)-N(3)	90.63(19)
N(2)-Mn(1)-N(3)	101.11(19)	N(1)-Mn(1)-N(3)	168.8(2)
N(5)-Mn(1)-N(3)	92.19(18)	C(1)-N(1)-C(5)	119.2(5)
C(l)-N(l)-Mn(l)	125.3(4)	C(5)-N(1)-Mn(1)	115.5(4)
C(10)-N(2)-C(6)	118.6(5)	C(10)-N(2)-Mn(1)	124.0(4)
C(6)-N(2)-Mn(1)	117.3(4)	C(11)-N(3)-C(15)	119.9(6)
C(11)-N(3)-Mn(1)	125.0(5)	C(15)-N(3)-Mn(1)	114.2(4)

C(16)-N(4)-C(20)	117.5(6)	C(16)-N(4)-Mn(1)	117.8(4)
C(20)-N(4)-Mn(1)	124.3(4)	C(25)-N(5)-C(21)	118.7(6)
C(25)-N(5)-Mn(1)	116.9(4)	C(21)-N(5)-Mn(1)	124.1(4)
C(30)-N(6)-C(26)	118.1(6)	C(30)-N(6)-Mn(1)	124.7(5)
C(26)-N(6)-Mn(1)	117.1(4)	N(1)-C(1)-C(2)	123.6(6)
C(3)-C(2)-C(1)	117.8(7)	C(4)-C(3)-C(2)	119.5(6)
C(3)-C(4)-C(5)	120.4(6)	N(1)-C(5)-C(4)	119.4(6)
N(1)-C(5)-C(6)	117.0(5)	C(4)-C(5)-C(6)	123.5(6)
N(2)-C(6)-C(7)	120.7(6)	N(2)-C(6)-C(5)	116.3(5)
C(7)-C(6)-C(5)	123.0(5)	C(6)-C(7)-C(8)	120.2(6)
C(9)-C(8)-C(7)	119.0(6)	C(8)-C(9)-C(10)	117.1(6)
N(2)-C(10)-C(9)	124.3(6)	N(3)-C(11)-C(12)	122.0(8)
C(13)-C(12)-C(11)	118.9(8)	C(12)-C(13)-C(14)	120.7(7)
C(13)-C(14)-C(15)	118.9(9)	N(3)-C(15)-C(14)	119.6(7)
N(3)-C(15)-C(16)	117.7(5)	C(14)-C(15)-C(16)	122.7(7)
N(4)-C(16)-C(17)	122.2(6)	N(4)-C(16)-C(15)	115.1(6)
C(17)-C(16)-C(15)	122.7(6)	C(16)-C(17)-C(18)	119.3(6)
C(19)-C(18)-C(17)	119.7(8)	C(18)-C(19)-C(20)	117.6(7)
N(4)-C(20)-C(19)	123.7(6)	C(22)-C(21)-N(5)	123.0(6)
C(23)-C(22)-C(21)	118.7(7)	C(22)-C(23)-C(24)	120.0(7)
C(25)-C(24)-C(23)	118.5(6)	N(5)-C(25)-C(24)	121.1(7)
N(5)-C(25)-C(26)	116.8(6)	C(24)-C(25)-C(26)	122.1(6)
N(6)-C(26)-C(27)	120.4(7)	N(6)-C(26)-C(25)	115.7(5)
C(27)-C(26)-C(25)	123.9(6)	C(26)-C(27)-C(28)	120.6(7)
C(29)-C(28)-C(27)	118.2(8)	C(28)-C(29)-C(30)	120.0(8)
N(6)-C(30)-C(29)	122.7(7)	I(2)-I(1)-I(3)	178.48(2)
I(5A)#1-I(4A)-I(5B)	177.74(11)	I(5A)-I(4B)-I(5B)#1	179.3(3)
I(4B)-I(5A)-I(4A)#1	0.81(18)	I(4A)-I(5B)-I(4B)#1	0.85(17)
I(7A)-I(6A)-I(6D)#2	177.25(11)	I(7B)-I(6B)-I(6C)#2	173.64(10)
I(7C)-I(6C)-I(6B)#2	171.92(9)	I(7D)-I(6D)-I(6A)#2	170.69(10)
I(7D)#3-I(7A)-I(6A)	169.15(11)	I(7C)#3-I(7B)-I(6B)	171.15(11)
I(7B)#3-I(7C)-I(6C)	174.05(11)	I(6D)-I(7D)-I(7A)#3	176.44(12)

Symmetry transformations used to generate equivalent atoms:
1 -x+1, y, -z+3/2 #2 -x, -y, -z+1 #3 -x, y, -z+1/2

Table £5.
Hydrogen coordinates ($\times 10^4$) and isotropic displacement parameters ($A^2 \times 10^3$) for 2.

	X	y	I	U(eq)
H(1A)	2214	6137	3444	48
H(2A)	2967	6707	4401	50
H(3A)	3795	6397	4518	53
H(4A)	3838	5546	3681	49
H(7A)	3824	4754	2855	54
H(8A)	3771	3837	1962	53
H(9A)	2942	3272	1108	53
H(10A)	2205	3677	1182	48
H(11A)	1142	4866	420	58
	357	4112	-417	74

H(13A)	-53	2912	-139	95
H(14A)	313	2408	976	78
H(17A)	736	1910	2001	68
H(18A)	1191	1527	3141	88
H(19A)	1938	2472	3866	70
H(20A)	2212	3778	3427	60
H(21A)	1186	5130	2822	48
H(22A)	512	6065	2804	51
H(23A)	161	7453	2097	57
H(24A)	511	7931	1415	53
H(27A)	919	8353	904	54
H(28A)	1329	8652	290	81
H(29A)	1958	7482	378	73
H(30A)	2174	6081	1067	59

Hydrogen atoms are labelled according to the atom to which they are attached. All hydrogens were refined using the riding model (the positional parameters of the riding atoms have same e.s.ds as the atom on which they ride). All hydrogens were fixed a common U(iso) value (= 1.2 times the U(iso) of the atom to which they are attached).

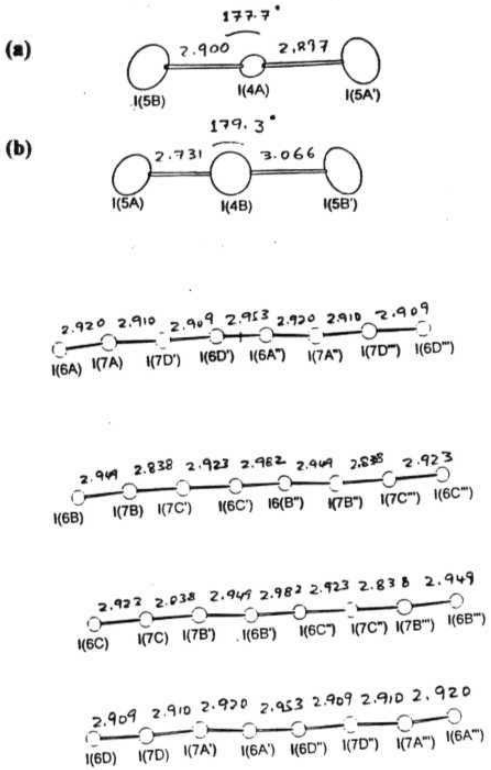

Figure E1. Disordered anions in *2* : (a), (b) One of the I_3^- anions disordered in 2 positions; (c), (d), (e), (f) the I_8^{2-} infinite chain disordered in 4 positions.

APPENDIX F. Crystallographic tables for $[Ni(phen)_3](I_3)_2 \cdot CH_3CN$ (3).

Table **F1.**
Crystal data and structure refinement for $[Ni(phen)_3](I_3)_2 \cdot CH_3CN$ (3).

Crystal Data :		
Structural formula	$[Ni(phen)_3](I_3)_2 \cdot CH_3CN$	
Empirical formula	$C_{38}H_{27}I_6N_7Ni$	
Formula weight	1401.78	
Melting point	533 K	
Temperature	293(2) K	
Crystal system	Triclinic	
Space group	P $\bar{1}$ (No.2)	
Unit cell dimensions	a =10.01(2) A	a = 78.78(2) deg.
	b= 12.581(4) A	β = 86.63(4) deg.
	c= 18.003(2) A	γ = 67.59(5) deg.
Volume	2055(3) A^3	
Z	2	
No. reflns. used for cell	25	
Cell measurement theta min/max	6.21/13.00	
Crystal shape	Needles	
Crystal colour	Brown	
Density (calculated)	2.266 Mg/m^3	
Absorption coefficient	5.016 mm^{-1}	
F(000)	1300	
Crystal size	50x .20x .15 mm	
Data Collection :		
Diffractometer	Enraf Nonius CAD-4	
Radiation type	MoK_α	
Wavelength	0.71073 A	
Radiation source	Fine focus sealed tube	
Monochromator	Graphite	
Measurement method	Omega-2theta	
Standard reflns.	2 measured every 60 min.	
Theta range for data collection	2.20 to 24.99 deg.	
Index ranges	$0 \le h \le 10$, $-13 \le k \le 14$, $-21 \le l \le 21$	
Reflections collected	7507	
Independent reflections	7057 [R(int) = 0.0210]	
Mean intensity/sigma	19.88	
No. reflns. [F > 4 sigma(F)]	4569	
Absorption correction	Semiempirical	
Max. and min. transmission	0 999 and 0.699	
Solution and Refinement :		
Atom sites soln. - primary	Patterson	
Atom sites soln. - secondary	Difference fourier	
Atom sites soln - hydrogens	Geometrical	

Treatment of hydrogen atoms	Riding model
Refinement method	Full-matrix least-squares on F^2
Data / restraints / parameters	6209 / 3 / 455
Goodness-of-fit (S) [F>4sigma(F)]	1.084
Goodness-of-fit (S) (all data)	1.211
Final R indices [F>4sigma(F)]	R1 =0.0609 wR2 = 0.1395
R indices (all data)	R1 =0.1075 wR2 = 0.1869
Maximum shift/esd	0.290 for x C37
Mean shift/esd	0.003
Largest diff peak and hole	1.997 and -1.946 e.A^{-3}

Computer Programs :

Data collection	CAD-4 system
Cell refinement	CAD-4 system
Data reduction	CAD-4 system
Structure solution	SHELXS-86
Structure refinement	SHELXL-93
Molecular graphics	ORTEP
Publication material	SHELXL-93

$R1 = \Sigma||F_o| - |F_c||/\Sigma|F_o|$

$wR_2 = [\Sigma\{w(F_o^2 - F_c^2)^2\}/\Sigma(wF_o^4)]^{1/2}$

$w^{-1} = [\sigma^2(F_o^2) + (0.0785P)^2 + 9.4097P]$, $P - (F_o^2 + 2F_c^2)/3$

$S = [\Sigma\{w(F_o^2 - F_c^2)^2\}/(n-p)]^{1/2}$

Table F2.
Atomic coordinates (x 10^4) and equivalent isotropic displacement parameters (A^2 x 10^3) for 3. U(eq) is defined as one third of the trace of the orthogonalized Uij tensor.

	x	y	z	U(eq)
Ni	429(1)	6626(1)	2434(1)	32(1)
I(1)	1148(1)	3227(1)	346(1)	54(1)
1(2)	3811(1)	2322(1)	1221(1)	51(1)
I(3)	6408(1)	1501(1)	2179(1)	69(1)
I(4)	8386(2)	1199(1)	4168(1)	133(1)
I(5)	7043(1)	1652(1)	5594(1)	67(1)
1(6)	5497(1)	2309(1)	6967(1)	88(1)
N(l)	730(7)	8218(5)	2244(3)	33(2)
N(2)	1500(7)	6559(5)	1397(3)	31(2)
N(3)	-1568(7)	7369(6)	1857(4)	37(2)
N(4)	-5(7)	5128(5)	2433(4)	35(2)
N(5)	-414(7)	6875(6)	3501(4)	36(2)
N(6)	2274(8)	5649(6)	3108(4)	40(2)
C(l)	423(9)	9002(6)	2680(5)	37(2)
C(2)	582(10)	10063(7)	2450(5)	47(2)
C(3)	1027(10)	10348(7)	1739(5)	49(3)
C(4)	1372(9)	9532(7)	1258(5)	38(2)
C(5)	1867(10)	9739(7)	508(6)	51(3)
C(6)	2257(9)	8923(7)	64(5)	44(2)

C(7)	2177(8)	7797(7)	350(4)	35(2)
C(8)	2642(10)	6871(7)	-53(5)	45(2)
C(9)	2518(11)	5819(8)	284(5)	56(3)
C(10)	1937(9)	5708(7)	995(5)	42(2)
C(11)	1640(8)	7579(6)	1084(4)	33(2)
C(12)	1225(8)	8478(6)	1549(5)	34(2)
C(13)	-2325(10)	8486(8)	1554(5)	48(2)
C(14)	-3632(10)	8840(8)	1174(5)	52(3)
C(15)	-4196(10)	8050(8)	1101(5)	51(3)
C(16)	-3462(10)	6865(8)	1408(5)	45(2)
C(17)	-3952(10)	5963(8)	1348(5)	51(2)
C(18)	-3216(10)	4857(8)	1656(5)	54(2)
C(19)	-1853(9)	4511(7)	2033(5)	40(2)
C(20)	-999(10)	3351(7)	2355(5)	44(2)
C(21)	303(10)	3115(7)	2681(6)	50(3)
C(22)	770(10)	4015(7)	2716(5)	43(2)
C(23)	-1309(9)	5368(7)	2096(4)	37(2)
C(24)	-2151(9)	6572(6)	1778(4)	33(2)
C(25)	-1752(10)	7542(8)	3680(5)	51(3)
C(26)	-2172(14)	7694(10)	4414(6)	74(4)
C(27)	-1163(13)	7116(10)	4977(6)	76(3)
C(28)	261(11)	6403(9)	4827(5)	57(3)
C(29)	1425(14)	5718(10)	5377(6)	80(4)
C(30)	2686(14)	5044(10)	5189(6)	77(4)
C(31)	3071(12)	4984(9)	4421(6)	62(3)
C(32)	4413(12)	4285(9)	4184(7)	75(4)
C(33)	4645(12)	4317(9)	3445(7)	71(4)
C(34)	3577(9)	4998(8)	2920(6)	57(3)
C(35)	1980(9)	5624(7)	3858(5)	41(2)
C(36)	576(10)	6319(7)	4054(5)	42(2)
C(37) (0.30)	3477(3)	1571(3)	3719(4)	35(6)
C(38) (0.30)	4268(3)	2058(4)	4131(4)	466(113)
N(7) (0.30)	3014(9)	1082(9)	3402(8)	154(20)

*The site occupation factors of disordered sites are given after the respective atom labels.

Table F3.
Anisotropic displacement parameters ($Å^2 \times 10^3$) for 3

	U11	U22	U33	U23	U13	U12
Ni	39(1)	27(1)	32(1)	-8(1)	-5(1)	-14(1)
I(1)	62(1)	39(1)	57(1)	-7(1)	-10(1)	-14(1)
I(2)	55(1)	35(1)	61(1)	-15(1)	2(1)	-12(1)
K3)	67(1)	62(1)	83(1)	-20(1)	-19(1)	-23(1)
I(4)	156(1)	142(1)	51(1)	-23(1)	11(1)	0(1)
I(5)	67(1)	71(1)	50(1)	-9(1)	-10(1)	-12(1)
I(6)	61(1)	137(1)	73(1)	-42(1)	12(1)	-36(1)
N(l)	40(4)	32(3)	33(3)	-11(3)	0(3)	-18(3)
N(2)	39(3)	20(3)	37(3)	-16(2)	-2(3)	-9(3)

N(3)	39(4)	31(3)	40(4)	-7(3)	3(3)	-12(3)
N(4)	40(4)	28(3)	34(3)	-5(3)	-4(3)	-9(3)
N(5)	37(3)	36(3)	42(4)	-13(3)	6(3)	-19(3)
N(6)	52(4)	31(3)	42(4)	**-4(3)**	-13(3)	-18(3)
C(l)	44(4)	29(4)	44(4)	-17(3)	2(4)	-13(3)
C(2)	61(6)	34(4)	51(5)	-24(4)	14(4)	-17(4)
CO)	68(6)	24(4)	62(6)	-12(4)	-3(5)	-22(4)
C(4)	41(4)	28(4)	42(4)	-9(3)	3(4)	-11(3)
C(5)	59(5)	29(4)	65(6)	-2(4)	-7(5)	-19(4)
C(6)	50(5)	39(4)	46(5)	-2(4)	12(4)	-22(4)
C(7)	37(4)	31(4)	38(4)	-6(3)	-5(4)	-12(3)
C(8)	68(6)	42(4)	28(4)	**-6(3)**	-1(4)	-24(4)
C(9)	73(6)	49(5)	44(5)	-23(4)	12(5)	-15(5)
C(10)	53(5)	35(4)	43(5)	-12(4)	6(4)	-21(4)
C(ll)	32(4)	25(4)	42(4)	-13(3)	-11(3)	-8(3)
C(12)	45(4)	20(3)	45(4)	-7(3)	-6(4)	-20(3)
C(13)	53(5)	40(5)	52(5)	-10(4)	2(4)	-19(4)
C(14)	55(6)	45(5)	54(5)	-12(4)	-15(5)	-11(4)
C(15)	35(5)	61(6)	58(6)	-12(4)	-12(4)	-16(4)
C(16)	52(5)	45(5)	38(5)	-11(4)	5(4)	-19(4)
C(17)	47(5)	64(5)	53(5)	-22(4)	-1(4)	-29(4)
C(18)	63(5)	64(5)	60(5)	-34(4)	7(4)	-41(4)
C(19)	49(5)	40(4)	41(4)	-19(3)	10(4)	-22(4)
C(20)	58(5)	37(4)	49(5)	-10(4)	5(4)	-29(4)
C(21)	57(6)	19(4)	74(6)	-8(4)	6(5)	-14(4)
C(22)	63(5)	29(4)	40(5)	-3(3)	7(4)	-23(4)
C(23)	58(5)	36(4)	31(4)	-15(3)	13(4)	-31(4)
C(24)	49(4)	31(4)	26(4)	-4(3)	-1(3)	-23(3)
C(25)	56(5)	56(5)	50(5)	-12(4)	10(4)	-30(4)
C(26)	100(8)	67(6)	58(6)	-27(5)	21(6)	-32(6)
C(27)	106(8)	107(7)	47(5)	-45(5)	29(5)	-65(6)
C(28)	81(6)	70(6)	41(5)	-10(4)	6(5)	-52(5)
C(29)	126(9)	83(7)	40(5)	-8(5)	-28(6)	-46(7)
C(30)	112(8)	57(6)	60(6)	12(5)	-48(6)	-34(6)
C(31)	84(7)	54(5)	49(6)	12(4)	-24(5)	-35(5)
C(32)	68(7)	50(6)	94(9)	17(6)	-31(6)	-18(5)
C(33)	55(6)	59(6)	84(8)	-9(6)	-24(6)	-3(5)
C(34)	27(5)	55(6)	78(7)	-11(5)	-6(5)	-2(4)
C(35)	47(5)	36(4)	45(5)	2(4)	-15(4)	-23(4)
C(36)	63(5)	44(4)	30(4)	**-6(3)**	-9(4)	-30(4)

The anisotropic displacement factor exponent takes the form:
$-2\pi^2[h^2a^{*2}U11 + ... + 2hka^*b^*U12]$

Table F4.
Bond lengths [A] and angles [deg] for 3.

Bond distances :

Ni-N(5)	2.084(7)	Ni-N(6)	2.086(7)

Ni-N(4)	2.089(7)	Ni-N(3)	2.094(7)
Ni-N(2)	2.096(6)	Ni-N(l)	2.098(7)
I(1)-I(2)	2.891(4)	I(2)-I(3)	2.928(3)
I(4)-I(5)	2.882(2)	I(5)-I(6)	2.925(2)
N(1)-C(1)	1.315(10)	N(1)-C(12)	1.344(10)
N(2)-C(10)	1.331(10)	N(2)-C(11)	1.353(10)
N(3)-C(13)	1.336(10)	N(3)-C(24)	1.370(11)
N(4)-C(22)	1.328(10)	N(4)-C(23)	1.372(11)
N(5)-C(36)	1.334(10)	N(5)-C(25)	1.341(11)
N(6)-C(34)	1.314(11)	N(6)-C(35)	1.360(11)
C(1)-C(2)	1.385(12)	C(2)-C(3)	1.357(13)
C(3)-C(4)	1.401(12)	C(4)-C(12)	1.387(11)
C(4)-C(5)	1.422(13)	C(5)-C(6)	1.350(13)
C(6)-C(7)	1.441(12)	C(7)-C(8)	1.405(12)
C(7)-C(11)	1.414(11)	C(8)-C(9)	1.393(13)
C(9)-C(10)	1.379(12)	C(11)-C(12)	1.457(11)
C(13)-C(14)	1.385(13)	C(14)-C(15)	1.345(14)
C(15)-C(16)	1.400(12)	C(16)-C(24)	1.393(12)
C(16)-C(17)	1.420(14)	C(17)-C(18)	1.324(13)
C(18)-C(19)	1.431(13)	C(19)-C(20)	1.406(11)
C(19)-C(23)	1.406(12)	C(20)-C(21)	1.363(13)
C(21)-C(22)	1.393(13)	C(23)-C(24)	1.441(10)
C(25)-C(26)	1.390(14)	C(26)-C(27)	1.36(2)
C(27)-C(28)	1.41(2)	C(28)-C(36)	1.423(12)
C(28)-C(29)	1.455(14)	C(29)-C(30)	1.29(2)
C(30)-C(31)	1.42(2)	C(31)-C(32)	1.39(2)
C(31)-C(35)	1.419(12)	C(32)-C(33)	1.33(2)
C(33)-C(34)	1.370(14)	C(35)-C(36)	1.410(12)
C(37)-N(7)	1.142(2)	C(37)-C(38)	1.472(2)

Bond angles :

N(5)-Ni-N(6)	79.8(3)	N(5)-Ni-N(4)	95.6(3)
N(6)-Ni-N(4)	91.1(3)	N(5)-Ni-N(3)	95.8(3)
N(6)-Ni-N(3)	169.3(3)	N(4)-Ni-N(3)	79.5(3)
N(5)-Ni-N(2)	169.2(3)	N(6)-Ni-N(2)	95.8(3)
N(4)-Ni-N(2)	94.4(2)	N(3)-Ni-N(2)	90.1(3)
N(5)-Ni-N(1)	91.5(3)	N(6)-Ni-N(1)	96.7(3)
N(4)-Ni-N(1)	170.3(2)	N(3)-Ni-N(1)	93.1(3)
N(2)-Ni-N(1)	79.2(2)	I(1)-I(2)-I(3)	176.24(3)
I(4)-I(5)-I(6)	174.87(4)	C(1)-N(1)-C(12)	117.2(7)
C(1)-N(1)-Ni	129.5(6)	C(12)-N(1)-Ni	113.1(5)
C(10)-N(2)-C(11)	117.5(7)	C(10)-N(2)-Ni	129.3(6)
C(11)-N(2)-Ni	113.0(5)	C(13)-N(3)-C(24)	116.6(7)
C(13)-N(3>.Ni	129.5(7)	C(24)-N(3)-Ni	113.8(5)
C(22)-N(4)-C(23)	117.1(7)	C(22)-N(4)-Ni	129.8(6)
C(23)-N(4)-Ni	113.1(5)	C(36)-N(5)-C(25)	118.7(7)
C(36)-N(5)-Ni	112.5(5)	C(25)-N(5)-Ni	128.7(6)
C(34)-N(6)-C(35)	118.2(8)	C(34)-N(6)-Ni	129.9(7)
C(35)-N(6).Ni	111.6(5)	N(1)-C(1)-C(2)	1228(8)
C(3)-C(2)-C(1)	120.1(8)	C(2)-C(3)-C(4)	118.7(8)

C(12)-C(4)-C(3)	116.8(8)	C(12)-C(4)-C(5)	120.1(8)
C(3)-C(4)-C(5)	123.1(8)	C(6)-C(5)-C(4)	122.3(8)
C(5)-C(6)-C(7)	119.7(8)	C(8)-C(7)-C(11)	117.0(7)
C(8)-C(7)-C(6)	123.7(8)	C(11)-C(7)-C(6)	119.3(7)
C(9)-C(8)-C(7)	118.6(8)	C(10)-C(9)-C(8)	119.9(9)
N(2)-C(10)-C(9)	123.3(8)	N(2)-C(11)-C(7)	123.7(7)
N(2)-C(11)-C(12)	116.6(7)	C(7)-C(11)-C(12)	119.7(7)
N(1)-C(12)-C(4)	124.2(7)	N(1)-C(12)-C(11)	117.0(7)
C(4)-C(12)-C(11)	118.8(7)	N(3)-C(13)-C(14)	122.7(9)
C(15)-C(14)-C(13)	120.3(9)	C(14)-C(15)-C(16)	120.1(8)
C(24)-C(16)-C(15)	116.6(9)	C(24)-C(16)-C(17)	119.0(8)
C(15)-C(16)-C(17)	124.4(9)	C(18)-C(17)-C(16)	121.7(9)
C(17)-C(18)-C(19)	121.2(9)	C(20)-C(19)-C(23)	116.5(8)
C(20)-C(19)-C(18)	124.2(8)	C(23)-C(19)-C(18)	119.3(8)
C(21)-C(20)-C(19)	119.4(8)	C(20)-C(21)-C(22)	120.6(8)
N(4)-C(22)-C(21)	122.5(9)	N(4)-C(23)-C(19)	123.9(7)
N(4)-C(23)-C(24)	117.6(7)	C(19)-C(23)-C(24)	118.5(8)
N(3)-C(24)-C(16)	123.8(7)	N(3)-C(24)-C(23)	115.9(7)
C(16)-C(24)-C(23)	120.2(8)	N(5)-C(25)-C(26)	123.6(9)
C(27)-C(26)-C(25)	117.5(11)	C(26)-C(27)-C(28)	121.7(10)
C(27)-C(28)-C(36)	116.1(9)	C(27)-C(28)-C(29)	127.1(9)
C(36)-C(28)-C(29)	116.8(9)	C(30)-C(29)-C(28)	122.8(10)
C(29)-C(30)-C(31)	122.2(10)	C(32)-C(31)-C(35)	117.4(10)
C(32)-C(31)-C(30)	124.8(10)	C(35)-C(31)-C(30)	117.6(10)
C(33)-C(32)-C(31)	119.1(10)	C(32)-C(33)-C(34)	121.2(11)
N(6)-C(34)-C(33)	122.6(11)	N(6)-C(35)-C(36)	117.7(7)
N(6)-C(35)-C(31)	121.3(8)	C(36)-C(35)-C(31)	120.9(8)
N(5)-C(36)-C(35)	118.1(7)	N(5)-C(36)-C(28)	122.4(8)
C(35)-C(36)-C(28)	119.5(8)	N(7)-C(37)-C(38)	171.9(5)

Table F5.
Hydrogen coordinates ($\times 10^{2}$) and isotropic displacement parameters ($A^{2} \times 10^{3}$) for **3**.

	x	y	z	U(eq)
H(1)	84(9)	8838(6)	3164(5)	60(6)
H(2)	384(10)	10582(7)	2784(5)	60(6)
H(3)	1102(10)	11071(7)	1574(5)	60(6)
H(5)	1924(10)	10462(7)	316(6)	60(6)
H(6)	2577(9)	9087(7)	-425(5)	60(6)
H(8)	3024(10)	6959(7)	-534(5)	60(6)
H(9)	2827(11)	5192(8)	30(5)	60(6)
H(10)	1845(9)	5003(7)	1204(5)	60(6)
H(13)	-1960(10)	9049(8)	1601(5)	60(6)
H(14)	-4120(10)	9626(8)	968(5)	60(6)
H(15)	-5075(10)	8292(8)	847(5)	60(6)
H(17)	-4810(10)	6154(8)	1086(5)	60(6)
H(18)	-3591(10)	4294(8)	1627(5)	60(6)

H(20)	-1319(10)	2750(7)	2346(5)	60(6)
H(21)	885(10)	2346(7)	2881(6)	60(6)
H(22)	1659(10)	3829(7)	2947(5)	60(6)
H(25)	-2438(10)	7923(8)	3291(5)	60(6)
H(26)	-3106(14)	8172(10)	4516(6)	60(6)
H(27)	-1421(13)	7194(10)	5474(6)	60(6)
H(29)	1254(14)	5767(10)	5885(6)	60(6)
H(30)	3364(14)	4582(10)	5569(6)	60(6)
H(32)	5138(12)	3803(9)	4536(7)	60(6)
H(33)	5548(12)	3868(9)	3283(7)	60(6)
H(34)	3781(9)	5001(8)	2409(6)	60(6)

Hydrogen atoms are labelled according to the atom to which they are attached. All hydrogens were refined using the riding model (the positional parameters of the riding atoms have same e.s.ds as the atom on which they ride). All hydrogens were fixed to a common U(iso) value.

APPENDIX G.Crystallographic tables and figures for $[Mn(phen)_3](I_3)_2$ (1).

Table G1. Crystal data and structure refinement for 1.

Empirical formula	C12 H8 I2 Mn0.33 N2
Formula weight	452.32
Temperature	130 K
Wavelength	0.71073 A
Crystal system	Rhombohedral
Space group	R-3
Unit cell dimensions	a - 16.248(2) A alpha = 90 deg. b - 16.248(2) A beta = 90 deg. c - 25.757(5) A gamma = 120 deg.
Volume	5889(2) A^3
Z	18
Density (calculated)	2.296 Mg/m^3
Absorption coefficient	5.089 mm^-1
F(000)	3750
Crystal size	.22 x .38 x .76 mm
Theta range for data collection	2.14 to 25.00 deg.
Index ranges	0<=h<=8, -19<=k<=0, 0<=l<=30
Reflections collected	1337
Independent reflections	1247 [R(int) = 0.0528]
Refinement method	Full-matrix least-squares on F^2
Data / restraints / parameters	1247 / O / 151
Goodness-of-fit on F^2	1.109
Final R indices [I>2sigma(I)]	R1 = 0.0539, wR2 = 0.1325
R indices (all data)	R1 = 0.0609, wR2 = 0.1394
Largest diff. peak and hole	1.218 and -1.251 e.A^-3

$R1 = \Sigma||F_o| - |F_c||/\Sigma|F_o|$

$wR2 = [\Sigma\{w(F_o^2 - F_c^2)^2\}/\Sigma(wF_o^4)]^{1/2}$

$w^{-1} = [\sigma^2(F_o^2) + (0.0994P)^2 + 65.93P]$, $P = (F_o^2 + 2F_c^2)/3$

$S = [\Sigma\{w(F_o^2 - F_c^2)^2\}/(n-p)]^{1/2}$

Table G2. Atomic coordinates (x 10^4) and equivalent isotropic displacement parameters (A^2 x 10^3) for 1. U(eq) is defined as one third of the trace of the orthogonalized Uij tensor.

	x	y	z	U(eq)
I{1)	-70(1)	3896(1)	905(1)	33(1)
I(2)	0	5000	0	22(1)
I(3)	0	0	0	18(1)
I(4)	0	0	1104(1)	93(1)
Mn(l)	6667	3333	121(1)	15(1)
N(l)	7696(7)	4590(7)	589(3)	18(2)
N(2)	7005(8)	4612(8)	-363(3)	22(2)
C(l)	8017(9)	4609(11)	1060(4)	33(3)
C(2)	8591(10)	5413(11)	1337(5)	35(4)
C(3)	8846(11)	6269(12)	1125(6)	46(4)
C(4)	8572(11)	6319(11)	621(5)	33(4)
C(5)	1149(12)	2815(13)	-341(7)	52(5)
C(6)	1428(11)	2814(11)	140(7)	44(4)
C(7)	2066(12)	3667(11)	407(6)	36(4)
C(8)	2411(13)	3736(11)	915(5)	43(4)
CO)	6953(12)	5431(11)	-1122(5)	36(4)
C(10)	6667(10)	4617(11)	-836(4)	30(3)
C(ll)	7635(10)	5462(10)	-144(4)	25(3)
C(12)	7972(9)	5463(10)	364(5)	25(3)

Table G3. Selected bond lengths [A] and angles [deg] for 1.

I(1)-I(2)	2.9077(9)
I(2)-I(l)#l	2.9077(9)
I(3)-I(4)#2	2.844(2)
I(3)-I(4)	2.844(2)
Mn(1)-N(1)#3	2.237(10)
Mn(l)-N(l)	2.237(10)
Mn(l)-N(l)#4	2.237(10)
Mn(l)-N(2)#3	2.242(9)
Mn(1)-N(2)#4	2.242(9)
Mn(l)-N(2)	2.242(9)
I(l)-I(2)-I(l)#l	180.0
I(4)#2-I(3)-I(4)	180.0
N(1)#3-Mn(1)-N(1)	93.6(3)
N(1)#3-Mn(1)-N(1)#4	93.6(3)
N(l)-Mn(l)-N(l)#4	93.6(3)
N(1)#3-Mn(1)-N(2)#3	74.3(3)
N(l)-Mn(l)-N(2)#3	103.5(4)
N(1)#4-Mn(1)-N(2)#3	159.4(4)
N(1)#3-Mn(1)-N(2)#4	103.5(4)
N(1)-Mn(1)-N(2)#4	159.4(4)
N(1)#4-Mn(1)-N(2)#4	74.3(4)
N(2)#3-Mn(l)-N(2)#4	92.1(3)
N(1)#3-Mn(1)-N(2)	159.5(4)
N(1)-Mn(1)-N(2)	74.3(3)

N(l)#4-Mn(l)-N(2)	103.5(4)
N(2)#3-Mn(l)-N(2)	92.1(3)
N(2)#4-Mn(l)-N(2)	92.1(3)

Symmetry transformations used to generate equivalent atoms:
#1 -x,-y+l,-z #2 -x,-y,-z #3 -x+y+1,-x+1,z
#4 -y+1,x-y,z

Table G4. Anisotropic displacement parameters (A^2 x 10^3) for 1.
The anisotropic displacement factor exponent takes the form:
-2 pi^2 [h^2 a*^2 U11 + ... + 2 h k a* b* U12]

	U11	U22	U33	U23	U13	U12
Id)	34(1)	37(1)	28(1)	1(1)	-6(1)	16(1)
I(2)	15(1)	26(1)	21(1)	-5(1)	-2(1)	8(1)
I(3)	16(1)	16(1)	20(1)	0	0	8(1)
I(4)	130(2)	130(2)	19(1)	0	0	65(1)
Mn(l)	14(1)	14(1)	17(1)	0	0	7(1)
N(l)	12(6)	19(7)	23(4)	-6(4)	-3(4)	6(6)
N(2)	23(7)	30(7)	21(4)	7(5)	1(5)	20(6)
C(l)	20(9)	43(11)	25(5)	-7(6)	-2(6)	9(8)
C(2)	32(10)	44(12)	30(6)	-19(7)	-15(7)	19(10)
C(3)	32(10)	33(12)	62(9)	-20(9)	-4(9)	7(11)
C(4)	17(10)	30(11)	53(7)	-13(7)	-3(7)	12(9)
C(5)	29(11)	25(11)	84(11)	-7(9)	-6(10)	0(10)
C(6)	19(10)	15(10)	93(12)	0(9)	10(9)	4(8)
C(7)	33(11)	20(10)	61(9)	-3(8)	8(8)	18(9)
C(8)	50(13)	45(11)	51(8)	25(8)	14(8)	37(10)
C(9)	44(11)	39(10)	34(6)	5(7)	-6(7)	28(10)
C(10)	32(10)	49(11)	25(5)	4(6)	0(6)	32(9)
C(ll)	14(8)	20(9)	40(6)	5(7)	5(6)	7(8)
C(12)	10(8)	15(9)	49(7)	-10(7)	3(6)	5(8)

Table G5. Hydrogen coordinates (x 10^4) and isotropic displacement parameters (A^2 x 10^3) for 1.

	x	y	z	U(eq)
H(l)	7840(9)	4028(11)	1217(4)	69(20)
H(2)	8802(10)	5372(11)	1667(5)	69(20)
H(3)	9204(11)	6822(12)	1316(6)	69(20)
H(5)	760(12)	2238(13)	-504(7)	69(20)
H(6)	1200(11)	2236(11)	311(7)	69(20)
H(8)	2190(13)	3187(11)	1113(5)	69(20)
H(9)	6709(12)	5402(11)	-1452(5)	69(20)
H(10)	6215(10)	4040(11)	-979(4)	69(20)

(a)

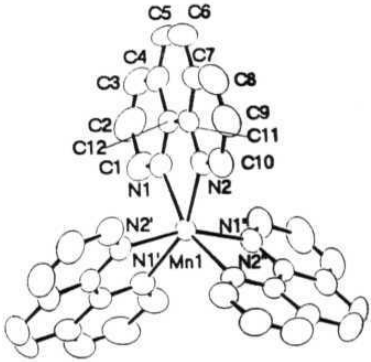

(b)

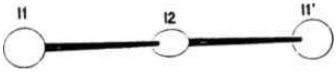

(C)

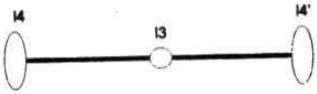

Figure G1. Views of the cation and anions of 1 (50% probability ellipsoids) at 130 K. (a) Cation $[Mn(phen)_3]^{2+}$, (b) 'normal' I_3^- (':-x, 1-y, -z), (c) 'short' I_3^- (':-x, -y, -z).

Table 6. Bond lengths [A] and angles [deg] for 1.

I(1)-I(2)	2.9077(9)
I(2)-I(1)#1	2.9077(9)
I(3)-I(4)#2	2.844(2)
I(3)-I(4)	2.844(2)
Mn(l)-N(l)#3	2.237(10)
Mn(1)-N(1)	2.237(10)
Mn(1)-N(1)#4	2.237(10)
Mn(l)-N(2)#3	2.242(9)
Mn(l)-N(2)#4	2.242(9)
Mn(1)-N(2)	2.242(9)
N(l)-C(l)	1.315(14)
N(l)-C(12)	1.38(2)
N(2)-C(10)	1.338(13)
N(2)-C(ll)	1.36(2)
C(l)-C(2)	1.37(2)
C(2)-C(3)	1.35(2)
C(3)-C(4)	1.39(2)
C(4)-C(12)	1.40(2)
C(4)-C(5)#5	1.44(2)
C(5)-C(6)	1.32(2)
C(5)-C(4)#5	1.44(2)
C(6)-C(7)	1.43(2)
C(7)-C(8)	1.41(2)
C(7)-C(ll)#5	1.42(2)
C(8)-C(9)#5	1.34(2)
C(9)-C(8)#5	1.34(2)
C(9)-C(10)	1.38(2)
C(ll)-C(12)	1.42(2)
C(ll)-C(7)#5	1.42(2)

I(l)-I(2)-I(l)#l	180.0
I(4)#2-I(3)-I(4)	180.0
N(l)#3-Mn(l)-N(l)	93.6(3)
N(l)#3-Mn(l)-N(l)#4	93.6(3)
N(l)-Mn(l)-N(l)#4	93.6(3)
N(l)#3-Mn(l)-N(2)#3	74.3(3)
N(1)-Mn(1)-N(2)#3	103.5(4)
N(1)#4-Mn(1)-N(2)#3	159.4(4)
N(l)#3-Mn(l)-N(2)#4	103.5(4)
N(1)-Mn(1)-N(2)#4	159.4(4)
N(1)#4-Mn(1)-N(2)#4	74.3(4)
N(2)#3-Mn(l)-N(2)#4	92.1(3)
N(l)#3-Mn(l)-N(2)	159.5(4)
N(l)-Mn(l)-N(2)	74.3(3)
N(l)#4-Mn(l)-N(2)	103.5(4)
N(2)#3-Mn(l)-N(2)	92.1(3)
N(2)#4-Mn(1)-N(2)	92.1(3)
C(l)-N(l)-C(12)	116.1(10)
C(l)-N(l)-Mn(l)	128.7(9)
C(12)-N(1)-Mn(1)	114.9(7)
C(10)-N(2)-C(ll)	118.3(11)
C(10)-N(2)-Mn(l)	126.9(9)
C(11)-N(2)-Mn(1)	114.8(7)
N(l)-C(l)-C(2)	125.3(14)
C(3)-C(2)-C(l)	118.9(13)
C(2)-C(3)-C(4)	119.7(14)

C(3)-C(4)-C(12)	117.9(14)
C(3)-C(4)-C(5)#5	125.0(14)
C(12)-C(4)-C(5)#5	117.1(14)
C(6)-C(S)-C(4)#5	122.2(14)
C(5)-C(6)-C(7)	122(2)
C(8)-C(7)-C(11)#5	116.2(13)
C(8)-C(7)-C(6)	126(2)
C(ll)#5-C(7)-C(6)	117.3(14)
C(9)#5-C(8)-C(7)	121.9(13)
C(8)#5-C(9)-C(10)	118.6(12)
N(2)-C(10)-C(9)	123.4(14)
N(2)-C(ll)-C(12)	118.5(11)
N(2)-C(ll)-C(7)#5	121.4(11)
C(12)-C(ll)-C(7)#5	120.1(12)
N(l)-C(12)-C(4)	121.9(12)
N(l)-C(12)-C(ll)	117.2(11)
C(4)-C(12)-C(ll)	120.9(12)

Symmetry transformations used to generate equivalent atoms:
#1 -x,-y+l,-z #2 -x,-y,-z #3 -x+y+l,-x+l,z
#4 -y+l,x-y,z #5 -x+l,-y+l,-z

APPENDIX H. Crystallographic tables and figures for $[Mn(bpy)_3](I_3)_{1.5}(I_8)_{0.25}$ (2)

Table H1. Crystal data and structure refinement for 2.

Empirical formula	C30 H24 I6.5 Mn1 N6
Formula weight	1348.3
Temperature	295 K
Wavelength	0.71073 A
Crystal system	Monoclinic
Space group	C 2/c
Unit cell dimensions	a = 29.374 (6) A a = 90° b = 12.980(3) A β = 121.05°(3) c = 23.368(5) A γ = 90°.
Volume	7632(3) A^3
Z	8
Density (calculated)	2.347 Mg/m^3
Absorption coefficient	5.633 mm^-1
F(000)	4924
Crystal size	. 12 x .14 x .36 mm
Theta range for data collection	2.0 to 25.0 deg.
Index ranges	0<=h<=34, 0<=k<=15, -27<=1<=23
Reflections collected	6833
Independent reflections	6694 [R(int) = 0.0400]
Refinement method	Full-matrix least-squares on F^2
Data / restraints / parameters	2235 / 0 / 213
Goodness-of-fit on F^2	1.78
Final R indices [I>3sigma(I)]	R1 = 0.0688, wR2 = 0.0830
R indices (all data)	R1 = 0.1839, wR2 = 0.1200
Largest diff. peak and hole	1.04 and -1.25 e.A^-3

$R1 = \Sigma || F_O| - |F_C| |/\Sigma | F_O|$

$wR2 = [\Sigma\{w(F^2 - F_C^2)^2\}/\Sigma(wF_O^4)]^{1/2}$

$w^{-1} = [\sigma^2(F_O^2) + (0.0008P)^2 + 0.000P]$, $P = (F_O^2 + 2F_C^2)/3$

$S = [\Sigma\{w(F_O^2 - F_C^2)^2\}/(n-p)]^{1/2}$

Table H2. Atomic coordinates (x 10^4) and equivalent isotropic displacement parameters (A^2 x 10^3) for 2.

	x	y	z	U(eq)
Mn(l)	1842 (1)	-28(3)	-2952(8)	38(2)
N(l)	2579(6)	517 (13)	-1999(8)	25(4)
N(2)	2562(6)	-542(13)	-2952 (8)	24(4)
N(3)	1668(7)	-1354(15)	-2518(9)	43(5)
N(4)	1199(7)	-902(15)	-3831(10)	48(6)
N(5)	1247(7)	930(14)	-2849(9)	39(5)
N(6)	1680(7)	1367 (14)	-3601(9)	38(5)
C(l)	2545(8)	991(18)	-1501(11)	41(6)
C(2)	3001(10)	1361 (22)	-921(13)	66(8)
C(3)	3455(10)	1109(20)	-865(12)	51(7)
C(4)	3509(10)	640(20)	-1353(11)	50(7)
C(5)	3032(8)	364 (17)	-1923(10)	31(6)
C(6)	3029(9)	-251(19)	-2495(11)	43(7)
C(7)	3495(9)	-461(18)	-2503(11)	41(6)
C(8)	3463(10)	-970(20)	-3023(12)	58(8)
C{9)	2983(9)	-1309(19)	-3513(12)	48(7)
C(10)	2529(9)	-1052(18)	-3483(11)	43(6)
C(ll)	1891 (10)	-1565(22)	-1865(13)	61 (8)
C(12)	1745(12)	-2359(23)	-1616(15)	76(9)
C(13)	1311(12)	-2916(27)	-2021 (16)	89(10)
C(14)	1070(10)	-2720(22)	-2674(13)	60(8)
C(15)	1227(10)	-1925(21)	-2939(13)	52(7)
C(16)	985(9)	-1637(19)	-3653(12)	43(6)
C(17)	512(13)	-2073(28)	-4161 (16)	98(11)
C(18)	307(13)	-1764 (27)	-4820(17)	91(11)
C(19)	511(11)	-1092(22)	-4977 (15)	68(8)
C(20)	963(10)	-630(22)	-4481(12)	59(8)
C(21)	1044(9)	711(19)	-2480(11)	47(7)
C(22)	652(9)	1283(20)	-2500(12)	48(7)
C(23)	479(9)	2075(20)	-2890(11)	49(7)
C(24)	647(9)	2368(19)	-3293(11)	47(7)
C(25)	1066(9)	1798(18)	-3238(11)	39(6)
C(26)	1321(10)	2054(22)	-3655(12)	53(7)
C(27)	1188(11)	2856(23)	-4042(13)	65(8)
C(28)	1410(12)	3099(26)	-4428(15)	87(10)
C(29)	1802(11)	2356(22)	-4383(14)	72(9)
C(30)	1890(9)	1520(20)	-3965(11)	46(7)
I(1)	2349(1)	5595(1)	-72(1)	94(2)
I(2)	3161(1)	3393(2)	424(1)	63(1)
I(3)	3934(1)	2301(2)	876(1)	69(1)
I(4)	0	-1361(3)	7500	154(4)
I(5)	688(2)	-1361(5)	-1065(2)	245(4)
I(6)	66(2)	-5003(4)	-594(5)	565(21)
I(7)	62(3)	-4907(5)	-1875(6)	627(32)

* U(eq) is defined as one third of the trace of the orthogonalised U_{ij} tensor.

Table H3. Selected bond lengths [A] and angles [deg] for 2.

I(1)-I(2)	2.972(3)
I(2)-I(3)	2.879(3)
I(4)-I(5)#1	2.888(5)

I(6)-I(7)	2.991(20)
I(6)-I(6)#2	2.995(26)
I(7)-I(7)#3	2.749(30)
Mn(1)-N(1)	2.274(13)
Mn(l)-N(2)	2.215(21)
Mn(l)-N(3)	2.190(23)
Mn(1)-N(4)	2.252(17)
Mn(l)-N(5)	2.258(23)
Mn(l)-N(6)	2.249(19)

I(1)-I(2)-I(3)	178.7(1)
I(5)#1-I(4)-I(5)#4	180.0(3)
I(6)-I(7)-I(7)#3	173.2(5)
I(7)-I(6)-I(6)#2	173.0(3)
N(l)-Mn(l)-N(2)	70.7(7)
N(3)-Mn(l)-N(4)	74.9(7)
N(5)-Mn(1)-N(6)	73.8(8)

Symmetry transformations used to generate equivalent atoms:
#1 -x,y,-z+l/2 #2 -x,-y-l,-z #3 -x,y,-z-l/2
#4 x,y, z+1

Table H4. Anisotropic displacement parameters (A*2 x 10^3) for 2.
The anisotropic displacement factor exponent takes the form:
-2 pi*2 [h^2 a**2 U11 + ... + 2 h k a* b* U12]

	U11	U22	U33	U12	U13	U23
Mn(1)	32(2)	43(2)	41(2)	3(2)	19(2)	2(2)
I(1)	155(2)	64(2)	99(2)	31(2)	90(2)	16(1)
I(2)	84(1)	64(1)	54(1)	-16(1)	45(1)	-7(1)
I(3)	62(1)	88(2)	60(1)	-5(1)	33(1)	-8(1)
I(4)	160(4)	87(3)	278(6)	0	157(4)	0
I(5)	210(4)	328(7)	237(5)	-122(5)	142(4)	-140(5)
I(6)	43(3)	60(2)	1178(44)	2(2)	19(10)	-71(12)
I(7)	107(6)	75(3)	1429(66)	28(3)	204(25)	71(11)

Table H5. Hydrogen coordinates (x 10^4) and isotropic displacement parameters (A^2 x 10^3) for 2.

	x	y	z	U(eq)
H(1A)	2198	1094	-1564	50
H(2A)	2985	1710	-570	70
H(3A)	3800	1312	-469	60
H(4A)	3845	493	-1310	60
H(7A)	3835	-278	-2127	60
H(8A)	3774	-1066	-3052	70
H(9A)	2954	-1719	-3872	60
H(10A)	2183	-1230	-3849	60

H(11A)	2179	-1135	-1554	30
H(12A)	1962	-2534	-1152	HO
H(13A)	1177	-3429	-1851	110
H(14A)	764	-3110	-2989	80
H(17A)	339	-2594	-4040	110
H(18A)	-24	-2058	-5157	110
H(19A)	167	-892	-5434	80
H(20A)	1132	-88	-4584	70
H(21A)	1193	144	-2175	70
H(22A)	490	1091	-2249	70
H(23A)	208	2496	-2896	70
H(24A)	498	2935	-3599	70
H(27A)	926	3317	-4058	90
H(28A)	1316	3700	-4706	90
H(29A)	1986	2448	-4619	90
H(30A)	2134	1008	-3944	60

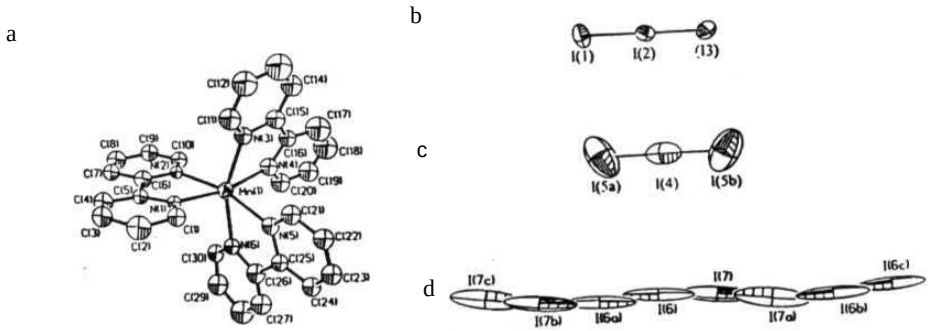

Figure 1. Views of the cation and anions in 2 (50% probability ellipsoids) at 298 K. (a) $[Mn(bpy)_3]^{2+}$ cation, (b), (c) the two crystallographically inequivalent I_3^- (a: -x, y, -z+1/2 ; b: x, -y-1, z-1/2), (d) the repeating unit of $(I_8^{2-})_n$ (a: -x, y, -z+1/2 ; b: x, -1-y, z-1/2; c: -x, -1-y, -2).

APPENDIX L Crystallographic tables for $[Cu(bpy)_3]I_8 \cdot CH_2Cl_2$ (6).

Table 11.
Crystal data and structure refinement for $[Cu(bpy)_3]I_8 \cdot CH_2Cl_2$ (6).

Crystal Data :

Structural formula	$[Cu(bpy)_3]I_8 \cdot CH_2Cl_2$	
Empirical formula	$C_{15.50}H_{13}ClCu_{0.50}I_4N_3$	
Formula weight	816.11	
Temperature	293(2) K	
Crystal system	Monoclinic	
Space group	C2/c (No.15)	
Unit cell dimensions	a =18.445(2) A	α = 90 deg.
	b = 19.951(1) A	β = 102.873(7) deg.
	c = 12.429(1) A	y = 90 deg.
Volume	4458.9(6) A^3	
Z	8	
No reflns. used for cell	25	
Cell measurement theta min/max	15.04/17.56	
Crystal shape	Rectangular	
Crystal colour	Dark brown	
Density (calculated)	2.431 Mg/m^3	
Absorption coefficient	6.178 mm^{-1}	
F(000)	2964	
Crystal size	.48 x .25 x .10 mm	

Data Collection :

Diffractometer	Enraf Nonius CAD-4
Radiation type	MoK_α
Wavelength	0.71073 A
Radiation source	Fine focus sealed tube
Monochromator	Graphite
Measurement method	Omega-2theta
Standard reflns.†	3 measured every 90 min.
Theta range for data collection	2.04 to 24.94 deg
Index ranges	-21≤h≤21, ft£k<23, 0<l<l
Reflections collected	3905
Independent reflections	3905 [R(int) - 0.0000]
Mean intensity/sigma	36.63
No. reflns.[F > 4 sigma(F)]	2660
Absorption correction	Statistical(DIFABS)
Max. and rain transmission	1.249 and 0.925

Solution and Refinement :

Atom sites soln. - primary	Patterson
Atom sites soln. - secondary	Difference fourier
Atom sites soln. - hydrogens	Geometrical
Treatment of hydrogen atoms	Riding model
Refinement method	Full-matrix least-squares on F^2

Data / restraints / parameters	3905/4/216	
Goodness-of-fit (S) [F>4sigma(F)]	0.883	
Goodness-of-fit (S) (all data)	0.915	
Final R indices [F>4sigma(F)]	R1 =0.0497	wR2 = 0.1375
R indices (all data)	R1 =0.0799	wR2 =0.1543
Maximum shift/esd	0.049	
Mean shift/esd	0.002	
Extinction coefficient	N/A	
Largest diff. peak and hole	1.586 and -0.992 e.Å^{-3}	

Computer Programs :

Data collection	CAD-4 system
Cell refinement	CAD-4 system
Data reduction	CAD-4 system
Structure solution	SHELXS-97
Structure refinement	SHELXL-97
Molecular graphics	ORTEP
Publication material	SHELXL-97

$R1 = \Sigma||F_o| - |F_c||/\Sigma|F_o|$

$wR_2 = [\Sigma\{w(F_o^2 - F_c^2)^2\}/\Sigma(wF_o^4)]^{1/2}$

$w^{-1} = [\sigma^2(F^2) + (0.0982P)^2 + 47.9340P]$, $P = (F_o^2 + 2F_c^2)/3$

$S = [\Sigma\{w(F_o^2 - F_c^2)^2\}/(n-p)]^{1/2}$

† The crystal showed a 15% decay of the standard reflection intensities. Hence, a decay correction was applied.

Table 12.

Atomic coordinates (x 10^4) and equivalent isotropic displacement parameters (Å^2 x 10^3) for 6. U(eq) is defined as one third of the trace of the orthogonalized Uij tensor.

	x	y	z	U(eq)
I(1)	1888(1)	9(1)	220(1)	114(1)
I(2)	2320(1)	-949(1)	1965(1)	78(1)
I(3)	2728(1)	-1984(1)	3713(1)	83(1)
I(4)	4316(1)	-2178(1)	2797(1)	73(1)
Cu	0	3403(1)	7500	46(1)
N(l)	-1192(3)	3346(3)	7830(5)	53(2)
N(2)	80(3)	2670(3)	8666(5)	53(2)
N(3)	320(3)	4181(3)	8552(4)	47(1)
C(l)	-1782(4)	3747(4)	7474(7)	64(2)
C(2)	-2369(5)	3773(5)	7998(9)	80(3)
C(3)	-2358(5)	3386(5)	8911(8)	84(3)
C(4)	-1762(5)	2960(4)	9258(7)	66(2)
C(5)	-530(6)	1916(4)	9628(7)	73(3)
C(6)	87(7)	1515(5)	9872(8)	87(3)
C(7)	707(6)	1708(4)	9506(8)	78(3)
C(8)	680(5)	2286(4)	8938(7)	65(2)
C(9)	-537(4)	2503(4)	9032(6)	55(2)
C(10)	-1202(4)	2947(4)	8698(6)	52(2)

C(ll)	720(4)	4121(4)	9566(6)	53(2)
C(12)	1034(5)	4691(5)	10187(7)	67(2)
C(13)	942(5)	5288(5)	9669(8)	74(3)
C(14)	528(5)	5356(4)	8634(7)	61(2)
C(15)	217(4)	4787(3)	8077(6)	46(2)
Cl(1) (0.50)	473(4)	-87(4)	2036(6)	116(2)
Cl(2) (0.50)	530(5)	913(4)	2601(8)	145(3)
C(16)(0.50)	651(7)	183(6)	3352(10)	39(3)

*The site occupation factors of the disordered sites are given after the respective atom labels.

Table I3.
Bond lengths [A] and angles [deg] for 6.

Bond distances :			
I(1)-I(2)	2.8663(11)	I(2)-I(3)	2.9703(10)
I(3)-I(4)	3.3919(10)	I(4)-I(4)#1	2.7827(13)
Cu-N(3)	2.031(6)	Cu-N(3)#2	2.031(6)
Cu-N(2)	2.041(6)	Cu-N(2)#2	2.041(6)
Cu-N(1)#2	2.327(6)	Cu-N(:)	2.327(6)
N(1)-C(10)	1.344(10)	N(1)-C(1)	1.345(10)
N(2)-C(8)	1.326(10)	N(2)-C(9)	1.359(10)
N(3)-C(11)	1.316(9)	N(3)-C(15)	1.340(9)
C(1)-C(2)	1.384(12)	C(2)-C(3)	1.369(14)
C(3)-C(4)	1.380(13)	C(4)-C(10)	1.369(11)
C(5)-C(6)	1.369(14)	C(5)-C(9)	1.384(11)
C(6)-C(7)	1.376(15)	C(7)-C(8)	1.346(12)
C(9)-C(10)	1.495(11)	C(11)-C(12)	1.423(11)
C(12)-C(13)	1.346(13)	C(13)-C(14)	1.348(12)
C(14)-C(15)	1.386(10)	C(15)-C(15)#2	1.478(14)
Cl(1)-C(16)	1.683(14)	Cl(2)-C(16)	1.717(15)

Bond angles :			
I(1)-I(2)-I(3)	177.61(3)	I(2)-I(3)-I(4)	86.04(2)
I(4)#1-I(4)-I(3)	172.20(2)	N(3)-Cu-N(3)#2	80.3(3)
N(3)-Cu-N(2)	97.3(2)	N(3)#2-Cu-N(2)	165.9(2)
N(3)-Cu-N(2)#2	165.9(2)	N(3)#2-Cu-N(2)#2	97.3(2)
N(2)-Cu-N(2)#2	88.4(3)	N(3)-Cu-N(1)#2	90.0(2)
N(3)#2-Cu-N(1)#2	94.3(2)	N(2)-Cu-N(1)#2	99.6(2)
N(2)#2-Cu-N(1)#2	76.2(2)	N(3)-Cu-N(1)	94.3(2)
N(3)#2-Cu-N(1)	90.0(2)	N(2)-Cu-N(1)	76.2(2)
N(2)#2-Cu-N(1)	99.6(2)	N(1)#2-Cu-N(1)	174.3(3)
C(10)-N(1)-C(1)	117.5(6)	C(10)-N(1)-Cu	110.7(5)
C(1)-N(1)-Cu	129.8(5)	C(8)-N(2)-C(9)	119.1(7)
C(8)-N(2)-Cu	121.3(6)	C(9)-N(2)-Cu	118.7(5)
C(11)-N(3)-C(15)	119.9(6)	C(11)-N(3)-Cu	124.5(5)
C(15)-N(3)-Cu	114.4(4)	N(1)-C(1)-C(2)	121.9(8)
C(3)-C(2)-C(1)	120.0(9)	C(2)-C(3)-C(4)	118.0(9)
C(10)-C(4)-C(3)	119.5(8)	C(6)-C(5)-C(9)	121.4(9)

C(5>C(6)-C(7)	118.3(8)	C(8)-C(7)-C(6)	118 5(9)
N(2)-C(8)-C(7)	124.1(9)	N(2)-C(9)-C(5)	118.6(8)
N(2)-C(9)-C(10)	117.3(6)	C(5)-C(9)-C(10)	124.0(8)
N(1)-C(10)-C(4)	123.0(7)	N(1)-C(10)-C(9)	114.6(6)
C(4)-C(10)-C(9)	122.4(7)	N(3)-C(11)-C(12)	121.4(7)
C(13)-C(12)-C(11)	117.0(8)	C(12)-C(13)-C(14)	122.0(8)
C(13)-C(14)-C(15)	118.6(8)	N(3)-C(15)-C(14)	121.1(6)
N(3)-C(15)-C(15)#2	114.8(4)	C(14)-C(15)-C(15)#2	124.0(5)
Cl(1)-C(16)-Cl(2)	76.7(6)		

Symmetry transformations used to generate equivalent atoms:
#1 -x+1, y, -z+1/2 #2 -x, y, -z+3/2

Table 14.
Anisotropic displacement parameters ($A^2 * 10^3$) for 6

	U11	U22	U33	U23	U13	U12
I(1)	137(1)	98(1)	102(1)	10(1)	17(1)	40(1)
I(2)	67(1)	83(1)	82(1)	-17(1)	12(1)	0(1)
I(3)	67(1)	97(1)	85(1)	10(1)	15(1)	-19(1)
I(4)	85(1)	64(1)	71(1)	7(1)	19(1)	-6(1)
Cu	50(1)	44(1)	46(1)	0	15(1)	0
N(l)	49(3)	59(4)	55(3)	-1(3)	20(3)	4(3)
N(2)	60(3)	46(3)	55(3)	3(3)	19(3)	-2(3)
N(3)	49(3)	54(3)	39(3)	-5(3)	13(2)	-1(3)
C(l)	61(4)	67(5)	68(5)	1(4)	25(4)	3(4)
C(2)	61(5)	69(5)	117(8)	-3(5)	34(5)	0(4)
C(3)	77(5)	92(7)	96(6)	-6(5)	50(5)	-9(5)
C(4)	72(5)	71(5)	63(5)	-3(4)	32(4)	-11(4)
C(5)	94(6)	64(5)	63(5)	13(4)	18(5)	-17(5)
C(6)	128(8)	50(5)	74(6)	17(4)	4(6)	4(5)
C(7)	102(7)	47(4)	82(6)	8(4)	16(5)	8(5)
C(8)	71(5)	61(5)	67(5)	8(4)	20(4)	9(4)
C(9)	63(4)	57(4)	47(4)	0(3)	18(3)	-12(4)
C(10)	56(4)	47(4)	56(4)	-9(3)	20(3)	-7(3)
C(ll)	60(4)	55(4)	45(4)	-1(3)	13(3)	-1(3)
C(12)	61(5)	75(5)	61(5)	-2(4)	4(4)	12(4)
C(13)	75(5)	67(5)	75(6)	-25(5)	7(5)	-5(5)
C(14)	71(5)	47(4)	67(5)	-5(4)	22(4)	-10(4)
C(15)	49(3)	42(3)	53(4)	-7(3)	25(3)	-1(3)

The anisotropic displacement factor exponent takes the form:
$-2K\ [h^2 a^{*2} U_{11} + \ldots + 2hka^*b^* U_{12}]$

Table 15.
Hydrogen coordinates (× 10) and isotropic displacement parameters (A^2 × 10) for 6.

	x	y	z	U(eq)
H(l)	-1795	4016	6858	95
H(2)	-2772	4053	7729	120
H(3)	-2740	3410	9287	125
H(4)	-1742	2684	9867	99
H(5)	-954	1791	9868	110
H(6)	88	1123	10276	130
H(7)	1134	1446	9647	117
H(8)	1108	2424	8723	98
H(ll)	800	3698	9882	80
H(12)	1291	4653	10918	101
H(13)	1170	5665	10037	110
H(14)	454	5775	8302	91

Hydrogen atoms are labelled according to the atom to which they are attached. All hydrogens were refined using the riding model (the positional parameters of the riding atoms have same e.s.ds as the atom on which they ride). All hydrogens were assigned fixed U(iso) values (= 1.5 x U(iso) of the atom to which they are attached.)

Table 16. Selected torsion angles and least square planes for 6

Selected torsion angles:

90.91 (0.04) 12 - I3 - I3_$l - I2_$1
93.21 (0.02) I1 - I3 - I3_$l - I1 $1

Least-squares planes (x,y,z in crystal coordinates) and deviations from them
(• indicates atom used to define plane)

5.7514 (0.0043) x + 14.2343 (0.0029) y + 6.7396 (0.0029) z = 1.2673 (0.0011)

* -0.0205 (0.0003) I1
• 0.0403 (0.0006) I2
* -0.0197(0.0003) I3
• -0.0001 (0.0000) I4

Rms deviation of fittjed atoms = 0.0246

5.7514 (0.0043) x - 14.2343 (0.0029) y + 6.7396 (0.0029) z= 7.8539 (0.0027)

Angle to previous plane (with approximate esd) = 88.97 (0.02)

* 0.0205(0.0003) I1_$1
* -0.0403 (0.0006) I2_$1
* 0.0197(0.0003) I3_$1
* 0.0001 (0.0000) I4_$1

Rms deviation of fitted atoms = 0.0246

6.3925 (0.0604) x + 14.3971 (0.0494) y + 6.3017 (0.0375) z - 8.9702 (0.0336)

* 0.0176(0.0051) N1
* -0.0044(0.0059) C1
* -0.0108 (0.0067) C2
* 0.0132(0.0068) C3
* -0.0001 (0.0061) C4
* -0.0154(0.0053) C10

Rms deviation of fitted atoms = 0.0120

2.6420 (0.0676) x + 10.2004 (0.0599) y + 9.8708 (0.0270) z = 11.3172 (0.0172)

Angle to previous plane (with approximate esd) =22.12 (0.44)

* -0.0183 (0.0051) N2
* 0.0095 (0.0054) C9
* 0.0007 (0.0062) C5
* -0.0029(0.0066) C6
* -0.0056 (0.0066) C7
* 0.0166 (0.0060) C8

Rms deviation of fitted atoms = 0.0111

- 17.1154 (0.0231) x + 2.5968 (0.0672) y + 6.8023 (0.0348) z = 6.3575 (0.0433)

Angle to previous plane (with approximate esd) - 76.72 (0.27)

* -0.0021 (0.0048) N3
* -0.0119 (0.0055) C11
* 0.0210(0.0061) C12
* -0.0166 (0.0066) C13
* 0.0022 (0.0059) C14
* 0.0074(0.0051) C15

Rms deviation of fitted atoms = 0.0124

- 17.1154 (0.0231) x - 2.5968 (0.0672) y + 6.8023 (0.0348) z = 3.8459 (0.0392)

Angle to previous plane (with approximate esd) = 14.96 (0.28)

* 0.0021 (0.0048) N3_$2
• 0.0119(0.0055) C11 $2
• -0.0210 (0.0061) C12_$2
• 0.0166 (0.0066) C13 $2
* -0.0022 (0.0059) C14_$2
* -0.0074(0.0051) C15 $2

Rms deviation of fitted atoms = 0.0124

$1 -x+1, y, -z+1/2
$2 -x, y, -z+3/2

APPENDIX J. Crystallographic tables for $[Fe(bpy)_3]I_9$ (8).

Table J1.
Crystal data and structure refinement for $[Fe(bpy)_3]I_9$ (8).

Crystal Data :

Structural formula	$[Fe(bpy)_3]I_9$	
Empirical formula	$C_{30}H_{24}FeI_9N_6$	
Formula weight	1666.50	
Melting point	445 K	
Temperature	293(2) K	
Crystal system	Monoclinic	
Space group	$P\ 2_1/c$ (No.14)	
Unit cell dimensions	a= 12.237(4) A	a = 90 deg.
	b = 22.496(4) A	β = 109.94(3) deg.
	c= 15.779(5) A	y = 90 deg.
Volume	4083(2) A^3	
Z	4	
No. reflns. used for cell	25	
Cell measurement theta min/max	9.74/14.07	
Crystal shape	Rectangular rods	
Crystal colour	Dark, shining green	
Density (calculated)	2.711 Mg/m^3	
Absorption coefficient	7.204 mm^{-1}	
F(000)	2996	
Crystal size	.40 x .25 x .15 mm	

Data Collection :

Diffractometer	Enraf Nonius CAD-4
Radiation type	MoK_α
Wavelength	0.71073 A
Radiation source	Fine focus sealed tube
Monochromator	Graphite
Measurement method	Omega-2theta
Standard reflns.†	2 measured every 60 min.
Theta range for data collection	2.04 to 25.00 deg.
Index ranges	$0 \le h \le 10$,† $0 \le k \le 26$, $-18 \le l \le 17$
Reflections collected†	6542
Independent reflections	6094 [R(int) = 0.0336]
Mean intensity/sigma	24.33
No. reflns. [F > 4 sigma(F)]	4222
Absorption correction	Statistical (DIFABS)
Max. and min. transmission	1.21 and 0.923

Solution and Refinement :

Atom sites soln. - primary	Patterson
Atom sites soln. - secondary	Difference fourier
Atom sites soln. - hydrogens	Geometrical
Treatment of hydrogen atoms	Riding model

Refinement method	Full-matrix least-squares on F^2
Extinction method	empirical
Data / restraints / parameters	5529 / 0 / 450
Goodness-of-fit (S) [F>4sigma(F)]	1.140
Goodness-of-fit (S) (all data)	1.213
Final R indices [F>4sigma(F)]	R1 = 0.0629 wR2 = 0.1266
R indices (all data)	R1 = 0.1033 wR2 = 0.1600
Maximum shift/esd	-0.021
Mean shift/esd	0.001
Extinction coefficient	0.0007(2)
Largest diff. peak and hole	1.683 and -1.277 e.$Å^{-3}$

Computer Programs :

Data collection	CAD-4 system
Cell refinement	CAD-4 system
Data reduction	CAD-4 system
Structure solution	SHELXS-86
Structure refinement	SHELXL-93
Molecular graphics	ORTEP
Publication material	SHELXL-93

$R1 = \Sigma||F_o| - |F_c||/\Sigma|F_o|$

$wR_2 = [\Sigma\{w(F_o^2 - F_c^2)^2\}/\Sigma(wF_o^4)]^{1/2}$

$w^{-1} = [\sigma^2(F_o^2) + (0.0982P)^2 + 91.6184P]$, $P = (F_o^2 + 2F_c^2)/3$

$S = [\Sigma\{w(F_o^2 - F_c^2)^2\}/(n-p)]^{1/2}$

† The crystal showed a decay of 50% with time. By then, about 90% of the data was collected and a decay correction was applied

Table J2.
Atomic coordinates (x 10^4) and equivalent isotropic displacement parameters (A^2 x 10^3) for 8. U(eq) is defined as one third of the trace of the orthogonalized Uij tensor.

	x	y	z	U(eq)
I(1)	1136(1)	527(1)	772(1)	71(1)
I(2)	2194(1)	1423(1)	2080(1)	48(1)
1(3)	3044(1)	2429(1)	3413(1)	58(1)
I(4)	4043(1)	3613(1)	4929(1)	67(1)
I(5)	5166(1)	4446(1)	6206(1)	58(1)
I(6)	6417(1)	5540(1)	7720(1)	68(1)
1(7)	4225(1)	5324(1)	8432(1)	56(1)
I(8)	2528(1)	5074(1)	9137(1)	84(1)
l(9A)(0.50)	8697(2)	5213(1)	9148(2)	68(1)
I(9B)(0.50)	9243(3)	5227(1)	9574(2)	81(1)
Fe	-1907(1)	2529(1)	989(1)	26(1)
N(l)	-3344(7)	2584(4)	1272(5)	28(2)
N(2)	-2705(7)	3132(4)	100(5)	25(2)
N(3)	-2561(8)	1868(4)	156(6)	34(3)
N(4)	-1248(8)	1868(4)	1830(5)	32(2)
N(5)	-476(7)	2557(4)	693(5)	25(2)

N(6)	-1096(7)	3147(4)	1838(5)	28(2)
C(l)	-3599(10)	2273(5)	1904(7)	34(3)
C(2)	-4619(10)	2370(6)	2096(7)	43(4)
C(3)	-5373(10)	2777(6)	1596(8)	42(3)
C(4)	-5134(10)	3102(6)	941(7)	43(4)
C(5)	-4133(10)	2980(5)	769(7)	32(3)
C(6)	-3777(9)	3274(4)	82(6)	26(3)
C(7)	-4497(11)	3663(5)	-560(8)	44(4)
C(8)	-4112(10)	3909(5)	-1210(7)	34(3)
C(9)	-2999(12)	3777(5)	-1168(7).	48(4)
C(10)	-2314(11)	3400(5)	-515(7)	39(3)
C(ll)	-3239(10)	1905(6)	-693(7)	40(3)
C(12)	-3628(11)	1419(5)	-1255(8)	45(4)
C(13)	-3285(10)	866(5)	-898(8)	41(3)
C(14)	-2595(11)	811(5)	-5(8)	43(3)
C(15)	-2243(9)	1322(5)	518(7)	31(3)
C(16)	-1496(9)	1323(5)	1445(7)	34(3)
C(17)	-1078(12)	812(6)	1953(8)	56(4)
C(18)	-355(12)	862(6)	2837(8)	57(4)
C(19)	-105(12)	1424(6)	3206(8)	52(4)
C(20)	-547(10)	1908(6)	2682(7)	42(3)
C(21)	-216(9)	2233(5)	68(7)	34(3)
C(22)	792(11)	2305(6)	-97(7)	46(4)
C(23)	1576(10)	2727(6)	352(7)	44(4)
C(24)	1336(9)	3053(5)	1003(7)	34(3)
C(25)	329(10)	2960(5)	1166(7)	36(3)
C(26)	-27(10)	3281(4)	1838(7)	31(3)
C(27)	699(11)	3688(5)	2452(8)	43(4)
C(28)	278(12)	3976(6)	3045(8)	55(4)
C(29)	-833(11)	3852(6)	3031(8)	47(4)
C(30)	-1478(11)	3445(5)	2421(8)	44(4)

*The site occupation factors of disordered sites are given after the respective atom labels.

Table J3.
Anisotropic displacement parameters (A × 10) **for 8**.

	U11	U22	U33	U23	U13	U12
I(1)	86(1)	54(1)	77(1)	-14(1)	33(1)	-2(1)
I(2)	48(1)	49(1)	49(1)	4(1)	20(1)	6(1)
I(3)	56(1)	70(1)	44(1)	-6(1)	14(1)	3(1)
I(4)	65(1)	78(1)	58(1)	1(1)	22(1)	7(1)
I(5)	60(1)	60(1)	57(1)	9(1)	23(1)	16(1)
I(6)	41(1)	81(1)	76(1)	-4(1)	12(1)	-13(1)
I(7)	64(1)	45(1)	56(1)	-2(1)	15(1)	4(1)
I(8)	80(1)	88(1)	90(1)	-29(1)	37(1)	-29(1)
I(9A)	93(2)	43(1)	90(1)	-2(1)	61(1)	-9(1)
I(9B)	112(2)	71(2)	72(1)	13(1)	49(1)	21(1)

Fe	21(1)	28(1)	28(1)	0(1)	6(1)	-2(1)
N(l)	15(5)	30(5)	34(4)	-6(4)	2(4)	-3(4)
N(2)	17(5)	34(5)	24(4)	0(4)	6(3)	6(4)
N(3)	24(5)	38(5)	38(5)	-6(4)	8(4)	-6(4)
N(4)	27(5)	40(5)	30(4)	8(4)	8(4)	-3(4)
N(5)	18(5)	28(5)	30(4)	2(4)	8(3)	6(4)
N(6)	24(5)	29(5)	37(4)	-4(4)	20(4)	-9(4)
C(l)	23(7)	41(7)	42(6)	11(5)	17(5)	0(5)
C(2)	34(8)	65(8)	33(5)	1(6)	15(5)	-17(6)
C(3)	14(7)	55(8)	52(7)	-15(6)	7(5)	-4(6)
C(4)	33(8)	56(8)	37(6)	2(6)	8(5)	10(6)
C(5)	23(7)	32(6)	38(6)	-10(5)	6(5)	1(5)
C(6)	26(7)	25(5)	22(5)	-7(4)	2(4)	-15(5)
C(7)	40(8)	36(7)	46(7)	1(5)	4(6)	6(6)
C(8)	42(7)	25(6)	35(5)	8(5)	11(5)	3(5)
C(9)	73(10)	27(6)	35(6)	5(5)	5(6)	-14(6)
C(10)	28(7)	37(6)	49(6)	-10(5)	8(5)	-9(6)
C(11)	36(7)	45(7)	33(6)	-3(5)	4(5)	-3(6)
C(12)	44(8)	39(7)	44(6)	0(6)	5(6)	-2(6)
C(13)	39(7)	34(6)	56(7)	-21(5)	24(6)	-9(6)
C(14)	61(8)	26(6)	48(6)	-7(5)	24(6)	-19(6)
C(15)	27(7)	31(6)	38(5)	7(5)	14(5)	4(5)
C(16)	24(7)	30(6)	48(6)	3(5)	12(5)	16(5)
C(17)	64(9)	49(8)	50(7)	14(6)	13(7)	11(7)
C(18)	57(9)	63(9)	55(7)	25(7)	25(6)	18(7)
C(19)	57(9)	56(8)	43(6)	20(6)	17(6)	6(7)
C(20)	44(8)	41(7)	41(6)	-4(5)	13(5)	-4(6)
C(21)	18(7)	37(6)	40(6)	6(5)	2(5)	-7(5)
C(22)	46(8)	64(8)	27(5)	-6(6)	12(5)	9(7)
C(23)	9(7)	81(10)	43(6)	5(6)	11(5)	-3(6)
C(24)	3(6)	57(8)	42(6)	-4(5)	8(5)	-8(5)
C(25)	27(7)	35(6)	37(6)	2(5)	0(5)	2(5)
C(26)	44(8)	15(5)	30(5)	1(4)	6(5)	-12(5)
C(27)	20(7)	50(8)	55(7)	-3(6)	9(5)	-5(6)
C(28)	63(9)	51(8)	57(7)	-25(6)	27(7)	-26(7)
C(29)	37(8)	59(8)	58(7)	-18(6)	31(6)	6(7)
C(30)	32(8)	44(7)	52(7)	-13(6)	10(6)	2(6)

The anisotropic displacement factor exponent takes the form:
$-2\pi^2[h\ a^*\ U11 + ... + 2hka^*b^*U12]$

Table J4.
Bond lengths [A] and angles [deg] for **8**

Bond distances :

I(1)-I(2)	2.8585(14)	I(2)-I(3)	3.0232(14)
I(3)-I(4)	3.509(2)	I(4)-I(5)	2.752(2)
I(5)-I(6)	3.408(2)	I(6)-I(9A)	3.019(3)
](6)-I(7)	3.277(2)	I(7)-I(8)	2.729(2)
I(8)-I(9B)#1	3.507(3)	I(9A)-I(9B)#2	2.817(4)

I(9A)-I(9A)#2	3.531(5)	I(9B)-I(9A)#2	2.817(4)
Fe-N(6)	1.950(8)	Fe-N(2)	1.956(8)
Fe-N(l)	1.960(9)	Fe-N(5)	1.961(9)
Fe-N(3)	1.966(9)	Fe-N(4)	1.974(9)
N(1)-C(1)	1.339(14)	N(1)-C(5)	1.353(13)
N(2)-C(6)	1.340(14)	N(2)-C(10)	1.36(2)
N(3)-C(11)	1.315(13)	N(3)-C(15)	1.355(14)
N(4)-C(20)	1.328(13)	N(4)-C(16)	1.355(14)
N(5)-C(21)	1.348(14)	N(5)-C(25)	1.360(13)
N(6)-C(26)	1.343(14)	N(6)-C(30)	1.35(2)
C(l)-C(2)	1.40(2)	C(2)-C(3)	1.35(2)
C(3)-C(4)	1.38(2)	C(4)-C(5)	1.37(2)
C(5)-C(6)	1.46(2)	C(6)-C(7)	1.40(2)
C(7)-C(8)	1.38(2)	C(8)-C(9)	1.37(2)
C(9)-C(10)	1.38(2)	C(11)-C(12)	1.38(2)
C(12)-C(13)	1.37(2)	C(13)-C(14)	1.38(2)
C(14)-C(15)	1.40(2)	C(15)-C(16)	1.436(14)
C(16)-C(17)	1.39(2)	C(17)-C(18)	1.38(2)
C(18)-C(19)	1.38(2)	C(19)-C(20)	1.36(2)
C(21)-C(22)	1.35(2)	C(22)-C(23)	1.36(2)
C(23)-C(24)	1.37(2)	C(24)-C(25)	1.36(2)
C(25)-C(26)	1.46(2)	C(26)-C(27)	1.41(2)
C(27)-C(28)	1.37(2)	C(28)-C(29)	1.38(2)
C(29)-C(30)	1.37(2)		

Bond angles :

I(1)-I(2)-I(3)	173.59(4)	I(7)-I(6)-I(5)	84.77(4)
I(2)-I(3)-I(4)	178.88(4)	I(8)-I(7)-I(6)	174.77(5)
I(5)-I(4)-I(3)	170.71(5)	I(7)-I(8)-I(9B)#1	169.48(6)
I(4)-I(5)-I(6)	176.29(4)	I(9B)#2-I(9A)-I(6)	173.50(9)
I(9A)-I(6)-I(7)	111.37(6)	I(9B)#2-I(9A)-I(9A)#2	5.23(7)
I(9A)-I(6)-I(5)	115.26(6)	I(6)-I(9A)-I(9A)#2	177.65(12)
N(6)-Fe-N(2)	90.7(3)	N(2)-Fe-N(3)	93.2(3)
N(6)-Fe-N(1)	94.8(4)	N(1)-Fe-N(3)	90.4(4)
N(2)-Fe-N(1)	81.5(4)	N(5)-Fe-N(3)	93.3(4)
N(6)-Fe-N(5)	81.6(4)	N(6)-Fe-N(4)	94.6(3)
N(2)-Fe-N(5)	94.4(4)	N(2)-Fe-N(4)	173.9(4)
N(1)-Fe-N(5)	174.6(4)	N(1)-Fe-N(4)	95.0(4)
N(6)-Fe-N(3)	173.9(4)	N(5)-Fe-N(4)	89.4(4)
N(3)-Fe-N(4)	81.9(4)	C(1)-N(1)-C(5)	118.6(10)
C(1)-N(1)-Fe	126.3(7)	C(8)-C(9)-C(10)	120.6(12)
C(5)-N(1)-Fe	115.1(8)	N(2)-C(10)-C(9)	122.3(12)
C(6)-N(2)-C(10)	117.3(9)	N(3)-C(11)-C(12)	124.2(11)
C(6)-N(2)-Fe	115.2(7)	C(13)-C(12)-C(11)	117.5(10)
C(10)-N(2)-Fe	127.4(8)	C(12)-C(13)-C(14)	119.8(11)
C(11)-N(3)-C(15)	118.5(10)	C(13)-C(14)-C(15)	119.2(11)
C(11)-N(3)-Fe	127.2(8)	N(3)-C(15)-C(14)	120.8(9)
C(15)-N(3)-Fe	114.2(7)	N(3)-C(15)-C(16)	114.8(9)
C(20)-N(4)-C(16)	119.0(9)	C(14)-C(15)-C(16)	124.4(10)
C(20)-N(4)-Fe	127.1(8)	N(4)-C(16)-C(17)	120.3(10)

C(16)-N(4)-Fe	113.7(6)	N(4)-C(16)-C(15)	115.2(9)
C(21)-N(5)-C(25)	117.1(10)	C(17)-C(16)-C(15)	124.4(11)
C(21)-N(5)-Fe	127.6(7)	C(18)-C(17)-C(16)	1198(13)
C(25)-N(5)-Fe	115.4(8)	C(17)-C(18)-C(19)	118.4(12)
C(26)-N(6)-C(30)	117.0(9)	C(20)-C(19)-C(18)	119.4(11)
C(26)-N(6)-Fe	115.3(7)	N(4)-C(20)-C(19)	122.9(12)
C(30)-N(6)-Fe	127.7(8)	N(5)-C(21)-C(22)	122.2(10)
N(1)-C(1)-C(2)	122.1(10)	C(21)-C(22)-C(23)	120.6(12)
C(3)-C(2)-C(1)	117.6(11)	C(22)-C(23)-C(24)	117.9(12)
C(2)-C(3)-C(4)	121.4(12)	C(25)-C(24)-C(23)	120.0(11)
C(5)-C(4)-C(3)	118.4(11)	C(24)-C(25)-N(5)	122.1(11)
N(1)-C(5)-C(4)	121.6(11)	C(24)-C(25)-C(26)	125.1(10)
N(1)-C(5)-C(6)	113.6(10)	N(5)-C(25)-C(26)	112.8(10)
C(4)-C(5)-C(6)	1248(10)	N(6)-C(26)-C(27)	122.1(11)
N(2)-C(6)-C(7)	122.2(10)	N(6)-C(26)-C(25)	114.8(9)
N(2)-C(6)-C(5)	114.5(9)	C(27)-C(26)-C(25)	123.1(11)
C(7)-C(6)-C(5)	123.3(11)	C(28)-C(27)-C(26)	118 8(12)
C(8)-C(7)-C(6)	119.9(12)	C(27)-C(28)-C(29)	119.3(12)
C(9)-C(8)-C(7)	117.5(10)	C(30)-C(29)-C(28)	118.4(12)
N(6)-C(30)-C(29)	124.3(12)		

Symmetry transformations used to generate equivalent atoms:
#1 -x+1,-y+1,-z+2 **#2 -x+2, -y+1, -z+2**

Table J5.
Hydrogen coordinates (× 10) and isotropic displacement parameters (A × 10) **for 8**.

	x	y	z	U(eq)
H(l)	-3082(10)	1983(5)	2226(7)	95(53)
H(2)	-4771(10)	2161(6)	2552(7)	72(44)
H(3)	-6070(10)	2840(6)	1696(8)	39(33)
H(4)	-5639(10)	3398(6)	623(7)	8(22)
H(7)	-5233(11)	3755(5)	-550(8)	91(54)
H(8)	-4588(10)	4154(5)	-1659(7)	104(56)
H(9)	-2705(12)	3944(5)	-1586(7)	69(44)
H(10)	-1557(11)	3326(5)	-493(7)	49(37)
H(ll)	-3471(10)	2281(6)	-930(7)	26(28)
H(12)	-4106(11)	1467(5)	-1852(8)	98(53)
H(13)	-3515(10)	530(5)	-1257(8)	21(25)
H(14)	-2367(11)	437(5)	246(8)	137(73)
H(17)	-1286(12)	439(6)	1696(8)	146(79)
H(18)	-44(12)	526(6)	3177(8)	104(57)
H(19)	361(12)	1471(6)	3806(8)	205(108)
H(20)	-349(10)	2284(6)	2932(7)	31(29)
H(21)	-746(9)	1950(5)	-260(7)	42(32)
H(22)	951(11)	2065(6)	-520(7)	66(41)
H(23)	2252(10)	2793(6)	221(7)	46(35)
H(24)	1864(9)	3336(5)	1333(7)	59(39)
H(27)	1449(11)	3760(5)	2457(8)	6(22)

H(28)	737(12)	4252(6)	3451(8)	31(29)
H(29)	-1135(11)	4041(6)	3426(8)	27(28)
H(30)	-2231(11)	3370(5)	2409(8)	27(29)

Hydrogen atoms are labelled according to the atom to which they are attached. All hydrogens were refined using the riding model (the positional parameters of the riding atoms have same e.s.ds as the atom on which they ride). All hydrogens were refined freely for U(iso) values.

Table J6. Selected least square planes for 8

Least-squares planes (x,y,z in crystal coordinates) and deviations from them
(* indicates atom used to define plane)

4.6504 x- 15.0120 y+ 7.4561 z = 0.3252

* -0.0130 I1
• 0.1099 I2
• -0.0111 I3
* -0.1939 I4
• 0.0310 I5
• 0.0985 I6
• -0.0665 I7
* 0.0451 I8

Rms deviation of fitted atoms • 0.0916

2.0531 x+ 21.7449 y+ 1.9699 z= 14.8954

Angle to previous plane = 62.79

• -0.0103 I6
• 0.0278 I9A
• -0.0278 I9A_$1
* 0.0103 I6 $ 1

Rms deviation of fitted atoms = 0.0210

- 0.4954 x+ 21.5001 y+ 4.5307 z = 15.0511

* 0.0225 I7
* -0.1178 I8
* 0.0633 I6
* -0.0979 I9A
0.1009 I9B
* 0.0979 I9A_$2
-0.1009 I9B $2

* -0.0633 16_$2
* -0.0225 17_$2
* 0.1178 18_$2

Rms deviation of fitted atoms = 0.0836

12.0382 x- 1.8144 y- 7.6691 z = 0.6595

Angle to previous plane = 80.28

* 0.0201 I1
* 0.1282 12
* -0.0535 I3
* -0.2273 I4
* -0.0067 I5
* 0.1392 I6

Rms deviation of fitted atoms = 0.1230

- 12.0382 x+ 1.8145 y+ 7.6690 z= 5.7738

Angle to previous plane = 0.00

* 0.0201 Il_$2
* 0.1282 I2_$2
* -0.0535 I3_$2
* -0.2273 I4_$2
* -0.0067 I5_$2
* 0.1392 16 $2

Rms deviation of fitted atoms = 0.1230

3.0020 x+ 15.8283 y+ 8.5723 z= 4.1583

* 0.0186 N1
* -0.0086 C1
* 0.0032 C2
* -0.0075 C3
* 0.0173 C4
* -0.0230 C5

Rms deviation of fitted atoms = 0.0148

1.9369 x+ 17.4251 y+ 8.2313 z = 5.0359

Angle to previous plane =7.16

* -0.0200 N2
* 0.0048 C6
* 0.0139 C7
* -0.0175 C8
* 0.0025 C9
* 0.0164 C10

Rms deviation of fitted atoms = 0.0141

- 11.7731 x - 1.1506y+ 9.1485 z= 2.9550

Angle to previous plane = 88.40

* -0.0122 N3
* 0.0052 C11
* 0.0057 C12
* -0.0094 C13
* 0.0023 C14
* 0.0084 C15

Rms deviation of fitted atoms = 0.0079

- 11.7128 x- 0.7743 y+ 9.4127 z = 3.0255

Angle to previous plane = 1.50

* 0.0141 N4
* -0.0158 C16
* 0.0119 C17
* -0.0060 C18
* 0.0041 C19
* -0.0083 C20

Rms deviation of fitted atoms • 0.0109

- 2.7697 x + 15.4728 y- 9.0127 z= 3.4505

Angle to previous plane = 89.70

• 0.0120 N5
* 0.0021 C21
* -0.0158 C22
• 0.0155 C23
• -0.0016 C24
• -0.0122 C25

Rms deviation of fitted atoms = 0.0115

- 1.7569 x+ 16.3952 y- 9.1582 z= 3.6841

Angle to previous plane = 5.42

* -0.0162 N6
• 0.0161 C26
• -0.0066 C27
• -0.0027 C28
• 0.0026 C29
• 0.0068 C30

Rms deviation of fitted atoms = 0.0102

$1 : -x+2,-y+1,-z+2
$2: -x+1, -y+1, -z+2

APPENDIX K. Crystallographic tables and figures for $[Zn(bpy)_3]I_{12}$ (9).

Table K1.
Crystal data and structure refinement for $[Zn(bpy)_3]I_{12}$ *(9).*

Crystal Data :

Structural formula	$[Zn(bpy)_3]I_{12}$	
Empirical formula	$C_{30}H_{24}I_{12}N_6Zn$	
Formula weight	2056.76	
Temperature	293(2) K	
Crystal system	Monoclinic	
Space group	$P\ 2_1/c$ (No. 14)	
Unit cell dimensions	a =12.515(4) A	a = 90 deg.
	b= 17.388(1) A	β = 92.950(9) deg.
	c = 22.589(1) A	y = 90 deg.
Volume	4909(1) A^3	
Z	4	
No. reflns. used for cell	25	
Cell measurement theta min/max	15.06/17.11	
Crystal shape	Rectangular	
Crystal colour	Lustrous black	
Density (calculated)	2.783 Mg/m^3	
Absorption coefficient	8.074 mm^{-1}	
F(000)	3648	
Crystal size	45x .23 x .20 mm	

Data Collection :

Diffractometer	Enraf Nonius CAIM
Radiation type	MoK_α
Wavelength	0.71073 A
Radiation source	Fine focus sealed tube
Monochromator	Graphite
Measurement method	Omega-2theta
Standard reflns.	2 measured every 90 min
Theta range for data collection	1.63 to 22.47 deg.
Index ranges	$-13 \le h \le 13$, $0 \le k \le 18$, $0 \le l \le 2$
Reflections collected	6375
Independent reflections	6375 (R(int) = 0.0000]
Mean intensity/sigma	26.95
No. reflns. [F > 4 sigma(F)]	4117
Absorption correction	Statistical(DIFABS)
Max. and min. transmission	1.04 and 0.810

Solution and Refinement :

Atom sites soln. - primary	Patterson
Atom sites soln. - secondary	Difference fourier
Atom sites soln. - hydrogens	Geometrical
Treatment of hydrogen atoms	Riding model
Refinement method	Full-matrix least-squares on F^2

Data / restraints / parameters	6375/0/442	
Goodness-of-fit (S) [F>4sigma(F)]	0.996	
Goodness-of-fit (S) (all data)	0.996	
Final R indices [F>4sigma(F)]	R1 = 0.0475	wR2 = 0.1131
R indices (all data)	R1 = 0.0874	wR2 = 0.1320
Maximum shift/esd	0.022	
Mean shift/esd	0.001	
Largest diff. peak and hole	1.456 and -1.421 e. A"^{3}	

Computer Programs :

Data collection	CAD-4 system
Cell refinement	CAD-4 system
Data reduction	CAD-4 system
Structure solution	SHELXS-97
Structure refinement	SHELXL-97
Molecular graphics	ORTEP
Publication material	SHELXL-97

$R1 = \Sigma||F_o| - |F_c||/\Sigma|F_o|$

$wR_2 = [\Sigma\{w(F_o^2 - F_c^2)^2\}/\Sigma(wF_o^4)]^{1/2}$

$w^{-1} = [\sigma^2(F_o^2) + (0.0627P)^2 + 31.1543P]$, $P = (F_o^2 + 2F_c^2)/3$

$S = [\Sigma\{w(F_o^2 - F_c^2)^2\}/(n-p)]^{1/2}$

Table K2.
Atomic coordinates (x 10^4) and equivalent isotropic displacement parameters ($Å^2$ x 10^3) for 9. U(eq) is defined as one third of the trace of the orthogonalized Uij tensor.

	x	y	z	U(eq)
1(1)	7749(1)	3702(1)	2785(1)	139(1)
I(2)	6962(1)	2616(1)	3560(1)	99(1)
I(3)	5962(1)	1517(1)	4443(1)	116(1)
I(4)	7158(1)	2539(1)	5560(1)	98(1)
1(5)	8106(1)	3388(1)	6481(1)	90(1)
I(6)	9221(1)	4382(1)	7560(1)	130(1)
I(7)	7579(1)	5692(1)	7204(1)	81(1)
1(8)	6290(1)	6929(1)	6927(1)	117(1)
I(9)	3774(1)	1046(1)	3819(1)	84(1)
I(10)	1835(1)	643(1)	3245(1)	110(1)
1(11)	8601(1)	4759(1)	8940(1)	82(1)
I(12)	8333(1)	5077(1)	10103(1)	92(1)
Zn	12615(1)	1760(1)	775(1)	57(1)
N(l)	13508(8)	1098(6)	175(4)	54(3)
N(2)	11744(8)	687(6)	699(4)	53(3)
N(3)	13635(10)	1406(7)	1528(5)	66(3)
N(4)	13701(9)	2700(6)	917(5)	58(3)
N(5)	11680(9)	2279(6)	34(5)	57(3)
N(6)	11355(9)	2342(6)	1196(5)	59(3)
C(l)	14385(11)	1349(8)	-86(6)	67(4)

C(2)	14854(13)	959(10)	-541(6)	76(4)
C(3)	14377(14)	285(11)	-737(6)	84(5)
C(4)	13484(13)	14(10)	-472(6)	82(5)
C(5)	13086(11)	434(7)	-8(5)	56(3)
C(6)	12125(11)	175(8)	313(6)	60(4)
C(7)	11675(13)	-540(9)	213(8)	84(5)
C(8)	10768(15)	-723(10)	533(9)	101(6)
C(9)	10378(14)	-207(11)	917(8)	100(6)
C(10)	10877(12)	503(9)	983(6)	74(4)
C(ll)	13626(13)	713(10)	1780(6)	78(4)
C(12)	14422(14)	465(10)	2199(6)	83(5)
C(13)	15247(13)	969(13)	2332(7)	89(5)
C(14)	15260(13)	1670(11)	2086(6)	78(4)
C(15)	14441(12)	1875(8)	1682(6)	60(4)
C(16)	14400(11)	2633(8)	1385(6)	61(4)
C(17)	15045(14)	3269(11)	1561(8)	95(5)
C(18)	14985(18)	3929(11)	1265(9)	107(6)
C(19)	14262(17)	4020(10)	791(10)	109(6)
C(20)	13636(13)	3379(10)	614(7)	84(5)
C(21)	11797(12)	2173(9)	-546(6)	73(4)
C(22)	11080(15)	2420(9)	-982(8)	89(5)
C(23)	10179(14)	2802(9)	-822(7)	81(5)
C(24)	10030(13)	2930(8)	-231(7)	72(4)
C(25)	10798(12)	2660(7)	186(7)	63(4)
C(26)	10702(11)	2777(8)	834(6)	58(4)
C(27)	9971(12)	3303(9)	1067(8)	80(4)
C(28)	9969(14)	3346(10)	1672(8)	86(5)
C(29)	10565(13)	2905(10)	2037(8)	80(5)
C(30)	11298(13)	2405(9)	1784(7)	78(4)

*The site occupation factors of disordered sites are given after the respective atom labels.

Table K3.
Anisotropic displacement parameters (A ▪ 10) for 9.

	U11	U22	U33	U23	U13	U12
I(1)	152(1)	136(1)	133(1)	-26(1)	52(1)	1(1)
I(2)	74(1)	107(1)	115(1)	-32(1)	-7(1)	22(1)
I(3)	92(1)	115(1)	140(1)	1(1)	-1(1)	-2(1)
I(4)	74(1)	87(1)	134(1)	22(1)	10(1)	3(1)
I(5)	79(1)	91(1)	100(1)	28(1)	17(1)	23(1)
I(6)	140(1)	167(1)	79(1)	-17(1)	-19(1)	65(1)
I(7)	87(1)	82(1)	74(1)	-6(1)	-4(1)	-11(1)
I(8)	165(1)	111(1)	77(1)	-8(1)	7(1)	53(1)
I(9)	102(1)	66(1)	87(1)	2(1)	27(1)	9(1)
1(10)	110(1)	112(1)	110(1)	-31(1)	26(1)	-19(1)
I(11)	85(1)	78(1)	82(1)	-2(1)	-1(1)	1(1)
I(12)	105(1)	88(1)	84(1)	-9(1)	7(1)	1(1)

Zn	62(1)	53(1)	57(1)	-3(1)	7(1)	-6(1)
N(l)	46(6)	53(7)	63(7)	-1(6)	7(5)	-2(5)
N(2)	50(6)	56(7)	54(6)	-8(6)	7(5)	-3(5)
N(3)	79(8)	65(8)	56(7)	1(6)	13(6)	0(7)
N(4)	71(8)	51(7)	52(7)	-12(6)	10(6)	-7(6)
N(5)	66(7)	57(7)	50(7)	K5)	8(6)	-6(6)
N(6)	67(7)	56(7)	54(7)	-14(6)	8(6)	-7(6)
C(l)	63(9)	68(10)	71(10)	-2(8)	6(8)	3(8)
C(2)	81(11)	84(12)	63(9)	2(9)	8(8)	11(9)
C(3)	94(12)	106(14)	53(9)	-9(9)	17(9)	22(11)
C(4)	94(12)	96(12)	54(9)	-18(9)	1(8)	26(10)
C(5)	68(9)	47(8)	49(8)	-1(6)	-15(7)	16(7)
C(6)	70(9)	51(9)	60(8)	7(7)	2(7)	-15(7)
C(7)	81(11)	62(10)	110(13)	-22(9)	8(10)	-11(9)
C(8)	106(14)	65(11)	135(16)	-5(11)	29(12)	-29(10)
C(9)	84(12)	94(14)	123(16)	-2(12)	24(11)	-16(11)
C(10)	83(11)	66(10)	74(10)	-1(8)	14(8)	-13(9)
C(11)	96(12)	83(12)	55(9)	11(8)	8(8)	2(9)
C(12)	99(13)	94(12)	56(9)	15(9)	7(9)	32(11)
C(13)	63(11)	123(16)	80(12)	-15(12)	-16(8)	26(11)
C(14)	85(12)	92(13)	57(9)	-14(9)	-1(8)	17(10)
C(15)	73(10)	57(9)	51(8)	-25(7)	7(7)	-3(8)
C(16)	62(9)	61(10)	60(9)	-20(7)	21(7)	-15(7)
C(17)	102(13)	95(14)	88(12)	-29(11)	10(10)	-32(11)
C(18)	144(19)	65(13)	113(16)	-14(12)	10(14)	-42(12)
C(19)	133(17)	58(11)	137(18)	-17(12)	14(14)	-16(12)
C(20)	89(12)	78(12)	87(11)	-1(10)	24(9)	-8(10)
C(21)	69(10)	84(11)	67(10)	20(8)	10(8)	9(8)
C(22)	101(13)	82(12)	84(11)	21(10)	-9(10)	0(11)
C(23)	84(12)	78(11)	81(12)	20(9)	-3(9)	10(9)
C(24)	81(11)	58(9)	75(11)	12(8)	3(9)	5(8)
C(25)	68(10)	42(8)	80(10)	-3(7)	12(8)	-18(7)
C(26)	58(9)	45(8)	73(10)	-11(7)	15(8)	-19(7)
C(27)	69(10)	65(10)	107(13)	-16(9)	23(9)	-9(8)
C(28)	90(13)	72(11)	96(13)	-29(10)	14(11)	2(10)
C(29)	78(11)	84(12)	79(11)	-33(10)	20(9)	-18(9)
C(30)	87(11)	80(11)	69(11)	-13(9)	20(9)	-16(9)

The anisottopic displacement factor exponent takes the form:
-2K [h a* U11+ ... + 2hka*b*U12]

Table K4.
Bond lengths [A] and angles [deg] for 9.

Bond distances :			
I(1)-I(2)	2.788(2)	I(2)-I(3)	3.074(2)
I(3)-I(9)	3.123(2)	I(3)-I(4)	3.374(2)
I(4)-I(5)	2.7681(19)	I(5)-I(6)	3.244(2)
I(6)-I(7)	3.1442(18)	I(6)-I(11)	3.3152(17)
I(7)-I(8)	2.7405(17)	I(9)-I(10)	2.7822(19)

I(11)-I(12)	2.7222(16)	Zn-N(l)	2.136(10)
Zn-N(6)	2.137(11)	Zn-N(4)	2.140(11)
Zn-N(3)	2.162(12)	Zn-N(2)	2.164(10)
Zn-N(5)	2.188(11)	N(1)-C(5)	1.328(15)
N(1)-C(1)	1.345(16)	N(2)-C(10)	1.327(17)
N(2)-C(6)	1.350(16)	N(3)-C(15)	1.330(17)
N(3)-C(11)	1.333(18)	N(4)-C(16)	1.341(17)
N(4)-C(20)	1.365(18)	N(5)-C(21)	1.338(16)
N(5)-C(25)	1.347(17)	N(6)-C(30)	1.339(16)
N(6)-C(26)	1.356(17)	C(1)-C(2)	1.387(19)
C(2)-C(3)	1.38(2)	C(3)-C(4)	1.38(2)
C(4)-C(5)	1.392(18)	C(5)-C(6)	1.503(18)
C(6)-C(7)	1.378(19)	C(7)-C(8)	1.41(2)
C(8)-C(9)	1.36(2)	C(9)-C(10)	1.39(2)
C(11)-C(12)	1.41(2)	C(12)-C(13)	1.38(2)
C(13)-C(14)	1.34(2)	C(14)-C(15)	1.38(2)
C(15)-C(16)	1.478(19)	C(16)-C(17)	141(2)
C(17)-C(18)	1.33(2)	C(18)-C(19)	1.38(3)
C(19)-C(20)	1.41(2)	C(21)-C(22)	1.37(2)
C(22)-C(23)	1.37(2)	C(23)-C(24)	1.38(2)
C(24)-C(25)	1.393(19)	C(25)-C(26)	1.489(19)
C(26)-C(27)	1.414(19)	C(27)-C(28)	1.37(2)
C(28)-C(29)	1.33(2)	C(29)-C(30)	1.41(2)

Bond angles '

I(1)-I(2)-I(3)	175.39(6)	I(2)-I(3)-I(9)	104.29(5)
I(2)-I(3)-I(4)	88.73(5)	I(9)-I(3)-I(4)	145.11(6)
I(5)-I(4)-I(3)	179.06(5)	I(4)-I(5)-I(6)	179.93(6)
I(7)-I(6)-I(5)	86.80(4)	I(7)-I(6)-I(11)	85.20(4)
I(5)-I(6)-I(11)	134.37(7)	I(8)-I(7)-I(6)	174.75(6)
I(10)-I(9)-I(3)	178.94(6)	I(12)-I(11)-I(6)	173.57(6)
N(1)-Zn-N(6)	163.5(4)	N(1)-Zn-N(4)	99.1(4)
N(6)-Zn-N(4)	92.8(4)	N(1)-Zn-N(3)	92.2(4)
N(6)-Zn-N(3)	101.8(4)	N(4)-Zn-N(3)	75.8(5)
N(1)-Zn-N(2)	76.3(4)	N(6)-Zn-N(2)	93.6(4)
N(4)-Zn-N(2)	169.9(4)	N(3)-Zn-N(2)	95.2(4)
N(1)-Zn-N(5)	90.8(4)	N(6)-Zn-N(5)	76.5(4)
N(4)-Zn-N(5)	96.4(4)	N(3)-Zn-N(5)	172.0(4)
N(2)-Zn-N(5)	92.7(4)	C(5)-N(1)-C(1)	117.8(11)
C(5)-N(1)-Zn	116.9(8)	C(1)-N(1)-Zn	124.7(9)
C(10)-N(2)-C(6)	118.5(12)	C(10)-N(2)-Zn	126.2(9)
C(6)-N(2)-Zn	115.3(8)	C(15)-N(3)-C(11)	117.7(13)
C(15)-N(3)-Zn	116.1(10)	C(11)-N(3)-Zn	125.1(10)
C(16)-N(4)-C(20)	119.4(12)	C(16)-N(4)-Zn	115.8(9)
C(20)-N(4)-Zn	124.3(10)	C(21)-N(5)-C(25)	116.7(12)
C(21)-N(5)-Zn	127.7(10)	C(25)-N(5)-Zn	114.9(9)
C(30)-N(6)-C(26)	119.4(12)	C(30)-N(6)-Zn	123.9(10)
C(26)-N(6)-Zn	115.6(8)	N(1)-C(1)-C(2)	123.6(14)
C(3)-C(2)-C(1)	117.4(15)	C(4)-C(3)-C(2)	120.0(14)
C(3)-C(4)-C(5)	118.5(16)	N(1)-C(5)-C(4)	122.6(14)

N(1)-C(5)-C(6)	115.2(11)	C(4)-C(5)-C(6)	122.1(13)
N(2)-C(6)-C(7)	123.0(13)	N(2)-C(6)-C(5)	115.5(11)
C(7)-C(6)-C(5)	121.5(13)	C(6)-C(7)-C(8)	116.9(15)
C(9)-C(8)-C(7)	120.2(16)	C(8)-C(9)-C(10)	118.8(16)
N(2)-C(10)-C(9)	122.5(15)	N(3)-C(11)-C(12)	123.0(16)
C(13)-C(12)-C(11)	116.7(16)	C(14)-C(13)-C(12)	120.9(16)
C(13)-C(14)-C(15)	118.9(16)	N(3)-C(15)-C(14)	122.7(14)
N(3)-C(15)-C(16)	114.8(13)	C(14)-C(15)-C(16)	122.5(14)
N(4)-C(16)-C(17)	119.5(15)	N(4)-C(16)-C(15)	116.2(12)
C(17)-C(16)-C(15)	124.2(15)	C(18)-C(17)-C(16)	121.2(18)
C(17)-C(18)-C(19)	120.6(18)	C(18)-C(19)-C(20)	117.6(18)
N(4)-C(20)-C(19)	121.6(17)	N(5)-C(21)-C(22)	124.1(15)
C(21)-C(22)-C(23)	118.7(16)	C(22)-C(23)-C(24)	119.1(15)
C(23)-C(24)-C(25)	118.6(15)	N(5)-C(25)-C(24)	122.7(13)
N(5)-C(25)-C(26)	115.3(13)	C(24)-C(25)-C(26)	122.1(14)
N(6)-C(26)-C(27)	121.3(14)	N(6)-C(26)-C(25)	116.0(12)
C(27)-C(26)-C(25)	122.7(15)	C(28)-C(27)-C(26)	116.2(16)
C(29)-C(28)-C(27)	124.0(16)	C(28)-C(29)-C(30)	117.5(15)
N(6)-C(30)-C(29)	121.6(16)		

Table K5.
Hydrogen coordinates (* 10) and isotropic displacement parameters (A x 10) for 9.

	x	y	z	U(eq)
H(l)	14694	1808	46	101
H(2)	15466	1146	-708	114
H(3)	14658	12	-1047	126
H(4)	13155	-440	-601	122
H(7)	11954	-885	-53	127
H(8)	10437	-1199	481	152
H(9)	9787	-327	1133	150
H(10)	10593	863	1235	111
H(ll)	13068	379	1674	117
H(12)	14392	-16	2377	125
H(13)	15803	821	2597	134
H(14)	15812	2012	2185	117
H(17)	15519	3224	1890	142
H(18)	15437	4333	1379	161
H(19)	14189	4489	594	163
H(20)	13166	3419	282	126
H(21)	12404	1915	-660	110
H(22)	11200	2330	-1379	134
H(23)	9675	2973	-1110	122
H(24)	9429	3192	-113	107
H(27)	9518	3602	823	120
H(28)	9523	3707	1837	128
H(29)	10500	2925	2445	120

H(30)	11754	2111	2031	117

Hydrogen atoms are labelled according to the atom to which they are attached. All hydrogens were refined using the riding model (the positional parameters of the riding atoms have same e.s.ds as the atom on which they ride). All hydrogens were fixed to U(iso) values (=1.5xU(iso) of the atom to which they are attached)..

Table K6. Selected torsion angles and least square planes for 9

Selected torsion angles

66.97(0.03) I1 - I3 - I6 - I8
150.29(0 04) I1 - I3 - I6 - I12
-43.62 (0.06) I10 - I3 - I6 - I8
39.70(0.07) I10 - I3 - I6 - I12

Least-squares planes (x,y,z in crystal coordinates) and deviations from them
(* indicates atom used to define plane)

- 5.8543 (0.0032) x + 13.1176 (0.0050) y + 10.9326 (0.0100) z = 3.3246 (0.0042)

* 0.0401 (0.0005) I1
• -0.0766(0.0010) I2
• 0.0309(0.0007) I3
* 0.0128(0.0009) I9
• -0.0072 (0.0005) I10

Rms deviation of fitted atoms = 0.0416

9.6433 (0.0046) x + 11.0487 (0.0068) y + 0.2424 (0.0063) z - 13.8476 (0.0066)

Angle to previous plane (with approximate esd) = 81.83 (003)

* 0.0692(0.0007) I6
* -0.0748 (0.0011) I7
• 0.0414(0.0006) I8
• -0.0782 (0.0010) I11
• 0.0424(0.0006) I12

Rms deviation of fitted atoms = 0.0633

6.9029 (0.0578) x - 8.7733 (0.0867) y + 14.3431 (0.0936) z = 8.6249 (0.0842)

* -0.0125 (0.0082) N1

* -0.0014 (0.0095) C1
* 0.0107(0.0100) C2
* -0.0070 (0.0106) C3
* -0.0064 (0.0100) C4
* 0.0165 (0.0086) C5

Rms deviation of fitted atoms = 0.0103

6.9431 (0.0685) x - 6.6274 (0.1028) y+ 16.0386 (0.1068) z = 8.8082 (0.0738)

Angle to previous plane (with approximate esd) = 8.29 (0.93)

* 0.0122(0.0092) N2
* -0.0039(0.0101) C6
* -0.0031 (0.0118) C7
* 0.0023 (0.0137) C8
* 0.0057 (0.0133) C9
* -0.0132 (0.0111) C10

Rms deviation of fitted atoms = 0.0080

6.9834 (0.0583) x - 6.4295 (0.0934) y - 17.4078 (0.0786) z - 5.9545 (0.0979)

Angle to previous plane (with approximate esd) = 84.32 (0.38)

* 0.0036 (0.0088) N3
* 0.0037(0.0099) C11
* -0.0103(0.0104) C12
* 0.0099(0.0110) C13
* -0.0026(0.0102) C14
* -0.0044(0.0090) C15

Rms deviation of fitted atoms = 0.0066

9.1956 (0.0553) x- 5.3868 (0.1060) y - 14.4673 (0.1174) z = 9.8202 (0.1015)

Angle to previous plane (with approximate esd) = 13.38 (0.84)

* -0.0026(0.0091) N4
* -0.0003 (0.0096) C16
* -0.0052 (0.0123) C17
* 0.0131 (0.0143) C18
* -0.0155 (0.0134) C19
* 0.0105(0.0111) C20

Rms deviation of fitted atoms = 0.0096

6.1862 (0.0630) x + 15.0945 (0.0506) y - 1.6114 (0.1307) z = 10.6631 (0.0572)

Angle to previous plane (with approximate esd) = 82.99 (0.45)

- -0.0038 (0.0087) N5
* 0.0022(0.0105) C21
* 0.0018 (0.0112) C22
- -0.0039 (0.0110) C23
- 0.0022(0.0101) C24
* 0.0016(0.0090) C25

Rms deviation of fitted atoms = 0.0028

8.7502 (0.0509) x + 12.4286 (0.0693) y - 0.4348 (0.1244) z = 12.7884 (0.0395)

Angle to previous plane (with approximate esd) = 15.14 (0.70)

- 0.0060(0.0086) N6
» -0.0085 (0.0087) C26
- -0.0048 (0.0099) C27
* 0.0208 (0.0113) C28
- -0.0224 (0.0108) C29
* 0.0090(0.0098) C30

Rms deviation of fitted atoms = 0.0138

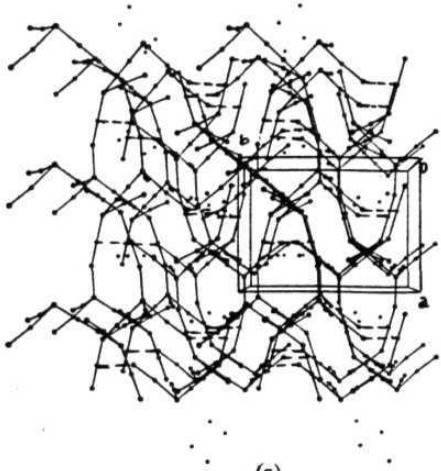

(a)

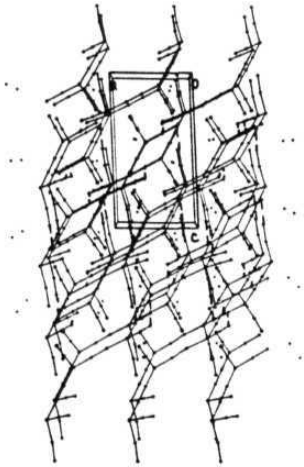

(b)

Figure K1. Views of packing of anion in 9. (a) viewed normal to ab plane, (b) viewed normal to ac plane. (the Zn atoms are shown as small circles and ligand molecules are omitted.)

APPENDIX L. Crystallographic tables and figures for $[Zn(phen)_3]I_{12}$ (10).

Table L1.
Crystal data and structure refinement for $[Zn(phen)_3]I_{12}$ (10).

Crystal Data :		
Structural formula	$[Zn(phen)_3]I_{12}$	
Empirical formula	$C_{36}H_{24}I_{12}N_6Zn$	
Formula weight	2128.78	
Temperature	293(2) K	
Crystal system	Triclinic	
Space group	P F (No.2)	
Unit cell dimensions	a =12.867(2) A	a = 85.34(1) deg.
	b = 14.047(2) A	P = 76.53(1) deg.
	c = 15.832(2) A	γ = 65.61(l) deg.
Volume	2531.1(6) A^3	
Z	2	
No. reflns. used for cell	19	
Cell measurement theta min/max	15.03/17.38	
Crystal shape	Rectangular	
Crystal colour	Lustrous brown	
Density (calculated)	2.790 Mg/m^3	
Absorption coefficient	7.826 mm^{-1}	
F(000)	1896	
Crystal size	.35 x .20 x .18 mm	
Data Collection :		
Diffractometer	Enraf Nonius CAD-4	
Radiation type	MoK_α	
Wavelength	0.71073 A	
Radiation source	Fine focus sealed tube	
Monochromator	Graphite	
Measurement method	Omega-2theta	
Standard reflns.	2 measured every 90 mm	
Theta range for data collection	1.59 to 24.96 deg.	
Index ranges	$-14 \le h \le 15, -16 \le k \le 16, 0 \le l \le 18$	
Reflections collected	8948	
Independent reflections	8856 [R(int) = 0.0000]	
Mean intensity/sigma	2494	
No. reflns.[F > 4 sigma(F)]	5478	
Absorption correction	Statistical (DIFABS)	
Max. and min transmission	1.03 and 0.899	
Solution and Refinement :		
Atom sites soln. - primary	Patterson	
Atom sites soln. - secondary	Difference fourier	
Atom sites soln. - hydrogens	Geometrical	
Treatment of hydrogen atoms	Riding model	

Refinement method	Full-matrix least-squares on F^2
Data / restraints / parameters	8856 / 0 / 496
Goodness-of-fit (S) [F>4sigma(F)]	0.970
Goodness-of-fit (S) (all data)	0.970
Final R indices [F>4sigma(F)]	Rl = 0.0565 wR2 = 0.1410
R indices (all data)	R1 =0.1026 wR2 = 0.1681
Maximum shift/esd	0.016
Mean shift/esd	0.001
Largest diff. peak and hole	1.664 and -1.843 e.Å^{-3}

Computer Programs :

Data collection	CAD-4 system
Cell refinement	CAD-4 system
Data reduction	CAD-4 system
Structure solution	SHELXS-97
Structure refinement	SHELXL-97
Molecular graphics	ORTEP
Publication material	SHELXL-97

$R1 = \Sigma||F_o| - |F_c||/\Sigma|F_o|$

$wR_2 = [\Sigma\{w(F_o^2 - F_c^2)^2\}/\Sigma\{wF_o^4)]^{1/2}$

$w^{-1} = [\sigma^2(F_o^2) + (0.0857P)^2 + 20.9707P]$, $P = (F_o^2 + 2F_c^2)/3$

$S = [\Sigma\{w(F_o^2 - F_c^2)^2\}/(n-p)]^{1/2}$

Table L2.
Atomic coordinates (x 10^4) and equivalent isotropic displacement parameters (Å^2 x 10^3) for 10. U(eq) is defined as one third of the trace of the orthogonalized Uij tensor.

	x	y	Z	U(cq)
I(1)	-263(1)	4827(1)	6606(1)	73(1)
I(2)	2032(1)	3461(1)	5862(1)	61(1)
I(3)	4552(1)	1983(1)	5109(1)	87(1)
I(4)	5508(1)	2510(1)	6496(1)	75(1)
I(5)	6551(1)	2856(1)	7778(1)	95(1)
1(6)	4217(1)	4576(1)	9205(1)	83(1)
1(7)	2376(1)	6055(1)	10296(1)	86(1)
1(8)	265(1)	8061(1)	11759(1)	110(1)
I(9)	-2023(1)	8487(1)	11433(1)	79(1)
1(10)	-4313(1)	8885(1)	11116(1)	111(1)
I(11) (0.75)	-6018(1)	10744(1)	12519(1)	87(1)
I(12) (0.75)	-7852(2)	12440(1)	13354(1)	83(1)
Zn(l)	2095(1)	7494(1)	7181(1)	44(1)
N(l)	298(9)	8228(8)	7857(6)	46(2)
N(2)	1705(9)	6174(7)	7749(6)	43(2)
N(3)	2177(9)	8860(7)	6457(6)	46(2)
N(4)	1651(8)	7338(7)	5962(6)	41(2)
N(5)	2698(9)	7850(7)	8240(6)	45(2)
N(6)	3943(9)	6569(8)	6852(7)	52(3)
C(l)	-391(12)	9245(10)	7879(8)	54(3)

C(2)	-1551(13)	9645(11)	8357(9)	65(4)
C(3)	-1989(13)	8995(12)	8829(9)	66(4)
C(4)	-1298(12)	7941(11)	8800(8)	58(3)
C(5)	-1706(13)	7159(13)	9254(9)	66(4)
C(6)	-1012(15)	6137(14)	9201(9)	75(5)
C(7)	162(12)	5761(10)	8681(8)	54(3)
C(8)	934(15)	4696(10)	8591(8)	63(4)
C(9)	2043(13)	4402(10)	8079(9)	59(3)
C(10)	2386(11)	5168(10)	7666(8)	53(3)
C(11)'	-157(10)	7570(9)	'8313(6)	42(3)
C(12)	599(11)	6468(9)	8253(7)	45(3)
C(13)	2483(13)	9575(10)	6685(9)	60(3)
C(14)	2470(13)	10438(11)	6157(9)	65(4)
C(15)	2170(13)	10523(11)	5383(9)	64(4)
C(16)	1842(11)	9790(9)	5118(8)	51(3)
C(17)	1461(11)	9837(10)	4320(8)	53(3)
C(18)	1181(11)	9095(10)	4090(8)	56(3)
C(I9)	1211(9)	8226(9)	4650(7)	43(3)
C(20)	932(11)	7425(11)	4443(8)	55(3)
C(21)	1005(12)	6625(11)	4984(8)	56(3)
C(22)	1382(12)	6609(10)	5756(9)	57(3)
C(23)	1869(9)	8938(8)	5675(7)	40(3)
C(24)	1573(10)	8158(9)	5424(7)	43(3)
C(25)	2086(14)	8502(10)	8912(9)	64(4)
C(26)	2575(17)	8693(12)	9535(9)	72(4)
C(27)	3750(2)	8140(15)	9473(11)	89(6)
C(28)	4461(15)	7425(12)	8776(9)	66(4)
C(29)	5686(16)	6806(16)	8665(13)	86(5)
C(30)	6274(16)	6160(17)	7999(12)	90(6)
C(31)	5750(11)	6045(12)	7335(10)	66(4)
C(32)	6324(13)	5406(14)	6605(12)	83(5)
C(33)	5741(15)	5345(15)	6011(13)	92(5)
C(34)	4561(13)	5955(12)	6150(9)	68(4)
C(35)	3868(13)	7314(10)	8163(8)	54(3)
C(36)	4527(12)	6637(10)	7441(9)	57(3)

*The site occupation factors of disordered sites are given after the respective atom labels.

Table L3.
Anisotropic displacement parameters (A × 10) for 10.

	U11	U22	U33	U23	U13	U12
I(1)	62(1)	80(1)	81(1)	-15(1)	-19(1)	-28(1)
I(2)	70(1)	57(1)	62(1)	1(1)	-18(1)	-29(1)
I(3)	71(1)	87(1)	95(1)	-11(1)	-2(1)	-29(1)
I(4)	60(1)	65(1)	82(1)	3(1)	-1(1)	-16(1)
I(5)	98(1)	88(1)	90(1)	-1(1)	-24(1)	-26(1)
I(6)	113(1)	86(1)	79(1)	27(1)	-55(1)	-56(1)

1(7)	99(1)	83(1)	103(1)	36(1)	-47(1)	-56(1)
1(8)	111(1)	103(1)	119(1)	-23(1)	-22(1)	**-44(1)**
I(9)	119(1)	57(1)	58(1)	-4(1)	-3d)	-40(1)
1(10)	86(1)	135(1)	93(1)	-37(1)	8(1)	-35(1)
I(11)	80(1)	78(1)	101(1)	13(1)	**-23(1)**	-30(1)
1(12)	99(1)	79(1)	59(1)	9(1)	2(1)	-36(1)
Zn(l)	53(1)	45(1)	36(1)	6(1)	-14(1)	-23(1)
N(l)	62(6)	50(6)	29(5)	13(4)	-14(5)	-27(5)
N(2)	56(6)	45(5)	27(5)	2(4)	-7(4)	-20(5)
N(3)	58(6)	48(6)	40(6)	4(4)	-10(5)	-29(5)
N(4)	48(5)	49(5)	33(5)	4(4)	-15(4)	-25(5)
N(5)	59(6)	41(5)	35(5)	11(4)	-8(5)	-22(5)
N(6)	59(6)	51(6)	45(6)	7(5)	-12(5)	-24(5)
C(l)	67(9)	50(7)	42(7)	0(6)	-8(6)	-24(7)
C(2)	78(10)	52(8)	54(8)	6(6)	-17(8)	-15(7)
C(3)	60(8)	76(10)	48(8)	-22(7)	-3(7)	-12(8)
C(4)	72(9)	63(8)	33(7)	**-4(6)**	-14(6)	-21(7)
C(5)	71(9)	91(11)	53(8)	-12(8)	9(7)	-58(9)
C(6)	104(13)	97(12)	41(8)	-8(8)	16(8)	-74(11)
C(7)	82(9)	67(8)	44(7)	21(6)	-33(7)	-54(8)
C(8)	112(13)	57(8)	45(8)	15(6)	-33(8)	-52(9)
C(9)	77(10)	50(7)	56(8)	8(6)	-27(8)	-29(7)
C(10)	52(7)	52(7)	47(7)	13(6)	-11(6)	-16(6)
C(ll)	58(7)	52(7)	20(5)	4(5)	-12(5)	-27(6)
C(12)	62(8)	52(7)	34(6)	10(5)	-13(6)	-35(6)
C(13)	77(9)	56(8)	62(9)	10(6)	-20(7)	40(7)
C(14)	89(10)	60(8)	67(9)	-4(7)	-7(8)	-56(8)
C(15)	81(10)	60(8)	43(8)	14(6)	1(7)	-33(8)
C(16)	56(7)	48(7)	49(7)	12(6)	-6(6)	-25(6)
C(17)	59(8)	51(7)	39(7)	3(5)	-10(6)	-14(6)
C(18)	57(8)	55(8)	37(7)	13(6)	-11(6)	-7(6)
C(19)	36(6)	57(7)	31(6)	1(5)	-7(5)	-14(5)
C(20)	59(8)	75(9)	32(6)	-2(6)	-16(6)	-25(7)
C(21)	69(9)	73(9)	40(7)	-1(6)	-15(6)	-42(7)
C(22)	69(9)	58(8)	58(8)	4(6)	-20(7)	-37(7)
C(23)	39(6)	43(6)	37(6)	2(5)	3(5)	-22(5)
C(24)	45(6)	45(6)	34(6)	8(5)	-5(5)	-16(5)
C(25)	85(10)	52(8)	55(8)	9(6)	-21(8)	-26(7)
C(26)	120(14)	71(10)	49(9)	6(7)	-35(9)	-55(10)
C(27)	144(18)	117(15)	63(11)	30(10)	-52(12)	-98(15)
C(28)	97(12)	85(10)	41(8)	19(7)	-24(8)	-60(9)
C(29)	89(13)	127(16)	84(13)	42(11)	**-53(11)**	-73(12)
C(30)	76(11)	140(17)	73(12)	36(12)	-37(10)	-58(12)
C(31)	40(7)	**85(10)**	75(10)	22(8)	r7(7)	-33(7)
C(32)	44(8)	91(12)	94(13)	11(10)	5(9)	-18(8)
C(33)	69(11)	108(14)	88(13)	-21(11)	-3(10)	-28(10)
C(34)	65(9)	74(10)	59(9)	-15(7)	-18(7)	-19(8)
C(35)	77(9)	60(8)	53(8)	22(6)	-26(7)	-52(8)
C(36)	71(9)	62(8)	50(8)	18(6)	-21(7)	-39(7)

The anisotropic displacement factor exponent takes the form:
-2% [h a* U11+... + 2hka*b*U12]

Table L4.
Bond lengths [A] and angles [deg] for 10.

Bond distances :

I(1)-I(2)	2.8029(15)	I(2)-I(3)	3.0472(16)
I(3)-I(4)	3.0263(18)	I(4)-I(5)	2.8504(18)
I(5)-I(6)	3.419(2)	I(6)-I(7)	2.743(2)
I(7)-I(8)	3.534(2)	I(8)-I(9)	2.914(2)
I(9)-I(10)	2.920(2)	I(10)-I(11)	3.240(2)
I(11)-I(12)	2.722(2)	Zn(1)-N(6)	2.144(11)
Zn(1)-N(1)	2.147(10)	Zn(l)-N(5)	2.174(10)
Zn(1)-N(3)	2.181(9)	Zn(l)-N(4)	2.187(9)
Zn(1)-N(2)	2.188(9)	N(l)-C(l)	1.332(15)
N(1)-C(11)	1.365(14)	N(2)-C(10)	1.318(15)
N(2)-C(12)	1.368(15)	N(3)-C(13)	1.322(15)
N(3)-C(23)	1.369(15)	N(4)-C(22)	1.294(15)
N(4)-C(24)	1.359(14)	N(5)-C(25)	1.328(17)
N(5)-C(35)	1.357(16)	N(6)-C(34)	1.338(17)
N(6)-C(36)	1.358(16)	C(1)-C(2)	1.402(19)
C(2)-C(3)	1.35(2)	C(3)-C(4)	1.375(19)
C(4)-C(11)	1.388(18)	C(4)-C(5)	1.474(19)
C(5)-C(6)	1.34(2)	C(6)-C(7)	1.44(2)
C(7)-C(12)	1.391(15)	C(7)-C(8)	1.410(19)
C(8)-C(9)	1.38(2)	C(9)-C(10)	1.386(18)
C(11)-C(12)	1.445(16)	C(13)-C(14)	1.412(18)
C(14)-C(15)	1.351(19)	C(15)-C(16)	1.388(19)
C(16)-C(23)	1.421(15)	C(16)-C(17)	1.444(18)
C(17)-C(18)	1.335(18)	C(18)-C(19)	1.443(16)
C(19)-C(24)	1.391(16)	C(19)-C(20)	1.397(17)
C(20)-C(21)	1.342(18)	C(21)-C(22)	1.411(17)
C(23)-C(24)	1.411(16)	C(25)-C(26)	1.38(2)
C(26)-C(27)	1.37(2)	C(27)-C(28)	1.42(2)
C(28)-C(35)	1.421(18)	C(28)-C(29)	1.43(2)
C(29)-C(30)	1.31(3)	C(30)-C(31)	1.43(2)
C(31)-C(32)	1.38(2)	C(31)-C(36)	1.420(19)
C(32)-C(33)	1.36(2)	C(33)-C(34)	1.37(2)
C(35)-C(36)	1.409(19)		

Bond angles :

I(1)-I(2)-I(3)	178.02(5)	I(4)-I(3)-I(2)	94.04(4)
I(5)-I(4)-I(3)	175.71(5)	I(4)-I(5)-I(6)	103.29(5)
I(7)-I(6)-I(5)	176.45(5)	I(6)-I(7)-I(8)	172.81(5)
I(9)-I(8)-I(7)	107.67(5)	I(8)-I(9)-I(10)	179.17(6)
I(9)-I(10)-I(11)	101.30(6)	I(12)-I(11)-I(10)	163.20(8)
N(6)-Zn(1)-N(1)	164.0(4)	N(6)-Zn(1)-N(5)	77.2(4)
N(1)-Zn(1)-N(5)	91.9(4)	N(6)-Zn(1)-N(3)	95 2(4)
N(1)-Zn(1)-N(3)	96.9(4)	N(5)-Zn(1)-N(3)	92.4(3)

N(6>Zn(l)-N(4)	99.4(4)	N(1)-Zn(1)-N(4)	93.5(4)
N(5)-Zn(1)-N(4)	168.3(3)	N(3)-Zn(1)-N(4)	76.8(3)
N(6)-Zn(1)-N(2)	93.2(4)	N(1)-Zn(1)-N(2)	76.8(4)
N(5)-Zn(1)-N(2)	99.1(3)	N(3)-Zn(1)-N(2)	167.0(4)
N(4)-Zn(1)-N(2)	92.1(3)	C(1)-N(1)-C(11)	118.1(11)
C(1)-N(1)-Zn(1)	126.7(8)	C(11)-N(1)-Zn(1)	115.3(8)
C(10)-N(2)-C(12)	118.0(10)	C(10)-N(2)-Zn(1)	128.7(8)
C(12)-N(2)-Zn(1)	113.4(7)	C(13)-N(3)-C(23)	119.2(10)
C(13)-N(3)-Zn(1)	128.1(9)	C(23)-N(3)-Zn(1)	112.7(7)
C(22)-N(4)-C(24)	119.7(10)	C(22)-N(4)-Zn(1)	126.7(8)
C(24)-N(4)-Zn(1)	113.4(7)	C(25)-N(5)-C(35)	118.8(12)
C(25)-N(5)-Zn(1)	129.0(10)	C(35)-N(5)-Zn(1)	112.2(8)
C(34)-N(6)-C(36)	118.1(12)	C(34)-N(6)-Zn(1)	127.8(10)
C(36)-N(6)-Zn(1)	114.1(9)	N(1)-C(1)-C(2)	121.9(12)
C(3)-C(2)-C(1)	119.9(13)	C(2)-C(3)-C(4)	119.0(13)
C(3)-C(4)-C(11)	119.6(13)	C(3)-C(4)-C(5)	123.4(14)
C(11)-C(4)-C(5)	117.0(12)	C(6)-C(5)-C(4)	121.7(13)
C(5)-C(6)-C(7)	120.8(13)	C(12)-C(7)-C(8)	116.5(13)
C(12)-C(7)-C(6)	119.8(13)	C(8)-C(7)-C(6)	123.6(12)
C(9)-C(8)-C(7)	119.9(12)	C(8)-C(9)-C(10)	119.0(13)
N(2)-C(10)-C(9)	123.2(12)	N(1)-C(11)-C(4)	121.5(11)
N(1)-C(11)-C(12)	116.8(10)	C(4)-C(11)-C(12)	121.7(11)
N(2)-C(12)-C(7)	123.4(12)	N(2)-C(12)-C(11)	117.6(10)
C(7)-C(12)-C(11)	119.0(12)	N(3)-C(13)-C(14)	122.0(13)
C(15)-C(14)-C(13)	119.3(12)	C(14)-C(15)-C(16)	120.6(12)
C(15)-C(16)-C(23)	117.7(12)	C(15)-C(16)-C(17)	124.7(12)
C(23)-C(16)-C(17)	117.6(11)	C(18)-C(17)-C(16)	122.0(12)
C(17)-C(18)-C(19)	120.8(12)	C(24)-C(19)-C(20)	118.0(11)
C(24)-C(19)-C(18)	118.6(11)	C(20)-C(19)-C(18)	123.3(11)
C(21)-C(20)-C(19)	120.3(11)	C(20)-C(21)-C(22)	118.4(12)
N(4)-C(22)-C(21)	122.6(12)	N(3)-C(23)-C(24)	119.0(10)
N(3)-C(23)-C(16)	121.1(10)	C(24)-C(23)-C(16)	119.9(11)
N(4)-C(24)-C(19)	121.0(11)	N(4)-C(24)-C(23)	117.9(10)
C(19)-C(24)-C(23)	121.1(10)	N(5)-C(25)-C(26)	123.9(15)
C(27)-C(26)-C(25)	117.8(15)	C(26)-C(27)-C(28)	121.5(15)
C(27)-C(28)-C(35)	115.7(15)	C(27)-C(28)-C(29)	125.4(15)
C(35)-C(28)-C(29)	118.9(15)	C(30)-C(29)-C(28)	121.3(16)
C(29)-C(30)-C(31)	123.0(17)	C(32)-C(31)-C(36)	117.4(15)
C(32)-C(31)-C(30)	125.9(15)	C(36)-C(31)-C(30)	116.7(16)
C(33)-C(32)-C(31)	121.4(15)	C(32)-C(33)-C(34)	117.9(16)
N(6)-C(34)-C(33)	123.9(15)	N(5)-C(35)-C(36)	119.1(11)
N(5)-C(35)-C(28)	122.3(13)	C(36)-C(35)-C(28)	118.5(14)
N(6)-C(36)-C(35)	117.3(12)	N(6)-C(36)-C(31)	121.2(13)
C(35)-C(36)-C(31)	121.5(13)		

Table L5.
Hydrogen coordinates (× 10) and isotropic displacement parameters ($A^2 \times 10^3$) for 10.

	x	y	z	U(eq)
H(l)	-95	9703	7569	64
H(2)	-2018	10356	8349	78
H(3)	-2747	9256	9167	80
H(5)	-2466	7381	9587	79
H(6)	-1291	5664	9503	90
H(8)	694	4192	8877	76
H(9)	2556	3701	8011	70
H(10)	3132	4961	7313	
H(13)	2715	9508	7209	72
H(14)	2667	10943	6340	77
H(15)	2182	11078	5024	76
H(17)	1410	10401	3956	63
H(18)	964	9140	3563	67
H(20)	694	7446	3927	66
H(21)	811	6093	4854	67
H(22)	1440	6053	6131	68
H(25)	1282	8851	8967	77
H(26)	2120	9180	9981	86
H(27)	4094	8235	9898	107
H(29)	6076	6862	9073	103
H(30)	7067	5758	7959	108
H(32)	7125	5008	6519	100
H(33)	6129	4905	5526	111
H(34)	4168	5941	5730	81

Hydrogen atoms are labelled according to the atom to which they are attached. All hydrogens were refined using the riding model (the positional parameters of the riding atoms have same e.s.ds as the atom on which they ride). All hydrogens were fixed U(iso) values (=1.2xU(iso) of the atom to which they are attached).

Table L6. Selected least square planes for 10

Least-squares planes (x,y,z in crystal coordinates) and deviations from them
(* indicates atom used to define plane)

4.6048 (0.0018) x + 11.6594 (0.0024) y - 7.4574 (0.0021) z = 0.5377 (0.0020)

- 0.0433(0.0010) I1
- 0.0611(0.0009) I2
* 0.0598(0.0010) I3
* 0.0805(0.0010) I4
- 0.0077 (0.0011) I5
* -0.1246 (0.0010) I6
- -0.0619 (0.0010) I7
- 0.2135(0.0013) I8

* -0.0994(0.0010) 19
* -0.4540 (0.0015) 110
* -0.1180 (0.0013) I11
* 0.3917(0.0012) 112

Rms deviation of fitted atoms • 0.1966

4.6696 (0.0022) x + 11.8067(0.0025) y - 7.1956 (0.0023) z = 0.8176 (0.0020)

Angle to previous plane (with approximate esd) = 1.10 (0.02)

- 0.0058(0.0007) I1
* -0.0012(0.0008) I2
* -0.0276 (0.0009) I3
- 0.0434 (0.0009) I4
* 0.0160(0.0010) I5
- -0.0687 (0.0009) I6
- 0.0324 (0.0007) I7

Rms deviation of fitted atoms • 0.0353

- 3.1168 (0.0052) x - 9.7399 (0.0059) y+ 10.3441 (0.0072) z = 4.2230 (0.0120)

Angle to previous plane (with approximate esd) = 13.77 (0.06)

- 0.0068(0.0005) I8
- -0.0328(0.0010) I9
- -0.0339(0.0007) I10
* 0.1380(0.0013) I11
* -0.0781 (0.0007) I12

Rms deviation of fitted atoms • 0.0741

4.6696 (0.0022) x + 11.8067 (0.0025) y - 7.1956 (0.0023) z = 3.7352 (0.0045)

Angle to previous plane (with approximate esd) = 13.77 (0.06)

* -0.0058 (0.0007) Il_$l
- 0.0012 (0.0008) I2_$l
- 0.0276(0.0009) I3_$l
- -0.0434(0.0009) I4_$l
* -0.0160 (0.0010) I5_$l
- 0.0687(0.0009) I6_$l
- -0.0324(0.0007) I7_$l

Rms deviation of fitted atoms = 0.0353

7.7130 (0.0509) x + 4.8481 (0.0700) y + 14.3942 (0.0335) z = 15.5206(0.0481)

- 0.0077 (0.0075) N1
- 0.0012(0.0088) C1
* -0.0121 (0.0097) C2
* 0.0139(0.0096) C3
- -0.0048 (0.0086) C4
- -0.0059 (0.0076) C11

Rms deviation of fitted atoms = 0.0087

7.7363 (0.0506) x + 4.2005 (0.0635) y + 14.4743 (0.0311) z = 15.1217 (0.0313)

Angle to previous plane (with approximate esd) = 2.% (0.58)

* 0.0068 (0.0076) N2
* 0.0036(0.0079) C12
* -0.0106 (0.0082) C7
* 0.0081 (0.0086) C8
* 0.0018(0.0090) C9
* -0.0097 (0.0087) C10

Rms deviation of fitted atoms = 0.0074

- 9.3199 (0.0489) x + 2.5126 (0.0731) y + 4.0746 (0.0833) z - 2.8219 (0.0997)

Angle to previous plane (with approximate esd) = 87.14 (0.36)

* 0.0065 (0.0081) N3
- -0.0068 (0.0097) C13
- 0.0070(0.0103) C14
- -0.0068 (0.0100) C15
* 0.0062(0.0088) C16
- -0.0060 (0.0079) C23

Rms deviation of fitted atoms = 0.0066

- 9.3291 (0.0436) x + 2.1398 (0.0728) y + 4.5516 (0.0714) z = 2.7455 (0.0720)

Angle to previous plane (with approximate esd) = 2.41 (0.91)

* -0.0017 (0.0079) N4
* 0.0013 (0.0080) C19
* -0.0038 (0.0088) C20
* 0.0035 (0.0093) C21
* -0.0008 (0.0090) C22
* 0.0014(0.0077) C24

Rms deviation of fitted atoms = 0.0024

4.9766 (0.0611) x + 11.7958 (0.0386) y - 7.0999 (0.0707) z = 4.7507 (0.0995)

Angle to previous plane (with approximate esd) - 80.29 (0.39)

* 0.0011 (0.0079) N5
* -0.0115 (0.0092) C25
* 0.0144 (0.0103) C26
* -0.0075 (0.0108) C27
* -0.0024 (0.0094) C28
* 0.0060(0.0081) C35

Rms deviation of fitted atoms = 0.0086

5.3196 (0.0664) x + 12.1365 (0.0454) y - 6.3655 (0.0928) z = 5.7224 (0.1083)

Angle to previous plane (with approximate esd) = 2.95 (0.84)

* -0.0147 (0.0089) N6
* 0.0040(0.0103) C31
* -0.0026 (0.0122) C32
* -0.0077 (0.0130) C33
* 0.0168 (0.0117) C34
* 0.0042(0.0091) C36

Rms deviation of fitted atoms = 0.0100

$1 : -x-1, -y+2, -z+2

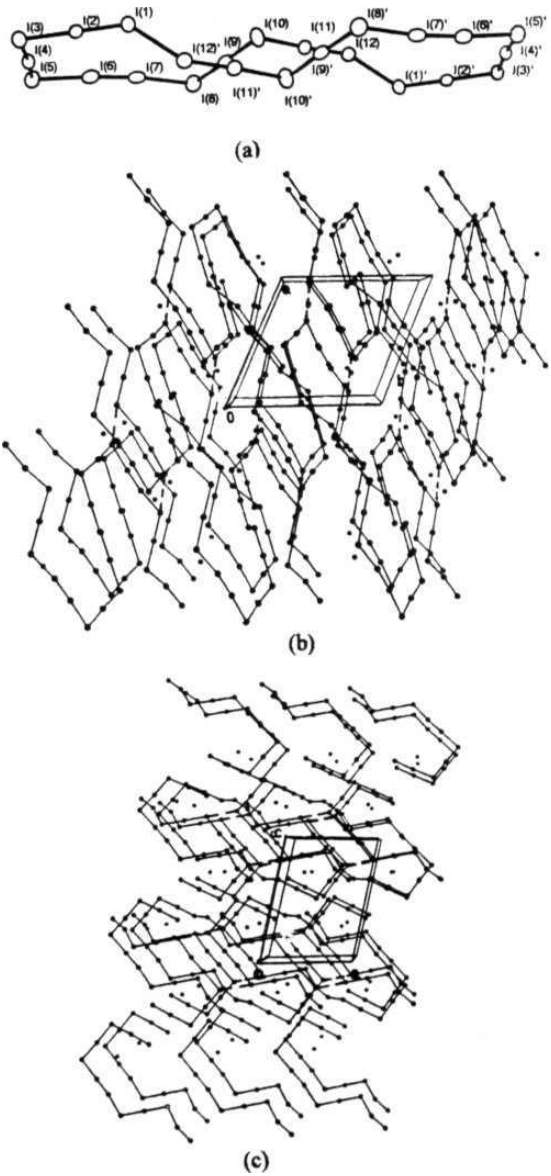

Figure L1. (a) The nearly planar dimeric **l** ring.
Views of packing in 10. (b) normal to ab plane, (c) normal to ac **plane**. (the Zn atoms are shown as small circles and ligand molecules are omitted.)

APPENDIX M. Selected crystallographic data for [bpyH]I_5 (11) and [bpyH]I_7 (12).

Table M1. Crystal data and structure refinement for [bpyH]I_5 (11).

Crystal Data:		
Structural formula	2-2'-bipyridinium pentaiodide	
Empirical formula	$C_{10}H_9I_5N_2$	
Formula weight	791.69	
Temperature	293(2) K	
Crystal system	Monoclinic	
Space group	$P2_1/a$ (No. 14)	
Unit cell dimensions	a = 8.3118(16) A	a = 90 deg.
	b = 25.29(3) A	β = 106.85(3) deg.
	c = 8.868(4) A	y = 90 deg.
Volume	1784(2) A^3	
Z	4	
No. reflns used for cell	20	
Cell measurement theta min/max	7.59/15.67	
Crystal shape	Plate	
Crystal colour	Shining black	
Density (calculated)	2.947 Mg/m^3	
Absorption coefficient	8.701 mm^{-1}	
F(000)	1392	
Crystal size	0.40 x 0.25 x 0.10 mm	
Data Collection :		
Diffractometer	Enraf Nonius CAW	
Radiation type	MoK_α	
Wavelength	0.71073 A	
Radiation source	fine focus sealed tube	
Monochromator	graphite	
Measurement method	omega-2theta	
Standard reflns.	2 measured every 60 min	
Theta range for data collection	2.40 to 25.01 deg.	
Index ranges	$0 \le h \le 9, 0 \le k \le 30, -10 \le l \le 10$	
Reflections collected	3367 [R(int) - 0.0447]	
Independent reflections	3138	
Mean intensity/sigma	30.40	
No. reflns., 1 > 2 sigma(I)	1543	
Absorption correction	Semiempirical	
Max. and min transmission	0.990 and 0.661	
Solution and Refinement :		
Atom sites soln. - primary	Patterson	
Atom sites soln. - secondary	difference fourier	
Atom sites soln. - hydrogens	geometrical	
Treatment of hydrogen atoms	riding model	
Refinement method	Full-matrix least-squares on F^2	
Extinction method	N/A	

Absolute structure	N/A
Data / restraints / parameters	3138/0/ 104
Goodness-of-fit(S) [l>2sigma(I)]	0.936
Goodness-of-fit(S) (all data)	0.936
Final R indices [l>2sigma(I)]	R1 = 0.1108, wR2 = 0.2790
R indices (all data)	R1 = 0.1763, wR2 = 0.3252
Maximum shift/esd	0.020
Mean shift/esd	0.001
Largest diff. peak and hole	4.421 and -3.299 e. A^{-3}

Computer Programs :

Data collection	CAD-4 system
Cell refinement	CAD-4 system
Data reduction	CAD-4 system
Structure solution	SHELXS-86
Structure refinement	SHELXL-93
Molecular graphics	ORTEP
Publication material	SHELXL-93

$R1 = \Sigma||F_o| - |F_c||/\Sigma|F_o|$

$wR2 = [\Sigma\{w(F_o^2 - F_c^2)^2\}/\Sigma(wF_o^4)]^{1/2}$

$w^{-1} = [\sigma^2(F_o^2) + (0.1664P)^2 + 61.460P]$, $P = (F_o^2 + 2F_c^2)/3$

$S = [\Sigma\{w(F_o^2 - F_c^2)^2\}/(n-p)]^{1/2}$

Table M2. Selected bond lengths [A] and angles [deg] for 11.

Bond distances :

I(1)-I(2)	2.796(4)	I(1)-I(3)	3.094(4)
I(3)-I(5)	3.393(3)	I(3)-I(4)	3.401(3)
I(4)-I(4)#1	2.780(5)	I(5)-I(5)#2	2.780(5)

Bond angles :

I(2)-I(1)-I(3)	179.74(8)	I(1)-I(3)-I(5)	120.04(8)
I(1)-I(3)-I(4)	120.36(8)	I(5)-I(3)-I(4)	119.50(9)
I(4)#1-I(4)-I(3)	177.76(12)	I(5)#2-I(5)-I(3)	177.23(12)

Intermolecular contacts :

(a) I...I contacts :

Distances:

I(2)...I(5)#3	4.143(4)	I(5)...I(2)#4	4.143(4)

Angles:

I(1)-I(2)-I(5)#3	148.81(8)	I(3)-I(5)-I(2)#4	73.70(6)

Symmetry transformations used to generate equivalent atoms:

#1 -x+1,-y,-z+1; #2 -x-1,-y,-z; #3 x+1/2, -y+1/2, z; #4 x-1/2, -y+1/2, z;

Table M3. Crystal data and structure refinement for $[bpyH]I_7$ (12).

Crystal Data :

Systematic name	2,2'-bipyridinium heptaiodide

Structural formula	[bpyH]I_7
Empirical formula	$C_{10}H_9I_7N_2$
Formula weight	1045.49
Temperature	293(2) K
Crystal system	Triclinic
Space group	$P\bar{1}$ (NO. 2)
Unit cell dimensions	a = 7.061(13) Aa = 98.860(17) deg.
	b - 10.096(2) A β = 90.03(5) deg.
	c = 14.699(3) A y = 96.91(5)deg.
Volume	1027.7(19) A^3
Z	2
No. reflns. used for cell	23
Cell measurement theta mm/max	13.47/14.67
Crystal shape	Rectangular rod
Crystal colour	Shining greyish-black
Density (calculated)	3.379 Mg/m^3
Absorption coefficient	10.562 mm^{-1}
F(000)	908
Crystal size	0.45 x 0.20 x 0.15 mm

Data Collection :

Diffractometer	Enraf Nonius CAD-4
Radiation type	MoK_α
Wavelength	0.71073 A
Radiation source	fine focus sealed tube
Monochromator	graphite
Measurement method	omega-2theta
Standard reflns.	2 measured every 90 min
Theta range for data collection	2.06 to 24.97 deg.
Index ranges	$-8 \leq h < 8$, $-11 < k < 11$, $0 < 1 \leq 17$
Reflections collected	2838 [R(int) - 0.0082]
Independent reflections	2799
Mean intensity/sigma	65.36
No. reflns., 1 > 2 sigma(l)	1831
Absorption correction	Statistical (DIFABS)
Max. and min transmission	1.098 and 0.625

Solution and Refinement :

Atom sites soln. - primary	Patterson
Atom sites sob. - secondary	difference fourier
Atom sites soln. - hydrogens	geometrical
Treatment of hydrogen atoms	riding model
Refinement method	Full-matrix least-squares on F^2
Extinction method	empirical
Absolute structure	N/A
Data / restraints / parameters	2797 / 0 / 113
Goodness-of-fit(S) [l>2sigma(I)]	1.635
Goodness-of-fit(S) (all data)	2.130
Final R indices p>2sigma0)]	R1 = 0.1095, wR2 = 0.3396

R indices (all data)	R1 = 0.1734, wR2= 0.4797
Maximum shift/esd	-0.010
Mean shift/esd	0.001
Largest diff. peak and hole	3.61 and -3.31 e.Å^{-3}

Computer Programs :

Data collection	CAD-4 system
Cell refinement	CAD-4 system
Data reduction	CAD-4 system
Structure solution	SHELXS
Structure refinement	SHELXL
Molecular graphics	ORTEP, ORTEX
Publication material	SHELX-97

$R1 = \Sigma||F_o| - |F_c||/\Sigma|F_o|$

$wR2 = [\Sigma\{w(F_o^2 - F_c^2)^2\}/\Sigma(wF_o^4)]^{1/2}$

$w^{-1} = [\sigma^2(F^2) + (0.2000P)^2 + 0.000P]$, $P = (F_o^2 + 2F_c^2)/3$

$S = [\Sigma\{w(F_o^2 - F_c^2)^2\}/(n-p)]^{1/2}$

Table M4. Selected bond lengths [A] and angles [deg] for 12.

Bond distances :

I(1)-I(2)	2.800(3)	I(2)-I(3)	3.106(3)
I(3)-I(4)	3.096(3)	I(3)-I(7)#1	3.432(6)
I(4)-I(5)	2.788(3)	I(5)-I(6)	3.493(6)
I(6)-I(7)	2.723(5)		

Bond angles :

I(1)-I(2)-I(3)	174.70(9)	I(4)-I(3)-I(2)	109.12(9)
I(4)-I(3)-I(7)#1	93.19(10)	I(2)-I(3)-I(7)#1	100.99(10)
I(5)-I(4)-I(3)	177.89(9)	I(4)-I(5)-I(6)	93.73(10)
I(7)-I(6)-I(5)	177.89(10)		

Intermolecular contacts :

(a) I...I contacts :

Distances:

I(1)...I(7)#2	3.859(3)	I(7)...I(1)#2	3.859(3)
I(5)...I(7)#3	4.033(3)	I(7)...I(5)#3	4.033(3)
I(4)...I(4)#4	4.191(4)	I(6)...I(6)#3	4.142(4)

Angles:

I(2)-I(1)-I(7)#2	167.76(9)	I(1)-I(7)#2-I(6)#2	87.51(7)
I(6)-I(5)-I(7)#3	96.37(6)	I(6)-I(7)-I(5)#3	82.58(7)
I(3)-I(4)-I(4)#4	108.16(6)	I(5)-I(6)-I(6)#3	72.97(6)

(b) I...ring contacts :

I(1)...N(2)#5	3.87(3)	I(2)...N(1)	3.88(2)

Symmetry transformations used to generate equivalent atoms:

#1 x-l,y-l,z; #2 -x+1, -y+2, -z; #3 -x+1, -y+3, -z+1; #4 -x+1, -y+2, -z+1; #5 x-1, y, z;

APPENDIX N.

Note on tbe anti-microbial properties of the polyiodide salts.

Iodine has been known for its anti-microbial properties and its use in purifying water from germs. But it has a disadvantage of subliming very fast, while most of the triiodides dissolve in water. A preliminary investigation was performed using some of the stable, water-insoluble polyiodide salts of metal complex cations. Complexes 1, 2, 3 and 10 were tested for their action on the microbes present in ordinary tap-water.

Preparation of nutrient medium (broth) of pH = 7.0 . 100ml of broth was prepared by weighing and mixing 0.5g of peptone, 0.3g of beef extract and 0.5g of NaCl in 100ml distilled water. 10ml of the above was transferred into 10 conical flasks of 100ml capacity. All the conical flasks were sealed with cotton plug, aluminium foil and closed tightly with a rubber-band. Then, they were sterilised in auto-clave at 15 pounds of pressure for 45 min. at 120°C. The conical flasks were treated as follows:

(1) Control without inoculation.

(2) Inoculation of tap water. 2ml of tap water was taken in test-tubes. One test-tube was kept without adding anything while in others, ~ 10mg of crystals of 1, 2, 3 and 10 were added under sterilised conditions, inside a lamina. The test-tubes were left inside for one hour. After one hour, 0.5ml of each sample including the untreated tap water were added into each of the conical flasks. For each compound, two samples were taken. The inoculated samples were kept in an incubator for one day (24 hours) after which, its optical density with respect to the first control sample as standard were measured. The absorption of the 680.0nm peak absorption is presented in Table N1.

Table **N1** Optical densities of samples tested for anti-microbial activity.

Sample treatment	**Optical** density
Control (without inoculation)	-0.047
With **inoculation** :	
Control without treatment	1.363
1 (a)	-0.026
1 (b)	-0.044
2 (a)	0.047
2 (b)	-0.027
3 (a)	1.112
3 (b)	0.950
10 (a)	-0.042
10 (b)	-0.039

The inoculated control set-up and the complex 3 treated sample showed growth of bacteria while complexes 1, 2 and 10 treated samples did not show any growth for after one day. On keeping the flasks covered (outside the incubator) for one more day resulted in development of turbidity in all solutions, the minimum among them, was in the iodine-rich 10.

The results showed that the Mn^{2+} complexes (1, 2) and the Zn^{2+} complex 10 show anti-microbial property, while the Ni^{2+} complex 3, does not.

Back cover: Space filling model of 2 and 8, showing polyiodide chains $(I_8^{2-})_n$ inside the cationic channels in $[Mn(bpy)_3](I_3)_{1.5}(I_8)_{0.25}$ (2), and the cations trapped inside the anionic channels of the polyiodide (I_{18}^{4-}) in $[Fe(bpy)_3]I_9$ (8).
(the iodine atoms are shown in violet colour.)